

Predicting the Potential for Natural Ventilation of Buildings in the Urban Environment

by

Jianqiang Li, BEng, MArch.S.

**Thesis submitted to the University of Sheffield for
the Degree of Doctor of Philosophy**

**School of Architecture
The University of Sheffield
October 2008**

Dedication

This thesis is dedicated to my beloved parents, wife and son.

Abstract

Natural ventilation is a rewarding technique for use in sustainable building design, due to its strengths in health, comfort, energy saving and economy. The speed-up of global warming and urbanisation urges us to effectively utilise this technique in the urban environment. However, the understanding of natural ventilation is far from adequate, because the effects of surrounding buildings on its driving forces and ventilation rates are complicated. Building regulations have put much emphasis on constructing air-tightened buildings to save energy, which makes it a challenge to predict ventilation potential at the design stages. This dissertation aims to develop a methodology for predicting the potential for natural ventilation of buildings in the urban environment.

Based on computational fluid dynamics, a virtual urban boundary layer wind tunnel was developed for predicting the wind pressure coefficients around a building. The investigations on the boundary condition, turbulence models and domain size suggest that the proposed settings are more appropriate for the purpose than other methods. The virtual wind tunnel was compared against the wind tunnel experiment, in both an isolated model and a group of models, to confirm its validity. The results verify that the virtual wind tunnel is suitable for predicting the mean wind pressure coefficients.

By coupling the virtual wind tunnel and airflow network models, the potential of natural ventilation driven by the combination of wind and buoyancy forces was calculated. The effects of planning parameters (floor area ratio, building density, and building space) on the potential were investigated, which provided the knowledge on natural ventilation at the planning stage. Finally, the developed methodology was applied to an urban building under various conditions. Some guidance on urban natural ventilation design was suggested. This methodology can be popularised to other projects, thus helping to develop better understandings of urban natural ventilation for decision makers, planners and designers.

Acknowledgements

I would like to express my sincere appreciation to my supervisor, Reader Ian Ward, for his excellent guidance, intellectual support, encouragement, and enthusiasm which made this dissertation possible.

My special thanks go to Professor Steve Sharples, Dr Fan Wang and Professor Jian Kang, for their helpful advice during the process of the project.

I am grateful to Dr. SB Chin and Dr Wei Yang, for their advice and guidance for developing the CFD models.

I would like to thank Dr Deniz Savas and Dr Richard Lukes for their help when using the high performance computing server ICEBERG. I thank Mrs Ruth Wildman for her help on the collection of the data.

Thanks also go to my colleagues at School of Architecture, University of Sheffield for their discussion of the thesis, and my friends for their help and encouragement.

I would like to thank Jenney, Helia and John for their help on the proof reading.

I wish to acknowledge the University of Sheffield for its financial support during the study.

My sincere thanks go to my beloved parents who always support my pursuit; my brothers and sisters for their support and encouragement. Lastly, my heartfelt gratitude is given to my wife Hongyan Ding, for her understanding, immense help and encouragement.

Table of Contents

Title Page	i
Dedication	ii
Abstract	iii
Acknowledgements	iv
Table of Contents	v
List of Figures	x
List of Tables	xiv
List of Symbols	xvi
CHAPTER 1 INTRODUCTION.....	1
1.1 BACKGROUND	1
1.2 RESEARCH PROBLEMS	2
1.3 GENERAL OBJECTIVES	5
1.4 RESEARCH SCOPE.....	6
1.5 STRUCTURE OF THE THESIS	7
CHAPTER 2 NATURAL VENTILATION OF BUILDINGS IN THE URBAN ENVIRONMENT.....	10
2.1 PRINCIPLES OF NATURAL VENTILATION	10
2.1.1 <i>Driving forces</i>	11
2.1.2 <i>Calculation methods</i>	15
2.2 NATURAL VENTILATION DESIGN	18
2.2.1 <i>Standards</i>	18
2.2.2 <i>Design strategies</i>	21
2.2.3 <i>Problems and solutions</i>	22
2.3 NATURAL VENTILATION AND URBAN ENVIRONMENTS	24
2.3.1 <i>Characteristics of the urban atmospheric boundary layer</i>	24
2.3.2 <i>Airflow around buildings</i>	31
2.3.3 <i>Natural ventilation in the urban environment</i>	35

2.4	SUMMARY	41
CHAPTER 3	METHODOLOGY	45
3.1	FUNDAMENTALS OF COMPUTATIONAL FLUID DYNAMICS	46
3.1.1	<i>Governing equations</i>	46
3.1.2	<i>Modelling turbulence</i>	47
3.1.3	<i>Near wall treatments</i>	52
3.1.4	<i>Discretisation</i>	54
3.1.5	<i>Solution</i>	55
3.2	CFD SETTINGS FOR NATURAL VENTILATION STUDIES IN THE URBAN ENVIRONMENT	56
3.2.1	<i>CFD code – FLUENT</i>	56
3.2.2	<i>Meshing</i>	58
3.2.3	<i>Solver settings</i>	59
3.2.4	<i>Boundary conditions</i>	60
3.2.5	<i>Turbulence models</i>	62
3.2.6	<i>Solution settings</i>	66
3.3	AIRFLOW NETWORK MODELS FOR VENTILATION RATE STUDIES.....	67
3.3.1	<i>Fundamentals of airflow network models</i>	67
3.3.2	<i>Airflow network model Codes – AIDA, COMIS</i>	68
3.3.3	<i>Settings</i>	70
3.4	PROCEDURE.....	70
3.4.1	<i>Survey of physical urban boundary layer wind tunnels</i>	70
3.4.2	<i>Development of a virtual urban boundary layer wind tunnel</i>	71
3.4.3	<i>Validation</i>	72
3.4.4	<i>Investigation of planning and the potential for natural ventilation</i>	73
3.4.5	<i>Evaluation of the potential for natural ventilation of an urban building ..</i>	74
3.5	RATIONALE	75
3.5.1	<i>Strength</i>	75
3.5.2	<i>Limitation</i>	76
3.6	SUMMARY	77

CHAPTER 4 DEVELOPING A VIRTUAL URBAN ATMOSPHERIC BOUNDARY LAYER WIND TUNNEL FOR NATURAL VENTILATION STUDIES	79
4.1 CONCEPT OF A VIRTUAL URBAN BOUNDARY LAYER WIND TUNNEL	80
4.1.1 <i>Background</i>	80
4.1.2 <i>Assumption</i>	82
4.1.3 <i>Structure</i>	84
4.2 MODELLING WIND IN THE URBAN ROUGHNESS AREA	85
4.2.1 <i>Modelling description</i>	86
4.2.2 <i>Grid sensitivity test</i>	88
4.2.3 <i>Turbulence model test</i>	90
4.2.4 <i>Friction velocity</i>	96
4.2.5 <i>Wind profile in the urban roughness area</i>	98
4.3 MODELLING EQUILIBRIUM BOUNDARY CONDITION	102
4.3.1 <i>Modelling description</i>	103
4.3.2 <i>Mean velocity profiles in the empty domain</i>	104
4.3.3 <i>Turbulence profile in the empty domain</i>	105
4.3.4 <i>Discussion</i>	107
4.4 IDENTIFICATION OF COMPUTATIONAL DOMAIN SIZE	111
4.4.1 <i>Normal pattern layout</i>	112
4.4.2 <i>Staggered pattern layout</i>	115
4.4.3 <i>Discussion</i>	118
4.5 SUMMARY	121
CHAPTER 5 VALIDATIONS OF THE VIRTUAL URBAN BOUNDARY LAYER WIND TUNNEL.....	124
5.1 STRATEGIES FOR VALIDATION	125
5.1.1 <i>Methodology</i>	125
5.1.2 <i>Criteria</i>	125
5.2 MODEL DESCRIPTION	126
5.2.1 <i>Wind tunnel experiments</i>	126
5.2.2 <i>Numerical models</i>	128
5.2.3 <i>Cases description</i>	132
5.3 RESULTS AND DISCUSSION	135
5.3.1 <i>Flow over the isolated model</i>	135

5.3.2	<i>Flow over the models in the neighbourhood region</i>	142
5.4	SUMMARY	150
CHAPTER 6	PLANNING AND THE POTENTIAL FOR NATURAL VENTILATION	152
6.1	BACKGROUND	153
6.1.1	<i>Previous findings</i>	153
6.1.2	<i>The current study</i>	154
6.2	EXPERIMENTAL SETTINGS	155
6.2.1	<i>Description of model parameters</i>	155
6.2.2	<i>Description of the method to calculate the potential for natural ventilation</i>	159
6.2.3	<i>Cases of the ventilation calculation</i>	161
6.2.4	<i>Criteria for the natural ventilation potential of the building</i>	165
6.3	RESULTS	165
6.3.1	<i>Floor area ratio</i>	165
6.3.2	<i>Building density</i>	174
6.3.3	<i>Building space and building gap</i>	181
6.4	DISCUSSION	187
6.4.1	<i>Planning parameters and natural ventilation potential</i>	188
6.4.2	<i>Opening area for natural ventilation in the urban environment</i>	190
6.4.3	<i>Natural ventilation modes in the urban environment</i>	192
6.4.4	<i>Guidelines of planning for natural ventilation in the urban environment</i>	192
6.5	SUMMARY	194
CHAPTER 7	A CASE STUDY TO EVALUATE THE POTENTIAL FOR NATURAL VENTILATION OF AN URBAN BUILDING	197
7.1	BACKGROUND	198
7.1.1	<i>Research context</i>	198
7.1.2	<i>Framework of predicting the potential for natural ventilation</i>	199
7.1.3	<i>Aims of this study</i>	200
7.2	EXPERIMENTAL PROCEDURE	201
7.2.1	<i>Description of the building and its urban environment</i>	201
7.2.2	<i>Parameters and methods</i>	204
7.2.3	<i>Numerical Model settings</i>	207

7.2.4	<i>Criteria of natural ventilation rates for the office building</i>	216
7.3	RESULTS.....	217
7.3.1	<i>Generation of the homogeneous urban wind profile</i>	217
7.3.2	<i>Wind pressure coefficients around the building</i>	219
7.3.3	<i>Nature Ventilation rate</i>	223
7.4	DISCUSSION.....	234
7.4.1	<i>Characteristics of wind pressure coefficients around the building in the urban environment</i>	234
7.4.2	<i>Natural ventilation design strategies in the urban environment</i>	235
7.4.3	<i>Simulation to predict the potential for natural ventilation</i>	236
7.5	SUMMARY	237
CHAPTER 8	239
8.1	MAIN CONCLUSIONS.....	239
8.1.1	<i>Development of the virtual urban boundary layer wind tunnel</i>	240
8.1.2	<i>Validations of the virtual urban boundary layer wind tunnel</i>	241
8.1.3	<i>Planning parameters and the potential for natural ventilation</i>	242
8.1.4	<i>Prediction of the potential of an urban building</i>	245
8.1.5	<i>Methodology for predicting the potential for natural ventilation</i>	246
8.2	LIMITATIONS	247
8.3	RECOMMENDATIONS	248
 BIBLIOGRAPHY		
APPENDIX A	AIR INFILTRATION DEVELOPMENT ALGORITHM	I
APPENDIX B	COMIS INPUT DATA OF THE ZONES OF THE JESSOP WEST BUILDING.....	III

List of Figures

<i>Figure 1.1 Organisation of the objectives</i>	5
<i>Figure 2.1 Schematic of wind pressure distributions on a building with a low-slopped roof with wind perpendicular to eav: Pressure (+), Suction (-).</i>	12
<i>Figure 2.2 Schematic of buoyancy flow driven by the temperature difference between the inside and the outside</i>	13
<i>Figure 2.3 Schematic of airflow driven by the combined wind and buoyancy forces: (a) assisting wind, (b) opposing wind with downward flow, (c) opposing wind with upward flow.</i>	15
<i>Figure 2.4 Urban atmospheric boundary layer profile</i>	25
<i>Figure 2.5 Wind field around the building in the atmospheric boundary layer (Murakami, 1993)</i>	31
<i>Figure 2.6 Wind pressure coefficients around a cube when normal to incident flow in the atmospheric boundary layer (Castro and Robins, 1977)</i>	
<i>Figure 2.7 Schematic of three flow regimes (Lee et al, 1980)</i>	33
<i>Figure 2.8 Threshold lines dividing flow into three flow regimes as function of the building (L/H) and canyon (W/H) geometries (Oke, 1988).</i>	34
<i>Figure 2.9 Pressure coefficient difference between front and back surfaces on the models within the different density roughness arrays at a free stream veolicty of 10ms^{-1}: A- normal pattern, S- staggered pattern. (Cheng et al, 2007)</i>	35
<i>Figure 4.1 Schematic of a typical urban atmospheric boundary layer wind tunnel (Lee, 1977)</i>	83
<i>Figure 4.2 Structure of the virtual wind tunnel</i>	84
<i>Figure 4.3 Layout of the urban roughness element area in the wind tunnel: The domain with dot lines represents one of the repeating units.</i>	87
<i>Figure 4.4 Comparison of mean velocity profiles in the urban canopy by the various turbulence models</i>	93
<i>Figure 4.5 Comparison of mean turbulence kinetic energy profiles in the urban canopy by various turbulence models</i>	94
<i>Figure 4.6 Comparison of mean velocity profiles by the various friction velocities</i> .	97
<i>Figure 4.7 Mean velocity vectors of the flow in the urban canopy at the height of $0.5 H_b$</i>	99
<i>Figure 4.8 Mean wind velocity profiles in the urban area by the various methods.</i>	100
<i>Figure 4.9 Mean turbulence kinetic energy profiles in the urban area by the various methods</i>	101

<i>Figure 4.10 Plan of the model for the horizontally homogeneous wind profile. The domain with dot lines represents the computational domain.....</i>	<i>104</i>
<i>Figure 4.11 Mean velocity profiles along the fetch in the empty domain.....</i>	<i>105</i>
<i>Figure 4.12 Turbulence kinetic energy profiles along the fetch in the empty domain</i>	<i>106</i>
<i>Figure 4.13 Turbulence dissipation rate profiles along the fetch in the empty domain</i>	<i>107</i>
<i>Figure 4.14 Comparison of equilibrium velocity profiles by the various methods..</i>	<i>108</i>
<i>Figure 4.15 Comparison of turbulence kinetic energy profiles by the various methods</i>	<i>109</i>
<i>Figure 4.16 Comparison of equilibrium turbulence dissipation rate profiles by the various methods</i>	<i>110</i>
<i>Figure 4.17 Schematic of the computational domain size of the models in the normal pattern layout. (a) Horizontal plan; (b) Section.</i>	<i>113</i>
<i>Figure 4.18 Pressure coefficient differences of the models in the various model densities along the streamwise fetch in the normal pattern layout.....</i>	<i>114</i>
<i>Figure 4.19 Pressure coefficient differences of the models in the various model densities along the lateral fetch in the normal pattern layout</i>	<i>115</i>
<i>Figure 4.20 Schematic of the computational domain size of the models in the staggered pattern layout: (a) Horizontal plan; (b) Section.</i>	<i>116</i>
<i>Figure 4.21 Pressure coefficient differences of the models in the various model densities along the streamwise fetch in the staggered pattern layout....</i>	<i>117</i>
<i>Figure 4.22 Pressure coefficient differences of the models in the various model densities along the lateral fetch in the staggered pattern layout</i>	<i>118</i>
<i>Figure 5.1 The inlet velocity profiles by the various methods. The dark dots represent the result of experiments with 5% error bars.</i>	<i>129</i>
<i>Figure 5.2 The inlet turbulence kinetic energy profiles by the various methods. The dark dots represent the result of experiments with 30% error bars.</i>	<i>130</i>
<i>Figure 5.3 The inlet turbulence dissipation rate profiles by the various methods ..</i>	<i>131</i>
<i>Figure 5.4 Schematic of the computational domain size of the isolated model.....</i>	<i>133</i>
<i>Figure 5.5 Comparisons of the mean velocity vectors at the central plan and section (a), (b): Wind tunnel experiment (Murakami and Mochida, 1988); (c), (d): The virtual wind tunnel; (e): The details of the velocity vectors at P1, P2 and P3.</i>	<i>137</i>
<i>Figure 5.6 Mean pressure coefficients along the vertical central line of the windward wall of the isolated model: The dark dots represent the experiment results with 15% error bars.</i>	<i>139</i>
<i>Figure 5.7 Mean pressure coefficients along the vertical central line of the leeward wall of the isolated model: The dark dots represent the experiment results with 20% error bars.</i>	<i>140</i>

Figure 5.8 Mean pressure coefficients along the vertical central line on the roof of the isolated model: The dark dots represent the experiment results with 20% error bars.....	141
Figure 5.9 Flow pathlines around the model in the normal pattern layout: Building density: (a) 5%, (b) 10%, and (c) 20%.....	143
Figure 5.10 Flow pathlines around the model in the staggered layout: Building density: (a) 5%; (b) 10%; (c) 20%.....	144
Figure 5.11 Comparison of the mean pressure coefficients along the vertical central line of the windward wall of the model in the normal pattern layout: The dark dots represent the experiment results with 30% error bars.....	146
Figure 5.12 Comparison of the mean pressure coefficients along the vertical central line of the leeward wall of the model in the normal pattern layout: The dark dots represent the experiment results with 30% error bars.....	147
Figure 5.13 Comparison of the mean pressure coefficients along the central line of the windward wall of the model in the staggered pattern layout: The dark dots represent the experiment results with 30% error bars.....	148
Figure 5.14 Comparison of the mean pressure coefficients along the vertical central line of the leeward wall of the model in the staggered pattern layout: The dark dots represent the experiment results with 30% error bars.....	149
Figure 5.15 Errors among the virtual wind tunnel, wind tunnel and real data.....	150
Figure 6.1 Schematics of the repeated unit in planning: (a) Normal pattern; (b) Staggered pattern.....	156
Figure 6.2 Pressure coefficient distributions along the central lines of the models of varying floor area ratios.....	167
Figure 6.3 Whole building ventilation rates of the buildings of varying floor area ratios.....	169
Figure 6.4 Purge ventilation rates of the buildings of varying floor area ratios....	171
Figure 6.5 Cooling ventilation rates of the large space of the buildings of varying floor area ratios.....	173
Figure 6.6 Pressure coefficient distributions along the central lines of the models of varying building densities.....	176
Figure 6.7 Whole building ventilation rates of the buildings of varying building densities.....	177
Figure 6.8 Purge ventilation rates of the buildings of varying building densities...	178
Figure 6.9 Cooling ventilation rates of the buildings of varying building densities	180
Figure 6.10 Pressure coefficient distributions along the central lines of the buildings of varying ratios of building height to building space.....	182
Figure 6.11 Whole building ventilation rates of the buildings of varying of the ratios of building height to building space.....	184
Figure 6.12 Purge ventilation rates of the buildings of varying of ratios of building height to building space.....	186

<i>Figure 6.13 Cooling ventilation rates of the buildings of varying of ratios of building height to building space</i>	<i>187</i>
<i>Figure 7.1 Framework of predicting the potential for natural ventilation of buildings in the urban environment: Dark shading indicates the input data.</i>	<i>200</i>
<i>Figure 7.2 Planning of the Jessop West Building: The domain enclosed by the dot lines stands for the computational domain.</i>	<i>202</i>
<i>Figure 7.3 Illustrations of the Jessop West Building: (a) view from the outside, (b) atrium in the centre, (c) double façade details.....</i>	<i>203</i>
<i>Figure 7.4 Schematic of the building section.....</i>	<i>204</i>
<i>Figure 7.5 Grids around the isolated building</i>	<i>211</i>
<i>Figure 7.6 Grids around the building with the urban surroundings</i>	<i>212</i>
<i>Figure 7.7 Zones of the Jessop West Building.....</i>	<i>214</i>
<i>Figure 7.8 Urban wind profiles at the building site (a) mean velocity profile; (b) turbulence kinetic energy profile; (c) turbulence dissipation rate profile</i>	<i>218</i>
<i>Figure 7.9 Contours of pressure coefficients on the facades of the isolated building</i>	<i>221</i>
<i>Figure 7.10 Contours of pressure coefficients on the facades of the building with urban surrounding buildings.....</i>	<i>222</i>
<i>Figure 7.11 Contours of pressure coefficients on the roofs. (a) the roof of the isolated building; (b) the building with urban surroundings</i>	<i>223</i>

List of Tables

<i>Table 2.1 Ventilation rate of buildings (rooms) for indoor air quality (CIBSE, 2003; ASHRAE, 2005).....</i>	<i>19</i>
<i>Table 2.2 Categories of ventilation rate for health (Ward, 2008)</i>	<i>20</i>
<i>Table 2.3 Required ventilation rate for the indoor environment (Wills et al, 1995) .</i>	<i>20</i>
<i>Table 2.4 Turbulence kinetic energy profile.....</i>	<i>29</i>
<i>Table 2.5 Methods and applications in natural ventilation in the urban environment</i>	<i>40</i>
<i>Table 3.1 Boundary condition settings in CFD models</i>	<i>62</i>
<i>Table 3.2 Characteristics of the urban atmospheric boundary layer wind tunnel in Sheffield (Hussain and Lee, 1980; Lee, 1977)</i>	<i>71</i>
<i>Table 4.1 Details of set-up grid of the urban roughness model. NWT stands for non-equilibrium wall function; EWT represents enhanced wall treatment.</i>	<i>88</i>
<i>Table 4.2 Comparison of six measured parameters among the four types of grid resolutions.....</i>	<i>89</i>
<i>Table 4.3 Comparison of mean pressure coefficients on the four surfaces of the model in the urban canopy by the various turbulence models.....</i>	<i>92</i>
<i>Table 4.4 Comparison of reattachment and recirculation lengths around the building by the various turbulence models.....</i>	<i>95</i>
<i>Table 4.5 Friction velocities and pressure gradients.....</i>	<i>97</i>
<i>Table 4.6 Details of the models for the lateral length study in the normal pattern layout.....</i>	<i>114</i>
<i>Table 4.7 Neighbourhood region in the urban environment for natural ventilation study</i>	<i>120</i>
<i>Table 5.1 Details of setting-up of the isolated model for the grid sensitivity test....</i>	<i>134</i>
<i>Table 5.2 Comparison of the average pressure coefficient difference on the model surfaces among the three grid resolutions. W1, W2, W3 and W4 represent the windward, leeward, lateral surfaces respectively; R1 stands for the roof.</i>	<i>135</i>
<i>Table 5.3 Comparison of the reattachment and recirculation length among experiments.....</i>	<i>138</i>
<i>Table 6.1 Parameters of the models of varying floor area ratios.....</i>	<i>157</i>
<i>Table 6.2 Parameters of the models of varying building densities</i>	<i>158</i>
<i>Table 6.3 Parameters of models of varying building space and gap.....</i>	<i>159</i>

<i>Table 6.4 Cases of the wind induced ventilation at the different levels</i>	162
<i>Table 6.5 Cases of natural ventilation combined wind and thermal buoyancy forces in the large space</i>	164
<i>Table 6.6 Ventilation criteria for the cases</i>	165
<i>Table 6.7 Average pressure coefficients on the building surfaces of varying floor area ratios. (the reference velocity is the gradient wind speed 9.65ms^{-1})</i>	166
<i>Table 6.8 Indices of the potential for natural ventilation of varying floor area ratios</i>	188
<i>Table 6.9 Indices of the potential for natural ventilatino of varying building densities</i>	189
<i>Table 6.10 Indices of the potential for natural ventiation of varying ratios of building height to building space</i>	190
<i>Table 7.1 Three cases of metrological conditions</i>	215
<i>Table 7.2 Ventilation functions and rates for the non-domestic building (Wills, 1995; Ward 2008)</i>	217
<i>Table 7.3 Natural ventilation rates of zones in winter with the different surrounding conditions</i>	226
<i>Table 7.4 Natural ventilation rates of the zones in summer with the different surrounding conditions</i>	227
<i>Table 7.5 Natural ventilation rates of the zones on the hottest days with the differnent surrounding conditions</i>	228
<i>Table 7.6 Natural ventilation rate under the average wind and no wind conditions in the urban context - winter</i>	231
<i>Table 7.7 Natural ventilation rates under the average wind and no wind conditions in the urban context - summer</i>	232
<i>Table 7.8 Natural ventilation rates under the average wind and no wind conditions in the urban context – the hottest days</i>	233

List of Symbols

Symbol	Definition	Unit
a	The side size of the square plan in the model	m
a'	Silhouette area of buildings	m^2
A	Area covered by buildings	m^2
A_r	Opening area recommended by the building regulation	m^2
A_u	Opening area of the building in the urban environment	m^2
C_d	Discharge coefficient	dimensionless
C_i	Flow coefficient of the 'i' th flow path	dimensionless
C_p	Pressure coefficient	dimensionless
C_{pd}	Pressure coefficient difference between the windward and leeward walls	dimensionless
E	Turbulence kinetic energy	m^2s^{-2}
F	Body forces	Pa
G_c	Building gap	m
H	Model height	m
\bar{H}	Average height of the group of buildings	m
H_b	Building height or urban roughness element height	m
H_d	Difference in height between two openings	m
H_s	Floor height	m

I	Turbulence intensity	dimensionless
K_v	Von Karman's constant (≈ 0.4)	dimensionless
L_t	Turbulence length scale	m
P	Pressure	Pa
P_b	Buoyancy force	Pa
P_i	Internal pressure	Pa
P_t	Total pressure combined wind and buoyancy forces	Pa
P_w	Wind pressure	Pa
ΔP	Pressure difference between P_t and P_i	Pa
Q_m	Mass flow rate	gs ⁻¹
Q_v	Volume flow rate	ls ⁻¹
R	Length of model distributions	m
Re	Reynolds number	dimensionless
S	Building distance	m
S_c	Building space	m
T	An eddy turnover time	s
T_i	interior air temperature	°C
T_o	outdoor air temperature	°C
ΔT	Time step	s
U	Mean velocity	ms ⁻¹

U_e	Friction velocity from the experience	ms^{-1}
U_g	Free stream velocity at Z_G	ms^{-1}
U_H	Mean velocity at roughness height	ms^{-1}
U_{ref}	Reference velocity at the reference height H_{ref}	ms^{-1}
U_{rsm}	Friction velocity deduced from Reynolds stress	ms^{-1}
U_*	Global friction velocity	ms^{-1}
U_τ	Surface friction velocity	ms^{-1}
U^+	Velocity parameter	dimensionless
u, v, w	Components of velocity along x, y and z axes respectively	ms^{-1}
u', v', w'	Components of fluctuating velocity along x, y and z axes respectively	ms^{-1}
y	The normal distance to walls	m
y^+	Near wall distance parameter	dimensionless
Z	Vertical height	m
Z_d	Zero displacement height	m
Z_g	Gradient wind level	m
Z_*	The height of roughness sublayer	m
α	Exponent of power law of wind velocity profile	dimensionless
β	Index for the potential of natural ventilation	dimensionless
δ	Boundary layer thickness	m

ϵ	Turbulence dissipation rate	$\text{m}^2 \text{s}^{-3}$
η	Kolmogorov length scale	m
λ	Building density	dimensionless
μ	Dynamic viscosity	Nsm^{-2}
ν	Kinematic viscosity	$\text{m}^2 \text{s}^{-1}$
\emptyset	Floor area ratio	dimensionless

CHAPTER 1

Introduction

1.1 Background

Natural ventilation is a reviving and rewarding technique to use in achieving a sustainable building. The employment of this technique in building design dates back thousands of years. For instance, wind catchers in traditional buildings are the particular devices for natural ventilation in Middle Eastern countries (Melaragno, 1982). However, the use of natural ventilation was largely abandoned with the advent of modern electrical air-conditioning, enabling people to comfortably enjoy an artificially controlled environment. The outbreak of the oil crisis in 1973 changed popular opinion on energy consumption. Society placed more emphasis on saving energy, using techniques such as enhancing envelope insulation, reducing air infiltration and applying renewable energy (Allard, 1998; Heiselberg, 2004). The increased air tightness of buildings and reduction of loss of heat meant saving energy; however, there appeared new problems with the indoor air quality and comfort. Inadequate ventilation can increase the risk of symptoms of SBS (Sick Building Syndrome) (Jakkola and Miettinen, 1995). As natural ventilation is an effective approach to improving indoor air quality, enhancing thermal comfort, reducing the energy consumption by cooling, as well as economical benefit (Emmerich et al., 2001), it has become a popular strategy for improving the built environment.

The importance of natural ventilation design has been emphasized in the whole building design process. Although ventilation of buildings is a mechanical issue, usually considered by building service engineering or mechanical engineering, the building's site, form and orientation can directly affect the airflow around the

building and the possibility of or potential for natural ventilation. Planners and architects have tried to consider natural ventilation as a factor in their design projects. The various design strategies for natural ventilation have been applied to various practices, such as the narrow building plan, the atrium, using the double façade and solar chimney as a shaft, the wind scoop and wind catcher, the wind cowl, and so on (CIBSE, 2005).

As the urban environment can significantly affect the potential for natural ventilation of a building, less effective natural ventilation will negatively affect the inhabitants' living quality, including health and comfort. As a result, the urban morphology has been considered in the assessment of air ventilation. For example, in order to achieve better city ventilation after the outbreak of SARS in 2003, the Hong Kong government organised an air ventilation assessment project to set up guidelines for urban planning in Hong Kong (Ng, 2008). In addition, due to the rapid urbanisation that is predicted to be an inevitable tendency over the next four decades (UN, 2008), urban land users are urged to consider natural ventilation in the planning of their buildings.

1.2 Research problems

Although natural ventilation techniques have been popularly applied in building design, the knowledge of the effects of surrounding buildings on their performance is still inadequate, especially in the urban environment. For example, British Standard (1991) has provided the principle of natural ventilation based on theory and empirical experiments, without taking into consideration the effects of the complicated surrounding buildings on the potential for ventilation. CIBSE (2005) has given guidance for natural ventilation design, but most data that this is based on is derived from studying an isolated building. As pointed out by some scholars, building density and layout can significantly affect the potential for natural ventilation (Khanduri et al., 1997; Lee et al., 1980), and neglecting the effect of building surroundings when designing a naturally ventilated building may result in poor ventilation (Syrios and Hunt, 2007).

In the meantime, there are no effective tools for predicting natural ventilation in the urban environment. The applications of traditional design methods by empirical equations, manual methods and wind tunnel experiments to predict airflow and natural ventilation are limited due to their low accuracy, high cost and long duration (Chen, 2004). Airflow network models are primarily restricted by the need to quantify the driving forces (Liddament, 1996). Even the popular CFD simulation has limitations, as its application to natural ventilation study restricted to considering the isolated building or the simple model, because CFD suffers from the challenge of computational resource, boundary conditions and accuracy. CIBSE (2005) points out that the application of CFD as the virtual wind tunnel is still an emerging issue in the simulation of natural ventilation.

So far, there are no comprehensive methods to holistically evaluate natural ventilation for the purpose of building design. Qualitative methods may be used to evaluate the possibility of natural ventilation in an urban scale region, but cannot guide natural ventilation design of the building in the region which is suitable for natural ventilation. This is because natural driven forces are determined by the climate, urban terrain and building surroundings, the building itself, and so on. For instance, Axley and Emmerich (2002) have proposed a method to assess the climate suitability of natural ventilation for cooling based on offsetting interior heating by natural ventilation. Ward (2003) has analysed the quality of natural ventilation potential in planning based on GIS (global information system) climate maps and wind flow regimes. This method may be useful in planning, but it cannot provide clear guidelines for building design in the urban environment. The multi-criteria method (Germano et al., 2005) has taken driven forces and constraints into account when assessing natural ventilation potentials of the building site at the preliminary design stage, but this method is limited considering the building site. In addition, the simple algebraic equation from the experimental model cannot be applied to a complex building. As a consequence, using the qualitative approach is not ideal for natural ventilation design in the urban environment.

Furthermore, the prediction of driven forces of natural ventilation is essential for natural ventilation design. As wind pressure can assist or oppose buoyancy, isolated

wind induced ventilation or buoyancy ventilation can inevitably cause the problems for building designers when choosing appropriate natural ventilation strategies. However, wind tunnel experiments usually ignore buoyancy ventilation on a small scale, because of the effect of low Reynolds number on viscosity (Lidden, 1999). A method to calculate natural ventilation rates in the urban canyon has been proposed in the URBVENT project (Guiaus and Allard, 2005). This method does not consider wind induced ventilation, so that it is limited to the deeper and longer street canyon, which only exists in the city centre. In a wide urban context, wind can still act as ventilation, just as well as buoyancy.

The inadequate knowledge, ineffective tools and evaluation methods for natural ventilation in the urban environment often puzzle planners and architects who attempt to use natural ventilation in their projects. As natural ventilation is affected by many factors, such as climate, urban terrain, surrounding buildings, building forms and so on, the decision of planning and building design will eventually determine the potential for natural ventilation. The multiple factors mean it is difficult for designers to choose an appropriate design strategy. In addition, a successful natural ventilation design strategy of one particular case may not be effective applied to other cases, because every building has its own specific conditions, which affect the potential for natural ventilation. Furthermore, the air tightness of buildings has been emphasized for energy saving by building regulations, whilst it is essential to obtain adequate ventilation for indoor air quality. How to choose an appropriate opening size is another complicated matter for architects to consider at the design stages.

Natural ventilation design should be thought through the design stages. During the design process, an effective, economical and flexible methodology for assessing natural ventilation can help planners and architects to quickly evaluate and optimise their schemes. This method should integrate qualitative and quantitative methods, and combine the natural ventilation driven by wind and thermal buoyancy forces in the urban environment. This methodology may be a comprehensive approach to predicting the potential for natural ventilation of buildings, considering many factors in the urban environment.

1.3 General Objectives

The prime aim of this research is to propose a methodology to predict the potential for natural ventilation of buildings in the urban environment. This methodology can be applied to planning, can be used in generic studies, and also to achieve guidelines for planners and building designers, as well as being used to evaluate the potential for natural ventilation of an urban building. The methodology consists of four objectives (see Figure 1.1):

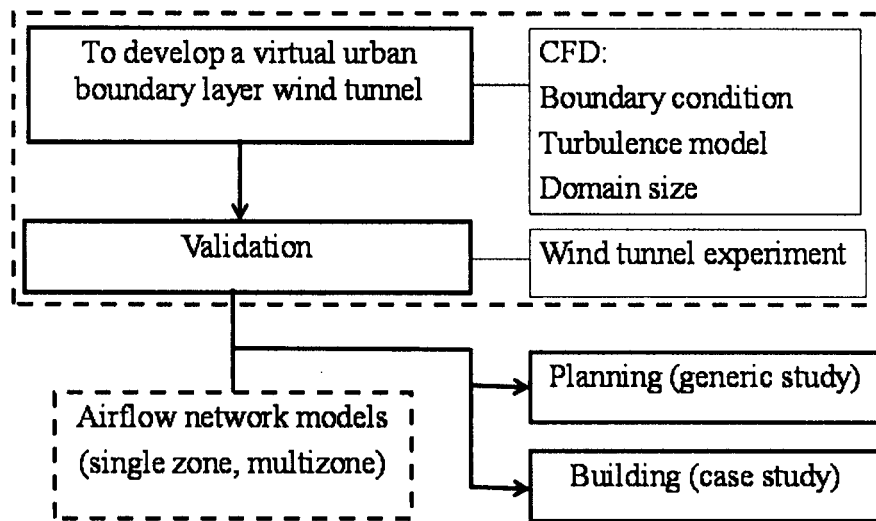


Figure 1.1 Organisation of the objectives

To develop a virtual urban boundary layer wind tunnel

The virtual urban boundary layer wind tunnel is specified as a computational model in which the wind flows around the studied building with a particular group of buildings can be tested in the same way that a physical wind tunnel can. It can be used to acquire wind pressure coefficients around the building, in order to study the potential for natural ventilation in the urban environment. Utilising the general CFD technique, this virtual wind tunnel explores the boundary conditions and computational domain size in the urban environment. Based on urban surrounding features, including building density, building layout and building form, specific guidelines for setting up the virtual wind tunnel are proposed. Compared with other

methods that predict wind pressure coefficients, the proposed approach is efficient, feasible and cost-saving, while retaining sensible results.

To validate the virtual urban boundary layer wind tunnel

Case studies on the isolated model and group models are performed by the established virtual wind tunnel. Their results of the average wind pressure coefficient are compared with those from physical wind tunnel experiments. The discrepancy between the virtual wind tunnel and the wind tunnel was presented. The validated virtual wind tunnel can build confidence in designers or engineers wishing to use these guidelines for building their models.

To develop the guidance of planning for natural ventilation in the urban environment

The effects of planning parameters on the potential for natural ventilation were investigated. These parameters include floor area ratio, building density, building space, and building gap. The guidelines provided the recommendation for the decision-makers, planners and designers. In addition, the established methodology may be useful for planners and architects to decide their projects at the early design stage, and optimise planning.

To apply the established methodology to an urban building for evaluating its potential for natural ventilation

It demonstrated a feasible approach for predicting the potential for natural ventilation of an urban building, in different seasons and with different surrounding conditions. This methodology can be popularised into other cases to analyse their potential for natural ventilation. The guidance of natural ventilation design of the building in the urban environment may help the designers to maximise the potential for natural ventilation.

1.4 Research Scope

Natural ventilation potential has been expressed through many parameters, including indoor air velocity (Su, 2003), degree days (Ghiaus and Allard, 2005), pressure

difference Pascal hours (PDPH) (Yang et al., 2005), and so on. The potential for natural ventilation in this study is defined by comparing natural ventilation rates with the criteria of the ventilation rate for health, thermal comfort and cooling in a building. It can also be expressed as the indices (the ratio of the natural ventilation rate to the criteria ventilation rate). The potential for natural ventilation is affected by the wind pressures around the building and the buoyancy force. The wind pressures around the building are dependent upon the wind speed, orientation, the surrounding buildings, the studied building's geometry, and so on. The buoyancy is determined by the outside and inside temperatures, and the vertical height difference between the openings.

The urban environment is specified as having characteristics of climate (wind speed, air temperature) and urban morphology. As natural ventilation in the urban environment is constrained by many factors, such as driven forces, noise from the outdoors, dust and pollution, and safety concerns, this research concentrated on the natural ventilation driven forces, and assumed the studied urban environment has fresh air, and is quiet and safe. As wind velocity is unstable, the prevailing wind usually used at the building design stages is mainly studied case. The air temperatures are set as the average temperatures in the winter, summer and on the hottest days. This study focuses a group of buildings in the urban context affecting the studied building, rather than focusing on the vegetation, or terrain.

Planning is specified as being the neighbourhood planning rather than the urban region planning, because the buildings outside of the neighbourhood region may have slight effects on the wind-induced ventilation of the studied building. The studied building is specified as being the low-rise building rather than the high-rise building, because the wind pressures on the high-rise building has different natural ventilation strategies as it may be less affected by the urban surrounding buildings.

1.5 Structure of the Thesis

This thesis states the details of the research, including a review of natural ventilation potential in the urban environment, methodology, results and discussion, and conclusions. The thesis is organised as follows:

Chapter 2 reviews the literature on natural ventilation potential in the urban environments. This includes natural ventilation driven forces and calculation methods; the current natural ventilation design standard and strategies and barriers, the characteristics of the urban atmospheric boundary layer and its numerical model; and the wind around an isolated building and buildings in the group. Chapter 2 also analyses the limitation of natural ventilation design. Finally, the research topics are identified.

Chapter 3 describes the research methodology and procedure used in this project. It introduces the fundamentals of the CFD technique and its application conditions in the wind environment. Airflow network methods for calculating natural ventilation rate are also presented. It highlights the fact that combining computational fluid dynamics and the multi-zone network is a good approach for studying the natural ventilation potential of buildings in the urban environment.

Chapter 4 presents the details of setting up an effective virtual wind tunnel for natural ventilation study in the urban environment, based on the CFD technique. The inlet boundary condition is studied, and the method for acquiring the urban atmospheric boundary layer profile is demonstrated. The effects of domain size on wind pressure coefficients are studied based on the various building layouts and building densities, in order to identify the neighbourhood scale for natural ventilation study.

Chapter 5 demonstrates the validation of the developed virtual urban boundary layer wind tunnel by the comparison of pressure coefficients around the models with those from the wind tunnel experiments. The pressure coefficients around the isolated model are used to validate the inlet wind profile and other boundary conditions. The pressure coefficients around the building in the group are used to validate the domain size setting in the virtual urban boundary layer wind tunnel.

Chapter 6 studies the effects of planning parameters on the potential for natural ventilation. By using the generic method, the selected planning parameters - including floor area ratio, building density and building space - are investigated in

**PAGE
NUMBERING
AS
ORIGINAL**

terms of their effects on the wind pressure coefficients around the building. The airflow rates of the building are calculated by inputting the wind pressure coefficients into the airflow network model. The potential for natural ventilation is presented by the comparison of the airflow rate with the criteria for health, thermal comfort and cooling. The guidance on planning for the potential for natural ventilation is developed.

Chapter 7 demonstrates the application of the methodology for predicting the potential for natural ventilation of an urban building. The cases in various seasons are presented. The comparison of the potential for natural ventilation in the isolated condition and the building in the urban context are shown. The comparison of results from the average wind condition and no wind condition are described. The guidelines for evaluating the potential for natural ventilation of an urban building, and design guidance for natural ventilation design of the building in the urban environment, are discussed.

Chapter 8 summarises the findings of the previous chapters, and presents their implications. The weakness of this research is discussed, and recommendations are made for future studies.

Chapter 6 studies the effects of planning parameters on the potential for natural ventilation. By using the generic method, the selected planning parameters - including floor area ratio, building density and building space - are investigated in terms of their effects on the wind pressure coefficients around the building. The airflow rates of the building are calculated by inputting the wind pressure coefficients into the airflow network model. The potential for natural ventilation is presented by the comparison of the airflow rate with the criteria for health, thermal comfort and cooling. The guidance on planning for the potential for natural ventilation is developed.

Chapter 7 demonstrates the application of the methodology for predicting the potential for natural ventilation of an urban building. The cases in various seasons are presented. The comparison of the potential for natural ventilation in the isolated condition and the building in the urban context are shown. The comparison of results from the average wind condition and no wind condition are described. The guidelines for evaluating the potential for natural ventilation of an urban building, and design guidance for natural ventilation design of the building in the urban environment, are discussed.

Chapter 8 summarises the findings of the previous chapters, and presents their implications. The weakness of this research is discussed, and recommendations are made for future studies.

CHAPTER 2

Natural Ventilation of Buildings in the Urban Environment

Natural ventilation has been studied a lot, but most literature focuses on the isolated building. As most people live in urban areas with the urbanisation, studying the natural ventilation potential of urban buildings has become a more important issue in achieving a healthy, thermally comfortable and energy efficient built environment. This chapter aims to critically review recent literature on natural ventilation in the urban environment, and identify the studied topics in this project.

This chapter consists of four sections. Firstly, the principles of natural ventilation, including driven forces and their calculation methods, are reviewed. Then natural ventilation design standards, strategies and solution approaches are discussed. Thirdly, wind characteristics around the buildings in the urban environment are discussed. The current research and practice on natural ventilation in the urban environment are critically reviewed. Finally, the limitations of the current study are summarised, and research topics on natural ventilation design in the urban environment are identified.

2.1 Principles of Natural Ventilation

Natural ventilation is the process of supplying outside air, and removing and diluting indoor air by means of naturally driving forces. According to two types of driven forces: wind pressure and buoyancy, it can be divided into wind induced ventilation and buoyancy ventilation. Natural ventilation performance can be manipulated by the purposely designed openings, such as windows, doors, trickle vents, ducts and so on.

As the air tightness of buildings has been emphasised by building regulations, the balance of ventilation rates for health and energy saving is more worthy of concern. The fundamentals of studying natural ventilation include its driving forces, calculation methods and design strategies.

2.1.1 Driving forces

Natural ventilation is driven by the pressure difference between the two openings of an airflow path. The natural driving forces are wind pressure or buoyancy induced by air density difference, or a combination of them both.

Wind pressure

According to Bernoulli's equation - that total pressure is constant along a streamline - the total pressure converts into static pressure and dynamic pressure when the wind impinges on buildings. Wind (dynamic) pressure is dependent upon wind speed and incidence, the shape of building and the surroundings, and is usually expressed as Equation 2.1. Broadly speaking, wind has pressure on the windward surface and suction on the leeward surface and roof (see Figure 2.1):

$$P_w = 0.5C_p \cdot \rho \cdot U_{ref}^2 \quad (2.1)$$

Where P_w is wind pressure on the building surface (Pa); C_p is wind pressure coefficient; ρ is air density (kgm^{-3}); and U_{ref} is the reference wind speed (ms^{-1}).

The wind pressure coefficients are dimensionless parameters used for describing pressure in the fluid field. This is because the pressure, forces and moments in the flow at moderate to high Reynolds numbers vary little with change in velocity for a given body. The wind pressure coefficients are almost independent of wind speed for a building with sharp corners because the flow separation points normally occur at the sharp edges (Awbi, 2003). However, they are dependent upon the wind direction relative to the building, the geometry of building, the opening size and the proximity of neighbouring buildings.

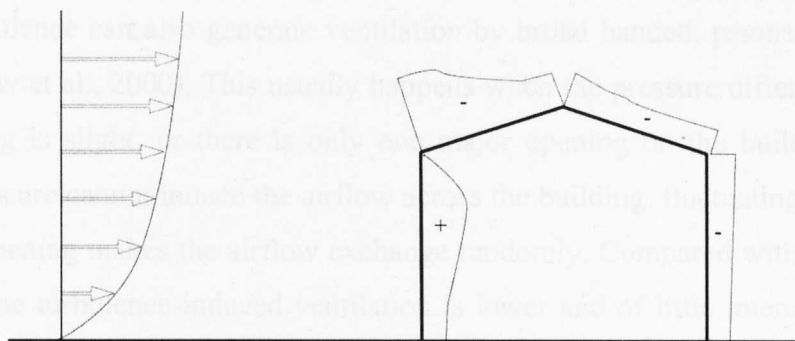


Figure 2.1 Schematic of wind pressure distributions on a building with a low-sloped roof with wind perpendicular to eave: Pressure (+), Suction (-).

There are five approaches to obtaining this data. The full scale measurement is the most accurate method, but it is impossible to use in building design due to expensive equipment and long periods of observation. The empirical method is the simplest method. Some manuals or standards, such as the AIVC guideline (Liddament, 1996), or British Standards (1997) has provided the pressure coefficients on the rectangular building for the wind load, but they may not be appropriate for studying natural ventilation in the urban environment, as they simplify the effect of the surrounding buildings on wind pressure coefficients. The algorithm or parametrical models (Grosso, 1992; Knoll et al., 1996; Sharag-Eldin, 1998) can estimate pressure coefficients by considering the surrounding effects based on extensive wind tunnel experiments and the established database. But the drawbacks are that simplifying the building geometry and the surroundings mean they cannot be applied into the complex condition. The wind tunnel experiment is an accurate method for acquiring pressure coefficients, provided that its atmospheric boundary layer profile over terrain is similar to that of the full scale test. As the wind tunnel is an expensive and time-consuming method, the current tendency is to apply CFD simulation to acquire the wind pressure coefficient (Burnett et al., 2005; Suh et al., 1997). However, using CFD as a virtual wind tunnel to calculate pressure coefficients in the complex arrangement of buildings is a challenging decision (CIBSE, 2005). Chang and Meroney (Chang and Meroney, 2003) point out that the adequate grid resolution, accurate inlet profile and improved turbulence model can replicate pressure coefficients just as the wind tunnel experiment can. Compared with the five other approaches, CFD has the potential for predicting the wind pressure coefficients of building in the urban environment, if the appropriate CFD conditions are established.

Wind turbulence can also generate ventilation by broad banded, resonant and shear layer (Straw et al., 2000). This usually happens when the pressure difference around the opening is slight, or there is only one major opening on the building. As the steady pressure cannot induce the airflow across the building, fluctuating pressure on the only opening makes the airflow exchange randomly. Compared with the average pressure, the turbulence-induced ventilation is lower and of little interest in natural ventilation studies (Etheridge and Sandberg, 1996).

Buoyancy force

Buoyancy force is generated by the different densities in warm and cold air, which increase with the height between the openings. The pressure gradient of the cold air declines more than that of the warm air with the increase in height, as the density of the former is larger than the latter. The warm air inside flows out at the top of the building and the cold air enters the building from the outside, at a position that is near the building's base (see Figure 2.2).

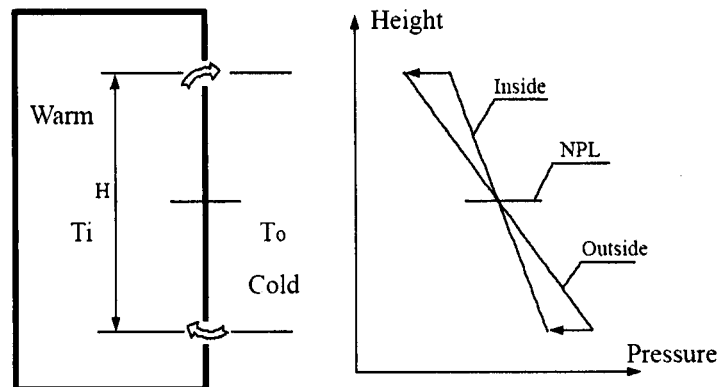


Figure 2.2 Schematic of buoyancy flow driven by the temperature difference between the inside and the outside

The neutral plan level (NPL) is the height at which the internal pressure is equal to the external pressure. The position of NPL is related to the size of the openings. When the opening areas at the upper level and the lower level are equal, the NPL is positioned in the middle between the openings. If the opening at the upper level is smaller than the lower level, the NPL moves down, and vice versa (CIBSE, 2005). In the multi-opening building, the openings at the higher level need to be larger than at the lower level in order to keep the same flow rate.

Buoyancy force is also derived from the Bernoulli equation. Its magnitude is dependent upon the temperature difference between the outside and inside, and the vertical distance between the openings. It can be expressed as Equation 2.2:

$$P_b = -273\rho gH_d \left(\frac{1}{T_o} - \frac{1}{T_i} \right) \quad (2.2)$$

where T_o is outdoor air temperature ($^{\circ}\text{C}$); T_i is internal air temperature ($^{\circ}\text{C}$); ρ is air density at outdoor air temperature; g is acceleration due to gravity (ms^{-2}); H_d is difference in height between two openings (m).

Combined wind and buoyancy forces

In most cases, natural ventilation is driven by the combined forces of wind and buoyancy. Wind force can assist or oppose buoyancy force, dependent on the opening positions and wind direction. Figure 2.3 shows the three types of airflow in a single-zone building: assisting wind, opposing wind with downward flow and opposing wind with upward flow. When warm air flows out from the upper opening in the leeward wall and cool air enters from the lower opening in the windward wall, the wind force can assist the buoyancy force. In this case, displacement ventilation occurs, and a stratified layer is established when the wind speed is low (Lidden, 1999). If the wind velocity is much larger than the buoyancy-induced velocity, the displacement will be destroyed, and the flow is less efficient than the no-wind flow at flushing the buoyant fluid from the space.

In general, the buoyancy ventilation assisted by wind flow can increase the ventilation rate. The airflow in the opposing wind condition is much more complicated. The airflow direction could be upward or downward, which are dependent upon whether wind or buoyancy is the dominating driving force. The solution for the flow rate as a function of the heat source strength shows some complex features (Li and Delsante, 2001). The airflow rates generated by the combined natural ventilation with opposing wind show multiple solutions, instability and hysteresis. These phenomena mean it is difficult to decide on a definite design solution. Andersen (2007) analysed the phenomena and concluded that a solution could be obtained, provided that difference between the indoor and outdoor temperature was known at the start.

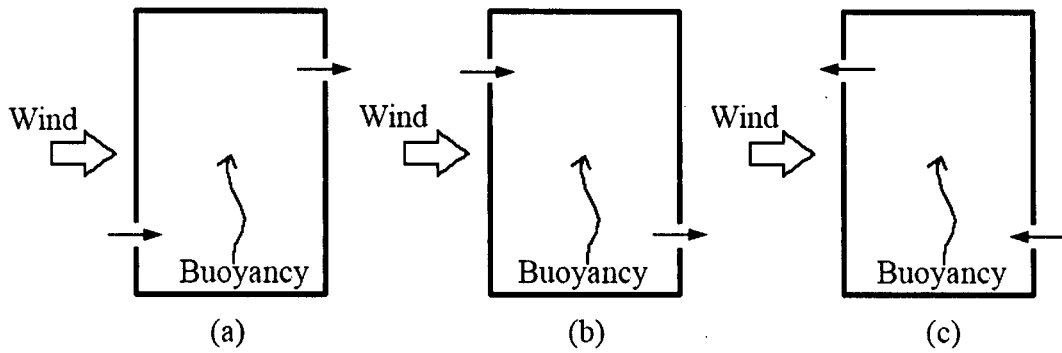


Figure 2.3 Schematic of airflow driven by the combined wind and buoyancy forces: (a) assisting wind, (b) opposing wind with downward flow, (c) opposing wind with upward flow.

The pressure acting on an opening for natural ventilation is the pressure difference (ΔP) between the total pressure (P_t) and the internal pressure (P_i). The total pressure (P_t) is expressed as Equation 2.3. The internal pressure (P_i) which responds to external pressure is dependent upon the external pressure distribution, opening size and building itself (Hee et al., 2007), but in a nominally sealed building it is smaller in magnitude than the external pressure on the building surface. Karava et al. (2006) found that the internal pressure coefficient is not uniform in a building with cross-ventilation when the opening area is larger than 10% of the wall, and that the average internal pressure should be considered for inflow calculation.

$$P_t = P_w + P_b \quad (2.3)$$

2.1.2 Calculation methods

During the design stages, the performance of natural ventilation needs to be evaluated by the relevant parameters. Both airflow rate and air velocity are usually used in this process. The airflow rate is the fresh air exchange rate between the inside and outside of buildings, so it is employed to assess the indoor air quality, or thermal comfort. Air speed is responsible for the heat exchange between the human body and environment. It usually indicates the indoor thermal comfort. Both parameters have their individual calculation methods, which have advantages and disadvantages for use in natural ventilation design.

Airflow Rate

Airflow rate is one of the main parameters for evaluating the performance of a ventilation system. It can be expressed as the volumetric flow rate (ls^{-1}), per occupant air flow rate ($\text{ls}^{-1}\text{p}^{-1}$), mass flow rate (gs^{-1}) and air change rate per hour (ACH). The airflow rate manifests how well the ventilation in the space is performing, compared with regulations and standards. However, since the flow through an opening is almost proportional to the square root of the pressure difference across the opening, the total flow rate may be approximated by:

$$Q_t = C_d A \left(\frac{2|\Delta P|}{\rho} \right)^{\frac{1}{2}} \quad (2.4)$$

where Q_t is total airflow rate; C_d is discharge coefficient; A is effective opening area; ρ is air density; ΔP is pressure difference between P_t and P_i .

The airflow rate is dependent upon the outside environment as well as the building itself. Awbi (2003) points out that the airflow rate is related to four main factors: wind speed and direction, internal and external air temperatures, the position and flow characteristics of all openings, and the pressure distribution over the building for specified wind direction. The amount of ventilation required is related to air quality and the thermal comfort standard. An individual requires about 7.5 ls^{-1} for respiration based on the rate of CO_2 generated by person at an active level (Lin and Deng, 2003), while typical air changes needed for thermal comfort require at least ten times this amount (Lidden, 1999).

To estimate the airflow rate, three types of method exist: empirical models, airflow network models and CFD models. Empirical models are experimental methods to estimate airflow rates, which include the British Standard method (1991), and the ASHRAE method (2001). The British Standard method assumes two-directional flow through a building and ignores all internal partitions; the ASHRAE method considers that the values of the wind coefficient are determined by shielding class and house height. Both methods use the formulae to calculate ventilation in single-sided and cross ventilation under the ideal conditions. Knowledge of the total effective leakage area of the building and the values of some empirical constants derived from a database of air infiltration measurements are a fundamental source of data. Empirical models are fast and convenient for designers, but these methods

cannot evaluate the ventilation rate of building in the complex environment, because their abstract conditions can cause low accuracy in results.

Airflow network models use flow equations to express the pressure difference acting on the flow paths, which interconnect the zones. Each zone can represent one or several rooms, assuming that the air in the zone is under homogeneous conditions. As these models represent the closest approximations to the true system of ventilation (Liddament, 1996), they are widely applied to the calculation of the airflow rate in complex buildings. However, these models are limited to the high space, in which the temperature difference between the upper and lower levels is distinct. In addition, their performance is determined by the accuracy of defining the wind pressure coefficient around external surfaces, for which one has to resort to using the wind tunnel or CFD modelling.

CFD modelling is a numerical method used to calculate air velocity, air temperature, pressure distribution and so on in the flow field, based on solving a set of partial differential equations for the conservation of mass, energy and momentum. CFD has been used to calculate the airflow rate (Li and Mak, 2007; Su et al., 2008). However, the CFD method is limited to modelling the simple building, due to computational resources and boundary conditions. For the complex building, especially at the design stage, it may be appropriate for the calculation of airflow rates in the building.

Three types of models have been used for different purposes. The empirical model is suitable for the simple building at the early design stage, because the airflow in the simple building is relatively simple and the model can obtain the result quickly. The airflow network model, especially the multizone model, is suitable for the complex building at the design stage, although it is not accurate in each zone because of its assumptions about the uniform zone. CFD is appropriate for the single large space due to its advantages on stratification compared with other methods, but the complicated boundary conditions and near wall grids make it impractical for the multizone building at the design stage. Asfour and Gadi (2007) compared the airflow rate predicted by the airflow network model and CFD model, and found that their discrepancy was less than 12%. This implies that the network model may have much more potential for applying in practice.

Air velocity

Air velocity is one of six factors affecting thermal comfort. The others are air temperature, mean radiant temperature, relative humidity, clothing and the activity of the occupant. Air velocity can modify the heat and mass exchanges around the human body by increasing the body's convective and evaporative heat loss rate. Air speed can maintain a naturally ventilated space about 2°C warmer than the air-conditioning space (Allard, 1998). However, excessive velocity can lead to draught. If above the recommended indoor air velocity of 0.8m/s, the paper on the table may be blown away.

Air velocity can be acquired from the empirical models, wind tunnel and CFD combined. Melaragno (1982) set up the tabulated data to calculate indoor air velocities. Ernest et al. (1991) presented an empirical correlation method to predict wind-induced indoor air velocity by the external wind pressure. Based on wind tunnel experiment data, Givoni (1998) proposed a method for estimating the average velocity inside a room. CFD is the most sophisticated tool for predicting air velocity indoors, as it can predict details of air flow within the domain being examined.

Comparing the methods used for calculating the airflow rate and air velocity, both can be acquired from empirical or correlation, scale model experiments and CFD. All the methods have advantages and disadvantages. Empirical or correlation methods based on the extensive experiments are quick, but not suitable for the complicated multizone building and environment. Scale model experiments are the most accurate but they are expensive and time-consuming. CFD is sophisticated, but the boundary condition and computational resource are restricted.

2.2 Natural Ventilation Design

2.2.1 Standards

Natural ventilation has mainly three functions on health, thermal comfort and cooling. Natural ventilation is a strategy for achieving acceptable indoor air quality, based on the supply of fresh air to a space and dilution of odours, and the limit to the concentration of carbon dioxide and airborne pollutants. The quantity of ventilation is determined by the amount and the nature of the domain pollutant source in a space.

Natural ventilation can also be used to keep occupants' thermal comfort. The suitable air movement by the air convection can maintain the human body a heat balance. Natural ventilation for cooling is generated by the exchange of cool fresh air outside and warm air inside.

One of the main functions of ventilation is for health, which is usually expressed by the indoor air quality (IAQ). Building regulation Part F (ODPM, 2006) classifies three ventilation strategies for adequate ventilation for health: extract ventilation, whole building ventilation and purge ventilation. Extract ventilation is used to minimise the water vapour and minimise the chance of pollutants spreading to other rooms. Whole building ventilation is to provide fresh air to the building and remove pollutants from the building. Purge ventilation is used to remove occasional high concentrations of pollutants and to improve thermal comfort or reduce overheating in summer. These types of ventilation can be accomplished by natural ventilation.

The international standards have various opinions on IAQ. Table 2.1 compares the ventilation rate for IAQ in dwellings and office buildings by the standards of CIBSE (2003) and ASHRAE (2005). The required ventilation rate for CIBSE is higher than ASHRAE. The reason is that the former is a rate for adequate ventilation, whilst the latter is the minimal requirement for health. Both standards are sensible, but they cannot show to what extent ventilation rates can be achieved by natural ventilation.

Table 2.1 Ventilation rate of buildings (rooms) for indoor air quality (CIBSE, 2003; ASHRAE, 2005)

Building / rooms		Ventilation rate	
		CIBSE	ASHRAE
Dwelling	Bathrooms	15ls ⁻¹	>2ACH
	Bedrooms	0.4 -1 ACH	3.5ls ⁻¹ per person
	Kitchen	60 ls ⁻¹	>5ACH
	Living rooms	0.4 -1 ACH	3.5ls ⁻¹ per person
	Toilet	> 5 ACH	>2ACH
Office	General	10 ls ⁻¹ per person	3.5 ls ⁻¹ per person
	Opening-plan	10 ls ⁻¹ per person	3.5 ls ⁻¹ per person

The categories of IAQ can clearly manifest the level of ventilation rate. Ward (2008) classified three categories of ventilation rate for IAQ according to the perceived air quality and the quantity of air supplied to a space (see Table 2.2). Assuming the area of the space is known, the ventilation for health can be represented by ls⁻¹m⁻² during the prediction of natural ventilation.

Table 2.2 Categories of ventilation rate for health (Ward, 2008)

Quality level (Category)	Perceived air quality		Required ventilation rate (ls^{-1} per person)
	% dissatisfied	decipol	
A	<10	<0.6	>16
B	10-20	0.6-1.4	7-16
C	>20	1.4	<7

For the thermal comfort standard in the naturally ventilated building, it is suggested that the adaptive comfort standard (ACS) by de Dear and Barger (2002) should be used. This standard complements thermal sensations, satisfaction and acceptability with the traditional method, which concerns four environmental factors (temperature, thermal radiation, humidity and air speed) and two personal factors (activity and clothing). This model has substituted Fanger's PMV method for natural ventilation study (ASHRAE, 2005). The adapted temperature in the naturally ventilated building for occupants is higher than predicted by the PMV model. Increasing indoor air speed can offset a higher temperature in summer. An air speed of about 0.25ms^{-1} is sufficient to give a cooling effect equivalent to a 1K reduction in the dry resultant temperature (Dry resultant temperature = $0.5 \times (\text{air temp.} + \text{mean radiant temp.})$), when indoor air speed is 0.1ms^{-1}). However, air speed is difficult to predict in natural ventilation design, so another approach to evaluate natural ventilation and thermal comfort is by means of the ventilation rate. In Table 2.3, Wills et al. (1995) state the required ventilation rates for the indoor environment.

Table 2.3 Required ventilation rate for the indoor environment (Wills et al, 1995)

Requirement	Air change rate (ACH)	Ventilation rate ($\text{ls}^{-1}\text{m}^{-2}$)
Health	0.5 to 1	0.4 to 0.8
Comfort	1 to 5	0.8 to 4
Cooling	5 to 30	4 to 25

The potential for natural ventilation in this study can be represented by the comparison of the natural ventilation rate and the required ventilation rate for the indoor environment, or the ratio of the natural ventilation rate to the required ventilation rate. Although natural ventilation potential has been expressed by many kinds of parameters, such as indoor air velocity (Su, 2003), degree days (Guiaus and Allard, 2005) pressure difference Pascal hours (PDPH) (Yang et al., 2005), these parameters are not suitable at the design stage, because indoor air velocity is very changeable, and degree days are not available to describe the difference between the building zones, and the PDPH method is too rough for the building design. The

parameter of ventilation rates is usually applied in the building design. Therefore, ventilation rates were employed in the study of the potential for natural ventilation.

The standards of ventilation are performance-based, and based on guidance. They usually answer what level of ventilation is adequate, but they cannot guide how to achieve them in building design. Karava et al. (2006) point out that the standards or codes should probably specify the window type, location on the façade and appropriate method to calculate the required airflow rate when natural ventilation is used.

2.2.2 Design strategies

Wind dominated ventilation strategies include single-side ventilation, cross ventilation, the ground floor ventilation and the wind induced top down ventilation. CIBSE (2005) provided guidance on these strategies. For example, for single side ventilation, the depth of the room is less than twice of the floor-to-ceiling height; for cross ventilation, the depth of the room is less than 5 times the floor-to-ceiling height. However, the crucial point for these kinds of strategies is to know the wind pressure difference around the inlet and outlet. These rules of thumb may be suitable for a building in the opening or lower building density area. In the urban environment, these strategies are not reliable, because the wind pressures around the building are significantly affected by the surrounding buildings. The top-down strategy (Gage et al., 2001) in the urban environment is restricted by wind pressure on the roof and the walls and the direction of the wind flow. Wind dominated ventilation strategies in the urban environment should be predicted prior to the decision of such strategies.

Buoyancy dominated ventilation strategies include chimney ventilation, atrium ventilation, double-skin façade ventilation and night ventilation. The air temperature difference between the inside and outside and the vertical distance between the openings determine the potential of the buoyancy force. Care should be taken over the position and form of the outlet, which is better situated in the larger wind suction zone. In addition, the outlet should be at a height at least half of one story above the ceiling of the top floor. In the case that the internal temperature is higher than outside, the outside warm air will pour into the building. The solution is to increase the internal air temperature by a solar radiation or using a fan. As a consequence, increasing the height of the opening on the roof is one of the strategies.

2.2.3 Problems and solutions

Natural ventilation design is a systemic process, since it is dependent on the climate, building surrounding and building itself and so on. There are inevitable problems during the design process due to the complicated mechanism of natural ventilation and its limited solutions. Heiselberg (2004) divided the procedure into four phases: the conceptual design stage, the basic design stage, the detailed design and the design evaluation. However, this classification ignores the preliminary design stage, at which design requirements and analysis investigations are necessary. So the process of natural ventilation design can be classified as having four stages: preliminary design, conceptual design, building design and design evaluation. Every design stage has its problems as well as tasks.

Natural ventilation design task and problems

The natural ventilation design task at the preliminary design stage is to evaluate the potential for natural ventilation of the region in the macro scale. The objects of the evaluation include the climate and the region. The climate determines the ventilation rate requirement of the building for heating and cooling. Axley and Emmerich (2002) proposed a method to evaluate the climate suitability by directly ventilated cooling and night cooling to offset the heat balance point of indoor and outdoor temperature. Ghiaus and Allard (2006) put forward a method to evaluate the potential for natural ventilation by using Degree-days with a variable base temperature. Pressure difference Pascal Hours (PDPH) was proposed as a method for evaluating the potential for natural ventilation in four cities in China (Yang et al., 2005), based on the comparison of the effective pressure difference and the required pressure difference. In addition, multi-criteria evaluation was presented to choose an appropriate site in the urban area (Germano et al., 2005). It can be seen that the evaluation of natural ventilation potential at the preliminary design stage may provide the basic information of the building region and help the planners and designers to select the appropriate site, but it cannot give the potential of the building site and building itself. Nor can it give suggestions for building area planning and design, because it does not consider the effect of the surroundings on the potential for natural ventilation.

At the conceptual design stage, the main ventilation design tasks are to decide the building form and ventilation strategies. This stage is usually fulfilled by intuition, precedents, general guidelines, and rules of thumb (Emmerich et al., 2001). Although the experience is helpful, it is difficult to decide the ventilation strategies if the building and surroundings are complicated. The earlier decision would considerably affect the eventual result. Therefore, the quantitative evaluation at this stage is necessary for natural ventilation design.

At the building design stage, the main ventilation design tasks are to find out the components of the ventilation system, including the opening size and position, and the detail of the components. The quantitative method is necessary. Airflow network models are often employed to decide the details of the components, but their problem is quantifying the driving forces and accounting for accurate openings in the building's surface.

At the design evaluation stage, the main tasks are to evaluate the performance of the proposed system relative to the design requirements. This is in order to determine if the design fulfils the targets of the project. The details of the building design can input the model of network models. CFD can be used to analyse the single space, but cannot be used to analyse the whole building.

Requirements on solution

The average method for the calculation of ventilation is commonly used in ventilation studies (Etheridge and Sandberg, 1996). This is due to the fact that the perceived effects of ventilation are over periods of time, and the time-averaged flow is much easier to study than the instantaneous flow. As a consequence, natural ventilation design concerns mean wind flow characteristics with respect to prevailing wind direction and mean wind speed. Swami and Chandra (1988) claimed that the average surface pressure coefficient were adequate for low-rise buildings. However, the average surface data is too rough to express the distribution of wind pressure. In the urban environment, a surface with the same average pressure data may have a different pressure distribution, which would affect the choice of positions of openings.

The tolerance error of natural ventilation design is larger than in other engineering sectors. Wind environment engineering is concerned with the general wind characteristics, such as mean wind speed, mean pressure and prevailing wind, while structural engineering is concerned with the extreme wind speed and peak pressure, which can cause large scale destruction.

The solution of ventilation requires different building details according to the design stages. At the early design stage, the building is a rough concept. The inside zone is not clear, so building would possibly be set as one zone. The flow path, building orientation, building forms could be taken into account. At the building design stage, the building configuration is determined, and this can provide the details for natural ventilation, including opening size and the shape of the windows. No matter what the design stage, natural ventilation should always consider the ventilation combined wind and buoyancy forces.

The average winter, the average summer and the hottest days can be used to describe the climate conditions. The outside temperature can be taken as the isothermal condition (Etheridge and Sandberg, 1996). Natural ventilation design has to consider the surroundings no matter what the design stage, as natural ventilation in the urban environment is affected by the wind environment and the surroundings.

The numerical simulation method is the most appropriate approach to study natural ventilation potential in the urban environment at the design stage. This is because it is much more flexible in modelling and accurate in generating mean data. It is also economical, compared with other methods. In order to improve its accuracy and extend its application, it is necessary to review its fundamental theory and applications in the urban environment.

2.3 Natural Ventilation and Urban Environments

2.3.1 Characteristics of the urban atmospheric boundary layer

The atmospheric boundary layer (ABL) is the lowest portion of the atmosphere which is directly affected by the earth's surface. Gradient wind speed is free from the earth's friction at the gradient height. Below the gradient height, the surface wind is affected by the earth's surface roughness. This layer is usually taken as the neutral

boundary layer, in which the heat flux is taken as zero. The atmospheric boundary layer can be simulated and is considered in building engineering (Simiu and Scanlan, 1986).

Urban atmospheric boundary layer

The characteristics of the urban atmospheric boundary layer is determined by the urban roughness length (Z_0), which is affected by urban structure, topography and building configuration. Generally, the wind speed is reduced from a maximum value at the top of the boundary layer to zero at the ground, which is caused by the friction drag of the surface and the protruding obstacles in the air flow. These retarding forces are transmitted through Reynolds stress through the boundary layer (ESDU, 1985).

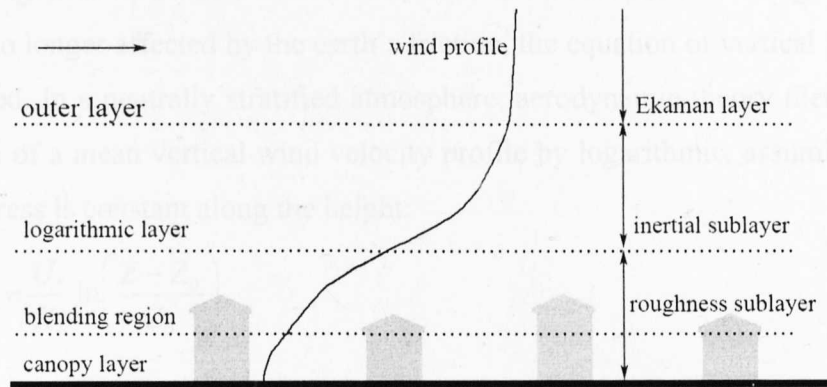


Figure 2.4 Urban atmospheric boundary layer profile

The urban area covered with various buildings and irregular spacing causes the non-uniformity flow field in the low part of the atmospheric boundary layer. The boundary layer can be divided into the outer layer and the inner layer (see Figure 2.4). In the outer layer, called the Ekman layer, the flow is dominated by diffusion, its effects, and the Coriolis force. The inner layer includes the roughness sublayer (RSL) and the inertial sublayer (ISL). Only the constant flux can be observed in ISL. In the urban area, the urban canopy sublayer is the layer below the average building height. The roughness sublayer is a non-equilibrium transition layer that means the mean flow is affected by the buildings, and is non-homogeneous and three-dimensional.

homogeneous and three-dimensional. The Monin-Obukhov similarity theory¹ is invalid within RSL. Turbulent shear stress from near zero inside the urban canopy increases up to a maximum value, which is typically observed at about twice the average building height (Kastner-klein and Rotach, 2004). This phenomenon has been observed by full scale and wind tunnel tests by Jimenez (2004) suggested that the ratio of boundary layer thickness to roughness height has to be larger than 40 before similarity laws can be expected.

Urban Wind Mean Velocity Profile

Log Law and Power Law

The atmospheric boundary layer consists of gradient wind and surface wind. The surface roughness is the main factor that affects the wind speed. As the gradient wind speed is no longer affected by the earth's friction, the equation of vertical wind speed is proposed. In a neutrally stratified atmosphere, aerodynamic theory then permits a derivation of a mean vertical wind velocity profile by logarithmic, assuming that the surface stress is constant along the height:

$$U = \frac{U_*}{K_v} \ln\left(\frac{Z - Z_0}{Z_0}\right) \quad (2.5)$$

where κ is Von Karman's constant, the ratio of friction velocity to the normalized mean shear $u(z) \cdot du/dz$ is constant, ~ 0.4 (Hogstrom, 1996), and Z is the height above ground, and Z_d is the zero plane displacement. An approximate value of Z_d is given by ESDU (1982):

$$Z_d = \bar{H} - Z_0 \left[4.3(1 - \lambda) + 10(\exp(-90\lambda^{1.5})) \right] \quad (2.6)$$

where \bar{H} is the average height of the surrounding buildings and λ is plan area density. For most application, the friction velocity U_* is simplified as:

$$U_* = 2.5U_{ref} / \ln(H_{ref}/Z_0) \quad (2.7)$$

¹ Monin-Obukhov similarity theory: It hypothesizes that the mean gradients and turbulence characteristics are dependent only on the height, while shear stress is constant in the boundary layer.

where U_{ref} is the reference velocity at reference height (H_{ref}); the roughness length (Z_0) is an empirical data, which is classified as 12 roughness classes varying from the sea surface to a regular building town (Wieringa, 1993). Z_0 values for dense low buildings in suburban area, a regular-built large town are 0.4-0.7m, and 0.7- 1.5m respectively. A theoretical approach for estimating Z_0 has been suggested by Lettau (1969) using the similarity principle:

$$Z_0 = \frac{\bar{H}\alpha}{2A} \quad (2.8)$$

where \bar{H} is the height of the average height of obstacles, α is silhouette area encountered and A is the area covered by obstacles. The observed values only approximate the theoretical model, which has been used to simulate urban conditions for wind tunnel experiments. There are also other basic methods to estimate the roughness length and displacement height, such as the MacDonald et al.'s (1998) method and the GIS (geographic information systems) method.

In other representations of the vertical wind profile, a simple power law is often used in engineering literature:

$$U = U_g \left(\frac{Z}{Z_g} \right)^\alpha \quad (2.9)$$

where α is an exponent representing all the friction factors, which is dependent on the terrain characteristics. For open country is 0.14, suburban settlement is 0.22 and inner city is 0.40, and Z_g (gradient wind level) is 270m, 370m and 460m respectively (ASHRAE, 2005).

Comparing logarithmic law with power law, Counihan (1975) insisted that the logarithmic law represented the lower 30-50m of the rural boundary layer very well, while power law was better to fit the higher range after the comprehensive view of full scale atmospheric data. Simiu and Scanlan (1986) agreed with this, and went on to say that the logarithmic law was regarded as a superior representation of wind profile by meteorologists in the lower atmosphere. The ratio of the boundary layer thickness to the roughness height determines whether or not the logarithmic layer survives, according to (Jimenez, 2004). He claimed that when the ratio was less than

40, the effects of the roughness extend across the boundary layer. However, both log law and power law do not describe the velocity profile in and around the buildings in urban areas. The roughness length generated by log law cannot describe the flow between the roughness elements, which is required for modelling wind pressure around the buildings.

Urban canopy profile

Recently, many researchers tried to establish methods to model the canopy flow. As the extrapolation of log law and power law down to the roughness sublayer cannot be accepted when there are problems in this sublayer, MacDonald (2000) proposed a method to describe the wind profile in the canopy sublayer according to the idea from the vegetation model. He divided the roughness sublayer into three regions and described them through a series of wind tunnel experiments. The profile in the canopy sublayer model was an exponential profile, in which the exponent was dependent on the ratio of front area density. Between UCL and ISL, the velocity profile must reduce to the semi-logarithmic profile above the wake diffusion height. The depth of ISL lay roughly between $2H$ and 0.15δ , where δ was the boundary layer height. Belcher et al. (2003) developed a theoretical model to adjust the spatially averaged time-mean flow in the canopy of the roughness elements.

However, these proposed methods still face problems. For example, they can only be applied to the building area if its density is lower than 0.3. The flow in the urban canopy layer is a complicated turbulence, which is impossible to express by the five proposed positions (Castro et al., 2006). In addition, the log law profile may be used above the ISL. The profile of the outer sub-layer, starting from the ISL up to the gradient height, is more suitably expressed by power law (Plate, 1999).

Turbulence Profile

As a turbulent flow, wind speed varies randomly with time and space. Turbulence intensity is a key factor to describing the atmosphere boundary layer for simulation. The longitudinal turbulence intensity is defined as:

$$I = \frac{u'}{u} \quad (2.10).$$

by the friction velocity, u'/U_* , v'/U_* , w'/U_* should be constant, where u' , v' , w' are components of fluctuating velocity along x, y and z respectively.

Turbulence intensity can also be described by turbulence kinetic energy (TKE) and turbulence dissipation rate. Turbulence kinetic energy represents the mean kinetic energy per unit mass associated with eddies in turbulent flow. It is expressed as Equation 2.11:

$$E = \frac{1}{2}(u'^2 + v'^2 + w'^2) \tag{2.11}$$

The turbulence profile has been studied by many researchers. The shear stress in the neutral ABL drops with the increase of height, so the turbulence kinetic energy has a function depending upon the height. The maximum TKE is near the roughness height (Rao and Nappo, 1998), while TKE has a maximum value near the ground and decreases with increasing height (Duynderke, 1988). Duynderke also observed that the stable ABL has a similar profile to the neutral ABL. Table 2.4 lists the different turbulence kinetic energy profiles.

Table 2.4 Turbulence kinetic energy profile

Authors	Turbulence kinetic energy profile	Comments
ESDU (1985)	$0.5U_*^2(1-Z/\delta)^2$	In practice, the co-variances uv and vw are small and can be ignored.
Rao & Nappo (1998)	$6(1-Z/\delta)^2$	Stable stratified boundary layer.
Hamlyn & Britter (2005)	$3.9U_*^2(1-Z/\delta)$	3.9 is derived from the near ground value of TKE in the experiment.

From the different expression of TKE by the above authors, it can be seen that the TKE decreases with height, and the maximum TKE is near the ground. In general, the TKE can be expressed as:

$$E = E_{\max} (1 - Z / \delta)^\alpha \tag{2.12}$$

E_{\max} is dependent upon the TKE near the ground. The neutral boundary layer height δ is usually dependent upon the friction velocity. The neutral boundary layer height is larger than the observed data. ESDU (1982) gives the experimental function to

estimate the boundary layer height ($\delta=U^*/6f$), where f is Coriolis parameter. According to the study by Duynkerke (1988), this data is obviously lower than the ideal neutral boundary layer, as the observational data are strongly influenced by stratification.

After the study of wind profile on atmospheric boundary layer, it can be concluded that the TKE profile is not constant, but is related to the height and the E_{max} near the ground. However, E_{max} is dependent upon the roughness length and friction velocity.

Turbulence in urban canopy layer

Reynolds stress has been found to increase with height from small values at Z_d (zero plane displacement) in the lower part of the roughness sublayer up to a virtually constant value (Rotach, 1999). Evidence for similar behaviours of Reynolds stress under observation include the investigations in Basel (Feigenwinter et al., 1999), and in Zurich (Rotach, 1993). The evidence for Reynolds stress varying with height in a wind tunnel came from a study conducted by Rafailidis (1997). This study shows that the Reynolds stress in the vicinity of the roof level is particularly dependent on the geometry of the roofs, with much larger vertical variability for slanted roofs than for flat ones. This work on Reynolds stress shows that a possible parameterization for the vertical characteristics of Reynolds stress has to include some information on the urban morphology. A function of local scaling variables can be derived to describe the data. Above roof level, the local scaling concept can be used to show that the mean velocity gradient is smaller than what would be predicted by a constant flux assumption. The maximum flux at the level of transition from the RSL to the ISL is appropriate to estimate the friction velocity U^* (Rotach, 1999).

The height of the maximum flux has been studied by many researchers. Oikawa and Meng (1995) observed the peak value of Reynolds stress at a level 1.5 times of the average building height when looked at the outer edge of a suburban area. Feigenwinter et al. (1999) measured values that were almost constant between the second and third level ($Z/\bar{H} = 1.5, 2.1, 3.2$). Christen et al. (2002) argued that turbulent shear stress and turbulent kinetic energy peaked just above roof-level. Kastner-Klein & Rotach (2004) employed a wind tunnel to test the central part of Nantes, France, a real world region of about 400m in diameter. The influence of

building pattern irregularities on the mean flow, shear stress, and turbulence kinetic energy distributions are clearly visible up to level $Z = 3H_b$. The shear stress and turbulence kinetic energy profile corresponding to both flow types in many cases show pronounced maxima in the region just above the average roof level (between H_r and $1.5H_b$).

From the above analyses, the current commonly used method from Richards and Hoxey (1993) is not appropriate to describe the urban boundary layer, as they described the wind velocity profile by log law, and assumed the turbulence kinetic energy was constant along the boundary layer. The effects of urban roughness on the wind profile should also be considered.

2.3.2 Airflow around buildings

Wind around the isolated building

Wind flow around a building is a considerably complex phenomenon. When impinging on the building, the flow generates curved mean streamlines, large adverse pressure gradients, sharp velocity discontinuities, flow separations and reattachments, cavity regions, recirculation zones, and strongly inhomogeneous turbulence, all as shown in Figure 2.5 (Murakami, 1993). This makes the prediction of wind pressure on the building facades impossible by the empirical data as well as catalogued algorithms, because there is a great variety of a mean and turbulent flow regime resulting from the flow within and over an arbitrary arrangement of non-uniform obstacles.

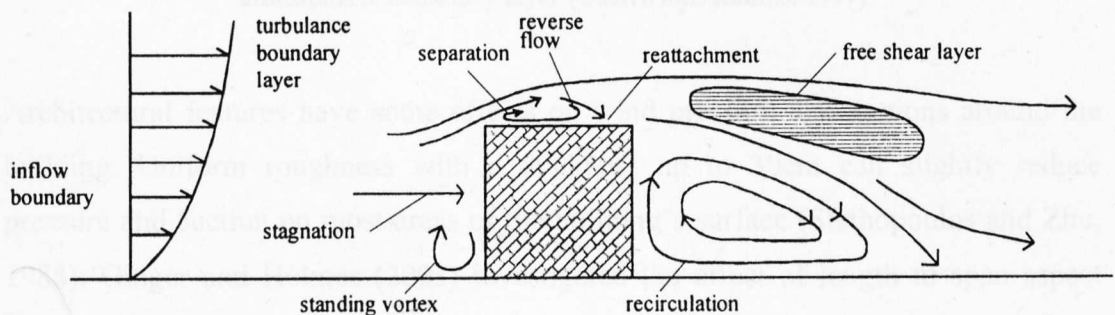


Figure 2.5 Wind field around the building in the atmospheric boundary layer (Murakami, 1993)

The windward pressure coefficient distribution around the isolated building has certain notable characteristics. From the boundary layer wind tunnel experiment on

the isolated cube (see Figure 2.6), it can be seen that the maximum data (stagnation point) is at about 0.8 the building height on the windward surface. It can also be seen that the lateral, roof and leeward surfaces experience suction.

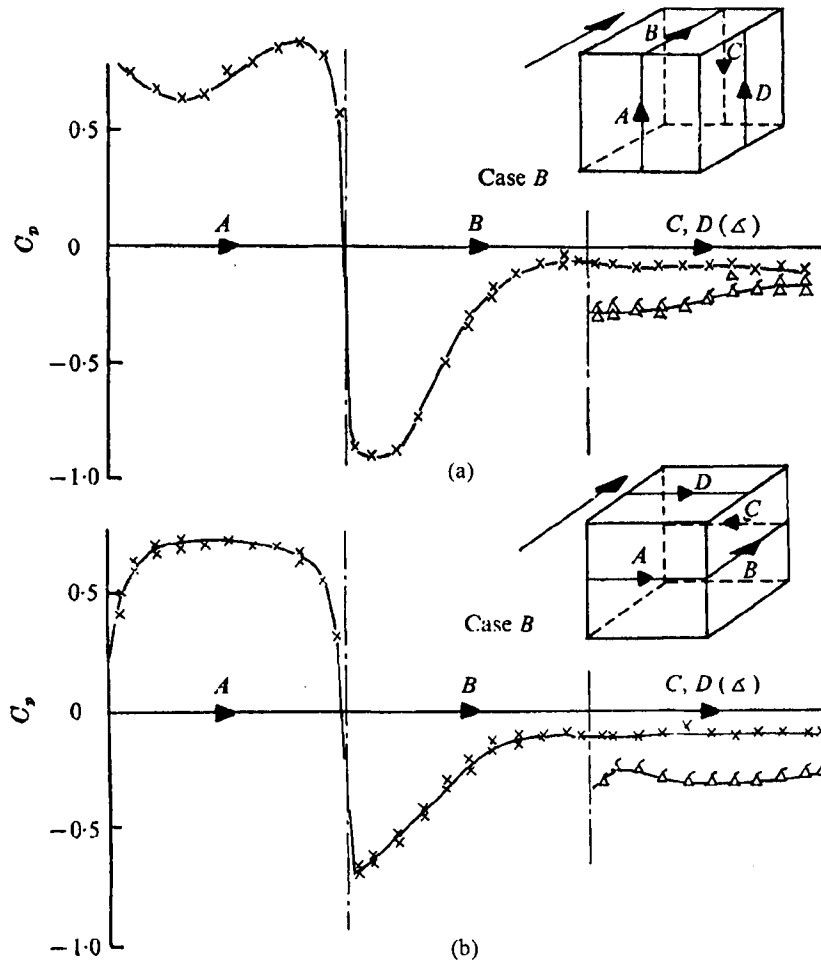


Figure 2.6 Wind pressure coefficients around a cube when normal to incident flow in the atmospheric boundary layer (Castro and Robins, 1977)

Architectural features have some effects on wind pressure distributions around the building. Uniform roughness with a thickness up to 30cm can slightly reduce pressure and suction on most areas of the building's surface (Stathopoulos and Zhu, 1988). Ginger and Holmes (2003) investigated the effect of length to span aspect ratio of a long low-rise building with a steep pitch roof on the external wind pressure distribution. Their result shows that the negative pressure coefficient of the leeward roof and wall significantly rises with the increase of length to span aspect ratio. However, the pressure on the building with the lower roof pitch and curved roof shape is less affected by the extension of the length. The effects of roof overhang

when the wind incidence is normal to gable wall was investigated by Wiik and Hansen (1997).

They concluded that the long roof overhang would change the pressure distribution on the low standing wall with an increase at the upper part of the wall, compared to a roof with no overhang. The odd-geometrical building has a relatively smaller wind pressure coefficients than that of the prismatic-shaped building (Suh et al., 1997). Suh et al. also point out that a larger opening on the surface can lead to the average pressure coefficient dropping by 25%, even 50% for the leeward surface, compared with the prismatic-shaped building. The above studies maintain that the wind pressure coefficients are dependent upon the geometry of the building. Besides the building itself, wind pressures around the building are also affected by the surroundings.

Wind around the building with surroundings

Wind in the urban environment can be divided into three flow regimes: the isolated roughness flow regime, the wake interference flow regime and the skimming flow regime (Lee et al., 1980) (see Figure 2.7). The isolated roughness flow regime means the flow pattern that appears around the building is almost same as the isolated building when the space between the buildings is wide. The wake interference flow regime indicates that the flow pattern is interfered with by the downstream building when the space between the buildings is reduced. When the space is even smaller, the skimming flow regime occurs with a stable circulatory vortex in the canyon, since the bulk of the flow does not enter into the canyon.

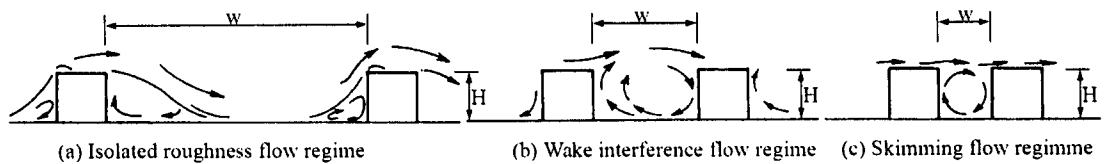


Figure 2.7 Schematic of three flow regimes (lee et al, 1980)

The flow regimes depend upon the critical combination of the ratio of height to width of canyon (H/W) and the ratio of height to length of canyon (H/L). Oke (1988) has proposed threshold lines that divide the flow into three flow regimes as a function of the two ratios. The isolated roughness flow regime happens at the conditions of

$H/W < 0.4$ for cubic building and $H/W < 0.3$ for row buildings. At closer spacing ($H/W < 0.7$ for cubic buildings and $H/W < 0.65$ for row buildings), the wake interference flow regime appears. When the spacing is even closer than that of wake interference flow regime, the skimming flow regime occurs (see Figure 2.8).

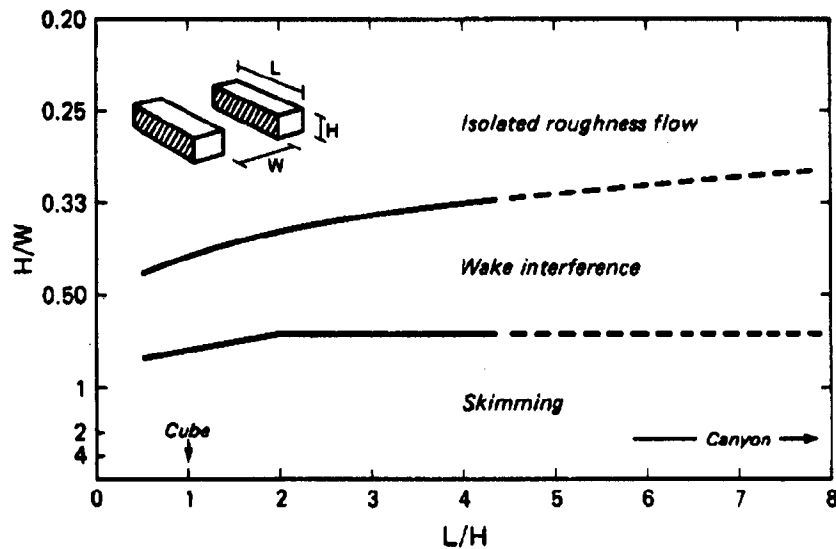


Figure 2.8 Threshold lines dividing flow into three flow regimes as function of the building (L/H) and canyon (W/H) geometries (Oke, 1988).

Wind pressure distribution around the building in the urban environment is affected by many factors. Lee et al. (1980) investigated wind pressure acting on a group of low-rise buildings by the boundary layer wind tunnel. They point out that the array pattern, frontal aspect ratio, side aspect ratio; fetch length and wind direction may all influence the wind pressure difference. The urban roughness length and the spacing between buildings can also affect pressure coefficients (Chang and Meroney, 2003).

Wind pressure coefficient distributions have certain characteristics in the urban environment. Cheng et al. (2007) investigated the flow around the cube in the urban-type area at the normal pattern (A) and staggered pattern (S). Their results showed that surroundings with a density of 6.25% (isolated roughness flow regime) had little effect on the pressure coefficient distribution, and the pressure coefficient distribution of the building was similar to that of the isolated building (see Figure 2.9). With the increase in building density, the maximum pressure coefficient difference moved near the top edge. Wind induced ventilation is reduced by high building density, but may still exist in the upper levels of buildings.

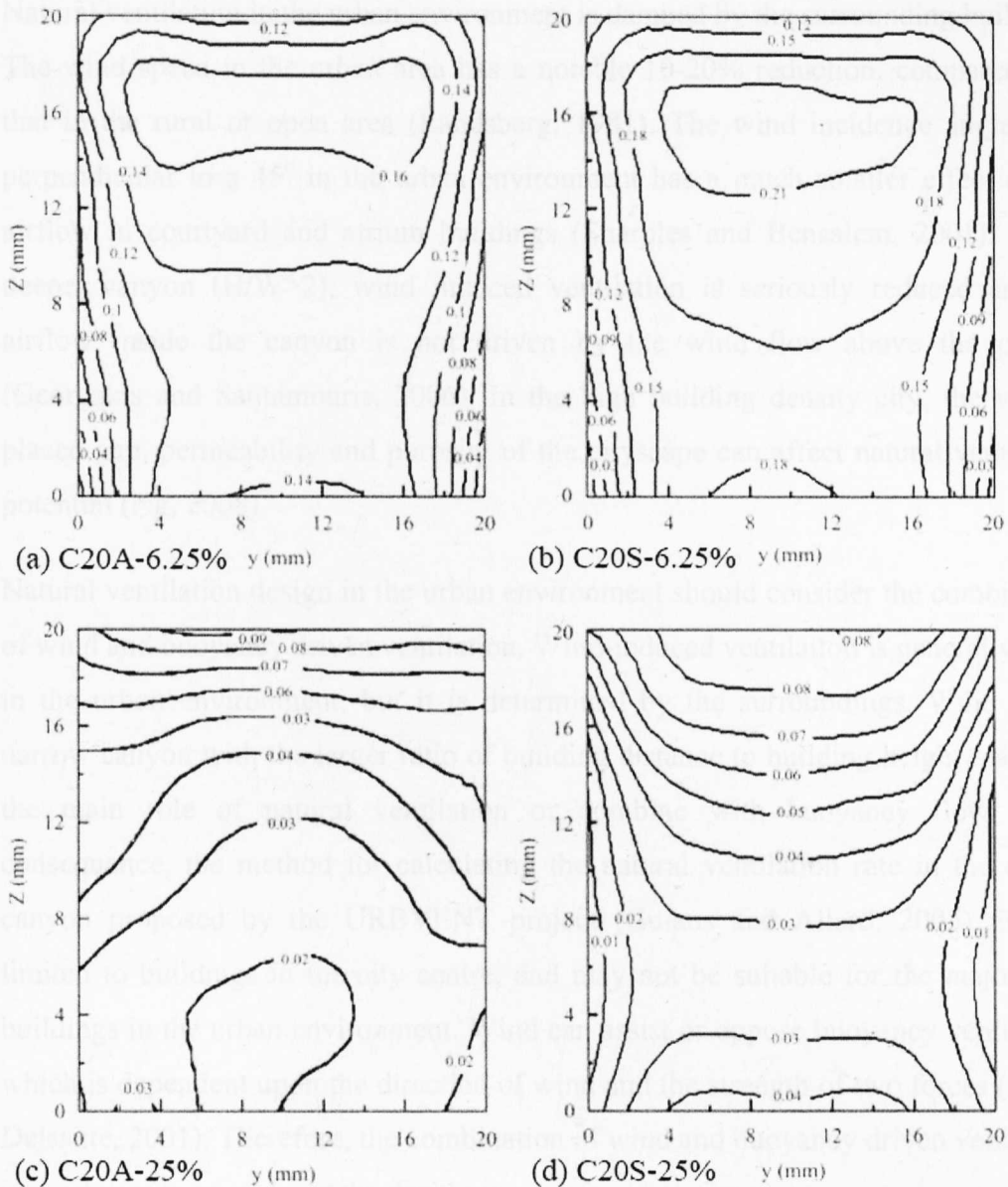


Figure 2.9 Pressure coefficient difference between front and back surfaces on the models within the different density roughness arrays at a free stream velocity of 10ms^{-1} : A- normal pattern, S- staggered pattern. (Cheng et al, 2007)

2.3.3 Natural ventilation in the urban environment

Wind pressure coefficients around the building in the urban environment are significantly affected by the building density, building space, building height and length and building layout. Compared with the isolated building, the building in the urban environment may have a low potential for wind induced ventilation.

Some characteristics

Natural ventilation in the urban environment is damped by the surrounding buildings. The wind speed in the urban area has a notable 10-20% reduction, compared with that in the rural or open area (Landsberg, 1981). The wind incidence angle from perpendicular to a 45° in the urban environment has a much smaller effect on the airflow in courtyard and atrium buildings (Sharples and Bensalem, 2001). In the deeper canyon ($H/W > 2$), wind induced ventilation is seriously reduced and the airflow inside the canyon is not driven by the wind flow above the canyon (Georgakis and Santamouris, 2006). In the high building density city, the vertical placed gap, permeability and porosity of the cityscape can affect natural ventilation potential (Ng, 2008).

Natural ventilation design in the urban environment should consider the combination of wind and buoyancy driven ventilation. Wind-induced ventilation is generally weak in the urban environment, but it is determined by the surroundings. Wind in the narrow canyon with the larger ratio of building distance to building height may play the main role of natural ventilation or combine with buoyancy flow. As a consequence, the method for calculating the natural ventilation rate in the deeper canyon proposed by the URBVENT project (Guiaus and Allard, 2005) may be limited to buildings in the city centre, and may not be suitable for the majority of buildings in the urban environment. Wind can assist or oppose buoyancy ventilation, which is dependent upon the direction of wind and the strength of two forces (Li and Delsante, 2001). Therefore, the combination of wind and buoyancy driven ventilation is necessary to consider at the design stage.

Planning and natural ventilation

The above studies show that building density, building height and building layout can all affect the potential of natural ventilation of a building. These parameters should be considered in planning in order to maximise a building's potential for natural ventilation. As the details of the buildings at this stage are in the development process, this study cannot provide the details of building design, but the guidance for decisions is necessary.

Rough guidance for planning can provide the planners with concepts of natural ventilation. Olgyay (1963) studied wind around buildings and gave the idea of utilising natural ventilation by the orientation of the building (not necessarily

perpendicular to wind direction), surrounding to create low and high pressure zones and opening positions. Pitts (2004) summarised the strategies of planning for natural ventilation by building layouts with long parallel rows, the larger building dimensions facing prevailing winds and flat and low-pitched roofs in order to increase air pressure differentials. These guides may enlighten the planner and designers, but cannot guide them at the design stage. One main reason is that there are many parameters that can affect natural ventilation potential, such as building density, spacing, height, opening position and size, and so on. These parameters may be interactive or contractive on natural ventilation, so they are confusing for the planners and designers. Planning for natural ventilation potential in reality is restricted by other issues, such as economy and the whole environment. Lower dense planning areas are better for natural ventilation, but will cost more in terms of land, and increase transport investments. Sensibly using the potential of natural ventilation in this stage will require quantitative analysis. Meanwhile, the comprehensive consideration of the parameters which mainly affect the potential of natural ventilation may provide appropriate guidance for the policy-makers, planners and designers.

Building design and natural ventilation

Building design in the urban environment affects the performance of natural ventilation. Some characteristics of buildings can assist natural ventilation in the urban environment. A building with atrium in the urban environment has more effective natural ventilation than a building with open courtyard (Sharples and Bensalem, 2001). Bauman et al. (1988) performed a wind tunnel study on wind pressure distribution on an attached two-story building in long building rows for a range of wind directions, building spacing, and building geometries. Their test indicated that the jack roof was a potential device for natural ventilation, even if used in a small building space. The building height also determines the strategy of natural ventilation in the urban environment. For example, top to down ventilation can be used in the low or medium rise building in the urban environment (Gage et al., 2001).

However, these factors may be interactive or contractive. A quantitative study is necessary at the building design stage in order to decide the opening components, size and position of the buildings and evaluate the whole natural ventilation system.

CIBSE (2005) provided the natural ventilation design strategies, but this guidance was not for a building in the urban environment. The guidance for the potential of natural ventilation of buildings in the urban environment would benefit designers.

Methods and applications

The methods used to study natural ventilation in the urban environment include field tests, scale experiments and numerical simulation and empirical analysis (see Table 2.5). These methods can be classified as indirect and direct methods. Some indirect methods combine the external models for the wind outside the building and internal models for the airflow inside the building. The external models include wind tunnel experiments (Ng, 2008; Su, 2003), parametrical models (van Moeseke et al., 2005) and empirical models (Ward, 2003), and were employed to acquire pressure coefficients around the building in the urban environment. The internal models include airflow network models (Ng, 2008), empirical models for ventilation rate (Ward, 2008) or air speed in the room (Su, 2003). Other methods directly test ventilation rates: field tests were employed to estimate the ventilation rate of rooms by trace gas (Georgakis and Santamouris, 2006); salt bath experiments were used to test ventilation rate driven by the combined forces of wind and buoyancy in the model (Syrios and Hunt, 2007); and CFD models were applied to calculate the air speed in a room (Ayata and Yildiz, 2006).

Comparing the direct and indirect methods, the former is theoretically more accurate than the latter. However, the direct methods may be unrealistic at the design stages. Field tests are limited to the tested type of building and the period of time, so they cannot be used at the design stage. Salt bath experiments are restricted by the simple models of buildings, which can affect the accuracy of the result. CFD is a desirable method for studying natural ventilation, but its direct model for combining the external and internal in the urban environment is difficult and complicated. This is because the Reynolds number of the building is more than one order of magnitude larger than that in rooms, so that numerous grids are required (Jiang and Chen, 2001). In addition, the complicated urban environment also requires a large number of grids. Furthermore, the combination of wind and buoyancy ventilation adds to the difficulty of using the CFD model, which was only used in the single building (Allocca et al., 2003). At present, with the limited computing resources and short time available -

which is rather common in most design projects, it seems unaffordable to use direct CFD modelling.

Choosing the appropriate method is dependent upon the aims and requirements of the project. This research aims to predict the potential for natural ventilation in the urban environment for the purpose of building design. It requires modelling the characteristic of urban environments and buildings; meanwhile, it requires calculating the ventilation rate driven by the combined forces of wind and thermal buoyancy in the multi-zones of buildings. In the indirect methods, CFD is a more accurate method than the parametrical and empirical models for calculating the pressure coefficient around the building in the urban environment. CFD also avoids the expensive, time consuming and inflexible wind tunnel experiment. Airflow network models are the sensible choice for calculating the ventilation rate in multizone buildings, because it is more accurate than empirical analysis and easier to combine natural ventilation driven by wind and thermal buoyancy in the multizone building than in CFD. Coupling CFD and the airflow network model is a reasonable approach to predicting the potential for natural ventilation in the urban environment.

Table 2.5 Methods and applications in natural ventilation in the urban environment

Authors	Methods	Applications	Findings	Remarks
Georgakis and Santamouris (2006)	Field test	A deep urban canyon	The potential of natural ventilation in the deep canyon is seriously reduced	A deep canyon is the specific case in the urban environment.
Ng-E (2008)	Wind tunnel + network model	A high density city	The amount of vertically placed gaps, permeability and porosity affect the ventilation and wind environment.	The general guidelines for preliminary design stage
Su (2003)	Wind tunnel + VENT15W	A residential building area	To estimate wind driven ventilation	Buoyancy ventilation is neglected.
Syrios and Hunt (2007)	Salt bath experiment	Series types of urban canyons	Neglecting the surroundings when designing naturally-ventilated buildings may result in poor ventilation	The surroundings in the model are too simple.
Ayata and Yildiz (2006)	CFD	A new building design in the urban environment	A rectangular box with 1:1.7 dimensional ratio is an optimal choice for natural ventilation.	Buoyancy ventilation is neglected. The model is too simple.
Van Moeeske et al. (2005)	Parametrical model + TAS	A building in the urban environment	Both vertical and horizontal pressure coefficient are important for the calculation.	Limitation of urban models based on parametrical model
Ward (2003)	GIS map + empirical equations	An urban area	Building density can reduce natural ventilation potential.	The general guidelines for the pre-design stage
Germano (2007)	Multicriteria analysis + Mesoscale atmospheric modelling	An urban region	The urban area has lower natural ventilation potential than that of rural area.	Only for building site, not for building

2.4 Summary

Natural ventilation is driven by the combination of wind and buoyancy forces. For wind force, the key parameter is the wind pressure coefficients around the building. It can be acquired from a full scale test, a wind tunnel experiment, empirical analysis, parametrical modelling and CFD. The buoyancy force is dependent upon the temperature difference between external and internal, and the vertical distance between the openings. Wind can assist or oppose the buoyancy force. This is dependent on the strength of the two force and wind flow direction.

Airflow rate and air velocity in the building are mainly used to describe the ventilation of the building. Both can be calculated by empirical equations and CFD, but the airflow rate is easier and more accurate than air speed in the room to describe the ventilation of the building. In the complicated multi-zone building, Airflow network models are popular methods for calculating airflow rate. The airflow rate can be taken as an index for describing the potential of ventilation on health, thermal comfort and cooling in the building.

Natural ventilation design is a systematic process, including preliminary design, conceptual design, building design and design evaluation stages. Every stage has its own requirements and problems, but the quantitative analysis as well as qualitative study is needed from the early design stage. The quantitative method requires the data to describe the external environment and internal ventilation rate. As a consequence, generating the wind pressure coefficients around the building and ventilation rates in the room are the main tasks for this study.

In the urban atmospheric boundary layer, the wind profile is so complicated that it is difficult to describe by the empirical profiles. The commonly used method is not suitable for describing the urban boundary layer profile. The rule is that the maximum turbulence kinetic energy occurs at the roughness sublayer.

The wind around a building is a complicated phenomenon. Building features can impact wind pressure distribution around the building. In the urban environment, the building height, spacing and layout can affect the wind pressure distribution. In the urban canyon, the largest pressure coefficient is near the top edge of the windward

surface. Natural ventilation in the urban environment is significantly affected by the surrounding buildings, compared with the isolated building. Building density, spacing and height, and layout can affect the potential of natural ventilation. However, the effect of wind direction between 0 and 45 degree is not distinctive.

Coupling CFD and airflow network models is an approximate method for predicting the potential for natural ventilation design in the urban environment. It is determined by its objective and requirement. CFD can be used to acquire the wind pressure coefficients around the building in the urban environment. After inputting the pressure coefficient into the network models, this can be used to calculate the ventilation rates in the multizone building. This method is more sensible and efficient than other methods for natural ventilation design.

The guidance for planning and natural ventilation needs to develop, as the planning parameters that affect the potential of natural ventilation are so complicated that rough strategies will not do for guidance. In addition, comprehensive consideration of these parameters is required. The guidance for natural ventilation design in the urban environment also needs to improve. Natural ventilation in the urban environment is significantly affected by surroundings. It is necessary to consider the building in the urban environment instead of the isolated building to achieve the optimum natural ventilation in buildings. The quantitative study on the building in the urban environment would provide sensible guidance for the designer.

The literature on the principle of natural ventilation, natural ventilation design and natural ventilation and urban environments were reviewed. The limitations of the current understanding on natural ventilation design in the urban environment tend to express research issues as follows:

To promote a virtual urban atmospheric boundary layer wind tunnel for natural ventilation study

The pressure coefficients around the building in the urban environment are essential parameters for natural ventilation design. However, the current methods, including empirical analysis, parametrical model, wind tunnel and the general CFD, are not appropriate for measuring it. This virtual wind tunnel aims to acquire the pressure coefficient around the building in the urban environment for natural ventilation study.

Its specified requirement needs to find the appropriate boundary conditions and computational domain. It will investigate the effects of the computational domain, boundary conditions, and grid distribution on the quality of the pressure coefficient and develop systematic rules for the CFD setting for the study of natural ventilation. The investigation of turbulence models is also carried out. The conditions of setting up a virtual wind tunnel for natural ventilation study in the urban environment are developed. In addition, it is necessary to validate the result through comparison with the physical wind tunnel and other research in the similar conditions to illustrate and quantify uncertainty, understand capabilities, and develop guidelines for application and applicability.

To develop guidance of planning for natural ventilation design

The guidelines or strategies of planning for natural ventilation cannot comprehensively consider the effects of planning parameters on natural ventilation potential, so that they cannot provide guidance for the policy-makers, developers and planners. The purpose of this study is to develop the guidance of planning for natural ventilation potential. It investigates the effects of planning parameters on natural ventilation through the proposed virtual wind tunnel and airflownetwork models. Planning parameters are from the data that policy-makers, developers, designers and occupants are concerned by. The study of natural ventilation by combining wind and buoyancy forces can provide more practical guidance for optimising planning.

To develop guidance of building design for adequate natural ventilation in the urban environment

Natural ventilation design of a building in the urban environment requires quantitative study as well as qualitative study. The objective of this study is to develop guidance of natural ventilation design of buildings in the urban environment. It shows the methodology frame to predict natural ventilation potential of the building in the urban environment. The comparison of the isolated building and the building with surroundings demonstrates the effects of surrounding buildings on natural ventilation. It implies the design guidance for natural ventilation. In addition, the difference of natural ventilation potential in the various seasons implies the design strategies in the urban environment.

The three research issues set up the main objectives for the next study. The following chapter will discuss the methodology, including the fundamentals of methods, procedures, experiment settings, and the rationale for the methodology approach.

CHAPTER 3

Methodology

As the wind around a building is a complicated turbulent phenomenon, and the urban environment comprises of complex ground topography, it is difficult to predict wind forces around a building in the urban environment. Natural ventilation design in the urban environment requires a method that can calculate the external ventilation driving forces and take into consideration the effects of surrounding buildings as well as the natural ventilation rates of the building. Unfortunately, traditional methods such as empirical models, parametrical models, wind tunnel experiments and even the common CFD method, cannot meet the requirements of natural ventilation design in the urban environment. It is necessary to develop a holistic method to solve the above problems. Compared with other methods, numerical simulation is much more accurate, economical, flexible, and informational for use in the study of architectural environment design (Chen, 2004). With the rapid development of computational hardware and software, numerical simulation is a promising approach to achieving this objective. This chapter discusses a numerical methodology coupling CFD and airflow network model for natural ventilation study in the urban environment.

This chapter consists of four sections. Firstly, the fundamentals of CFD and the employed CFD code – FLUENT – are briefly introduced, focusing on the external wind environment. Next, the CFD applications in the urban environment are reviewed and the CFD settings for urban natural ventilation study are described. Thirdly, the theory of airflow network models and their applications for the calculation of ventilation rate are discussed with the demonstration of the procedures.

Finally, the rationale of the methodology is discussed, including its strength and weakness.

3.1 Fundamentals of Computational Fluid Dynamics

CFD is a numerical technique to quantitatively predict the phenomenon of fluid flow by means of computer-based simulation. The fluid flow observes the conservation laws of physics, which are defined by a set of partial differential equations for conservation of mass, momentum, and energy. So the task of CFD is to solve these governing equations, involving modelling turbulence, near wall treatment, spatial and temporal discretisation and solution. CFD has become an efficient research method with some unique advantages over other methods including physical experiments and theoretical analyses. For the building industry, CFD has been employed to analyse the external environment, such as wind load around the building and the pedestrian wind environment, and the internal environment, such as airflow velocity and temperature, heat transfer, and so on. All of CFD's strength is derived from its fundamentals.

3.1.1 Governing equations

The governing equations of wind flow in the urban environment for natural ventilation study have certain notable factors. One aspect is that wind in the urban environment can be seen as an incompressible flow with constant density, because its Mach number (the ratio of wind speed to sound speed in air) is lower than 0.3 (Anderson, 2007). Another factor is that the atmospheric boundary layer can be taken as the neutral atmospheric boundary layer, since the effect of temperature on the wind flow near the ground can be neglected (Castro, 2003). Therefore, the simulation of wind in the urban environment is based on continuity and momentum equations.

Continuity Equations

Continuity equations mean that the rate of increase of mass in the fluid element equals the net rate of flow of mass into the fluid element. The density of incompressible flow is constant and the divergence of velocity is zero. These equations can be simplified as Equation 3.1:

$$\frac{\partial u_i}{\partial x_i} = 0 \quad (3.1)$$

Where u_i is the mean velocity in the x_i direction, with $i = 1, 2,$ or 3 representing the streamwise x , spanwise y or vertical z directions respectively.

Momentum Equations

Momentum equations, also called Navier-Stoke equations, are derived from Newton's second law, which states that the rate of momentum increase of a fluid particle is equal to the sum of forces on the fluid particle. It is expressed as Equation 3.2:

$$\frac{\partial \rho u_i}{\partial t} + \text{div}(\rho u_i u) = -\frac{\partial P}{\partial x_i} + \text{div}(\mu \text{grad} u_i) + F \quad (3.2)$$

Where u stands for mean velocity, u_i is the mean velocity in the x_i direction, with $i = 1, 2,$ or 3 representing the streamwise x , spanwise y or vertical z directions respectively. P is pressure, ρ is fluid density, F denotes body forces (such as gravity, centrifugal and Coriolis forces), μ is dynamic viscosity, and t denotes time. The first left term is the instantaneous acceleration term (unsteady term), followed by the convection term; the first term in the right side is the pressure gradient term; next is the viscous dissipation term; the last term is the body force.

3.1.2 Modelling turbulence

Modelling turbulence is a necessary approach to solving the governing equations of wind flow. Although directly solving the equations by DNS (Direction Numerical Simulation) without approximate or any simplified model is theoretically possible, its rigid requirement of $Re^{9/4}$ grids spatial resolution and temporal discretisation make it restricted in theoretical research, and it is too computationally expensive and unrealistic to apply to the engineering practice (Li et al., 2006; Murakami, 1998). A feasible approach is to solve the equations indirectly with the aid of turbulence models, including RANS (Reynolds Averaged Navier-Stokes), LES (Large Eddy Simulation) and DES (Detached Eddy Simulation). The following briefly introduces their concepts and reviews the current research and applications in the wind environment.

RANS models

The random turbulence flow in RANS is decomposed into mean and instantaneous components, and all the equations are time averaged to remove the fluctuating component. Equation 3.2 can be expressed as instantaneous Navier-Stokes equations as the following Equation 3.3:

$$\frac{\partial \rho u_i}{\partial t} + \frac{\partial \rho u_i u_j}{\partial x_j} = -\frac{\partial P}{\partial x_i} + \frac{\partial}{\partial x_j} \left[\mu \left(\frac{\partial u_i}{\partial x_j} + \frac{\partial u_j}{\partial x_i} \right) - \overline{\rho u'_i u'_j} \right] + F \quad (3.3)$$

Where u_i, u_j are velocities in x_i, x_j direction respectively, t is time, ρ is density, P is mean pressure, μ is dynamic viscosity, $\overline{\rho u'_i u'_j}$ is Reynolds stresses, and u'_i, u'_j are fluctuating velocity components in x_i, x_j direction respectively.

In RANS equations, the new term known as Reynolds Stresses $\overline{\rho u'_i u'_j}$ appears. In order to solve the equation, the main task of turbulence modelling is to develop computational procedures of sufficient accuracy and generality to predict the Reynolds stresses and the scalar transport terms. This includes two typical methods: the models based on the Boussinesq hypothesis and stress-transport models. The Boussinesq hypothesis assumes that the Reynolds Stresses have a linear relationship with the mean velocity gradients, expressed as Equation 3.4:

$$-\overline{\rho u'_i u'_j} = \mu_t \left(\frac{\partial u_i}{\partial x_j} + \frac{\partial u_j}{\partial x_i} \right) - \frac{2}{3} \rho k \delta_{ij} \quad (3.4)$$

Where μ_t is turbulence viscosity (also called eddy viscosity due to its analogy with the laminar viscosity μ), and $k \equiv \frac{1}{2} \overline{u'_i u'_i}$ is turbulence kinetic energy (E); δ_{ij} is the Kronecker data ($\delta_{ij} = 1$ if $i = j$ and $\delta_{ij} = 0$ if $i \neq j$). Note that μ_t is not a fluid property.

RANS turbulence models based on the Boussinesq hypothesis include three kinds of methods to calculate μ_t . According to the variable in the equation, it is divided into zero equation, one equation, and two equation models.

Zero equation turbulence models (algebraic turbulence models) calculate turbulence viscosity from the flow variables directly, and do not require the solution of any additional equations. As a consequence, it may not be able to properly consider convection and diffusion of turbulent energy. These models are often too simple for

use in general situations, but can be quite useful for simpler flow geometries, or in start-up situations.

In the one equation turbulence model (Spalart-Allmaras), turbulence viscosity is expressed by the one variable, turbulent kinematics eddy viscosity (see Equation 3.5).

$$\nu_t = \kappa^2 L_t \quad (3.5)$$

Where k is turbulence kinetic energy, L_t is the turbulence length scale. This turbulence model is mostly applied into aerospace with high speed flow, and is not suitable for the wind environment study.

Two equation turbulence models are defined by two extra transport equations to represent the turbulent property of the flow (see Equation 3.6). One variable is turbulent kinetic energy (κ). The other variable is dependent upon what type of two-equation model it is. The turbulent dissipation rate, (ϵ) or specific dissipation rate (ω) are commonly used.

$$\mu_t = C_\mu \rho \kappa^2 / \epsilon \quad (3.6)$$

The standard κ - ϵ model is a semi-empirical model, which uses the constants from experiments in the transport equation. It is the most popular and widely used in engineering, as it can provide robust and efficient results, while computational cost is lower (Li et al., 2006). However, it is well known that the standard κ - ϵ model has a disadvantage, as it overestimates turbulence kinetic energy at the impinging region (Murakami, 1993). This could be due to the fact that this model assumes that the flow is fully turbulent and is isotropy flow.

In order to overcome the drawbacks of the standard κ - ϵ model, a series of improved κ - ϵ equation turbulence models was developed, such as the RNG κ - ϵ (Yakhot and Orszag, 1986), and the Realizable κ - ϵ (Shih et al., 1995), and so on. The RNG κ - ϵ has the same form as the standard κ - ϵ by the Renormalization Group (RNG) theory, except it uses a modified equation for ϵ to account for non-equilibrium strain rates method and different model coefficient. The Realizable κ - ϵ model intends to address the shortcomings of the traditional κ - ϵ turbulence model by adopting a new eddy-viscosity formula, involving a variable C_μ and a new model equation for dissipation, based on the dynamic equation of the mean-square vorticity fluctuation. It improves

performance on the massive separation and high mean shear rate, based on the application of certain constraints to the normal Reynolds stresses to ensure that these remain positive at all times. The term ‘realizable’ means that the model satisfies certain mathematical constraints on the normal stress, consistent with the physics of turbulent flows. This model attenuates the stagnation point anomaly without leading to worse results in the wake. However, care should be taken to ensure that the two equation model assumes the flow is an isotropy flow, and does not consider stress-driven secondary flows.

A series of κ - ω models, including the standard κ - ω (Wilcox, 1998) and the Shear-stress transport (SST) model (Menter, 1994), are more accurate than the standard κ - ϵ models near the wall layers. The standard κ - ω has a simple low Reynolds number formulation and has the ability to compute flows with weak adverse pressure gradients. The SST model blends the advantages of κ - ϵ and κ - ω models. The difference between the k - ϵ and SST models is that the k - ϵ is difficult to integrate to the wall. The SST model accounts for the transport of shear stress, and also includes limiters that are difficult to make numerically stable in the k - ϵ . An improved near wall formulation reduces the near wall grid resolution requirements. However, there is a fundamental defect, due to neglecting rotation, anisotropy, and non-equilibrium effects.

Note that these models based on the Boussinesq hypothesis assume that the Reynolds Stresses are isotropic. As a consequence, they are not valid in the complex flow with strong curvature, or strongly accelerated or decelerated flow. An alternative approach of RANS is to model anisotropy Reynolds stress components for each of the terms in Reynolds stress tensor, such as the RSM (Reynolds Stress Model) turbulence model. The RSM model is the most elaborate RANS turbulence model, since it avoids making the isotropic Boussinesq approximation by solving additional transport equations for each of the individual Reynolds stresses. It solves additional transport equations for each of the individual Reynolds stresses, as well as an equation for the dissipation rate. This means that 5 additional transport equations are required in 2D flows, and 7 additional transport equations must be solved in 3D flows. Since the RSM accounts for the effects of streamline curvature, swirl, rotation, and rapid changes in strain rate in a more rigorous manner than other RANS models, it has

great potential to give accurate predictions for complex flows. However, the accuracy of the RSM is still limited by the closure assumptions used to model various terms in the exact transport equations for the Reynolds stresses. For this reason, the RSM does not always provide results that are superior to those of simpler models for all classes of flows (Murakami, 1998). For the dissipation rate equation, most RSM models use the same equation as standard k - ϵ turbulence model, which is generally believed to be the weakest part of the two equations model. Compared with other RANS models, although its shortcoming with computational cost and instability for practice is distinct, the RSM is a better model to predict the flow with anisotropic quantities.

LES

The LES models are advanced turbulence models based on Kolmogorov's theory that the large eddies of the flow are dependent on the geometry of the flow involved, while the smaller scales of eddies are more universal. By using a space-filtered subgrid-scale model, the LES models directly solve the time-dependent larger eddies, and simulate the smaller eddies through a subgrid-scale turbulence model using the Boussinesq hypothesis. The attractions of LES models are that they reduce the error induced by solving the large eddies. Despite the accuracy, the LES models require higher computational resources and are time-consuming. In addition, the time steps and wall function are not well known and need further validation.

DES

The DES models combine RANS modelling with LES for applications such as high-Re external aerodynamics simulations. The unsteady RANS model is employed in the near wall region; while the LES model is used in the regions away from the near-wall to capture the unsteady flow phenomena in areas of physical interest, such as wakes or recirculation zones. The advantage of the DES model is that it avoids the high quality grid requirement of the LES, and saves computational cost and time, while still considering the unsteady turbulence model. Unsteady RANS models used near the wall region can save more grids than the requirement of the sub-grid scale model of the LES. This hybrid model is often used for the application of high-Re external aerodynamics simulations, because the flow is not crucially dependent on the near wall regions, but, rather, dominated by the dynamics of body-scale motions,

hardly dependent at all on the viscous dominated process on the body surfaces. After the comparison of LES , DES and RANS models in the wall-mounted cubes, Schmidt and Thield (2002) concluded that the DES model had the capability to predict unsteady flow around the cubes with the coarse grid near the wall.

3.1.3 Near wall treatments

Turbulence is dramatically affected by the presence of the walls, which largely change the gradient of velocity and turbulence in the near wall region. Therefore, accurately modelling turbulence in this region will determine the whole flow region.

The Reynolds number (Re) can be used to express the effect of walls. The Re expresses the relationship between inertial and viscous forces as Equation 3.7.

$$Re = \frac{\text{inertial force}}{\text{viscous force}} = \frac{Uy}{\nu} \quad (3.7)$$

Where U is velocity, y is the normal distance to walls, ν is kinetic viscosity. Inertial force is the dominant force when the distance is far from the wall and the effect of the viscous force can be neglected. However, when the distance is close to the wall, the viscous force will be larger or more dominant than the inertial force.

In order to describe the velocity and the distance near the wall, two dimensionless parameters are introduced: a velocity parameter (U^+) and a distance parameter (y^+):

$$U^+ = \frac{U}{U_\tau} \quad (3.8)$$

$$y^+ = \frac{\Delta y U_\tau}{\nu} \quad (3.9)$$

Where U is velocity, U_τ is friction velocity, Δy is the distance from measured point to the wall, ν is kinematic viscosity.

The near wall region can be subdivided into two layers: the inner layer and the outer layer. The inner layer includes the laminar 'viscous sublayer' (inner), buff layer (interim) and log-law region. The fluid velocity in the viscous sublayer ($y^+ < 5$) has a linear relationship with the distance to the wall ($U^+ = y^+$). The buffer layer region ($5 \leq y^+ \leq 30$) has a complicated flow, and there is no appropriate method to describe it. Usually it is combined with the log-law region. Shear stress in the log-law region

($30 < y^+ < 500$) is assumed to be constant. The velocity and the distance to the wall have the following relationship:

$$U^+ = \frac{1}{K_v} \ln y^+ + B \quad (3.10)$$

where K is Von Karman constant (≈ 0.4), B is related to surface roughness ($= 5.45$ when the surface is smooth). The boundary between the inner and outer layer is determined by the Reynolds number. The outer layer is usually described by power law.

As most turbulence models, except κ - ω models, are valid only for fully developed turbulence, they need to consider some appropriate models for the wall-bounded flow. There are two approaches to dealing with the flow near walls. The first is by considering wall functions, including standard and non-equilibrium, which employ semi-empirical formulae to bridge the viscosity-affected region between the wall and the fully-turbulent region. This obviates the need to modify the turbulence models to account for the presence of the wall. As the standard wall function tends to be less reliable when the flow has severe pressure gradients and is in strong non-equilibrium, the non-equilibrium wall function based on two layer theory improves the quality of its prediction under the condition that the flow is involved in separation, reattachment, recirculation and subjected to a severe pressure gradient. Wall functions are an economical, robust, and reasonably accurate approach for the studied region above the viscosity-affected region. However, the wall function cannot solve the variables near the wall region. Another approach is the near wall model, modifying the turbulence models to enable the viscosity affected region near the wall, including the viscous sublayer. But it needs a fine mesh near the wall ($y^+ < 5$). However, its hypothesis about the constant-shear and local equilibrium flow conditions is limited.

Different turbulence models have various requirements of y^+ . The wall function and non-equilibrium wall function require that y^+ is larger than 30, but near 30 is better, while the enhanced wall treatment requires that y^+ is around 1 and less than 5 (Fluent, 2006). y^+ is not particularly required for κ - ω turbulence models, as they can be applied throughout the region, provided that the near-wall mesh resolution is sufficient.

3.1.4 Discretisation

Since the partial differential equations defining the spatial, physical and temporal characteristics of fluid flow cannot be solved directly, they should be discretised to algebraic equations, which can be solved by computation. The methods of discretisation are classified into three methods: FDM (finite difference method), FEM (finite element method) and FVM (finite volume method). FVM is popular due to its speed and efficiency, as this method directly integrates the equation in the full modelling in the domain. FVM uses the centre node to represent the value and properties of the finite cell, resulting in a system of algebraic equations which can be solved iteratively to obtain the distribution of the flow properties at all node locations.

Computational domain is spatially discretised into a number of grids or meshes, in which the nodes represent the information of the fluid. The grid types include structured grid and unstructured grid, which use a mixture of hexahedral, tetrahedral, pyramidal, and prismatic geometries. Structure grids are appropriate for simple geometries, resulting in saving computational resources and time, but need more effort to decompose the domain. Unstructured grids are flexible and easy to generate in the complex geometries, but may cost more in terms of computational resources and time. Hexahedra grids are superior to tetrahedral grids, as the former are known to introduce smaller truncation errors, which are the differences between the partial derivatives in the governing equations and their discrete approximations, and display better iterative convergence (Franke et al., 2004). The quality of grid also affects the computational result. The ratio of grid stretching should be less than 1.3 between consecutive cells in the region of high gradients in order to keep truncation error small (Franke et al., 2004). The grid resolution around the physical flow should be fine enough to capture the important physical phenomena. The angle between the normal vector of a cell surface and the line connecting the midpoints of its neighbours should be as small as possible as it can, and ideally parallel.

Temporal discretisation is employed into the unsteady state flow, in which the time is translated into discrete time steps. Time steps cannot be exactly calculated and they depend on the quality of spatial discretisation and system, but they are usually smaller than the period time of the oscillations. The variable of time makes the competing time much longer than the steady flow, which takes the flow to be time

averaged and independent. In the urban boundary layer wind tunnel, the steady fan speed means the wind can be taken as a steady flow (Franke et al., 2007).

3.1.5 Solution

The discreted momentum transport equations still cannot be solved, as the convection terms contain non-linear quantities and there is no equation for pressure which exists in every momentum equations. Non-linear equations usually adapt iterative methods, which are more efficient than other methods. The term of pressure is deduced from the guessed velocity components, and then used to solve the momentum equations. After the velocity field is improved, the result is used for the next iteration. The iteration proceeds until convergence occurs. The basic method used is SIMPLE, but the improved SIMPLEC is more popular for us in the wind field study.

Convergence occurs when the solution approaches the exact solution. There are three mathematical concepts for judging whether or not the convergence is successful. One is to specify the residential error, which is how much the initial error has dropped. When the residential reduces to the specified data, the solution can be regarded as convergence. The standard of 0.001 is used in industrial applications, although a residential error of lower than 5 orders of magnitude is recommended (Franke et al., 2004). Stability is another criterion for convergence, as the unstable data - even the round off error - can cause oscillations or divergence. The third criterion is to check the integrated quantities before concluding the solution is converged.

As the computational solution depends on the quality of the grid, a grid independence test is necessary to ensure that the grid resolution has slight effect on the solution. Grid independence is to successive refinement of an initially coarse grid until certain key results do not change. It usually requires at least three systematically and substantially refined grids in order to estimate the error in the solution by Richardson extrapolation (Stern et al., 2001) in the asymptotic range. The refinement of entire grids or local grids based on some refinement criterion can be used to estimate the grid independent solution, providing that the grid size is not in the asymptotic range (Franke et al., 2004).

CFD is a complicated computational system used to simulate the fluid phenomena by solving the governing equations. This system requires setting up the turbulence model, near wall treatments, discretisation and the solution. All of work is difficult for individuals who aim at using the application to achieve their own CFD codes. Fortunately, the commercial CFD codes provide the platform for general users, but these users still need to adapt CFD settings for their purposes.

3.2 CFD Settings for Natural Ventilation Studies in the Urban Environment

As the commercial CFD code is a general system and spans wide disciplines, it is necessary to set the appropriate conditions for any particular purpose. In order to avoid solution errors from the users themselves, some disciplines have produced best-practice guidelines. Examples of these are civil construction and HVAC in QNET-CFD (Castro, 2003), pedestrian wind environment (Franke et al., 2004; Yoshie et al., 2007), and flow and dissipation in the urban environment (Franke et al., 2007). However, natural ventilation study in the urban environment has certain requirements. It concerns the mean wind pressure distribution on the building façade (Swami and Chandra, 1988), which is distinguished from other disciplines, such as the extreme wind pressure for structure engineering and the air pollution diffusion for chemical engineering. As a consequence, natural ventilation study in the urban environment needs to define its own CFD settings.

This section concentrates on the CFD settings for natural ventilation study in the urban environment. The commercial CFD code and computer resource used in this study are briefly introduced. Based on the relevant theory, published resources and experiments, the section discusses meshing, the solver, boundary conditions, the turbulence model and the solution for the purpose of studying natural ventilation in the urban environment.

3.2.1 CFD code – FLUENT

Since CFD involves complicated mathematical calculations and requires various computer hardware and software, the best thing to do is to employ the commercial CFD code. All of the commercial CFD codes, such as PHONEICS, CFX, STAR-CD,

and FLUENT and so on, have common properties, so FLUENT was employed. FLUENT is one of the most powerful commercial CFD codes, and uses finite-volume method to solve the governing equations of conservation of mass, momentum, energy and other relevant fluid variables. At the University of Sheffield, FLUENT version 6.3 is available as CFD software which can be accessed on the campus website, and also can be run at the High Performance Computing and Grid Computing System, ICBERG. This system, supplied by Sun Microsystems, holds 2.4GHz AMD Opteron (PC technology) processors. It has high throughput facts and figures: processors: 320; Performance: 300GFLOPs; Main Memory: 800GB, Filestore: 9TB; Temporary disk space: 10TB. The capability of computational software and hardware ensures that the numerical experiments process normally.

The procedure of FLUENT simulation consists of three steps: pre-processor, solver and post-processor (Fluent, 2006). Firstly, the computational domain is meshed by GAMBIT, which is the pre-processor code of FLUENT, to decompose the domain into volumes. Secondly, the meshed model is imported into the FLUENT solver and the boundary condition and initial data are set. Every mesh consists of a set of non-linear algebraic equations of dependent variables. A pressure-based solver is used for the low-speed incompressible flows, because it can save time and computational resource by solving the equations sequentially. A point implicit linear equation solver is used in conjunction with an algebraic multigrid (AGM) method to solve the resultant scalar system of equations for the dependent variable in each cell. As the three components of velocity may not satisfy the continuity equation, a Poisson-type equation for pressure is derived from the continuity equation and the linearized momentum equations. The pressure correction equation is then solved to obtain the necessary corrections to the pressure and velocity field, so that continuity is satisfied. Since pressure does not appear explicitly in the continuity equation for incompressible flow, the procedure must be devised to obtain the pressure field. SIMPLIC is suitable for this study, as it refines expression for the variable flux through each cell face and accelerates convergence. FLUENT stores discrete values of the variables at the cell centre; however, values of the variables are required at the cell faces, so the convection terms in the equations must be interpolated from the cell centre values. This is accomplished using an upwind scheme. Thirdly, the results after convergence are examined, and their report can be visualized or quantitatively

expressed. If the results are not satisfactory, revisions of the physical or numerical model are necessary.

3.2.2 Meshing

As the pre-processor of CFD simulation, meshing aims to decompose the computational domain into a large number of grids for spatial discretisation. Two crucial issues which significantly affect the solution are domain geometry and grid quality during the meshing phase.

Domain geometry

The geometry of the computational domain is determined by the characteristics of the wind flow around the studied building. Firstly, three dimensions are essential for the simulation of the wind flow around the building, as wind flow is a turbulent flow with anisotropic characteristics. Many experiments have confirmed that the two dimensional flow leads to the recirculation length being longer than three dimension (Li et al., 2006). Since the flow is turbulent, the simulation should also be three dimensional, even though the cost is much greater (Shah and Ferziger, 1997). Secondly, the domain size is determined by the turbulence flow around the studied building. According to Franke et al.'s (2004) recommendation, for the single building, the inlet boundary is at least $5H_b$ (building height) in front the building, and the downstream fetch is $15H_b$ to keep the turbulence fully developed. Lateral fetch and the distance between the top and the roof should be $5H_b$. These distances can avoid the effect of boundaries on turbulence flow. In the urban area, the building height takes the height of the tallest building. In addition, the blockage ratio is defined as the ratio of the projected area of the model, and the domain section should be considered. It is usually less than 3% in order to avoid the blockage effect. However, the neighbourhood effect on the wind pressure around the building in urban environment is still an open issue. This issue will be explored further in the next chapter.

For the isolated building study, the computation domain size was $6H_b$ for the upstream fetch and the downstream fetch was $15H_b$; the spanwise fetch was $6H_b$ and the vertical height was $6H_b$. As the building was situated in the urban environment,

the computation domain size was determined by the fully developed turbulence domain and the neighbourhood regions.

Grid quality

Grid quality is dependent upon whether or not the grids can capture the characteristics of flow around the model. In general, the distribution of grids in the domain is dense near the model, especially near the separation edge, as the grid quality should be high to keep the truncation error small. In order to reduce the number of grids, the grid stretch ratio can be used, but should be less than 1.3 (Franke et al., 2004). As the flow is more complicated in the wake region than in the upstream region, the wake region should therefore have denser grids than the upstream region. The choice of structured or unstructured grid is determined by the complexity of the models. It is expected that this study will use the structured grid, as it is more accurate and saves time on computing, but it takes longer in terms of meshing. The unstructured grid can save not only time on meshing, but also provide a convenient framework for local grid adaption (Kim and Boysan, 1999). Furthermore, the grid equiangle skewness should be less than 0.9 (Fluent, 2006), otherwise, it would cause the problem of convergence.

Grid quality can be improved during the solution. As the grid is usually accomplished in the pre-processor, it can be refined or coarsened based on the geometric and numerical solution data in the solver by means of adaption. However, the adaption should be based on an initial grid that is fine, so it can capture the essential features in the flow field.

In this study, the grids complied with the above rules. In addition, most cases employed the structured grid. Boundary layer grids and size function were employed to keep the denser grid near the wall in order to meet the near wall treatment ($y^+ < 5$). The grid stretch ratio was less than 1.3 and the grid equiangle skewness was less than 0.8. The complex models had 8 layer grids near the walls, unstructured grids around the models and structured grids far from the models. The combination of unstructured and structured grids saves grids and time on meshing.

3.2.3 Solver settings

The solver setting in this study followed the characteristics of wind flow and the parameters being studied. Wind flow in the urban environment can be seen as being an incompressible flow, because its Mach number (the ratio to the speed of sound in air) is considerably less than 0.3. So the numerical method was set as a pressure-based solver, which solved the momentum equations separately, and was faster and more efficient than the density-based solver. The atmospheric boundary layer can be seen as neutrally stratified flow, because the effect of temperature difference near the ground is slight. The energy equation can be neglected when studying wind. Steady state flow was acceptable for urban natural ventilation study at the design stage. The time averaged steady flow can meet most engineers' requirements on the mean property of the flow (Franke et al., 2004). Although the time dependent, unsteady flow was usually more accurate than the steady flow, its time consuming, and its expense may be unaffordable at the design stage.

3.2.4 Boundary conditions

The boundary conditions specified by the physical characteristics of atmospheric boundary layer outside the computational domain determine the whole flow in the domain. They enter the discretisation equations by suppression of the link to the boundary side and modification of the source terms.

Inlet

The inlet velocity boundary condition is usually used in the wind environment, as the atmospheric boundary layer profile is well known. The inlet boundary requires an equilibrium boundary, which does not have a velocity gradient along the streamwise direction. There are several methods by which the inlet boundary conditions can be defined. Richards and Hoxey (1993) proposed a method to describe the wind profile by the Equations 3.11, 3.12 and 3.13. The velocity profile is usually described by the power-law or log-law. This method has been commonly used (Blocken et al., 2007; Hu and Wang, 2005; Reichrath and Davies, 2002), but it has drawbacks in terms of the decay of turbulence profiles along the fetch (Hargreaves and Wright, 2007).

$$U = \frac{U_*}{K_v} \ln\left(\frac{Z + Z_o}{Z_o}\right) \quad (3.11)$$

$$k = \frac{U_*^2}{\sqrt{C_\mu}} \quad (3.12)$$

$$\varepsilon = \frac{U_*^3}{K_v(Z + Z_o)} \quad (3.13)$$

Where U is wind velocity; U_* is friction velocity, which can be derived from the reference height and reference velocity by Equation 3.11; K_v is von Karman' constant (~ 0.4); Z_o is surface roughness length; C_μ is a constant (~ 0.9); κ is turbulence kinetic energy; ε is turbulence dissipation rate and Z is the vertical height.

Another method is from the wind tunnel experiment, as used by Yoshie, et al. (Yoshie et al., 2007), was to use the profile from the wind tunnel experiment to predict wind environment around the building. Yoshie et al. point out that the accuracy of the turbulence kinetic energy and the turbulence energy dissipation rate will determine whether or not the solution is successful. However, the wind tunnel experiment cannot be commonly used in practice, and the wind tunnel is inflexible for different conditions. Here, this study tried to use the urban roughness element model to acquire the inlet boundary conditions. The details can be seen in Chapter 4.

Outlet

The outflow condition was imposed on the outlet, in which the flow was fully developed and there were zero normal gradients for all flow variables except pressure. The details of the flow velocity and pressure were not known prior to solution of the flow problem. This can be express as Equation 3.14.

$$\frac{\partial u}{\partial x} = 0, \frac{\partial v}{\partial x} = 0, \frac{\partial w}{\partial x} = 0, \frac{\partial \kappa}{\partial x} = 0, \frac{\partial \varepsilon}{\partial x} = 0 \quad (3.14)$$

Top boundary

A symmetry boundary condition was imposed on the top boundary. That means there is no convective flux across it, expressed as Equation 3.15.

$$\frac{\partial u}{\partial z} = 0, \frac{\partial v}{\partial z} = 0, w = 0, \frac{\partial \kappa}{\partial z} = 0, \frac{\partial \varepsilon}{\partial z} = 0 \quad (3.15)$$

Lateral boundaries

Fully developed flow conditions were usually imposed on the lateral boundaries, as in Equation 3.16:

$$\frac{\partial u}{\partial y} = 0, v = 0, \frac{\partial w}{\partial x} = 0, \frac{\partial \kappa}{\partial x} = 0, \frac{\partial \varepsilon}{\partial x} = 0 \quad (3.16)$$

Ground

Since the bottom wall of the wind tunnel is smooth, the effect of roughness here is slight, and the wall function based on smooth-wall log-law is incorrect used on the roughness surface (Castro, 2003). So the ground of the computational domain can be regarded as a smooth wall by using enhanced wall treatment.

Building walls

The building walls were set as wall boundary conditions with no slip condition ($u=0$, $v=0$). Smooth wall were imposed, as the enhanced wall function with a fine mesh resolution at the near wall may be better for the strong non-equilibrium bluff body flow (Castro, 2003).

Table 3.1 Boundary condition settings in CFD models

Boundary	Setting	Comments
Inlet	Equilibrium wind profile from the urban roughness and equilibrium boundary layer simulation	Inlet velocity boundary
Outlet	Zero normal gradient condition except pressure	Outflow boundary
Bottom	Smooth wall, using enhanced wall treatment or near-wall model	Wall boundary with roughness height zero
Top	Free slip, flux normal to the boundary is zero	Symmetric boundary
Sides	Free slip, flux normal to the boundary is zero	Symmetric boundary
Building walls	Smooth wall, using enhanced wall treatment or near-wall model	Wall boundary with roughness height zero

3.2.5 Turbulence models

As there is no single turbulence which can solve a class of turbulence problems, the criteria of choosing an appropriate model are dependent on the physical character of the research object, the required level of accuracy, the available computational resources and the amount of available time and the specification of the models. This can be simplified as 'fit-for-purpose' (Castro, 2003).

Criteria of natural ventilation study in urban environments

As one branch of wind engineering, natural ventilation in the urban environment can take the criteria of other branches in wind engineering as references. Wind engineering has its own physical characteristics. Compared to meteorology and oceanography, its Reynolds numbers are smaller, and the complexities caused by rotation and stratification can usually be ignored (Ferziger, 1990). For the high Re flow around the bluff bodies, separation is an essential flow feature with large adverse pressure gradient. The wall function, based on log law, is inadequate to simulate the near wall region. However, near wall treatment is quite fundamental in wind engineering (Murakami, 1998). In addition, the standard κ - ϵ turbulence model is not appropriate for wind engineering, as it generates too much turbulence kinetic energy in the upstream of the impingement region and doesn't produce a separation region on the top of the body. This results in inaccurate levels of surface pressure. Qualitative analysis is more reliable than quantitative analysis in the complex wind flow field. The accuracy required is generally lower than mechanical and aeronautical engineering. Errors of approximate 30% are acceptable for wind engineering (Stathopoulos and Baskaran, 1996).

Natural ventilation also has its own peculiarities. Mean pressure coefficients around the building surface can be regarded as the target for a natural ventilation study (Swami and Chandra, 1988). The trends of pressure coefficient distributions can meet the needs of the planners and designers at the early design stage. If applied carefully and over a limited range, RANS turbulence models are capable of predicting the trends reasonably well (Ferziger, 1990). The steady state of RANS equations are efficient enough to simulate the wind tunnel's reality as the time averaged approach flow conditions in the wind tunnel are stable (Franke et al., 2007).

The Applications of the RANS turbulence models

The standard k - ϵ model has been used widely in wind engineering. Stathopoulos (1993) carried out a numerical simulation of wind-induced pressure on buildings by utilising the standard k - ϵ turbulence model, and concluded that this model is suitable for normal wind directions while differences exist in oblique wind cases. Wiik & Hussin (1997) compared the pressure coefficient on the roof overhang and gable wall of a low rise building in a CFD experiment and compared it against the wind tunnel

test. They stated that CFD, using the basic k - ϵ turbulence model, could predict the pressure at the windward side of the houses generally well, but that the CFD tests underestimated the pressure at the windward side of the edge, and overestimated the negative pressure at the leeward side of the edge. They stated that it may cause the overestimation of wind pressure coefficient on the windward surface as well as turbulent kinetic energy. Hu & Wang (2005) studied the street level wind around a built-up area by using the standard k - ϵ model. Their results concluded that the k - ϵ turbulence model was capable of performing a satisfactory simulation when the model and layout were not complicated; however the complicated model and the large height difference between the models can lead to relatively lower values. Therefore, the k - ϵ turbulence model is not suitable for studying the wind around a building's area, as it cannot simulate separation area, and overestimates kinetic energy at the windward area.

Instead of the standard k - ϵ , the improved k - ϵ models are more popular for study of the wind environment. These models reduce the overproduction of turbulence around the stagnation points on the upwind side of the building. Zhang et al. (2005) investigated a group of buildings by using the RNG k - ϵ turbulence model, and the study proved that the numerical results were similar to those of the wind tunnel. However, after testing on various shaped buildings, Endo et al. (2006) claimed that the RNG model was not appropriate for studying complicated building shapes. According to the experiments taken by Shih et al. (1995), the Realizable k - ϵ turbulence model can predict complex turbulence flows and remove the deficiencies of the k - ϵ eddy viscosity model. Compared with the value obtained from direct numerical simulation, the reattachment length by the Realizable k - ϵ has less than 1% error (Sagrado et al., 2002). However, these two equation turbulence models still have problems when predicting anisotropic turbulence flow. RANS turbulence models require lower computational resources, so have been popularly applied to research and engineering practice.

The RSM model was not used widely, as it takes more computational time compared with other RANS model. However, the RSM is more realistic than other RANS models (Meroney et al., 1999). If the anisotropic flow is more important for the studied variables, it is necessary to utilise the RSM model.

The application of LES

LES is an advanced model for simulating turbulence, as it directly calculates a large eddy while modelling the small eddies with a subgrid-scale model. Tutar & Oguz (2002) investigated turbulent wind flow around two parallel buildings with different wind directions and building arrangement by LES. The simulation results showed that the LES model can overcome the disadvantages of the RANS turbulence model and the LES model was promising for studying wind around buildings. Jiang et al. (2003) studied natural ventilation in buildings by the LES model. They concluded that the LES model was capable of simulating around and within models. Compared with other methods, the LES model provides the most accurate results, and was particularly valuable in studying instantaneous flow. However, though the model in Jiang et al.'s study was simple, it took the fast workstation one week to calculate the results. There were still some discrepancies between the LES results and the experimental data. This was due to the coarseness of the meshes used in the simulation. The current applications of the LES turbulence model in wind engineering and natural ventilation are limited to the simple and isolated model. The LES model is not a feasible approach for the study of group buildings in the urban environment in the practices.

RANS versus LES

RANS and LES turbulence models have been compared in some studies. The results from Cheng et al.'s (2003) study showed that both the LES and the RANS (standard $k-\epsilon$) turbulence models had the ability to not only reasonably predict the main characteristics of the mean flow in the array of cubes, but also capture the flow structures in the proximity of a cube. These included such things as separation at the sharp leading top and side edges, recirculation in front of the cube, and the arch-type vortex in the wake. However, the LES usually obtains better overall quantitative results, which are similar to the experiment data. Rodi (1997) compared the RANS with the LES on the flow around bluff bodies. The results showed that the main feature of the flow could be predicted reasonably well. However, the standard $k-\epsilon$ model produces poor results, due to the excessive turbulence production in the stagnation flow. The two-layer approach that resolved the turbulence near wall region problem can yield improved results, but the RANS model under predicted

turbulence fluctuations. In the summary of the turbulence models used in wind engineering, Murakami (1998) pointed out that the LES can better predict the reverse flow region behind the building, followed by the RSM and the $k-\epsilon$ model. In the urban canopy layer, the air flow is an unsteady turbulence flow, so the traditional steady state flow cannot catch the characteristics of unsteady flow. The RANS, DES and LES turbulence models were compared on the application of wall-mounted cubes (Schmidt and Thield, 2002). The results demonstrated that DES was able to capture the most dominant flow pattern like LES, while the RANS only provided a poor representation of the unsteady flow phenomena, because the RANS models had a major problem with strong curvature, so cannot be used for unsteady flow.

In summary, some RANS models are generally sufficient for prediction of the mean pressures around the building. The standard $k-\epsilon$ is not suitable for use in wind engineering. The improved $k-\epsilon$ is a more feasible and efficient for studying wind flow in the urban environment, but has shortcomings in the wake area. The RSM is more realistic for use in the urban wind environment than other RANS models. As wind flows are inherently anisotropic, the appropriate turbulence model for wind engineering should be able to model the anisotropy of turbulent flow, such as the Reynolds stress model. The LES is particularly appropriate to the scientific principle and transient turbulent study (Li et al., 2006). In addition, use of the two-layer method near the wall region can improve results.

It is still confusing to decide which turbulence model is most appropriate for the study of natural ventilation in the urban environment. So the comparison of the turbulence models prior to application is necessary. The improved $k-\epsilon$, recent developed the SST $k-\omega$, RSM and LES were all carried out under the same conditions and subsequently compared.

3.2.6 Solution settings

The governing equations were discretized by the finite volume method in the FLUENT code. The spatial terms in the equations were solved by the upwind scheme, which can eliminate the oscillation and provide better convergence for convective terms. Since the first order upwind scheme assumed the cell centre value represents a cell averaged value, it cannot predict rapid variations in the flow properly. The second

order upwind scheme was employed due to its more accurate values, which were from the Taylor series expansion of the cell centred solution. The pressure-velocity coupling in this study employed the SIMPLIC method, because this method was more appropriate for the complex flow than SIMPLE, and was more steady than the PISO algorithm (Fluent, 2006). The solution of CFD technique was dependent upon the convergence criteria. In this study, the convergence criteria were based on two rules. The first was that the residuals are 10^{-5} . The second was that the difference of mass flux of inlet and outlet were less than 0.001. The near wall treatment was set as an enhanced wall treatment, as the turbulence flow around the building had a large adverse pressure and curve line.

As a sophisticated technique to simulate flow phenomena, CFD codes need a high level of computational resources. It was not feasible to study natural ventilation in one model including the external and internal features of buildings, because the large difference scale and grid resolution caused the need for unaffordable computational resource (Zhai, 2006). The simulation of the flow by CFD in the multi-zone building was challenging for the current computational resource and boundary condition settings, so airflow network models had been popular in the building design stage.

3.3 Airflow Network Models for Ventilation Rate Studies

3.3.1 Fundamentals of airflow network models

Airflow network models are used to simulate different airflow paths in buildings by a number of nodes and lines, representing building zones and flow paths respectively. Each zone of a multi-zone building is represented by one equation. The equations are solved iteratively until the summation of the mass flow rate turns to zero (Bahadori and Haghghat, 1985).

In the multi-zone building, the total mass of air entering into the building is balanced by a corresponding mass of air leaving out of the building and the summation of mass of all zones in the building must be equal to zero. It can be expressed as Equation 3.17:

$$\sum_{i=1}^j Q_{mi} = 0 \quad (3.17)$$

Where Q_{mi} is mass airflow rate through the ' i 'th flow path, (kg/s); j is the total number of flow paths into the zones. For the ' i 'th flow path, mass flow through it is expressed as Equation 3.18:

$$Q_{mi} = \rho C_i (P_{ti} - P_{ii})^n \quad (3.18)$$

Where C_i is the flow coefficient; ρ is the density of air through the opening; n is flow exponent; P_{ii} is the total pressure combined wind pressure and buoyancy force at the ' i 'th opening (see the detail of driven forces in Chapter 2). P_i is the internal pressure, which is a unique data for each zone to balance the flow rate.

Airflow network models have the capability of simulating the flow within the zones. Compared with the CFD experiments, the airflow network model is reasonable of the calculation of airflow rate. The network models are recommended as a valid method for studies that have no access to laboratory or full-scale testing facilities (Asfour and Gadi, 2007). However, these methods are restricted by the need to quantify the driving force and to account accurately for all openings in the building .

3.3.2 Airflow network model Codes – AIDA, COMIS

Airflow network models can be classified in two categories: single zone models and multizone models. The single zone models are the basic method for calculating the airflow rate in the well-mixed single zone. They are easy to use and valuable for assessing the airflow rate in the simple building, such as a house at the early design stage. However, the single zone model cannot be used in most buildings with more than just one well-mixed zone. The multizone models are the methods used to calculate air infiltration and ventilation rates in buildings with a number of zones.

A single zone model – AIDA

AIDA (Air Infiltration Development Algorithm) is a single zone model used to calculate air infiltration and ventilation rate (Liddament, 1996). It can resolve flow rates for any number of defined openings, and calculate ventilation rates driven by a combination of wind pressure and thermal buoyancy in a single zone. AIDA requires inputting the outside and inside temperature, wind speed and pressuring coefficient around the openings and defining the volume of the zone and opening height and flow exponent. The equations are solved by iteration. As the original code written by

the BASIC difficult to define the flow coefficient, the improved code uses the opening area to define the flow coefficient, which can be seen in Appendix A, written by Matlab. AIDA is an easy to use and accurate way of approaching ventilation analysis of simple buildings at the early design stage, such as the planning stage with no details of the building configuration.

A multizone model – COMIS

There many types of multizone model, such as CONTAM , BREEZE (BRE, 1994) and COMIS (Feustel, 1999), and so on. Although these models are different from each other in details, they have a number of similar characteristics. Based on the mass balance equation, the nonlinear dependence of air flow rate on pressure difference is calculated by using an iterative method. Compared with 14 other airflow network models, the results showed that COMIS had a good agreement with them (Warren, 2000).

The multizone model COMIS (Conjunction of Multi-zone Infiltration Special) is an inter-zone air flow model used to calculate the complexity of flow in a building (Feustel, 1999). The COMIS model has various modules used to calculate air flow through large vertical openings, single-side ventilation, and different opening configuration. The COMIS needs to input the airflow driven forces, including wind velocity, pressure coefficient around the external openings, external and internal temperature and mechanical ventilation force. It can calculate quasi-steady-state air flow and distribution by time steps that are based on external conditions and schedules. Its output includes the flow rate, air change rate, mean age of air, air change efficiency, and so on.

The COMIS model has been validated for calculating airflow rate in some multizone buildings. Haghghat and Megri (1996) carried out a comprehensive validation of COMIS and COTAM. Their results showed that the predicted air change rates were within 20% difference with the measurement of air change rates, and that the two models showed excellent agreement. Zhao et al.(1998) compared this model with a measurement of the airflow rate in an airtight house, and concluded that COMIS was a satisfactory model for simulating airflow. Dascalaki et al. (1999) investigated the airflow through large openings using the full scale test and the COMIS simulation,

and their results showed good agreement. However, the successful applications of COMIS are dependent upon the input data from users and their experience (Roulet et al., 1999).

3.3.3 Settings

The choice of an appropriate airflow network model for the application needed to consider the building details and the requirement of the accuracy of results. At the planning stage, the building details were unknown and planners did not need to give the exact data of the airflow rate, so AIDA was suitable for the planning and study of the potential for natural ventilation. Details of the setting of the COMIS model can refer to Chapter 6. At the building design stage, the natural ventilation system in the building was known, so the multizone model COMIS was suitable for the prediction of the natural ventilation rate in the building. The setting of COMIS in the model of the studied building in the urban environment can be seen in Chapter 7.

3.4 Procedure

3.4.1 Survey of physical urban boundary layer wind tunnels

The purpose of this survey was to analyse the mechanism of a physical boundary layer wind tunnel prior to establishing a virtual urban wind tunnel. The atmospheric boundary layer wind tunnel has been a well-known technique for studying wind around the building since Davenport et al. studied the World Trade Centre in 1964. However, wind tunnel experiments that are restricted by expense and time and are inflexible mean they cannot be popularised in the building design.

The commonly used urban boundary layer wind tunnel originally introduced by Counihan (1969) is based on the use of spire and barrier wall to generate an initial turbulence flow, followed by a fetch of roughness elements representative of the urban terrain. Its parameters are scaled to the neutral atmospheric boundary layer. The gradient wind is a free stream velocity on the top. The urban roughness area is composed of regular elements. The fetch of the urban roughness elements accounts for the main part of the equipment. The turntable behind the roughness area is used to mount the tested model. The mechanism of an urban boundary layer wind tunnel

can be divided into three parts. The first part is used for generating turbulence flow, the second part is for establishing an urban wind profile, and the third is for testing the model.

Based on the same mechanism of the urban boundary layer wind tunnels, the urban boundary layer wind tunnel at the University of Sheffield was chosen as a prototype. This wind tunnel had been compared with the theoretical model and other wind tunnels and the results showed this wind tunnel can be seen as a validated wind tunnel for the study of wind pressures around the buildings. The details of this wind tunnel can be acquired from the literatures (Hussain and Lee, 1980; Lee, 1977). Table 3.2 summarises the characteristics of this wind tunnel:

Table 3.2 Characteristics of the urban atmospheric boundary layer wind tunnel in Sheffield (Hussain and Lee, 1980; Lee, 1977)

Parameters	Data
Work section	1.2m × 1.2m
Length	7.2m
Turntable dimension	1.1m (diameter)
Scale ratio	1:350
Depth of boundary layer	0.8m
Free stream velocity (U_g)	9.65ms ⁻¹
Friction velocity	0.065 U_g
Power law exponent	0.28
Roughness length	3mm

3.4.2 Development of a virtual urban boundary layer wind tunnel

The virtual urban boundary layer wind tunnel based on CFD was derived from the prototype of a physical wind tunnel. However, it was difficult and unnecessary to directly simulate the wind tunnel, because the urban roughness element area and the models in the wind tunnel require enormous computational resources. The more feasible and efficient approach was to divide the whole process of the physical wind tunnel into three parts: the urban roughness model, the equilibrium boundary model and the tested model.

The purpose of the urban roughness model was to determine the appropriate grid, turbulence model and urban wind profile in the urban environment. In order to save the computational resource, the model took one of the repeated units of the urban roughness area. The infinite length of the urban roughness area can be repeated by

using the periodic boundary condition in the CFD. Grid sensitivity tests on the urban roughness model were carried out in order to ensure the results were independent of grids used. Then the various turbulence models, including RANS and LES, were employed to test the same urban roughness model. Their results were compared to choose a suitable turbulence model fit for purpose, because the complicated urban environment was limited by the computational resource. A fully developed turbulent flow was generated after the flow passed an infinite length of urban roughness area.

The equilibrium boundary layer model was used for achieving a horizontally homogeneous boundary layer wind profile, which can avoid the effect of decay of wind profiles along the wind direction on the tested result. The profile was generated by the flow from the urban roughness area crossing a long empty domain. The wind profile along the fetch was compared in order to obtain the equilibrium profile. The established equilibrium wind profile was compared with the wind tunnel experiment. Using the equilibrium wind profile as the inlet boundary condition, the models for the neighbourhood region study were carried out. The results presented the effects of the surrounding models in the neighbourhood region on the pressure coefficients on the model. The results can be used to decide the appropriate computational domain size for natural ventilation study in the urban environment.

3.4.3 Validation

The results of airflow around buildings in the urban environment simulated by the virtual wind tunnel were compared against those from the corresponding wind tunnel experiments. Two kinds of cases were considered in this study. Firstly, the isolated cube in the urban environment was carried out. Its result showed whether the setting of the boundary condition from the virtual wind tunnel was suitable or not. Secondly, the validated boundary condition was applied to the models of airflow in the group of buildings. The results demonstrated the difference between the virtual wind tunnel and the physical wind tunnel on the wind pressure coefficients around the building in the urban environment. There was discussion on the difference between them in order to confirm the possibility of its application to urban environment.

3.4.4 Investigation of planning and the potential for natural ventilation

During the development of urban land, floor area ratio (ϕ) and building density (λ) are the key parameters to managing and evaluating the quality of the living environment (Chakrabarty, 2001; Gao et al., 2006). Floor area ratio is defined as the ratio of the total floor area of the buildings to the area of the plot, and is an important index in planning. It indicates the extent of the usage of the land and city infrastructure for the governors, and regulates the planning of land in the urban area. Building density was defined as the ratio of building coverage of the total area. This specification had a close relationship with the quality of life of the inhabitants, such as determining the green land rate of the total area. This study aims to develop guidance for policy-makers, planners and designers to optimise planning and building design at the preliminary stage.

A generic planning model can be represented by three parameters: floor area ratio, building density and building space (gap). These parameters can be represented by one of the repeated units, as all of the buildings in planning had the same geometry. The floor area ratio can control the building height if the building density is known. The building density can determine the density of building in the planning. Building space (gap) can adjust the position of the building in the planning. By using the three parameters, this generic planning can generate a variety of planning layouts. It is known that building distance in planning can affect the wind pressure distribution on the building. Under the same building densities, the normal pattern has the lowest building distance, and the staggered pattern has the largest. So these two typical pattern layouts were investigated.

This investigation of planning and the potential for natural ventilation potential were performed by coupling the validated virtual wind tunnel and the airflow network model. The planning parameters included building density (λ), floor area ratio (ϕ), the streamwise interval between buildings (S_C) and the lateral gap between buildings (G_C). The scale of models was 1/350, similar to the established virtual wind tunnel. The first step was to investigate the effects of floor area ratio on natural ventilation potential under the condition of constant building density, which was from typical planning in the urban environment. After that, the approximate floor area ratio could

be decided. The second step was to investigate the effects of building density on the potential for natural ventilation with the stable floor area ratio. Under the appropriate floor area ratio and building density, the third step was to investigate the effects of building space and gap on the potential for natural ventilation. These investigations provided a holistic way of understanding planning and the potential for natural ventilation.

The potential for natural ventilation can be quantitatively assessed at the planning stage. In terms of the functions of natural ventilation, as the ventilation rates for health, comfort and cooling can be taken as the criteria of the potential for natural ventilation. Building regulation Part F introduced an adequate ventilation rate for health and purge ventilation, which could be taken as criteria for health in winter. According to the three functions of ventilation, the whole building ventilation rate (ls^{-1}) for health and air change rate (ACH) for thermal comfort were applied to assess the potential for natural ventilation. Ventilation rate ($\text{ls}^{-1}\text{m}^{-2}$) was used to assess the potential for cooling.

3.4.5 Evaluation of the potential for natural ventilation of an urban building

Natural ventilation design requires quantitative analysis of its potential in the building site, since the natural ventilation system needs to decide its components and evaluate its performance. However, it is difficult to calculate the natural ventilation driving forces in the urban environment. The objective of this study was to apply the established methodology to evaluating the potential of natural ventilation of an urban building, and providing guidance for this design at the design stage.

Three steps were carried out to achieve the objectives. The first step was to investigate the wind pressure coefficients around the building. The isolated building and the building with surrounding buildings were accomplished by means of the virtual urban boundary layer wind tunnel. The results provided the wind pressure coefficients around the building for the next step of the study. The second step was to investigate the natural ventilation rates in the building by using the COMIS code under the three season cases: the average winter, the average summer and the hottest day. The third step was to compare the ventilation rate with the standards of

ventilation for health, thermal comfort and cooling. The comparison of the results and the corresponding criteria of natural ventilation presented the potential for natural ventilation of the zones of the building. The difference between the isolated building and the building with surrounding building demonstrated the effects of the surroundings on the potential for natural ventilation. The difference between the cases of the yearly average wind speed and no wind reflected the function of buoyancy ventilation and wind driven ventilation in ventilating the building in the urban environment. The guidance from this study can help designers choose the appropriate natural ventilation strategy in the urban environment.

3.5 Rationale

The above study demonstrates the fundamentals of methods like CFD and airflow network models, including their settings in this study as well as the process of this project. In order to achieve the aim of this study, it is necessary to identify the strength and limitation of the methodology.

3.5.1 Strength

CFD is a sophisticated technique used to simulate wind flow around a building. In recent years, many researchers have tried to apply CFD to predict wind pressures around buildings. Selvam (1997) studied the pressure around a building using difference inflow turbulence data. Suh et al. (1997) investigated the wind pressure coefficient around an odd-geometrical building. Wind-induced pressure at the external surface of a high-rise residential building was performed by CFD to optimise the building plan layout and location of windows (Burnett et al., 2005). Their results confirmed that the CFD had the same capability as the wind tunnel in helping designers at the planning stage. In addition, CFD has large advantages in terms of saving time, as well as being economical and informative. Compared to the wind tunnel experiment, the models generated by CFD can be much easier to set up and revise, and the information in the computational domain can be plotted flexibly.

Although it was found that CFD was difficult to simulate wind around the bluff body due to turbulence models and complicated physical phenomena (Murakami, 1998), CFD is much more appropriate for the study of natural ventilation, because at

the early design stage this study concerns the mean pressure coefficient, which can be achieved by using CFD. The dimensionless pressure coefficient difference based on pressure measurements on the external envelope of the building model can be used to evaluate the relative integral effectiveness of natural ventilation in different configurations (Cermak et al., 1984).

This methodology simplifies both the urban boundary layer wind tunnel experiment and the CFD test, but does not distort the results. Based on the mechanism of the urban boundary layer wind tunnel, the proposed virtual boundary layer wind tunnel simulates the typical urban boundary layer wind tunnel through CFD techniques, while avoiding the massive mesh of urban environments. Franke et al. (2007) state that RANS equations are an adequate representation of the wind tunnel's reality, as due to the time averaged approach, flow conditions in the tunnel do not change.

Coupling CFD and airflow network models can save computational resources when studying natural ventilation in the urban environment. Decomposing the external and internal models is feasible for these predictions, because the large scale difference between them can lead to unaffordable computational resources (Zhai, 2006). Airflow network models are better for simulating the multi-zone building than CFD, because the combined buoyancy and wind flow in the multizone building is so complicated that it requires much finer grids to capture the flow characteristics, and the solution is difficult to convergence. The association of CFD models for the wind pressure coefficients around the building and the airflow network models for the interior environment can achieve much more sensible results in the urban environment (van Moeseke et al., 2005).

3.5.2 Limitation

There may be some errors that occur when transferring the data from outside to inside. As the methodology consists of a sequence of models from the developing wind tunnel to the resulting ventilation, it is inevitable that errors will arise between the data output and input. The error can be reduced, provided that the computational resource is improved.

The methodology still has some deficiencies, due to CFD technique. For instance, steady state is actually an ideal state, but an unsteady instantaneous flow may affect the pressure distribution. The turbulence model and enhanced wall treatment still need to improve. However, the aim of simulation is not to get exact data, but to ascertain the relationship and tendency, especially at the design stage.

This study is limited to the model in the simplified cases. The prevailing wind was used for all of the models. This could lead to misunderstanding the effect of wind incidence on the potential for natural ventilation. This can be solved by using more models from various wind directions, but this needs more computing time. Note that this study emphasises the methodology, not the results of the building under the variety of conditions.

To sum up, the current methodology for predicting the potential for natural ventilation in the urban environment has many advantages in terms of saving time and money. The approach is feasible, as well being as simple and accurate as the physical wind tunnel. The limitations of this methodology are acceptable at the early design stage.

3.6 Summary

Wind flow in the urban environment can be taken as an incompressible flow with constant temperature, so its governing equations consist of Continuity Equations and Momentum Equations. Three dimensional models are essential for the simulation of the wind flow around the building in the urban environment. Steady state RANS equations can represent the wind flow in the urban boundary layer wind tunnel. There is no evidence for which RANS turbulence model is the most appropriate for the natural ventilation study. The near wall model or enhanced wall treatment is necessary to study wind flow around the building in the urban environment. The boundary conditions, especially the turbulence parameters, decide the accuracy of the solution of the mean pressure coefficients.

Coupling CFD and airflow network models is a feasible approach to predicting the potential for natural ventilation in the urban environment. CFD has the capability of predicting the average wind pressure coefficient around the building in the urban

environment, just as well as the urban boundary layer wind tunnel, providing that the CFD settings are appropriate. Airflow network models are the optimum choice for calculating the ventilation rate in the complex building. They can easily and accurately calculate natural ventilation rates driven by the combined wind and thermal buoyancy forces in the multizone building.

There are still some open issues after this study. The current method used to describe the inlet boundary conditions still need to improve; the computational domain size for natural ventilation study in the urban environment should consider the effect of the neighbourhood buildings on the studied building. In addition, choosing an appropriate turbulence for the natural ventilation study in the urban environment needs to be investigated. All of the issues are discussed in the next chapter.

CHAPTER 4

Developing a Virtual Urban Atmospheric Boundary Layer Wind Tunnel for Natural Ventilation Studies

CFD is a sophisticated technique used to study airflow around and in a building. It has been applied to evaluate the pedestrian wind environment (He and Song, 1999; Hu and Wang, 2005; Yoshie et al., 2007), as well as to predict wind pressure on a building (Burnett et al., 2005; Reichrath and Davies, 2002). For natural ventilation studies, it has been used to study wind induced cross ventilation in a building (Evola and Popov, 2006), and the combined natural ventilation driven by wind and thermal buoyancy forces (Allocca et al., 2003). However, the current application of CFD to natural ventilation study in the urban environment is a challenging issue, as it is restricted by the urban boundary condition, turbulence model, and computational resource (CIBSE, 2005). This chapter presents an approach to develop a virtual urban atmospheric boundary layer wind tunnel for natural ventilation study, based on the CFD technique.

This chapter consists of four sections. The background and concept of a virtual urban atmospheric boundary layer wind tunnel are described first. The second to the fourth sections demonstrate the procedure of developing the concept. The second section shows the modelling wind in the urban roughness area in order to identify grid resolution and turbulence model in the urban area. This section also provides the fully developed inlet boundary layer for the next step in the study. In the third section, the development of the inlet boundary condition in the empty domain to the development of the equilibrium boundary condition for the test model is explained.

In section four, the computational domain size with different layouts and densities for natural ventilation study is explored.

4.1 Concept of a virtual urban boundary layer wind tunnel

4.1.1 Background

Although the atmospheric boundary layer wind tunnel is well known as an effective simulation tool to study airflows in and around buildings, it is not appropriate for natural ventilation study at the planning and building design stage. This is because it is expensive, time consuming, and not amenable to parametric changes. Recently, the rapid development of numerical algorithms and computational resources made CFD a promising approach from which to study natural ventilation, due to its advantages on saving time and cost, and its informative results, avoiding the shortcomings of wind tunnels (Chen, 2004). Ayard (1999) investigated the ventilation properties of a room with various opening configurations using CFD. Jiang & Chen (2001) studied single-side and cross natural ventilation in buildings through use of various CFD turbulence models. All of their studies have presented the potentials of CFD in the study of natural ventilation.

However, the current CFD technique still has some deficits. One aspect is from itself, including software and hardware, such as the physical approximation model, iterative error, discretisation error and the limited computational resources, and so on. These kinds of problems will be solved by further scientific research and industrial improvement. Another aspect is from users' knowledge and experiences. These uncertainties include the domain size and meshing, boundary conditions and the users' settings on the model. The general purpose of commercial CFD codes cannot be applied to specific situations, although they provide a good platform for the users. The definition of computational domain size, grid resolution, boundary conditions and turbulence models can significantly affect the accuracy of the results. Guidelines or recommendations are needed for specific applications (Cowan et al., 1997; Franke et al., 2004).

The application of CFD to natural ventilation in the urban environment needs the users' guidelines due to its purpose and requirement. Natural ventilation study mainly uses the mean wind pressure distribution around the building (Swami and Chandra, 1988), which is distinguish from civil construction for the peak wind forces and pedestrian wind environment for the wind velocity at the level below body height. In addition, the application of CFD in the urban environment needs to adapt to much more complicated conditions. The computational domain should be large enough to meet the requirement of turbulence development and the effect of neighbourhood scale on pressure distributions around the building. Also, the large urban roughness height means the boundary condition in the urban environment is difficult to simulate, because the turbulence in and around the urban canopy layer is complicated. Boundary conditions and computational domain size represent the complexity of studying natural ventilation in the urban environment.

Three types of methods used to model urban boundary layer profile have problems when used in the urban environment. One method proposed by Richards and Hoxey (1993) describes the mean wind velocity profile using the equations of power law (exponent decided by terrain types) or logarithmic law (friction velocity and roughness length). The turbulence intensity feature is described by the profiles of turbulence kinetic energy and the dissipation rate of kinetic energy respectively. This method simplifies the surface roughness region, and may be suitable for studying the region above the urban canopy, but it is not appropriate to study wind around buildings in the urban area. This is because the equation's laws take the action above the height of urban roughness length plus displacement height, which is higher than building height. Another method used by Yoshie et al. (2007) is to interpolate the data from wind tunnel experiments into the CFD model. This method is much more accurate, but the wind tunnel is inflexible for the different cases and it cannot be employed by the common project. It is suitable for the purposes of research but not for application. The third approach is to directly simulate the roughness elements as in a wind tunnel by CFD (Miles and Westbury, 2003). However, this method may be infeasible and unnecessary, since lots of urban roughness elements occupy a large portion of computational resources, and decline its distribution for the area of interest.

It is necessary to generate the appropriate inlet boundary profile in the urban environment for natural ventilation study.

Computational domain size consists of the fully developed flow region and the region being studied. The fully developed flow region has been confirmed by many researchers, such as Franke et al. (2004). They recommend that the location of model is at least $5H$ away from the inlet, lateral and top boundary, and $15H$ in front of the outlet boundary. The blockage ratio of the domain should be less than 3%. The neighbourhood region for the urban natural ventilation needs to be looked at when determining computational domain size. The neighbourhood region is defined as the region in which the pressure coefficient difference between the windward and leeward surfaces of the studied building is affected by the surrounding buildings, but slightly affected by the outside. The rough neighbourhood region from wind tunnel experiences, such as $6-10H$, neglects the differential flow field around the building and does not consider the effects of building densities or layouts. Therefore it still needs the investigation of neighbourhood regions in the CFD condition in order to optimise the domain size in the application.

It is necessary to return to the physical wind tunnel to avoid the difference between physical model and numerical model. In order to minimise the error and ambiguity from users in the study of natural ventilation, a virtual urban boundary layer wind tunnel was conceived, which was a numerical approach to simulate physical wind tunnel based on CFD. It concerns how to form an urban wind profile, what the minimum requirement of the computational domain size is, what the strategies of grid distribution are, and the effect of turbulence models.

4.1.2 Assumption

A virtual urban boundary layer wind tunnel in this study was specified as the numerical neutral atmospheric boundary layer wind tunnel for the study of natural ventilation in the urban environment. Based on CFD theory, this virtual wind tunnel was established according to the requirement and 'fit for purpose' (Castro and Graham, 1999), although studying wind in the urban environment using CFD has many difficulties. These include a high Reynolds number, the complexity of the flow

field with impinging, the sharp edge, the large ground roughness and the unlimited domain (Murakami, 1998). Since the effect of density stratification on the flow around the building is generally weak, and can be neglected when studying the exterior wind environment (Castro, 2003), the neutral atmospheric boundary layer was a reasonable condition in this wind tunnel.

The mechanism of traditional urban boundary layer wind tunnels provided the concept of establishing virtual urban boundary layer wind tunnels. In the typical wind tunnel (see Figure 4.1), the uniform wind generated by the fan crosses the complicated obstacles to generate the urban wind profile. The honeycomb located in the inlet flare acts to straighten the flow, while the fence and spires generate the turbulent flow as well as the atmospheric boundary layer. The regular arrays of roughness elements on the wind tunnel ground represent the natural occurrence of full scale surface roughness to establish the urban wind profile. The test models are mounted on the turntable. Wind velocity profile and turbulence intensity in the wind tunnel in the centre of the turntable are measured to ensure accuracy, and then compared with the full scale experiment. The process of the wind flow from the uniform to the urban boundary layer in the urban boundary layer wind tunnel implies that the virtual wind tunnel may reproduce its route to simulate wind flow in the urban environment.

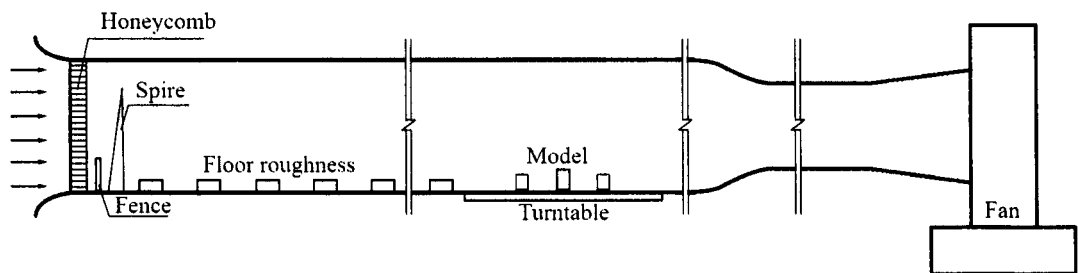


Figure 4.1 Schematic of a typical urban atmospheric boundary layer wind tunnel (Lee, 1977)

The virtual wind tunnel imitated the mechanism of the typical boundary layer wind tunnel. The turbulence flow produced by the castellated fence and spires in the wind tunnel can be formed by the pressure gradient in CFD, so that it can avoid the cost of the simulation of fences and spires. According to Cook's (1978) conclusion, the wind

profile developed naturally over a long fetch of roughness is more accurate than through the artificial method by barrier and mixing-device. The major part of the virtual wind tunnel is the flow across the long roughness fetch, which should be an equilibrium boundary layer after the urban roughness area, which means the wind profile would not be affected by the fetch. Usually a fetch length of about 250~1000 times of the roughness element height (Cook, 1978) can meet the needs of fully developed wind profile. The wind tunnel has constant fan speed, so the steady state flow - with average time and mean data - is appropriate to be simulated by CFD.

4.1.3 Structure

Instead of modelling the whole wind tunnel, including urban roughness elements and building models, the simulation can be divided into three steps (see Figure 4.2). The first step is to simulate wind in the urban roughness area, in order to acquire the steady urban wind profile after the infinite length of urban roughness elements. The resulting urban wind profile is used in the next step to fully develop the turbulent flow into equilibrium boundary conditions in the empty domain. Then the equilibrium mean wind profile is taken as the inlet boundary condition in the third step in studying the CFD domain size. By separating the simulation of the whole wind tunnel, the massive grids of the whole model can be avoided and the accuracy can be improved. It can also increase the chances of choosing the appropriate grids and turbulence model in the CFD application.

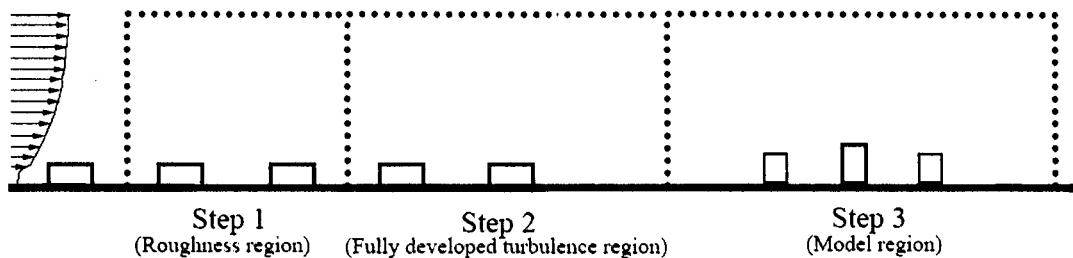


Figure 4.2 Structure of the virtual wind tunnel

A typical urban boundary layer wind tunnel at the building science department of the University of Sheffield was sampled due to its validation and successful applications. Its boundary layer free velocity (U_g) is 9.65m/s, and the height of models was 0.036m (Lee, 1977). The Reynolds number (based on the free stream velocity and

model height) was about 19000, and its roughness Reynolds number was 1261, so the flow on it was independent of the Reynolds number effect (Snyder and Castro, 2002). From the analysis, the main task was to identify the requirements of the virtual wind tunnel for studying the potential for natural ventilation on the inlet profile, the grid distribution, and the turbulence model. It was also necessary to decide the minimum - but still effective - computational domain size, especially the natural ventilation region in the urban neighbourhood.

4.2 Modelling Wind in the Urban Roughness Area

The urban roughness area in the wind tunnel plays a major role in generating the urban wind profile. It acts as a momentum sink, generating a profile of Reynolds stress through the layer, which, in turn, controls the mean velocity profile and the characteristics of the turbulence. Its function is determined by the density, the geometry of roughness elements and the fetch length. The fetch length of the roughness area determines whether or not the wind profile is fully developed.

Several problems arise when modelling wind in the urban roughness area. Firstly, it is impossible to model the whole length of the fetch, due to limited computational resources. The solution is to utilise the periodic boundary condition based on the CFD numerical advantage. The model can use one of the repeated units of the roughness element instead of the whole urban roughness area. Secondly, the surface shear stress is not clear, since the surface friction velocity is not the same as the friction velocity from logarithm law (Cheng et al., 2007). Thirdly, wind in the urban canopy layer has a complicated turbulence flow. Wind tunnel experiments in the urban roughness area was investigated by MacDonald et al., (1998), who proposed a method to model the mean wind profile in the urban canopy layer. Castro et al. (2006) studied turbulence characteristics over urban-type roughness using wind-tunnel measurements, and subsequently argued an appropriate turbulence model. Coceal et al. (2006) investigated the regular urban-like cubic arrays of obstacles with direct numerical simulations, concluding that it was impossible to describe using the steady turbulent model. However, the objective of this section is to acquire the mean wind profile for the purpose of application. Neither DNS nor LES models can be afforded for the practices.

This section identified an appropriate turbulence model for the simulation of wind in the urban environment through comparing RANS models with LES on mean wind pressure coefficients around the buildings. Meanwhile, the surface friction velocity and surface stress were investigated. This illustrated how the surface stress affected the wind profile and pressure coefficient on the surfaces. Wind character in the urban canopy was analysed and the inlet condition was evaluated for the next step in the study on the fully developed wind profile.

4.2.1 Modelling description

The periodic boundary condition was employed to study wind in the urban roughness area. As the urban wind profile in the wind tunnel was formed after the wind flow across a long urban roughness elements fetch, it is difficult to model the whole roughness fetch in CFD. This is because it consists of many boxes that are the same volume, and a regular layout of units. But one of the repeated urban roughness element units can represent the whole urban roughness element's fetch by using the periodic boundary condition in CFD. It is sensible to achieve the same wind profile of this unit as the whole roughness fetch. The periodic boundary is determined by streamwise pressure gradient or mass flow rate. The gradient pressure of the periodic boundary is deduced from the surface shear stress along the vertical domain:

$$\frac{\partial(P)}{\partial z} = \frac{\rho U_{\tau}^2}{L_z} \quad (4.1)$$

Where U_{τ} is surface friction velocity, L_z is the height of the computational domain, P is pressure.

The boundary conditions of the model were set as follows: the periodic boundary condition was imposed to the streamwise and lateral boundaries. The boundary condition at the top of the domain was symmetrical (free slip). The bottom and obstacle surfaces were taken as no-slip walls, with zero roughness height. The flow was maintained by a cyclic streamwise pressure gradient.

The computational domain size of this model was determined by the repeating unit of the fetch of the urban roughness elements. The repeating units in the original urban roughness element's fetch - being 4.5m long and 1.2m wide - is shown in Figure 4.3. The plan size of the roughness element was a square with the edge size (L) 75mm, and its height (H) was 36mm (Hussain and Lee, 1980). The distance between two near elements along streamwise dimension (S_c) was 150mm, and the lateral distance was 75mm, half of that in streamwise. The plan area density (λ) was 16.7%. In order to reduce the cost of computational resource, the vertical dimension was set as $6H_b$, so the streamwise, lateral and vertical dimensions were $6L$, $2L$ and $6H$ respectively.

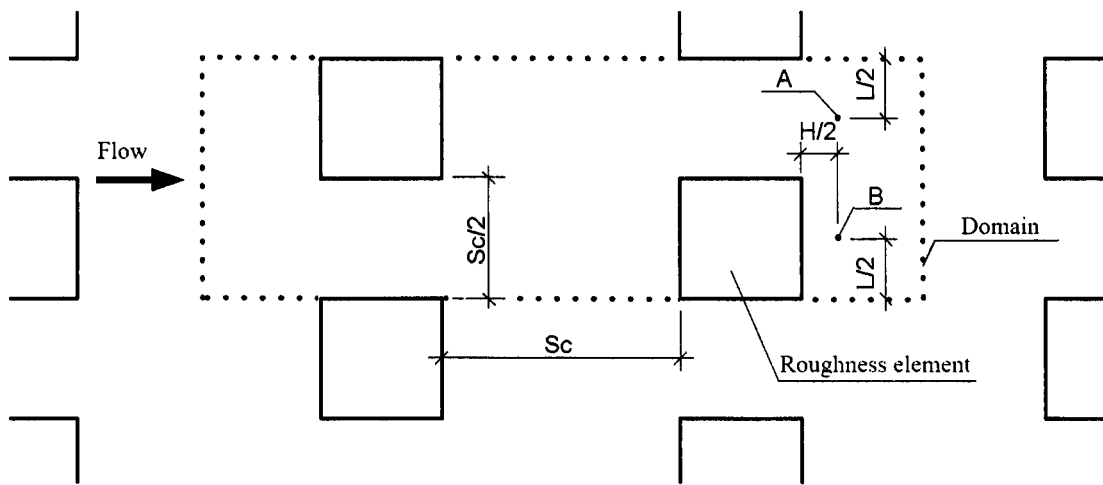


Figure 4.3 Layout of the urban roughness element area in the wind tunnel: The domain with dot lines represents one of the repeating units.

The CFD solver was set according to the characteristics of the flow and the purpose of this study. The wind flow can be regarded as incompressible turbulent flow as the density stratification around the buildings is very weak. The numerical solution of the governing equations: the mass conservation (Continuity) equations and the momentum conservation equations (Navier-Stokes), adapt finite volume method, while energy equation was not concerned since neutral atmospheric boundary layer is routine in the urban boundary layer wind tunnel. The discretised equations were solved by means of segregated method. Pressure-velocity coupling was employed using the SIMPLIC algorithm. Turbulence models were applied, including RANS turbulence models and LES was used as reference during the study of the mean wind profile in the urban canopy. As RANS turbulence models have various types, the improved turbulence models were compared and chosen depending on the condition

of the study. The solution was based on the secondary order upwind scheme difference, after using the first order upwind scheme, while the convergence criterion was based on the reduction of all the scaled solution residuals under the threshold of 10^{-5} . All the calculations were performed using the commercial CFD code FLUENT 6.3 by the high performance computing cluster at the University of Sheffield.

4.2.2 Grid sensitivity test

The purpose of the grid sensitivity test was to keep the numerical error minimal, or meet the requirement of the purpose, so it was not necessary to make the resolution close to the experiment result in this phase. By systematically increasing the number of meshes and comparing flow profiles, the errors should be reduced each time until the error is acceptable or neglected. As the surface shear stress is an open issue, here the common friction velocity U_* acquired from experimenting was taken as the surface friction velocity in this test.

Table 4.1 Details of set-up grid of the urban roughness model. NWT stands for non-equilibrium wall function; EWT represents enhance wall treatment.

Mesh type		G1	G2	G3	G4
Grid points per element	Nx	8	16	18	24
	Ny	8	22	26	36
	Nz	8	16	18	24
Stretch ratio		1	1.25	1.2	1.1
The smallest first grid length (H)		1/8	1/69	1/65	1/73
Wall treatment		NWF	EWT	EWT	EWT
Grid points in domain dimensions	Lx	48	96	108	144
	Ly	16	44	52	48
	Lz	48	36	41	62
Total grids		35,840	140,800	213,408	601,344

Four types of grid were used to study grid sensitivity based on the standard $\kappa\text{-}\epsilon$ turbulence model using the second order discretisation. The domain size is $6L \times 2L \times 6H$. The coarsest grid, G1, was used on the advice of Tseng et al (2006) who claimed that at least 6 - 8 grid points across the bluff body can meet the requirement of reasonable tests. The total grids of G2 are nearly four times of G1 and less than a quarter of G4. G1 employed the non-equilibrium wall function (NWF), and the other three grids utilised enhanced wall treatment (EWT) based on two-layer theory. As

the enhanced wall treatment has very fine grid requirements for the grid near the wall, the stretch ratio 1.25, 1.2 and 1.1 was applied to G2, G3 and G4 with the minimum grid. The first grids near the wall were $1/69H$, $1/65H$ and $1/73H$ respectively. Table 4.1 describes the details of set-up of the urban roughness elements. L_x , L_y , L_z are streamwise, lateral and vertical dimensions respectively.

Six parameters related to the wind profile were investigated in the grid sensitivity test. There were four local data: the mean velocity (U) and the mean turbulence kinetic energy (E) at the point A and B (see Figure 4.3) at the half of roughness element height (H), and two global data of the plan across the domain: the mean velocity (U_H), and the mean turbulence kinetic energy (E_H) at the height (H). Table 4.2 describes the percentage difference normalized in the finest grid G4. It can be seen that the mean velocity difference among the four types is less than 5%. However, the difference of the mean turbulence kinetic energy between G1 and G4 is about 30 percentage points. This could be due to the coarse grid of G1 as well as the non-equilibrium wall function which are not suitable to be applied into urban canopy layer. G2 and G3 show the difference with G4 as less than 6%, although the grid of G4 is more than four times of G2, and almost three times of G3. G3 is considerably better than G2.

Table 4.2 Comparison of six measured parameters among the four types of grid resolutions

Grids	Difference (%)					
	U_A	E_A	U_B	E_B	U_H	E_H
G1 vs. G4	2.2	32.9	5.3	29.0	-3.8	4.8
G2 vs. G4	1.7	3.3	-0.3	-4.1	1.9	5.8
G3 vs. G4	1.2	2.5	1.2	-0.1	1.6	4.2

From this study, the grid resolution of G3 can acquire a satisfactory wind profile. This grid resolution can be explained by Coceal et al.'s (2006) experiments, the dissipation rate in the urban canopy can be estimated as $\varepsilon \approx 2.5U_*^3 / H_b$, where U_* is defined as the friction velocity and the maximum value of dissipation rate at the top of array is $\varepsilon \approx 34U_*^3 / H_b$. the Kolmogorov length scale is $\eta \equiv (\nu^3 / \varepsilon)^{1/4} \approx 0.0075H_b$, so the smallest grid size is about 2η and 4η , which can meet the criterion that the

smallest length scale should capture the major part of the dissipation spectrum (it is typically larger than Kolmogorov length scale). The above grid sensitivity test shows that grid G3 can be seen as an independent grid.

4.2.3 Turbulence model test

As the turbulence model is an approximate approach to solve Navier-Stoke equations, there is no accurate turbulence model for any turbulence flow, even for the sophisticated Large-eddy Simulation (LES). The Turbulence model tests aim to choose an appropriate model for the purpose of studying natural ventilation in the urban environment. There are different opinions on the application of turbulence models in the urban environment. Some researchers claim that RANS models can be used to predict mean airflow data in the urban environment except the peak pressure coefficient in the arrays of blocks (Chang and Meroney, 2001; Nozawa and Tamura, 2002). Cheng et al. (2003) stated that both LES and RANS models could simulate the main characteristics of the mean flow. Lien & Yee (2004) investigated the flow in and over three dimensional arrays using RANS turbulence models. When they compared the data with the wind tunnel experiments the results showed good agreement for mean flow velocities. This implies that RANS models may be accurate enough to warrant its application to the prediction of mean flows in and over other more complex urban-type roughness arrays. On the other hand, some researchers claimed that RANS turbulence models were not appropriate to be applied to the urban environment because the characteristics of pressure and velocity in the urban canopy were dominated by the unsteady turbulent flow, meaning it could not be captured by the steady RANS (Coceal et al., 2006). As a consequence, turbulence model tests should be performed prior to its application for natural ventilation study in the urban environment.

Using the independent grid resolution G3 and the same boundary conditions, RANS turbulence models and LES models were compared in terms of their effects on mean pressure coefficients, recirculation lengths and wind profiles in and above urban canopy and reattachment lengths. Mean pressure coefficients were chosen as the parameter to check the turbulence model, as they represented the wind driven force in the urban environment for natural ventilation of the buildings. The wind profiles in

and above the urban canopy provided the appropriate inlet boundary condition for the next step of the study. The reattachment and recirculation lengths demonstrated the capability of the turbulence model to predict turbulent flow. The roughness of the obstacle wall has only a minor effect on the quantitative results (Castro, 2003), so the roughness of the model surfaces can be regarded as that of a smooth wall. As LES is only used in unsteady flow, its time step size has to be small enough to capture the smallest size eddy. The smallest grid was $1/65H$ and the time step should be smaller than the ratio of the smallest grid length to the maximum velocity, so the time step size was set as $\Delta t = 0.002T$. An eddy turnover time for the large eddies shed by the cubes is $T = U_H/H$. The initial duration $100T$ (4600 time steps) was generally adequate according to the steady result. Every time step includes 10 iterations. Statistics were collected and averaged over a further duration of $10T$ to ensure convergence.

Mean pressure coefficient on the model surfaces

Table 4.3 describes the results of the mean pressure coefficients on the four surfaces of the model by using different turbulence models. In general, both RANS and LES have a similar capability to predict the mean pressure coefficient on the building. Their results show that the windward surface encounters pressure, and the leeward surface and roof encounter suction. The maximum difference between their results is less than 50%. Compared with LES, RANS models overestimate the pressure coefficient on the windward surface, and underestimate it on the lateral surface and roof. The result shows that the standard and the improved $\kappa-\epsilon$ turbulence models overestimate the windward pressure coefficient, especially the REA model, which is about 28% larger than the LES model, while the pressure coefficient on the leeward wall by the $\kappa-\epsilon$ turbulence models is underestimated compared with the LES model. The SST model shows the closest result to the LES than other $\kappa-\epsilon$ turbulence models on the windward surface, but it underestimates the suck force on the leeward surface. Comparing all of the RANS models with the LES, it can be seen that the results of the RSM model are the closest to that of the LES. Their difference is less than 18%, which is acceptable for the early design stage, avoiding the need for expensive computational resources. However, the RSM model is the seven-equation RANS model, which requires more computational resources than the other two equation models. Among the two equations models, the SST model is an appropriate model to

predict the wind pressure coefficients around the building in the urban environment, as the discrepancy with LES is less than 22%.

Mean wind profile in the urban canopy layer

The turbulent flow in the urban canopy determines the complicated pressure distributions on the building surface. In order to understand the effect of turbulence models on the pressure distribution and choose an appropriate turbulence model for the next step of the study, the mean wind velocity profile and the turbulence energy profile in the urban canopy layer were investigated using various turbulence models at point B (see Figure 4.3).

Table 4.3 Comparison of mean pressure coefficients on the four surfaces of the model in the urban canopy by the various turbulence models

Turbulence model		Windward	Leeward	Lateral	Roof	
Steady RANS	Two- equation models	STD $k - \varepsilon$	0.0601	-0.0399	-0.0591	-0.0607
		RNG $k - \varepsilon$	0.0628	-0.0364	-0.0601	-0.0652
		REA $k - \varepsilon$	0.0635	-0.0361	-0.0624	-0.0658
		SST $k - \omega$	0.0499	-0.0268	-0.0574	-0.0664
	Seven- equation model	RSM	0.0574	-0.0329	-0.0635	-0.0633
unsteady		LES	0.0497	-0.0342	-0.0659	-0.0762

The mean wind velocity profile in the urban canopy is underestimated by the RANS model, when compared with the LES model. Figure 4.4 shows the mean velocity profile in the urban canopy layer using various turbulence models. All of the turbulence models have similar velocity profiles. The velocity increases from the bottom to the top of the urban canopy. Taking the profile provided by the LES as the criterion, the velocity profile from the SST model is the worst model for predicting velocity profile: the discrepancy is up to 15%. Among all of the RANS turbulence models, the RSM model is the best model for predicting velocity profile. The discrepancy of mean velocity between the RSM and LES is less than 8%. It also has been observed by Santiago et al. (2007) that the velocity in the urban canyon is underestimated by CFD compared with the wind tunnel experiment.

The turbulence kinetic energy profiles provided by the various turbulence models are considerably different. Figure 4.5 illustrates the mean turbulence kinetic energy profile normalized with the square of the free stream velocity, using various turbulence models below building height. RANS turbulence models have similar profiles, which are largely different from the LES, especially in the region near the ground. The reason can be due to the instantaneous flow and near wall treatment. The LES can directly calculate the unsteady flow and turbulence length larger than the subgrid. The RANS models utilise the approximate assumption on the wall treatment in steady state. The RNG model shows the largest discrepancy of turbulence kinetic energy with the LES, a discrepancy figure of about 50%. It further confirmed Xie and Castro's (2006) observation that the RANS models underestimated turbulence in the urban canyon. There is still more work for researchers to do in improving the near wall treatment and the RANS turbulence models.

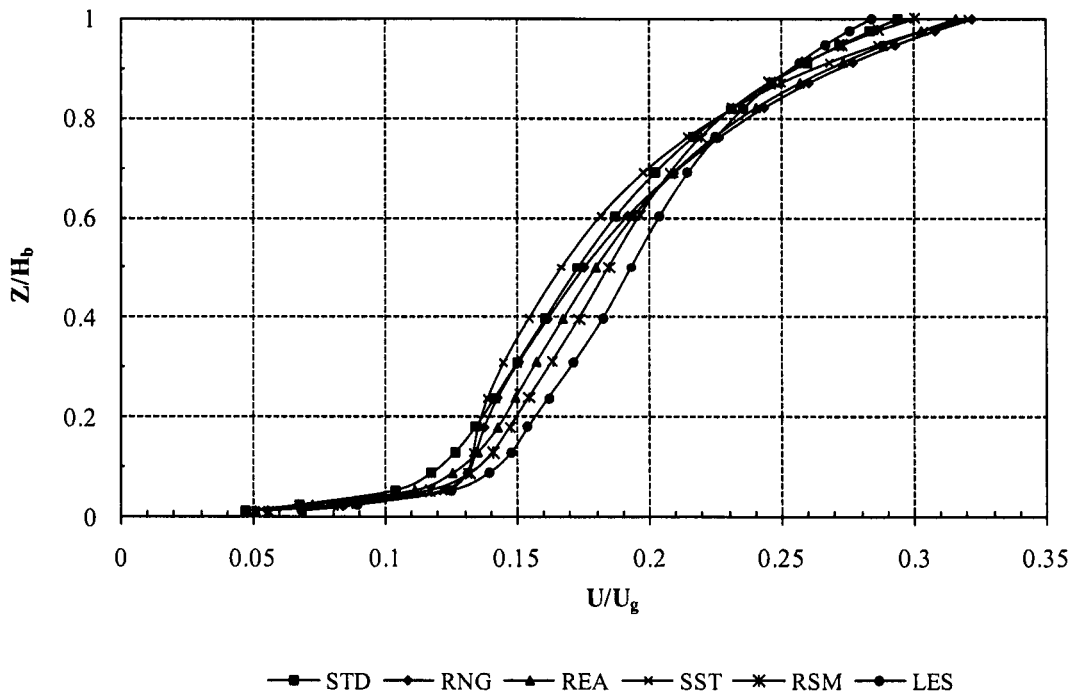


Figure 4.4 Comparison of mean velocity profiles in the urban canopy by the various turbulence models

Reattachment length and recirculation length

Reattachment length and recirculation length imply the capability of turbulence models on predicting turbulence flow. Table 4.4 shows the comparison of reattachment length and recirculation length around the model in the urban area by various turbulence models. In general, all the turbulence model can generate separation, which is contrary to the opinion that the standard $\kappa\text{-}\epsilon$ cannot acquire separation around the bluff body (Murakami and Mochida, 1988). The reason may be due to the employment of the enhanced wall treatment, which requires finer grids than the wall function. The recirculation length of the LES is the shortest among all of the turbulence models, measuring about 1.43 times of the building height. The RANS turbulence models underestimate the reattachment lengths on the roof and overestimate the recirculation lengths. Among all of the RANS models, the results of the RSM model are the closet to those of the LES model.

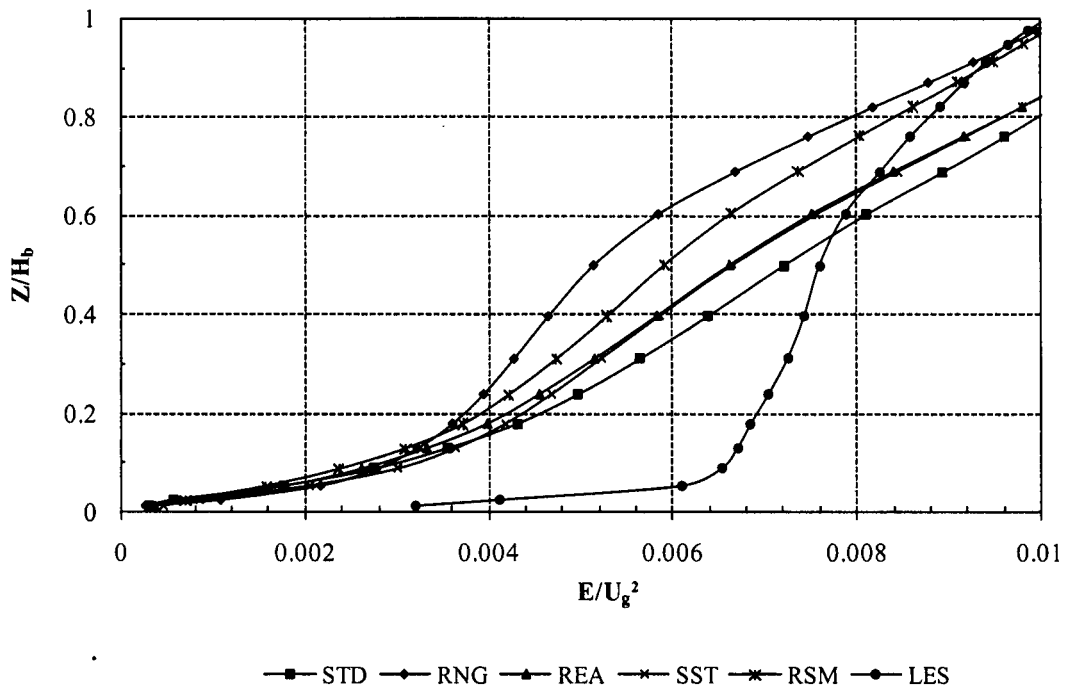


Figure 4.5 Comparison of mean turbulence kinetic energy profiles in the urban canopy by various turbulence models

The nature of RANS models is a steady-state methodology, which cannot accurately predict the transient wind field (Li et al., 2006). Therefore, the current strategy for turbulence models is to get the averaged mean wind profile by using the steady RANS turbulence model. This is because the unsteady RANS provides results that

are only marginally more accurate, while costing more in terms of time and computational resource than the steady RANS models.

The choice of an appropriate turbulence model depends on its purpose, and also upon compromises of computational resource and physical modelling. Considering computational resources and an end purpose of designing for natural ventilation, the current accuracy of the RSM is acceptable, although the LES is best choice. The comparison of turbulence models confirmed that the RSM model is the best RANS model, and its results are very close to the sophisticated LES turbulent model, which is further evidence that the RSM model can be used to study wind flow around the building for the purpose of designing for natural ventilation. The RSM turbulence model is more appropriate than the two equation turbulence models, such as the standard $k-\epsilon$ and its improved turbulence model, because they still have problems in capturing accurate separation and reattachments, as well as assuming wind as isotropic flow.

Table 4.4 Comparison of reattachment and recirculation lengths around the building by the various turbulence models

Turbulence models	Reattachment length (roof) (L)	Reattachment length (lateral wall) (L)	Recirculation length (H)
STD	0.07	0.25	1.75
RNG	0.09	0.41	1.81
REA	0.08	0.35	2.00
SST	0.16	0.51	2.06
RSM	0.11	0.31	1.56
LES	0.39	0.33	1.43

The RSM turbulence model also has some problems. It is not only sensitive to the fine grid, but also it is difficult to converge. This is probably because the RSM model is close to describing the characteristics of turbulence. As these are random and anisotropic, The RSM model cannot be simplified as steady state. An alternative is the SST turbulence model. The SST has a better result on the pressure coefficient than velocity in the canyon. In the street canyon, the wind pressure on building facades are the subject of this study. This implies that one turbulence model is not suitable to study any parameters. In this study, the RSM turbulence model is the appropriate model to study the wind profile in the urban environment, because this simple model can utilise the anisotropic wind flow in the urban environment. The

SST is the appropriate model to study the wind pressure coefficient around the building in the complicated urban environment.

4.2.4 Friction velocity

Friction velocity can be used to determine the pressure gradient along the boundary layer, as it is derived from measuring shear stress near the surface. It affects the Reynolds stress along the vertical boundary layer, which involves the velocity profile and turbulence profile. It is usually taken from the log law equation (see Equation 4.2).

$$U_* = U_{ref} \cdot K_v \cdot \ln\left(\frac{Z_0}{Z_{ref}}\right) \quad (4.2)$$

Where U_{ref} is the reference velocity at the reference height Z_{ref} , the roughness length Z_0 is an empirical data. Criticisms have been made that the surface friction velocity is different from U_* . This is because the former is deduced from surface shear stress, and the latter is from the logarithm law in the inertial sublayer (ISL) (Cheng and Castro, 2002; Kastner-klein and Rotach, 2004). There is no clear correlation between them, as U_τ is related to the roughness element volume and arrangement. The question arises of which surface friction velocity can be used to calculate the pressure gradient.

In this study, three kinds of friction velocities were investigated to identify the appropriate one for the wind profile. The three friction velocities were U_* , U_{rsm} , and U_e . The former two are from wind tunnel experiments (Lee, 1977): $U_* = 0.0065U_g^2$; U_{rsm} was deduced from the Reynolds stress near the surface area. U_e was from the experience of Cheng et al. (2007), who argued that the surface shear stress was 25% larger than that measured in inertial sub-layer. Table 4.5 shows the three kinds of surface friction velocity, and the correspondent pressure gradient along the boundary layer. The pressure gradient was obtained from equation 4.1. Pressure gradient from U_{rsm} was smaller than that from U_* , which was smaller than U_e .

Table 4.5 Friction velocities and pressure gradients

	U_*	U_{rsm}	U_e
U_T (ms^{-1})	0.627	0.621	0.701
ΔP (Pam^{-1})	-2.23	-2.19	-2.79

The pressure gradient can change the velocity profile above the building height, but only slightly affect the profile below the building height. Figure 4.6 shows the mean velocity profiles (below 6 times the building height with 3 pressure gradients) against the result from the wind tunnel experiment. Pressure gradients can significantly affect the profile above the building's height. The large pressure gradient makes the velocity increase rapidly along the vertical boundary layer. Compared with the wind tunnel experiment, the pressure gradient from U_{rsm} generates the best profile out of the three pressure gradients. The discrepancy of the profile from U_* with that of the wind tunnel is less than 10%. The surface friction velocity derived from the wind tunnel is usually larger than its real data. The reason is attributed to the limited fetch of the urban roughness area for generating the fully developed flow. The profile from U_e shows a larger velocity increase than the wind tunnel test; however, the profile below the building height is only slightly affected by the pressure gradient.

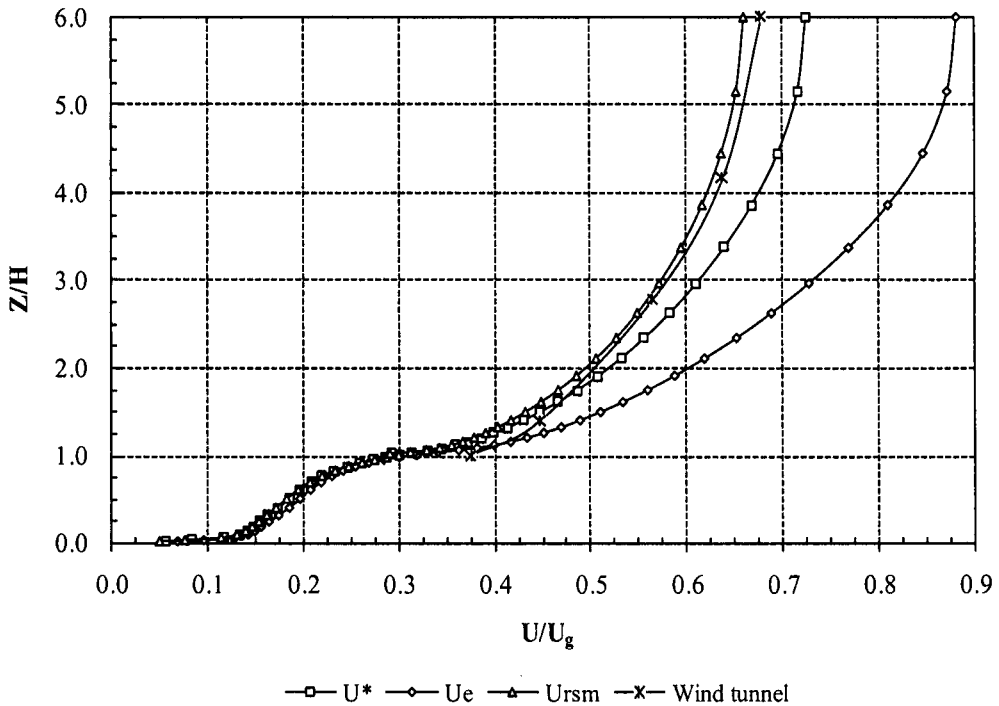


Figure 4.6 Comparison of mean velocity profiles by the various friction velocities

From the above results, it can be seen that simulation can generate more accurate wind profiles than algorithms, such as log law or power law. Simulation directly concerns the effect of the roughness surface on the roughness sub layer, as well as in the urban canopy layer, while algorithmic methods are not suitable for describing the profile around the building. In addition, this is further evidence that Richards and Hoxey's (1993) assumption - of a constant shear stress along the boundary layer for a wind profile - is inaccurate. As the data of a velocity profile and a turbulence profile from the wind tunnel is difficult to acquire at design stage, the method using the pressure gradient is a readily available approach to gaining the urban wind profile. The estimate of surface friction velocity from the log law equation can be used to calculate the pressure gradient along the vertical boundary layer.

4.2.5 Wind profile in the urban roughness area

Wind profiles in the urban canopy layer are unstable in the different positions. The velocity at a different position - even in the same horizontal plan - is considerably different (see Figure 4.7), because the flow in this layer is interfered with by the surrounding buildings, and is not fully developed. In order to describe wind profile, Castro et al.(2006) performed four points to represent the mean profile in the wind tunnel experiment. MacDonald (2000) took the five weighted average profile behind the nearest upwind model 0.5H by a pulsed-wire anemometer in the wind tunnel. As the different position of measured points, their profiles are different. This implies that the mean wind profile acquired from some random points is not accurate. Compared with some points of the wind tunnel tests, the area-weighted averaged data of the urban roughness area in CFD would more accurately represent the mean data of wind profiles.

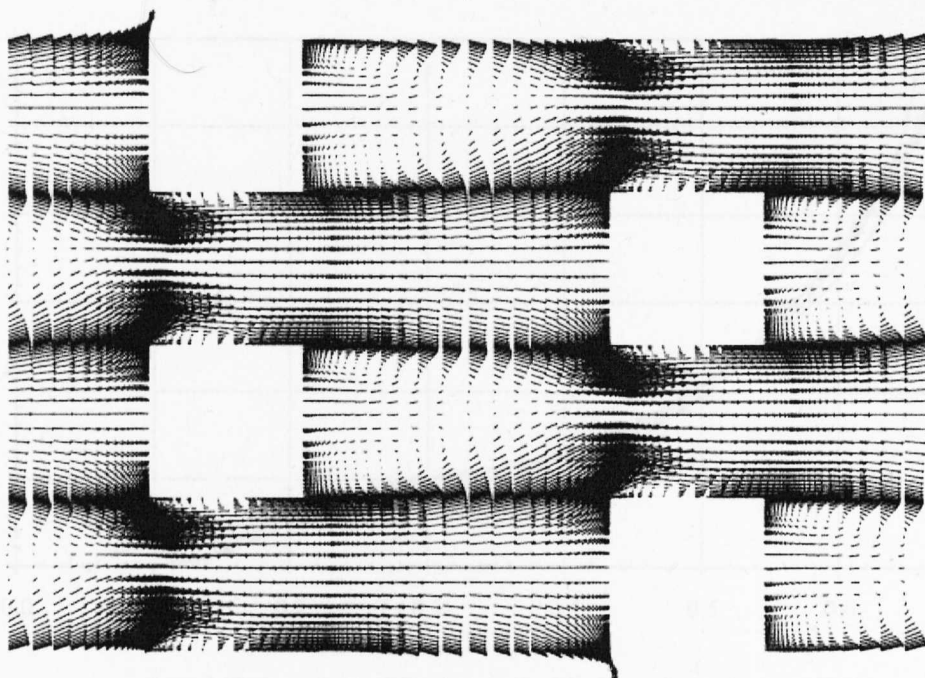


Figure 4.7 Mean velocity vectors of the flow in the urban canopy at the height of 0.5 Hb

Mean Velocity Profile

The mean velocity profile in the urban roughness area as measured by CFD shows good agreement with the profiles generated by other theoretical algorithms and the wind tunnel experiment. Figure 4.8 illustrates the present velocity profile compared with the methods of MD (MacDonald, 2000) and KR (Kastner-klein and Rotach, 2004) as well as the wind tunnel test (Hussain and Lee, 1980). The height of the domain is normalized by the building height (H_b) and mean velocity and TKE are normalized by free stream velocity (U_g). The data above $2H_b$ from CFD are much closer to the results of the wind tunnel experiment. The difference between them below $2H_b$ could be because the wind tunnel test is based on the point and present test on the average weighted area. Below the building's height, the CFD method has a similar profile to the MD method, with the largest difference being less than 8%, but the wind tunnel experiment did not provide the result of velocity, due to the difficulty of testing velocity near the ground. As the present result shows good agreement with other methods, especially the MD method, this further confirms that the mean wind profile in the urban roughness area should not be expressed by the simple power law or log law.

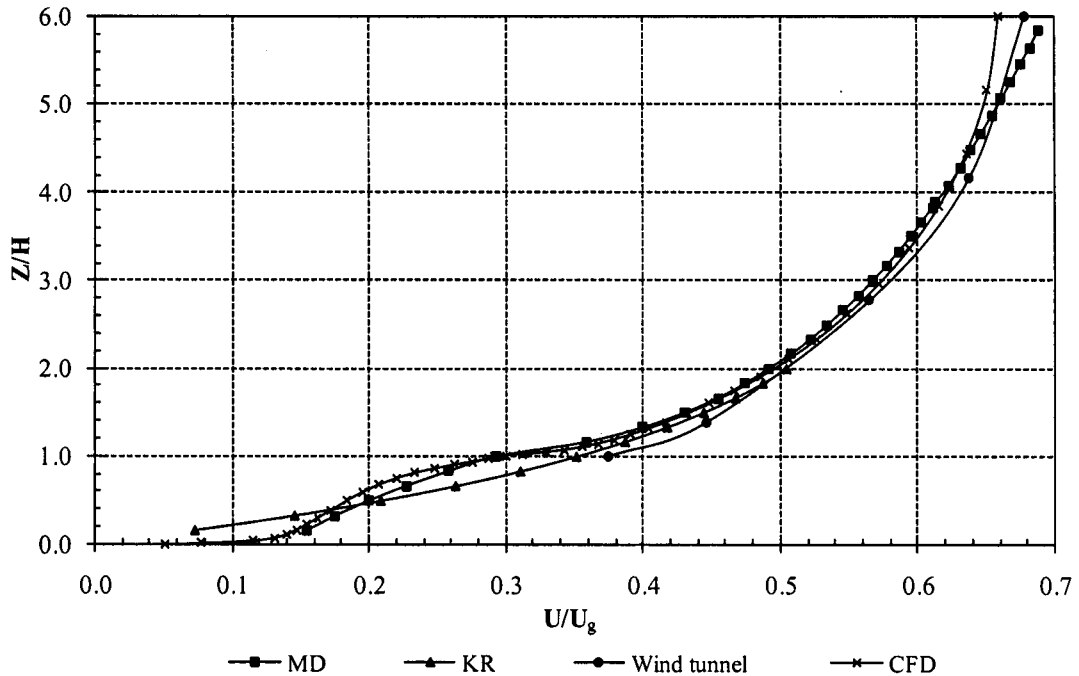


Figure 4.8 Mean wind velocity profiles in the urban area by the various methods

Turbulence Kinetic Energy Profile

Turbulence kinetic energy (TKE) describes the mean of kinetic energy per unit mass associated with eddies in turbulent flow along the vertical boundary layer. Figure 4.9 shows TKE profiles generated by the wind tunnel experiment, KR method and the CFD test. Below the building's height, TKE dramatically decreases as the distance from the ground increases. The maximum TKE is just above the building's height, at which point surface stress also reaches its maximum. As the wind tunnel test was conducted above the building height, and not including the region below building height, the valid data are limited. Above the building height, TKE profiles are varied, depending upon the methods used. The TKE profile generated by the KR method is lower than those generated by CFD and wind tunnel test. The CFD result demonstrates the TKE profile like a spline against the irregular curve profile from the wind tunnel test. The larger TKE profile difference between the CFD method and the wind tunnel test is because an equilibrium boundary layer had not yet been fully achieved (Lee, 1977). It is also confirmed that the TKE profile is like a curve shape (ESDU, 1985; Rao and Nappo, 1998). The ideal distribution should represent a constant shear stress followed by a gradual decrease to zero at the top of the boundary layer, similar to the distributions reported by Cheng and Castro (2002).

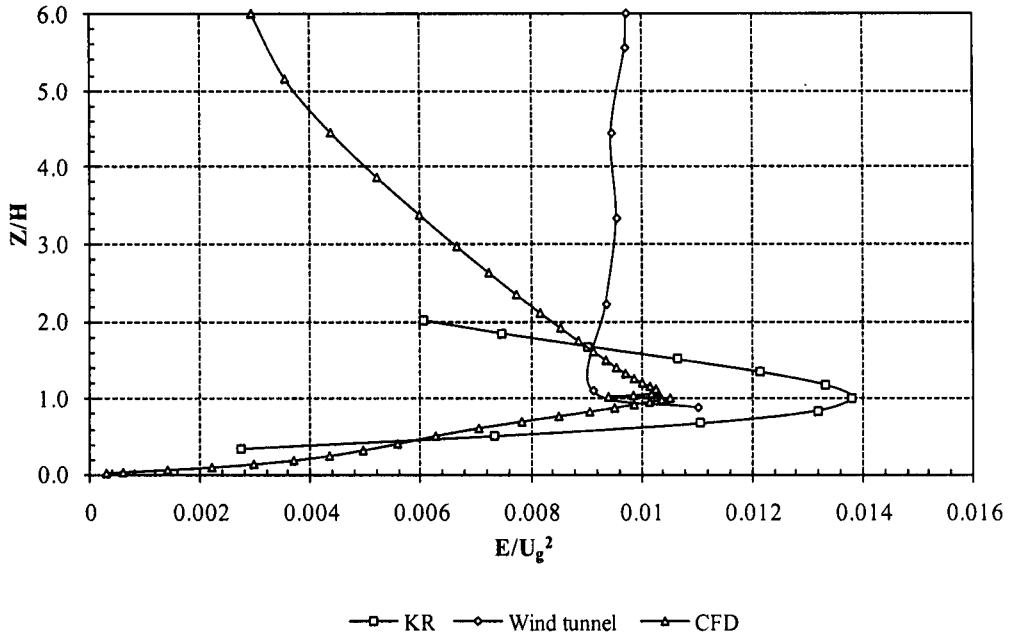


Figure 4.9 Mean turbulence kinetic energy profiles in the urban area by the various methods

In an urban roughness area, the TKE profile has certain characteristics. The maximum turbulence kinetic energy occurs around the building's height. Below this height, the turbulence kinetic energy increases as the height increases. Above the height of the maximum level of turbulence kinetic energy, the data decrease with the increase of height. This characteristic explains why the peak strike of TKE profile occurs near the ground in Hargreaves and Wright's (2007) observation on the CFD application.

Using one of the repeating units of the urban roughness element area and period boundary conditions in CFD can acquire a reasonable mean wind profile in the urban roughness element area, as compared with the wind tunnel experiment. The pressure gradient generated by the friction velocity from log law can much more accurately express the wind profile than the surface stress velocity can. Comparing the results of various RANS turbulence models with the LES, the RSM model is the best turbulence model to predict the wind profile in the urban area in RANS models. The SST model is a more sensible and feasible turbulence model for predicting the mean wind pressure coefficient around the building in the urban environment. This is because the RSM is rather sensitive and more costly in terms of time and

computational resource. The two-layer wall treatment and near wall model are necessary when studying mean wind flow around the building in the urban area.

This method is much more accurate for expressing the wind profile in the urban area. It provides the data in the urban canopy which is difficult to acquire from the wind tunnel experiment. The wind velocity profile considers the roughness length effect. The limited urban roughness element fetch in the wind tunnel can be extended by the period boundary layer in CFD, so the turbulence kinetic energy profile is improved. Compared with the common method RH, this method considers the effect of urban roughness, while avoiding the complexities of urban roughness element modelling.

The above study presented the mean wind profile in the urban roughness area. The wind profile in the urban canopy layer is changeable depending upon position. However, the equilibrium boundary layer should be established before studying the wind around the building in the virtual urban wind tunnel, because the non-equilibrium boundary layer can impact on the pressure around the building. The wind profile after the urban roughness area would be taken as the inlet profile for the next step in the study: developing the equilibrium boundary layer.

4.3 Modelling equilibrium boundary condition

An equilibrium boundary condition in the wind tunnel is that the wind profile remains horizontally homogenous in the empty domain. The first step is usually confirming the equilibrium boundary condition, prior to mounting the models on the turntable (Lee, 1977). The wind flow passes a long distance from the last roughness element to the turntable, and reaches the equilibrium condition around the turntable. In the virtual wind tunnel, the objective is to investigate the wind profile beyond the urban roughness element area, and identify the equilibrium boundary condition for modelling.

The non-equilibrium boundary condition commonly occurs in the CFD applications. The velocity and turbulence profiles decay along the fetch, even though there are no obstructions due to the wall function (Blocken et al., 2007; Hargreaves and Wright,

2007). Another reason is that the commonly-used inlet boundary condition recommended by Richards and Hoxey (1993) is not appropriate for assuming the constant pressure and constant shear stress in the urban boundary layer wind tunnel, which could lead to a larger difference between inlet and outlet wind profile. The solution for this problem is to replace the wall function problem with the enhanced wall treatment, which is based on two-layer theory and employs the improved inlet boundary condition. This section tries to use the equilibrium boundary condition from the urban roughness area and develop an equilibrium wind profile in the empty domain. The fully developed turbulence profile would be used as the inlet profile for the model test.

4.3.1 Modelling description

After passing the fetch of the urban roughness area, the flow requires a distance to build fully developed turbulence in the empty domain. Behind the last urban roughness element, the flow has complicated phenomena in the wake region, including separation and recirculation. In this region, the turbulent wind flow is not fully developed, and the data of the wind profile changes with the increase in distance. According to Versteeg and Malasekera (2007), the domain of fully developed turbulence after the obstacle should be not less than 10 times the height of the obstacle. However, this distance may be not enough for the flow past the urban roughness element area, as the maximum turbulence energy around the building height could require a long distance for the development of turbulence.

This model consists of one unit of repeated roughness elements and a long empty domain along the downstream direction (see Figure 4.10). The repeated unit represented the last unit of the urban roughness element in the wind tunnel. The empty domain was employed to check whether or not the flow was fully developed. The domain size after the urban roughness element was set as $40H$, which was enough to ensure the flow was fully developed, as compared with $20H$ in the wind tunnel experiment. The vertical dimension was $6H$ — the same as the urban roughness area model, and the lateral dimension was dependent upon the width of one unit of the urban roughness element and twice the roughness element length.

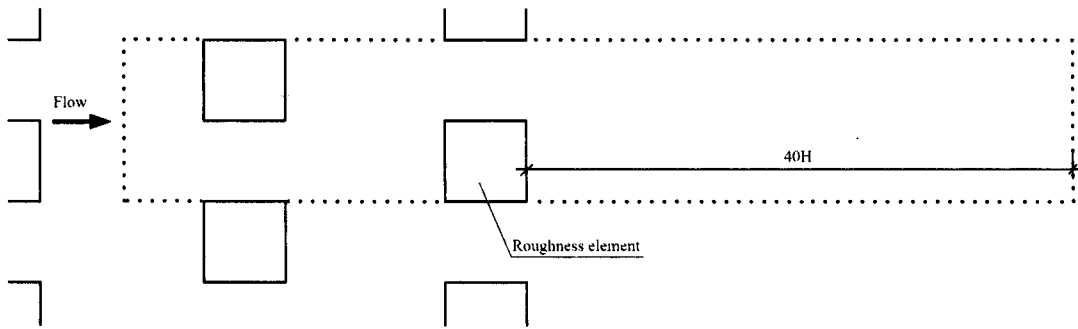


Figure 4.10 Plan of the model for the horizontally homogeneous wind profile. The domain with dot lines represents the computational domain.

The basic equations for the numerical simulation were shown in Chapter 3. Following the suggestion from section 4.2, the RSM turbulence model and the enhanced wall treatment based on two-layer theory near the wall were employed in this test. All physical quantities were normalized by the representative values. The representative length was the roughness element height, H . The representative velocity was the free stream velocity, U_g . The inlet boundary was interpolated from the outlet boundary condition of urban roughness element area model in section 4.2, because the flow had passed a long fetch of urban roughness area. The lateral boundary was set as the periodic boundary conditions, and the top was set as a symmetric boundary. The outlet was set as an outflow boundary. The ground was set as a wall boundary with zero roughness height. Based on the independent grid of the urban roughness area model G3, the grid of the empty domain was tested on three grids: $32 \times 24 \times 16$, $48 \times 32 \times 24$ and $72 \times 48 \times 36$. The difference in mean velocity in the domain centre and outlet of the three grids is less than 1%. So the grid $48 \times 32 \times 24$ was chosen as the grid to test the inlet profile.

4.3.2 Mean velocity profiles in the empty domain

The mean velocity profile tends to be fully developed behind the obstacle in the empty domain. Figure 4.11 shows the five vertical profiles at the points behind the obstacle $1H$, $10H$, $20H$, $30H$ and $40H$ respectively. The velocity at the same level below the building height increases with the extension of the fetch, but the magnitude of the increase between the same distances is different. The change of the velocity profile in the first $10H$ is rather large, due to the disturbed and not fully developed turbulence flow. This change scope in the second $10H$ and is smaller than

the first $10H$, but is still larger than 30%. Only in the fourth $10H$ does the velocity in the last interval increases less than 7%.

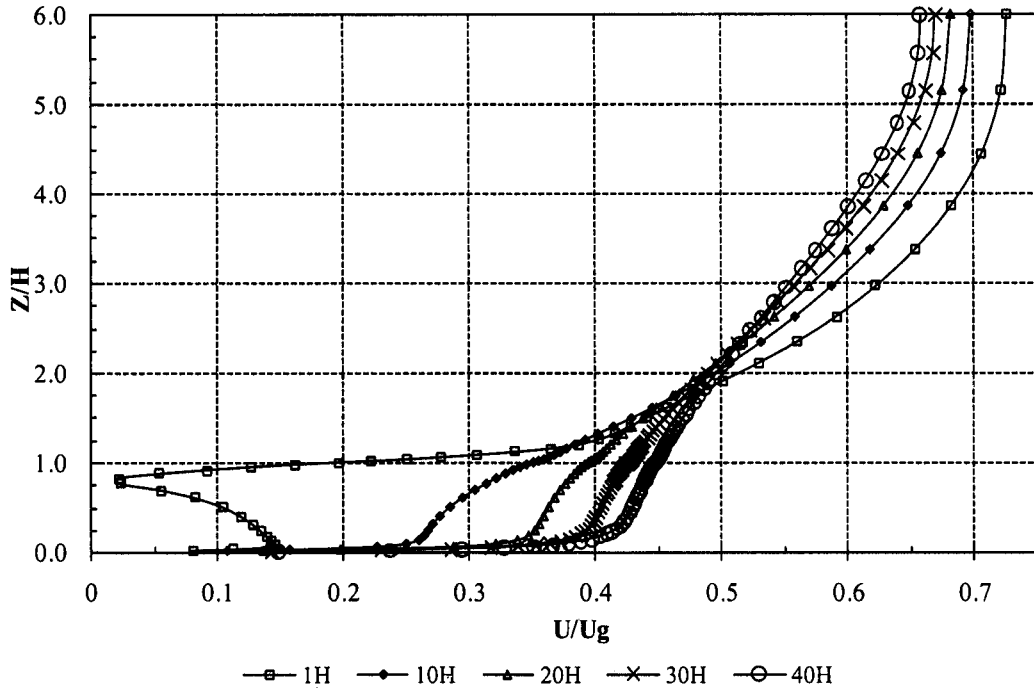


Figure 4.11 Mean velocity profiles along the fetch in the empty domain

The velocity at the same level above the building height declines along the fetch, but the difference is not as large as below the building height. In general, the profiles above the building height are fairly similar, and the difference in the $10H$ is less than 5%. The wind velocity profile tends towards equilibrium. As the difference of the velocity profile among the fourth $10H$ is smaller than 7%, the mean velocity profile at the position of $40H$ behind the obstacle can be seen as the equilibrium velocity profile.

4.3.3 Turbulence profile in the empty domain

The turbulence kinetic energy profile in the empty domain changes with the extension of the fetch. Figure 4.12 illustrates the TKE profiles at five positions behind the roughness element $1H$, $10H$, $20H$, $30H$ and $40H$. The position of the maximum TKE rises up, and the magnitude of the maximum TKE drops down with the increase of the fetch. At $1H$, the maximum TKE occurs around the building

height with an especially large magnitude, which is overestimated by CFD. This is because the adverse pressure and velocity gradient around the wall dramatically affect the turbulence. At $40H$, the maximum TKE is up to $2.3H$ and the magnitude of the maximum TKE reduces by $0.0065U_g^2$, which is similar to what happens in the wind tunnel. The changes of the maximum data in every $10H$ interval along the fetch reduce with the increase of the fetch. The discrepancy of the magnitude and position of the maximum TKE at $30H$ and $40H$ is less than 8%. The vertical profiles above $5H$ are close, which means that TKE may not be affected by the roughness. The turbulence profile at $40H$ can be taken as the equilibrium turbulence profile.

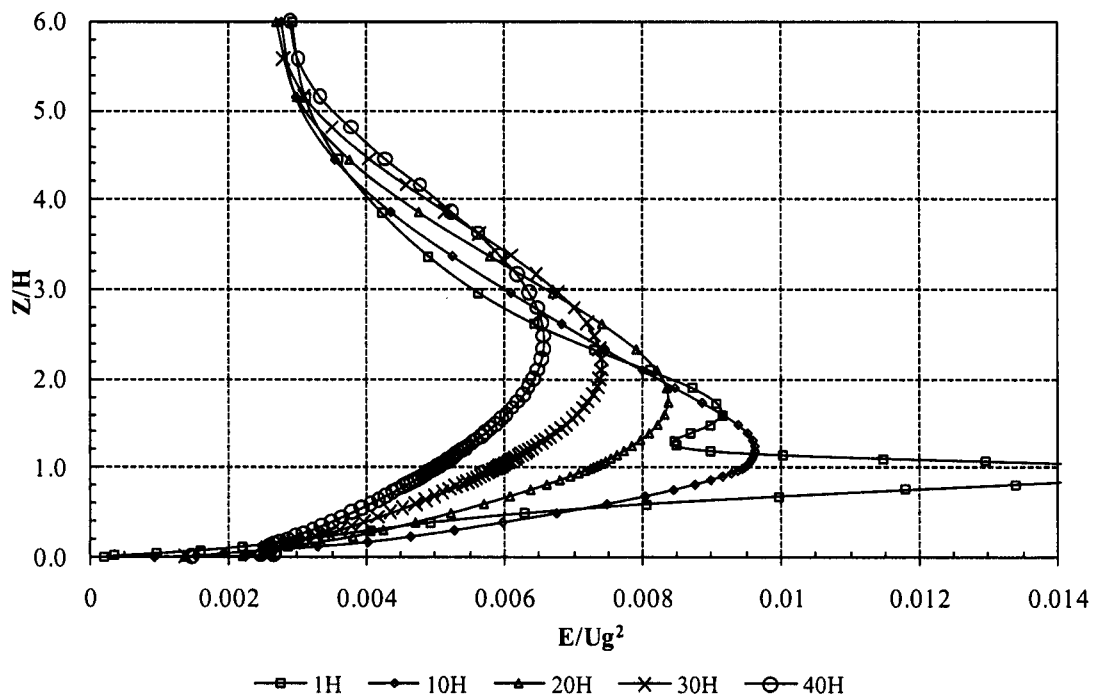


Figure 4.12 Turbulence kinetic energy profiles along the fetch in the empty domain

The turbulence energy dissipation rate profile represents another parameter of turbulence in the boundary layer. Figure 4.13 shows the turbulence energy dissipation rate profiles at five positions along the fetch in the empty domain. In general, the dissipation rate reduces dramatically with the increase of height, and tends towards zero at the boundary layer height. At the position of $1H$, the dissipation rate has a large magnitude at the building height, which is related to the maximum turbulence kinetic energy at this position. With the increase of the fetch, the difference of dissipation rate among the $10H$ intervals drops down. In the fourth $10H$, the difference is smaller than 8%, which can further confirm that the turbulence profile

at the $40H$ behind the obstacle in the empty domain the equilibrium turbulence profile.

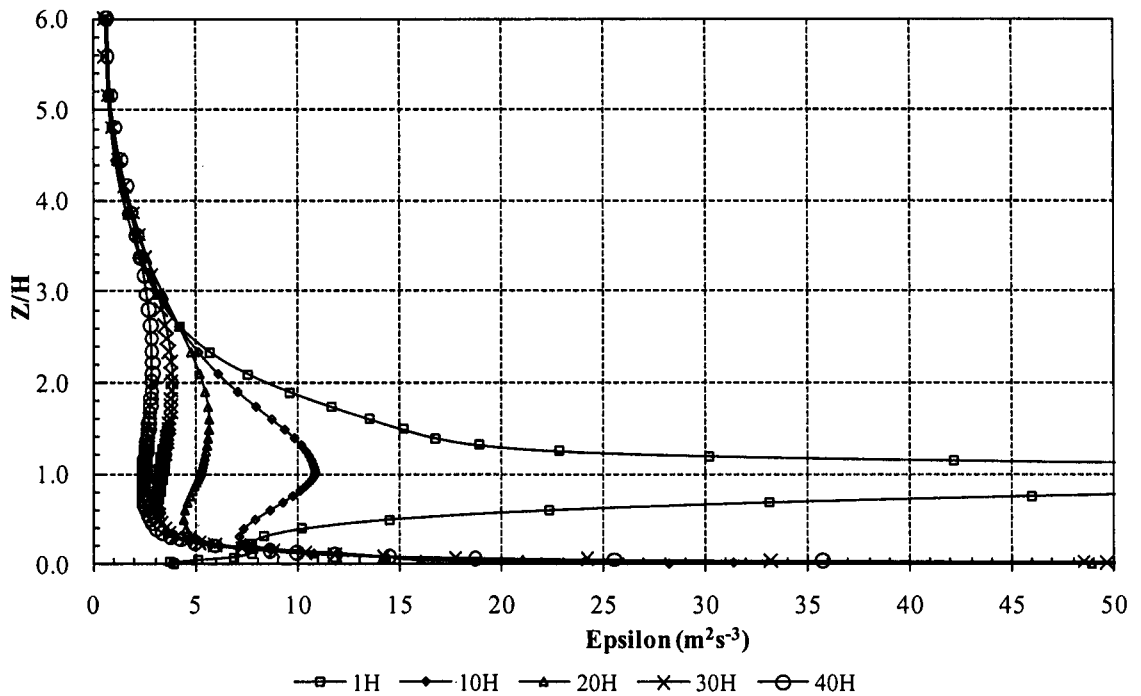


Figure 4.13 Turbulence dissipation rate profiles along the fetch in the empty domain

4.3.4 Discussion

After the study of modelling the equilibrium boundary condition, the major findings are as follows. The wind profile behind the obstacle develops from the disturbed condition to the equilibrium condition in the empty domain. Along the streamwise direction, the difference of profiles in the $10H$ gradually drops down. The equilibrium wind profile is achieved after the wind passes $40H$ behind the obstacle. The wind velocity below the building height increases rapidly to equilibrium at $40H$, whilst the wind velocity above the building height decreases slightly. The equilibrium TKE profile reaches its maximum data above the ground at $2.3H$. The TKE reduces with the increase of the boundary layer height. The turbulence kinetic energy dissipation rate decrease dramatically near the ground, and then reduces with the increase of boundary layer height.

The current equilibrium boundary velocity profile in the urban environment is distinguished from log law and power law profiles (see Figure 4.14). Both empirical

algorithms are, in general, used to describe the profile above the building height. The discrepancy of the profiles from present, power and log law above the building height is less than 5%, while the present profile has larger differences from the empirical laws below the building height. The velocity at the same height on the present profile is larger than those on other profiles. This is because both the log law and power law are not suitable for the profile near the ground. Log law is derived from the inertial sublayer, in which the shear stress is constant, but this is not true for the profile below the roughness height (Cheng and Castro, 2002). Power law does not consider the region below the roughness height, and it is only suitable for the outer sublayer of atmospheric boundary layer (Simiu and Scanlan, 1986). When using the empirical algorithm velocity profile, the profile near the ground is interpolated – and thus not real data.

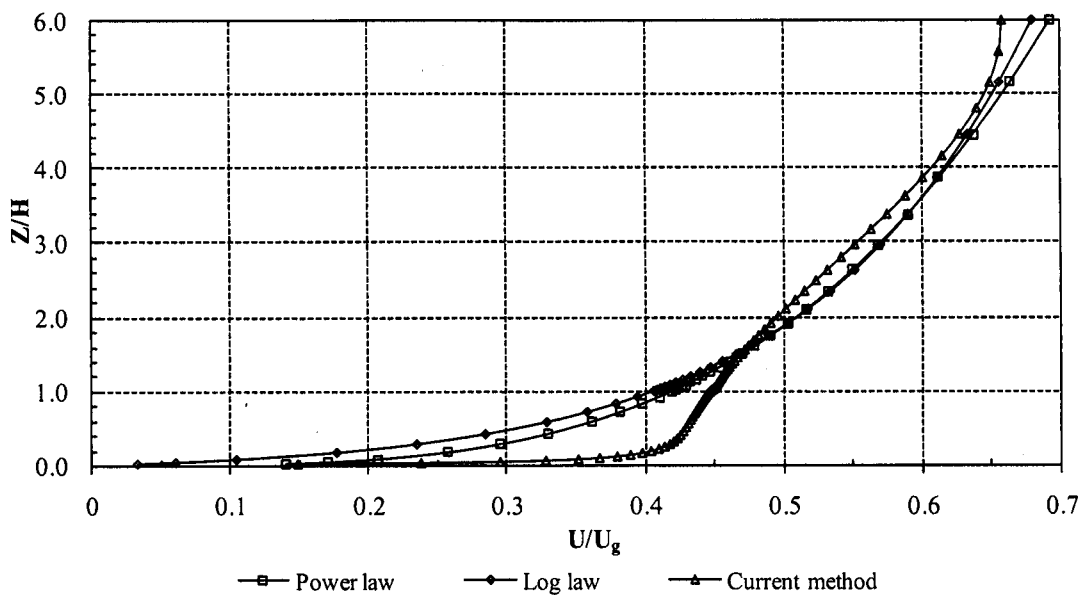


Figure 4.14 Comparison of equilibrium velocity profiles by the various methods

The equilibrium turbulence kinetic energy profile in the urban environment has two distinctive characteristics. One is that its maximum turbulence kinetic energy occurs at 2.3 times of the building height (see Figure 4.15). In the physical wind tunnel, the friction velocity (U_*) is usually obtained from this level, in which the shear stress is constant. Consequently, the friction velocity (U_*) is smaller than the surface friction velocity (U_s). Another characteristic is the shape of profile is a spline, which is

divided into two parts by the maximum TKE. These two characteristics can be used to make a decision about the appropriate equilibrium profile to use in the urban environment.

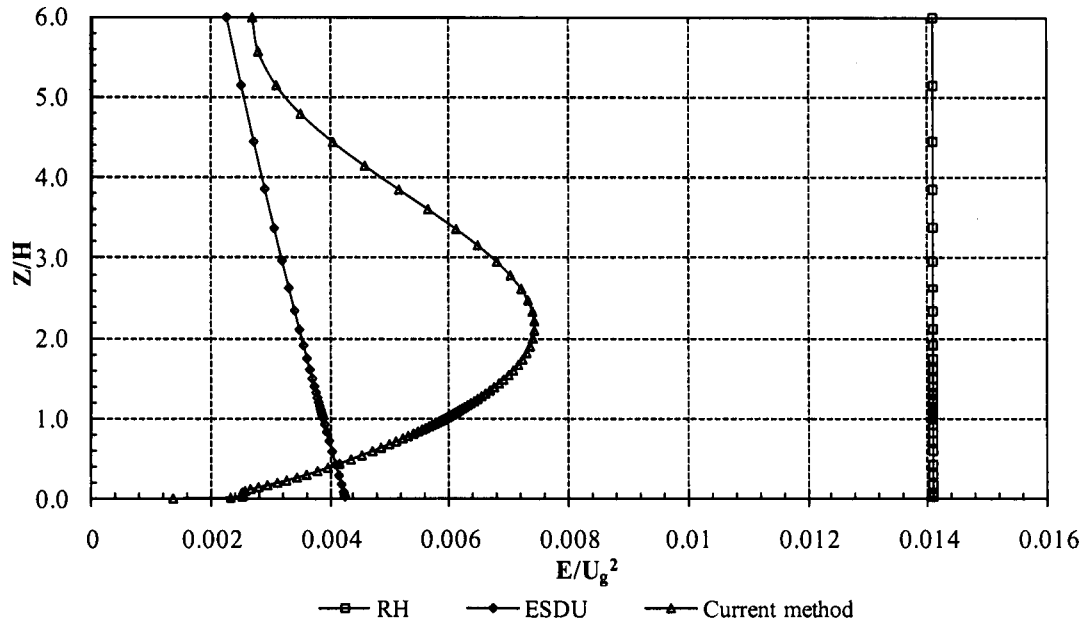


Figure 4.15 Comparison of turbulence kinetic energy profiles by the various methods

The current TKE profile from the simulation of the wind tunnel is distinguished from other methods. The commonly used RH method (Richards and Hoxey, 1993) described the turbulence kinetic energy as a constant, because it assumed that the shear stress was constant along the height. This assumption is only appropriate for the inertial sublayer, in which the shear stress is constant, so this method cannot be used to describe the TKE profile in the urban environment. ESDU's (1985) method¹ deduced an equation to describe the TKE profile. This profile presents the TKE reduces with the increase of boundary layer height, but it does not consider the effect of the ground on the profile. Both methods are unsuitable for describing turbulence kinetic energy profile in the urban environment. The profile from Yoshie et al.'s (2007) test in the urban boundary layer wind tunnel can further confirm the two characteristics of the TKE profile are appropriate for use in the urban environment.

¹ ESDU (1985) defined the shear stress along the vertical boundary layer as $\tau z = -\rho U_*^2 (1 - Z/\delta)^2$, so $E = 0.5 U_*^2 (1 - Z/\delta)^2$.

Associated with TKE, the turbulence kinetic energy dissipation rate is another parameter used to describe the special characteristics of turbulence. It has a correlation with turbulence kinetic energy, expressed as Equation 4.3 (Fluent, 2006):

$$\varepsilon = \frac{C_{\mu}^{1/2} E^{3/2}}{Z} \quad (4.3)$$

where $C_{\mu} = 0.09$; E is turbulence kinetic energy, and Z is the vertical height at the boundary layer.

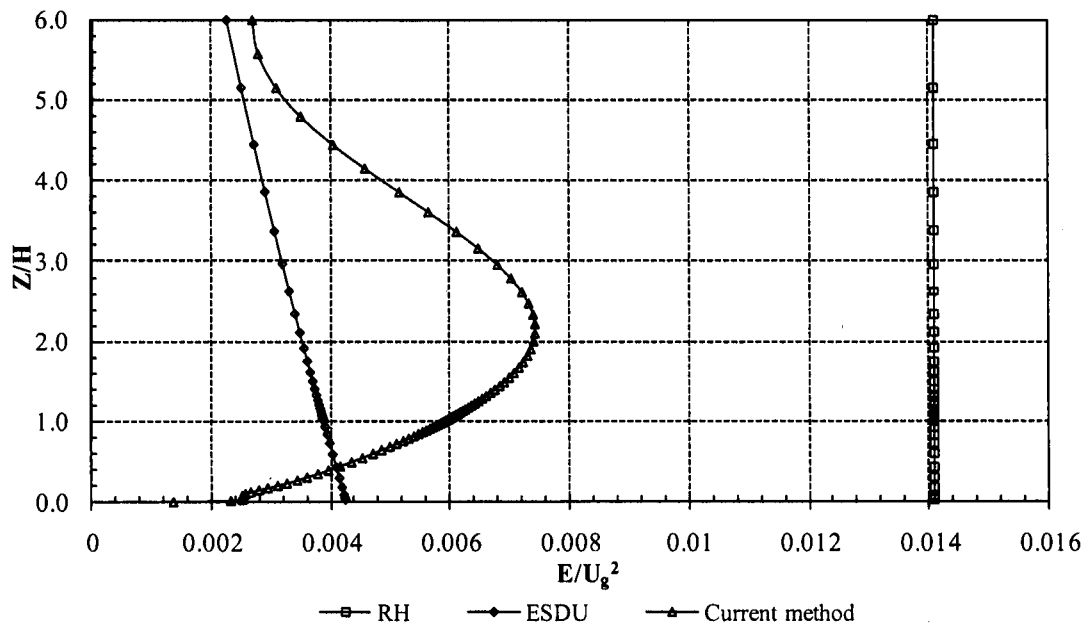


Figure 4.16 Comparison of equilibrium turbulence dissipation rate profiles by the various methods

The present profile reflects the tendency of the turbulence kinetic energy dissipation rate along the vertical boundary layer. It drops down with the increase of the height of the boundary layer (see Figure 4.16). The present profile and that of the RH method show a similar trend here. However, the latter exaggerates the dissipation rate near the ground, which is due to the overestimation of turbulence kinetic energy in this location. This discrepancy leads to the wind profile not being at equilibrium, and the near-ground turbulence profile would affect the accuracy of the results. Using the CFD model with the fine grid can be a way of obtaining turbulence data near the ground.

The current method is an appropriate approach for expressing the equilibrium inlet velocity profile in the urban environment. Unlike the empirical algorithm, it considers the effects of walls on the wind profiles near the ground region. In the scale wind tunnel test, the velocity near the ground is restricted by the equipment, and it is difficult to test. The interpolated wind velocity around the ground would cause errors when a different wind profile crosses the building. In addition, the wall treatment is set as the enhanced wall treatment instead of the wall function. The commonly-used wall function requires that the first grid near the wall is larger than the sand grid roughness height (K_s), which is about 30 times the roughness length (Z_0) (Franke et al., 2004). In the urban environment, the roughness length is between 0.7m ~ 5m, so the first grid is larger than the building height. The wall function is not suitable for the study of wind around the building in the urban environment. The enhanced wall treatment with zero roughness height is the only choice for the wall treatment. The wind profile from the present method can be taken as the inlet boundary for the next step in the study.

4.4 Identification of Computational Domain Size

Since wind belongs to a three-dimensional turbulence flow, it is necessary to simulate it in the three dimensional computational domain, which is enclosed by its boundaries. In the external wind environment, a box consisting of six faces is commonly used to represent boundaries. Computational domain size is dependent upon the purpose of study and computational resource. It is impossible to model the large domain while keeping the accuracy of model on the building being studied, because the computational domain size in the urban environment is restricted by computational resources. In addition, it is unnecessary to set a large computational domain size, because the surrounding buildings beyond the neighbourhood region have slight effects on the studied building. It is necessary to find the appropriate computational domain size for the purpose of study under the current conditions.

The computational domain size consists of two aspects of spatial requirement: the spatial requirement for the turbulence fully developed, and area of the building in question. As the fully developed space has been established (Franke et al., 2004), the following study set the inlet and lateral boundaries $6H$ away from the nearest

building and the outlet boundary $15H$ behind the last building. The top boundary is $5H$ away from the building. The area of the building being studied is determined by the purpose of the study. The average wind pressure coefficient on the building for natural ventilation study in the urban environment requires investigating the neighbourhood region.

The cases of the investigation on the neighbourhood region were determined by building layouts and building densities. According to the three-flow regimes - isolated roughness flow, wake interference flow and skimming flow (Hussain, 1978) - three typical densities (5%, 10%, and 20%) at both of normal and staggered patterns were studied. It can be assumed that the pressure coefficient difference (C_{pd}) between windward and leeward walls tended to be constant outside the neighbourhood region. The pressure coefficients in this study were normalized by the free stream velocity (U_g) instead of free streamwise velocity at building height.

The study was divided into two steps. The first step was to investigate the effects of the streamwise fetch on the pressure coefficient difference between the windward and leeward walls, with the lateral boundary taken as a periodical boundary. The surfaces of the ground and models were set as the wall boundary with smooth condition. After that, the constant streamwise fetch was achieved and can be applied into the next step to investigating the effect extending the lateral fetch on C_{pd} .

4.4.1 Normal pattern layout

The normal pattern layout is an ideal layout of models, in which the model space and gap are the same (see Figure 4.17). The air movement in this layout will be more sheltered by the surrounding buildings than other types of layouts. Normal pattern layout can be described by the model distance (S) and model density (λ). When the model is a cube, the model distance (S) and model density (λ) and model height can be expressed as Equation 4.4:

$$S = \frac{H}{\sqrt{\lambda}} \quad (4.4)$$

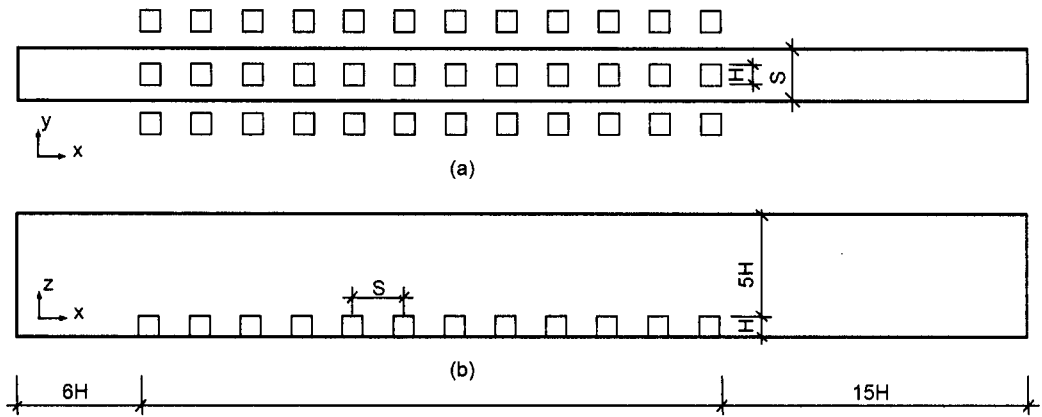


Figure 4.17 Schematic of the computational domain size of the models in the normal pattern layout. (a) Horizontal plan; (b) Section.

The neighbourhood region in the streamwise direction was investigated by taking one array of 12 elements along the wind direction as the object. Figure 4.18 describes the effect of the streamwise fetch on C_{pd} . In general, the continuous constant data appears with the increase of the streamwise fetch. So the fetch with the first constant data implies that a building outside this fetch may not affect the central building. Namely, the fetch can be shortened while considering its effect in order to save computational resources. For instance, the minimum upstream fetch with 5% building density appears after $9H$ (the third elements). The data along the fetch from $9H$ to $45H$ remains constant. So the elements among this range may be omitted as they do not affect the first element. The tolerant error can be defined as the ratio of the difference of C_{pd} between the tested and the constant C_{pd} to the constant C_{pd} . If the tolerant error is set as 5%, it can be concluded that $9H$ in the upstream fetches of the three kinds of building densities can meet the requirement. As for the downstream fetch, its effect is lower than the upstream fetch, but the range of $5H$ or the first element is required. So the streamwise fetch needs $14H$ in the normal pattern layout. In addition, building density has a significant effect on wind pressure difference. C_{pd} of 5% is just one in three of 20% and half of 10%. That means the lower density of buildings in the urban environment have a larger potential for natural ventilation.

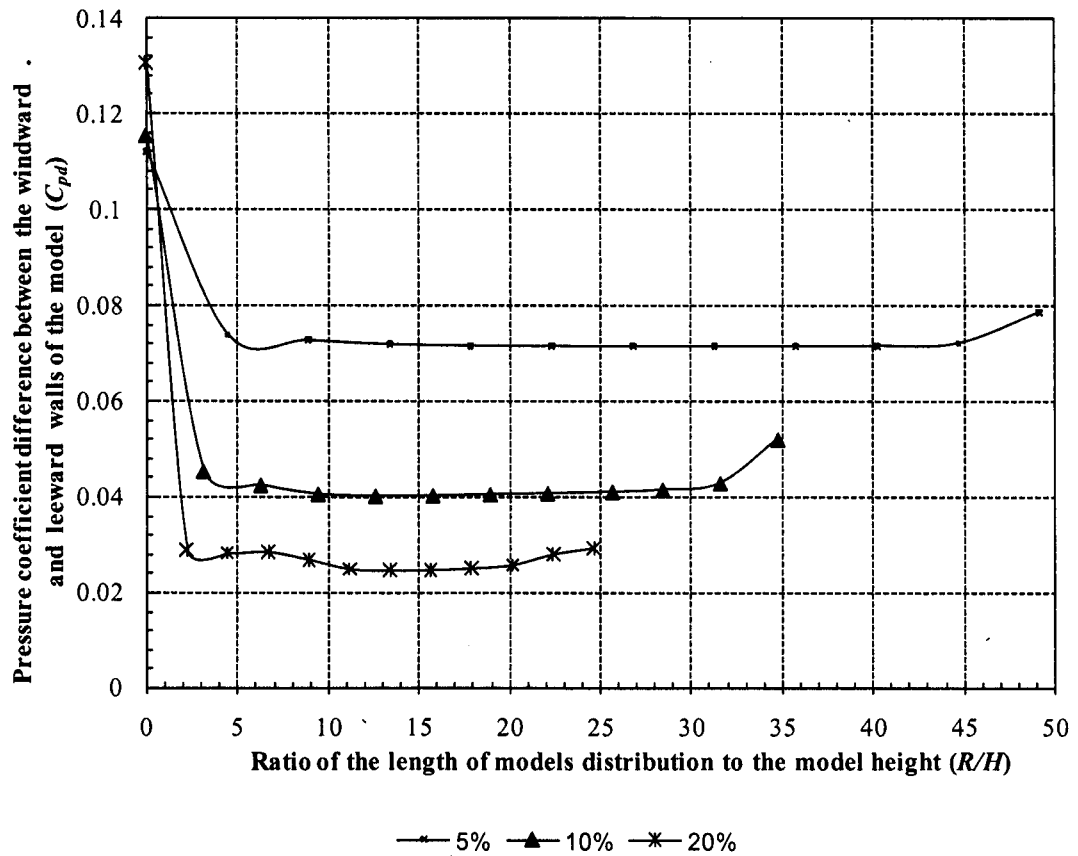


Figure 4.18 Pressure coefficient differences of the models in the various model densities along the streamwise fetch in the normal pattern layout

Based on the efficient element along the streamwise fetch from the above study, Table 4.6 summarises the layouts of three model density for the lateral fetch study. The simplified streamwise fetch remains constant, and the 4 elements in the lateral fetch are set, which is enough to investigate the effects of extension of the lateral fetch on C_{pd} . As the normal pattern is symmetrical, the symmetrical boundary is applied to the lateral boundary, and other boundaries are same as the streamwise fetch study

Table 4.6 Details of the models for the lateral length study in the normal pattern layout

Model density	Fetch in streamwise direction		Fetch in lateral direction	
	Elements (No.)	Length (H)	Elements	Length (H)
5%	5	18.77	4	13.91
10%	6	16.8	4	9.98
20%	7	13.44	4	7.22

The C_{pd} of the central model is affected by the first near model along the lateral direction. Figure 4.19 shows the result of the variation of C_{pd} along the lateral fetch in the three model density. These data are from the same row elements in every area density. R/H means the distance of the element from the side to the central model to the building height. It can be seen that the C_{pd} of the central model are affected by the nearest lateral model, but other models only have slight effects on the lateral fetch. The first lateral model in the lower density area impacts on the C_{pd} of central model larger than that in the higher density. In general, a lateral fetch of five times the building height can meet the requirements of a wind-induced ventilation study. For the high density area, the lateral neighbourhood region can be determined by the first element along the lateral direction.

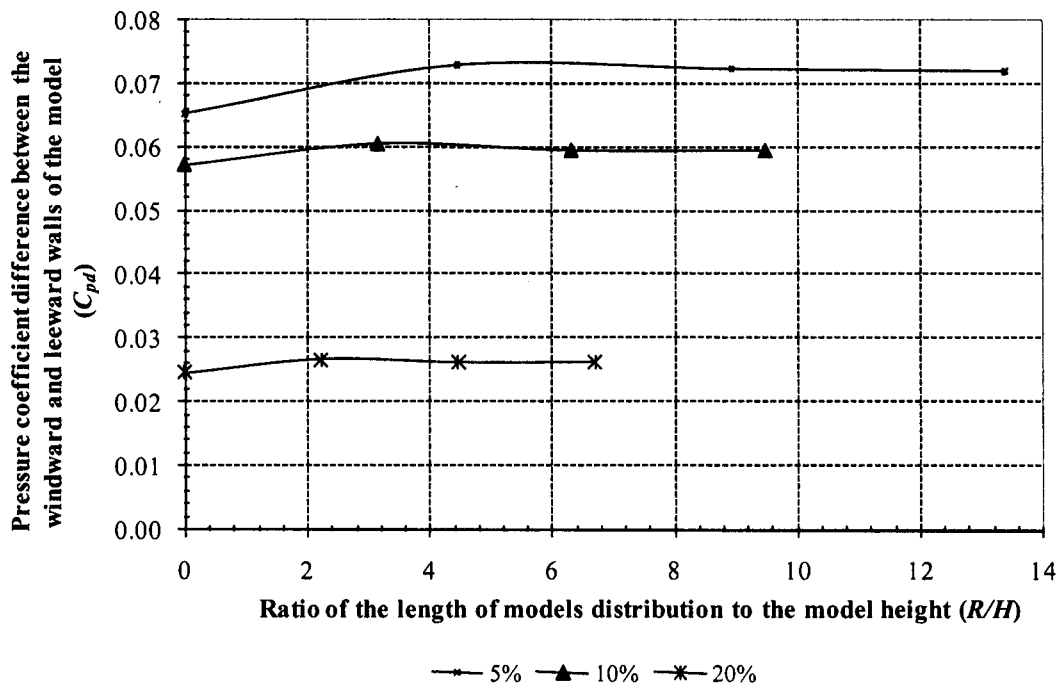


Figure 4.19 Pressure coefficient differences of the models in the various model densities along the lateral fetch in the normal pattern layout

4.4.2 Staggered pattern layout

The staggered pattern is another typical layout in the urban environment. Assuming that the building height is the same as the building width, the equation of building distance (S) and model density (λ) can be expressed as follows:

$$S = \sqrt{\frac{2}{\lambda}} H \quad (4.5)$$

The study of the neighbourhood region in the staggered pattern was to investigate the streamwise fetch firstly. One array was taken from the repeated units in the lateral direction as the model (see Figure 4.20). Lateral boundaries were set as the periodic boundary condition, which means the surroundings were considered in the model. The inlet boundary condition utilised the equilibrium boundary from section 4.3. The outlet boundary was set as the outflow boundary condition. Other boundary conditions were the same as those in the normal pattern layout study.

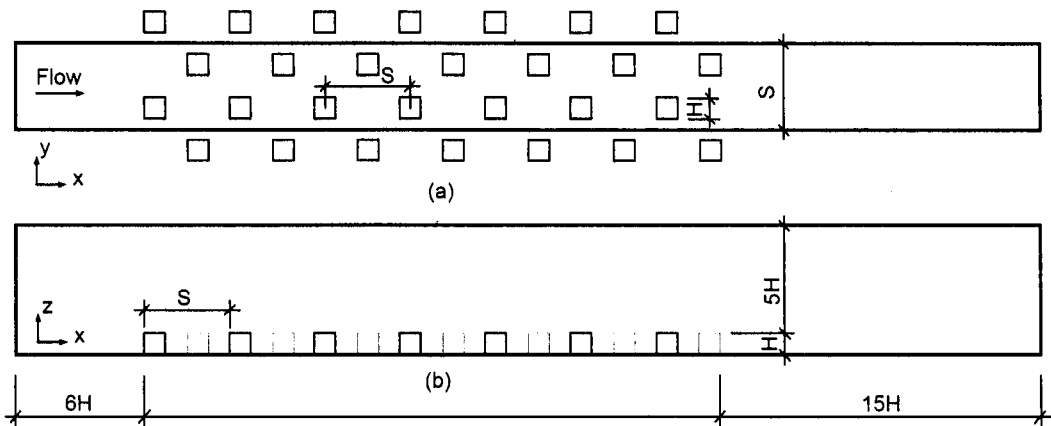


Figure 4.20 Schematic of the computational domain size of the models in the staggered pattern layout: (a) Horizontal plan; (b) Section.

The C_{pd} of the models along the streamwise direction in the staggered pattern with three model densities are shown in Figure 4.21. With the extension of the fetch, the C_{pd} generally drops down along the streamwise direction, but the reduction tends to small. The upstream fetch size should be at least $13H$. The models outside of this distance has effect on the C_{pd} less than 5% of the lowest data. The downstream fetch also affects the C_{pd} . The downstream fetch size requires $5H$ length or the first element in the wake region. The upstream fetch has more effect on the C_{pd} than the downstream fetch. Care should be taken, as the upstream fetch in the high density area can significantly affect the wind-induced driven force. The driven force is reduced by 85% for the 20% density, and 12% for the 5% density. The neighbourhood region in the streamwise direction can be determined by the upstream fetch $13H$ and the downstream fetch $5H$, or the first element in the wake region.

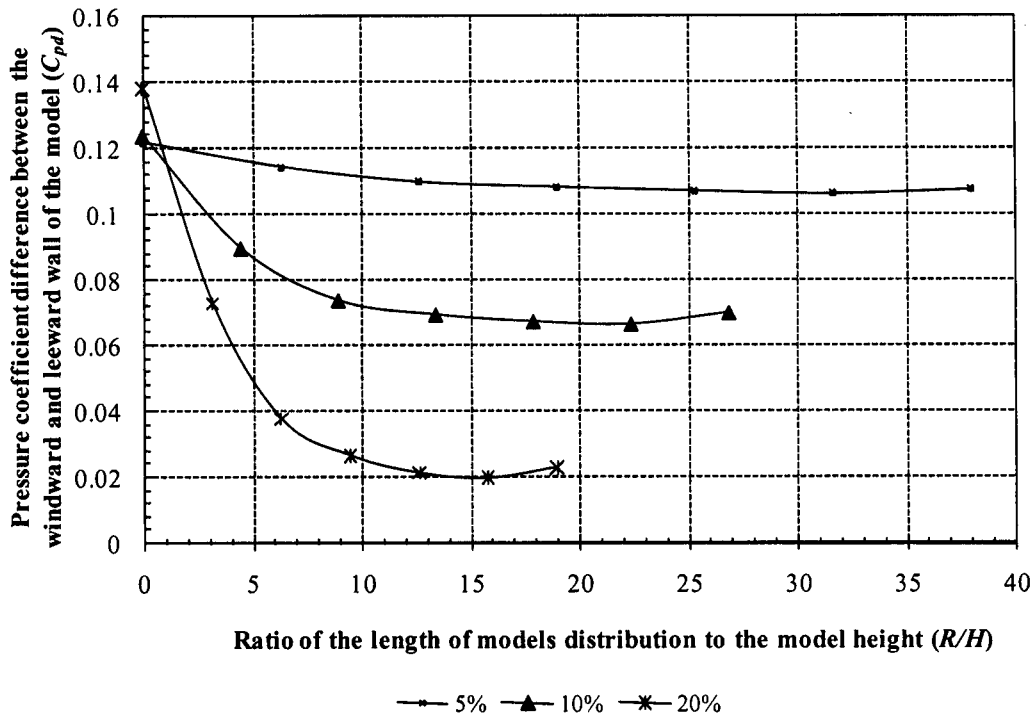


Figure 4.21 Pressure coefficient differences of the models in the various model densities along the streamwise fetch in the staggered pattern layout

The models in the lateral fetch in the staggered pattern have little effect on the C_{pd} of the central model. Figure 4.22 shows the effect of models in the lateral fetch on the C_{pd} of the central model in the three model density. In general, the maximum difference of C_{pd} between the central element and the element on the lateral fetch is less than 10% compared with the central data. The maximum lateral fetch which affects the C_{pd} of the central element is about $6H$. The first, nearest lateral element plays the main role in affecting the C_{pd} . The C_{pd} of other elements along the lateral direction keep a constant value, which means they slightly impact the C_{pd} of the surrounding models. The lateral fetch size in the lower model density is larger than in the higher area density. It can be concluded that the lateral neighbourhood region in the staggered pattern layout can be defined as $6H$ or the first lateral model in the side direction.

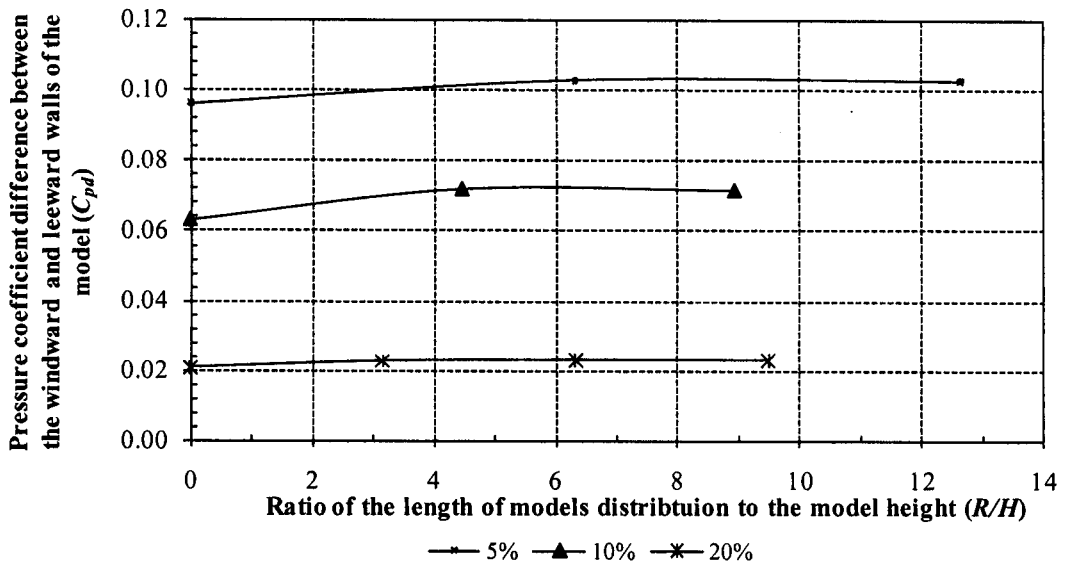


Figure 4.22 Pressure coefficient differences of the models in the various model densities along the lateral fetch in the staggered pattern layout

4.4.3 Discussion

The results from the computational domain size study confirm that the computational domain size should consider the neighbourhood region in the urban environment in a study about natural ventilation. The neighbourhood region is determined by the building density and layout pattern as well as the tolerant error. The upstream fetch is the main part of the neighbourhood region. Provided that the tolerant error is less than 5%, the upstream fetch for the normal pattern requires about $9H$ and for staggered pattern requires about $13H$. The lateral and downstream fetch can be decided by the nearest model around the building. The identified neighbourhood region can reduce unnecessary modelling, and save computational resources while keeping the result sensible. The computational domain size consists of the space for the turbulence fully developing and the neighbourhood region.

Neighbourhood region

The neighbourhood region is an area beyond which the surrounding buildings slightly affect the wind pressure distribution on the studied building in the urban environment. The neighbourhood region can determine the appropriate models of the surroundings for a study on natural ventilation in the urban environment, because the surroundings can significantly affect the potential of natural ventilation. Using the

neighbourhood region can avoid unnecessary modelling of the surroundings and save computational resource, while keeping the result sensible.

The results from the investigations on neighbourhood regions compensate for the results from the wind tunnel experiments. The wind tunnel experiment provides the conception of the neighbourhood region. Kiefer & Plate (1998) investigated the wind pressure coefficient of several built-up areas by using a wind tunnel. They claimed that the mean values were not significantly affected by the radius of model when it is larger than $10H$ in homogenous roughness field. From the wind tunnel experience, Franke et al. (2004) suggested the radius of the studied building area should be larger than $6H$. However, wind pressure coefficients are affected by building layout and building density. In addition, the numerical theory was different from the wind tunnel experiments. The present results consider the different cases of the flow field around the building. The suggestion of neighbourhood region provided the reference of neighbourhood region for CFD modelling.

Table 4.7 shows the result of current study on the neighbourhood region in the urban environment against other research. The region is normalized by the height of the building being studied. The current result provides the details of setting up the neighbourhood region around the building. In general, the upstream fetch of the current study is similar to the wind tunnel tests. The larger fetch from Lee et al. (1979) can be due to the limited urban roughness element fetch, which caused the turbulence flow in the wind tunnel to not tend toward equilibrium. Most work ignored the lateral and downstream fetches, or assumed they were the same as the upstream fetch. Actually, the flow field around the building is not the same. The CFD model should reduce the unnecessary model in the domain in order to save computational resources and improve efficiency. The current result suggests the downstream and lateral fetches can be reduced. In most cases, the downstream and lateral fetches can be determined by the first, nearest building in the corresponding directions. The length of upstream fetch is twice that of the downstream fetch and the lateral fetch. The upstream fetch in the normal pattern layout required a longer fetch than in the staggered pattern layout.

Table 4.7 Neighbourhood region in the urban environment for natural ventilation study

Authors	Method	Longitudinal Fetch		Lateral Fetch	
		upstream	downstream		
Cook (1972)	Wind tunnel	5 rows of buildings	n/a	n/a	
Soliman (1976)	Wind tunnel	12H	n/a	n/a	
Lee, et al (1979)	Wind tunnel	19H	11H	8H	
Kiefer & Plate (1998)	Wind tunnel	10H	10H	10H	
Franke et al. (2004)	experience	6~10H	6H	6H	
Current study	CFD	Normal	9H	5H or the first nearest building	5H or the first nearest building
		Staggered	13H	6H or the first nearest building	6H or the first nearest building

The neighbourhood region provides the guidance of model for natural ventilation study in the urban environment. The lateral and downstream fetch is shorter than the upstream fetch, so the concise model is appropriate for studying natural ventilation in the urban environment. The upstream fetch of the neighbourhood region is determined by the building density and pattern. The lateral and downstream fetch can be determined by the first near element.

Computational domain size

The computational domain size of the model in the urban environment should consist of two parts for the study of natural ventilation. The region in which turbulence can be fully developed is determined by the distance of the boundary away from the model. It has been observed and tested by many researchers, such as Franke et al.(2004). The neighbourhood region can refer to the suggestion in the above section, which is determined by the building density and layout pattern. The combination of the two parts means the region can guarantee the accuracy of the pressure coefficients of buildings in the urban environment. Meanwhile, this can avoid or reduce unnecessary models in the domain and make the simulation efficient.

The decision of the computational domain size usually receives guidance from the wind tunnel experiment. The difference between the wind tunnel and CFD makes the suggestion invalid. Another approach is to perform a computational domain size test by a series of trial-and-error tests (Hu and Wang, 2005). High accuracy is needed to perform domain size-sensitive tests, in order to ensure the solution is unaffected by the different downstream distance (Versteeg and Malalaserkra, 2007). However, the series of domain tests in the CFD requires extra work, and is costly and time-consuming. The present findings from the investigations of building densities and layout can help the users quickly determine the domain size for studying natural ventilation in the urban environment.

However, this study does not consider the vertical domain size, because the vertical height affects the wind flow less than the horizontal domain does, and the current vertical domain is larger than the suggested $4H$ (Yoshie et al., 2007). Further study should consider the effects of different height of the models on the domain size.

4.5 Summary

Because of the special requirements when studying natural ventilation in the urban environment, the virtual urban wind tunnel based on CFD was developed in this chapter. It provided a feasible and efficient approach to studying wind pressure around the buildings in the urban environment. The following conclusions have been drawn.

The virtual urban wind tunnel has the capability to simulate the mechanism of the physical urban boundary layer wind tunnel. Utilising the advantage of numerical simulation, it divided the procedure into three steps, which efficiently solved the limited computational resources, while concerning the effects of large urban roughness length.

According to the purpose for studying natural ventilation, mixed using RANS turbulence models can improve the efficiency of study. The RSM turbulence model with enhanced wall treatment is an essential turbulence model to study wind velocity in the urban environment. Comparing the RANS to LES turbulence models, two-

equation models overestimate the wind pressure on the windward wall, while at the same time underestimating the wind pressure on the leeward wall. The RSM turbulence model performs similarly to the LES. As the turbulent flow in the urban canopy has a large pressure gradient, enhanced wall treatment based on two-layer theory is necessary to express the turbulent flow in the urban canopy. However, the RSM model is difficult to converge, because RSM is sensitive to grid resolution, and tends to describe the characteristics of turbulence flow. An alternative method is to choose the SST $k-\omega$ turbulence model. The RSM model is used to calculate the flow far from the wall, and thus used to generate the inlet boundary of urban environment, while the SST is used to calculate the pressure coefficient in the urban environment.

Associated with the urban roughness elements model, friction velocity can be used to produce the wind profile in the urban area. The profile generated by the friction velocity from Reynolds stress is much more close to the experiment than the profiles generated by the surface friction velocity and the friction velocity from a wind tunnel. The reason is that the turbulence in the roughness area cannot fully develop due to the limited length of the roughness element fetch.

The equilibrium boundary condition for the model test was established at 40 times the obstacle height in the empty domain. The turbulence kinetic energy profile has two characteristics. The maximum data occurs at 2.3 times the model's height, and it decreases with height. It is more accurate than commonly used methods, such as the computational method proposed by Richard and Hoxey (1993) and experiment methods from wind tunnel tests. This is because the current profile considers the effects of urban roughness below the roughness height.

The computational domain size of the virtual urban wind tunnel consists of the fully turbulence developed domain and the neighbourhood region. The neighbour domain size of the virtual wind tunnel is dependent not only on the characteristic of building height, but also the density of the building area, building layout patterns, and the tolerance for error. The vertical domain is similar to the fully developed domain.

The virtual wind tunnel is more efficient and accurate for studying natural ventilation in the urban environment than the traditional wind tunnel and general CFD application are. The virtual wind tunnel establishes the equilibrium urban boundary layer condition, and provides guidelines on the choice of turbulence model and grids in the urban environment. Its results also provide more details than the physical wind tunnel.

CHAPTER 5

Validations of the Virtual Urban Boundary Layer Wind Tunnel

Computational simulation faces a critical question: to what extent can we have confidence in its results prior to application? Verification and validation are the primary approaches in building and quantifying this confidence. As mathematical or computational verification can be estimated using a grid refinement study (Franke et al., 2004), the main task for the applications is validation of the computational models in order to quantify the input uncertainty. This includes domain geometry, boundary conditions and physical model uncertainty including fluid density, viscosity and temperature and so on (Versteeg and Malalaserkra, 2007). The purpose of this chapter is to confirm whether or not the virtual wind tunnel had the capability to reproduce information usually obtained from the physical wind tunnel experiment for studying natural ventilation in the urban environment.

This chapter consist of three sections. Section 5.1 presents the methodology of validation in this study and shows the criteria for validation. Section 5.2 describes the wind tunnel experiments, numerical settings and the two kinds of models. The isolated model was used to validate the performance of the settings in the virtual wind tunnel. The models in the neighbourhood region were used to verify the performance of the flow over the group of models in the virtual wind tunnel. In section 5.3, the results of the flow characteristics and wind pressure coefficient distributions of the isolated building and the buildings in the neighbourhood region

are presented and discussed.

5.1 Strategies for Validation

5.1.1 Methodology

A wind tunnel experiment is an appropriate approach to use to validate the numerical simulation of the wind flow around buildings. The simulation for validation requires setting the same boundary conditions and models as the experiments, in order to accurately estimate error and uncertainty. However, the boundary condition in the full scale model is more complicated, and it is difficult to set its numerical model than in the wind tunnel experiment. The incident wind in the wind tunnel is usually steady, and there is no buoyancy effect, while the walls in the wind tunnel are usually flat and have little roughness (Castro, 2003). The time-averaged flow is commonly used in the experiment. The characteristics of the wind tunnel experiment simplify the numerical models in the simulation (Franke et al., 2004).

This study involves two different cases to clarify the errors and uncertainties of the virtual wind tunnel. The isolated cube in the urban environment was carried out firstly. Compared with the results from the wind tunnel experiment and other relevant literature, their discrepancies can confirm to what extent the virtual wind tunnel was an acceptable method. Using the confirmed boundary conditions and numerical setting, the buildings in the neighbourhood region were investigated. Their results were compared to those from the wind tunnel experiments, in order to confirm the dependability of the concept of a neighbourhood region in the virtual wind tunnel.

5.1.2 Criteria

The criteria for validating the virtual wind tunnel are dependent on the requirement of the natural ventilation study. Mean pressure coefficients around the building are central parameters in studying the potential for natural ventilation. This is because

the pressure coefficient is a non-dimensional parameter, which is independent of wind velocities (Awbi, 2003). When wind velocities at the reference height and pressure coefficients on the building surface are known, they can be used to calculate wind pressure on the building. Pressure coefficients are also essential data for the airflow network models to calculate the airflow rate in the interior zones. In addition, the previous wind tunnel experiment provided the information which mainly concerned mean pressure coefficients on the centre line of the windward and leeward walls, and the roof. In order to further understand the flow phenomenon, some flow characteristics, such as reattachment length and recirculation length, were compared with other similar wind tunnel experiments.

The discrepancy allowed in the numerical simulation for natural ventilation study could be larger than other engineering disciplines, such as aeronautical and structural engineering. Summer et al. (1986) thought that a discrepancy of 20% between numerical and full-scale tests could be satisfactory. For the numerical and wind tunnel test, this discrepancy could be larger, because the wind tunnel itself has the random error and systematic error. Stathopoulos and Baskaran (1996) suggested 30% discrepancy between CFD and wind tunnel could be acceptable. A discrepancy figure as high as 50% has been suggested as being tolerable (Castro, et al, 1999). This study took the discrepancy of 30% as criteria for wind pressure coefficient study for the purpose of natural ventilation.

5.2 Model Description

5.2.1 Wind tunnel experiments

This wind tunnel, built at the University of Sheffield three decades ago, had a working section of 7.2m (length) x 1.2m (width) x 1.2m (height), scaled as 1/350. The neutral urban boundary layer was generated by a castellated fence, a row of spires and a regular array of roughness elements. The free stream velocity was 9.65m/s at 0.8m height in the boundary layer height. Its mean streamwise velocity was described by a power-law profile with an exponent 0.28 representing urban

terrain boundary, with the roughness length 0.003m. The Reynolds number was approximately 1.9×10^4 , based on the building height as the characteristic length and free stream velocity. This value was larger than the required limiting value, to ensure the independence of the Reynolds number (Snyder and Castro, 2002).

This wind tunnel was validated by Lee (1977). After analysis of the wind profile at the turntable centre, it was found that the power law exponent was in good agreement with the full scale measurements in the urban terrain, with an exponent of 0.28 for the equilibrium boundary layer (Counihan, 1969). From the mean velocity profile plotted by the log-law form, the roughness length (Z_0) and friction velocity (U_*) were measured. It was found that Z_0 was 3mm and U_* was equal to $0.065U_g$. Compared with other urban boundary layer wind tunnel experiments, the data were in general agreement with others and the theory. Note that the shear stress rose to its maximum at half of the boundary layer height. That means the equilibrium boundary profiles were not fully achieved, because of the limited fetch of the urban roughness element. The turbulence intensity was, therefore, larger than that of the equilibrium boundary conditions. In general, the turbulence intensities in this wind tunnel were 0~20% larger than the suggestion by Davenport (1961). The integral turbulence length scale (L_t) measure at the three points 100mm, 250mm and 400mm were 255mm, 296mm and 314mm respectively, which matched the full scale atmospheric turbulence spectrum proposed by Harris(1968).

The wind profiles in the wind tunnel can be transferred to the turbulence kinetic energy profile and turbulence dissipation rate profiles.

$$E = \frac{1}{2}(u'^2 + v'^2 + w'^2) \approx -u'w' \quad (5.1)$$

Where E is turbulence kinetic energy (m^2s^{-2}); u' , v' and w' are components of fluctuating velocity along x, y and z axes respectively. Turbulence dissipation rate (ϵ) can be derived from the Equation 5.2

$$\varepsilon = C_{\mu}^{3/4} \frac{E^{3/2}}{L_t} \quad (5.2)$$

In this equation, ε is turbulence dissipation rate (m^2s^{-3}); C_{μ} is a constant, 0.09; L_t is the integral turbulence length scale.

The wind tunnel experiments performed by Hussain and Lee (1980) were used to validate the virtual wind tunnel. A series of experiments were carried out in this wind tunnel. They began investigating the influence of the upstream fetch on the central model, and then measured the mean pressure on various models covering a wide range of building shapes, group form and plan area density. These extensive investigations provided constructive information for the current validation.

5.2.2 Numerical models

Most CFD settings for the virtual urban boundary layer wind tunnel were described in Chapter 3 and Chapter 4. The following information summarises the settings and compares some numerical settings with the wind tunnel experiment.

Modelling settings

The modelling settings followed the characteristics of three-dimensional wind flow in the urban environment. The wind flow in the wind tunnel was set as a steady state, which can economically and efficiently meet the requirements for the mean pressure coefficients around the building. The wind flow is an incompressible flow, obeying the conservation of continuity and momentum equations. It can also be taken as a neutral condition, so the energy equation was not concerned. The pressure based solver was more appropriate than the density based solver for the incompressible flow. The turbulence model tests confirmed that the SST and the RSM model were more feasible and efficient than other turbulence models in the urban environment. The fine grids near the wall were essential in order to capture the turbulence, so the enhanced wall treatment based on the two-layer theory and near wall models were

employed. For pressure-velocity coupling, SIMPLIC was chosen. The second order upwind scheme for discretisation was used for the solution.

Boundary conditions

Boundary conditions in the urban environment specify the variables on the boundaries of physical models. They include the conditions of the inlet, outlet, sides, top, ground and the building models.

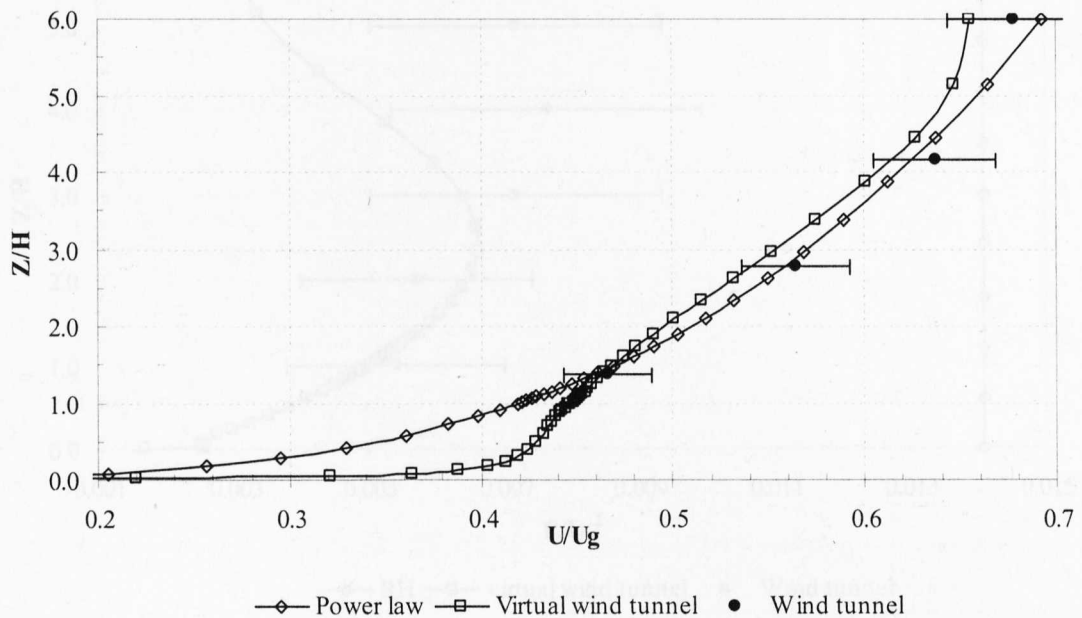


Figure 5.1 The inlet velocity profiles by the various methods. The dark dots represent the result of experiments with 5% error bars.

The inlet boundary condition of the virtual wind tunnel shows good agreement with that of wind tunnel experiment. Figure 5.1 shows the three types of velocity profiles: the power law, the virtual wind tunnel and the wind tunnel. The data from the wind tunnel experiment is shown with 5% error bars. The power law was commonly used to describe the atmospheric boundary layer in the urban terrain. Its exponent ratio was 0.28, which was gained from the wind tunnel experiment. The profile from the virtual wind tunnel was an urban equilibrium inlet profile generated by the urban roughness model in Chapter 4. It can be seen that both the power law and the virtual

wind tunnel can describe the wind profile in the urban environment as successfully as the wind tunnel. However, the difference between them is shown in the area below the building's full height. The velocity generated by the power law is lower than that generated by the virtual wind tunnel. This is because the wind flow at the roughness sublayer is not fully developed, so the power law is not suitable for predicting the velocity profile near the ground.

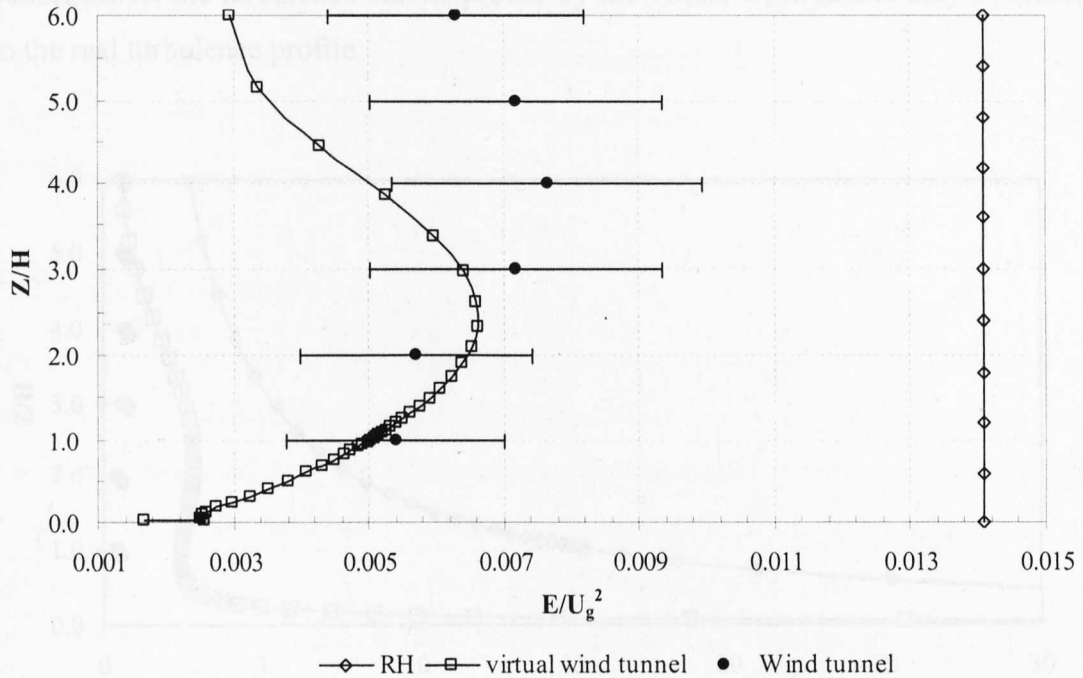


Figure 5.2 The inlet turbulence kinetic energy profiles by the various methods. The dark dots represent the result of experiments with 30% error bars.

The turbulence kinetic energy profile from the virtual wind tunnel is partly in agreement with that from the wind tunnel experiment and the common method. The three profiles are illustrated in Figure 5.2. The commonly used equation method (hereafter RH) proposed by Richards and Hoxey (1993) was to calculate turbulence kinetic energy by friction velocity, assuming that the shear stress is constant along the atmospheric boundary layer. Comparing the RH method with the result of the wind tunnel experiment, their discrepancy was beyond the error bar of 30%. It was suspect to use the equations to describe the turbulence kinetic energy profile. The profile generated by the virtual wind tunnel had certain characteristics. The

maximum data occurred at 2.3H. The kinetic energy dramatically declined with the increase of the height above the maximum data position, while decreasing below that height. Comparing the data from the virtual wind tunnel with the wind tunnel experiment, the former was less than the latter. Below the 3.5H, their discrepancy was within the 30% error, but above this height the error bar is exceeded. This could be because the fetch of the urban roughness elements in the physical wind tunnel was not long enough to reach the fully equilibrium boundary layer (Lee, 1977). As a consequence, the turbulence kinetic profile by the virtual wind tunnel may be closer to the real turbulence profile.

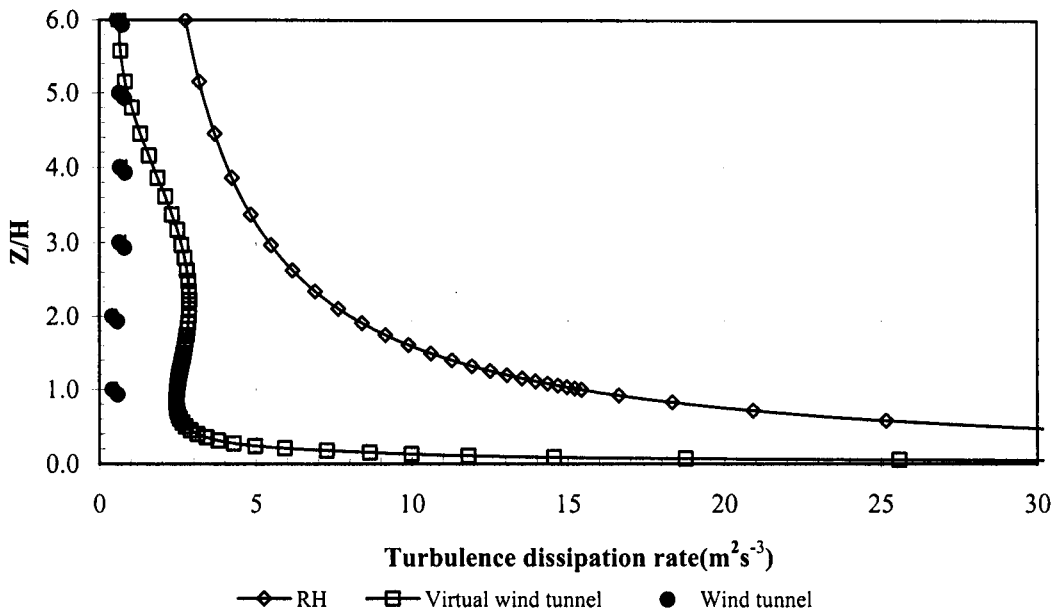


Figure 5.3 The inlet turbulence dissipation rate profiles by the various methods

The turbulence dissipation rate profile generated by the virtual wind tunnel is similar to that of the commonly used equation profile proposed by Richard and Hoxey (see Figure 5.3). The data dramatically decreases with the increase of height. The difference between the virtual wind tunnel and RH is the data near the ground. The turbulence dissipation rate of the wind tunnel experiment was calculated according the Equation 5.2. The turbulence length scale was set as 0.25m, which was from the experiment. The discrepancy between the virtual wind tunnel and the wind tunnel

experiment is larger near the ground.

Wall boundary conditions are mainly used at the bottom of the domain and on the surfaces of models. The roughness of the wall is set as zero, since the wall in the wind tunnel is flat and smooth, which has little effect on the wind flow. An enhanced wall treatment, combined with the two-layer model, was employed, as it can model the turbulence near the wall region. The outlet condition is set as the outflow boundary, which means no variable gradient on it. The boundary conditions of the top and lateral were set as a symmetric boundary condition, as the flow was not affected by the boundary. In theory, the flow can keep the same velocity and turbulence.

5.2.3 Cases description

Cases chosen from the wind tunnel experiments are determined by the objectives of this study. The first purpose was to clarify the effects of the virtual wind tunnel inlet boundary condition and the CFD settings on the reattachment and recirculation lengths and mean pressure coefficients. The results from the commonly used boundary condition and the present boundary condition were compared with those from the wind tunnel experiments. These were performed by the urban atmospheric flow across the simple model: an isolated cube. The second purpose was to clarify the effects of the neighbourhood region on the particular parameters. These tests were carried out by using the group of cubes with various plan density and layout patterns against the wind tunnel experiments.

Flow over the isolated model

The first case was the flow over the isolated cube in the urban atmospheric boundary layer. The tested cube had the same size as in the wind tunnel experiment, with the edge size being 36mm. Its computational domain size was the dimensions of 22H (streamwise), 13H (lateral), 6H (vertical) around the cube. The details of the domain are illustrated in Figure 5.4.

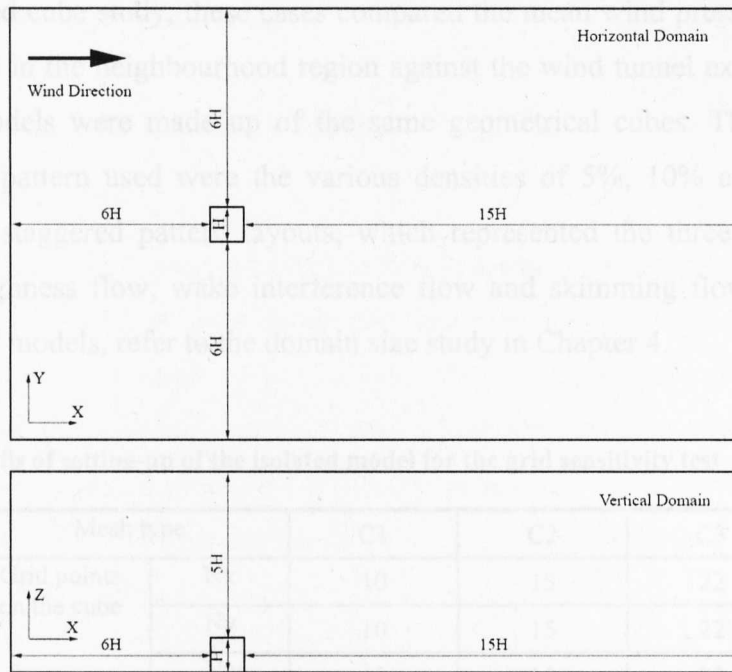


Figure 5.4 Schematic of the computational domain size of the isolated model

These dimensions between the building surfaces and the boundaries followed the recommendation of (Franke et al., 2004), neglecting the effect of the blockage ratio (less than 3%) and the boundaries on the flow.

A grid resolution study was performed in order to ensure that the grid was independent. Three types of grid sizes around the cube were used in a grid sensitivity study (see Table 5.1). The coarse grid C1 was 10 grids on every edge with a stretch ratio of 1.25; the corresponding medium size grid C2 had 15 grids on the edges with a stretch ratio 1.15, the fine size C3 had 22 grids on the edges with a stretch ratio 1.05. C2 had almost three times the grids that C1 had, and the grids of C3 were more than twice those of C2. Since the wall function was not efficient enough to predict the flow around the bluff body, the enhanced wall treatment was employed here instead.

Flow over the models in the neighbourhood region

Based on the confirmed boundary condition, independent grid, and turbulence model

in the isolated cube study, these cases compared the mean wind pressure coefficient of the model in the neighbourhood region against the wind tunnel experiments. The group of models were made up of the same geometrical cubes. The typical plan density and pattern used were the various densities of 5%, 10% and 20% in the normal and staggered pattern layouts, which represented the three flow regimes: isolated roughness flow, wake interference flow and skimming flow regimes. For details of the models, refer to the domain size study in Chapter 4.

Table 5.1 Details of setting-up of the isolated model for the grid sensitivity test

Mesh type		C1	C2	C3
Grid points on the cube	Nx	10	15	22
	Ny	10	15	22
	Nz	10	15	22
Stretch ratio		1.25	1.15	1.1
The smallest first grid length (H_b)		1/55	1/55	1/65
Wall treatment		EWT	EWT	EWT
Grid points in domain dimensions	Lx	55	76	104
	Ly	50	79	106
	Lz	30	43	59
Total grids		88,100	254,797	599,378

The computational domain size followed the suggestion made in Chapter 4. It consisted of two parts: one was the required domain for the fully developed flow, which was that the distance from the inlet, and lateral boundary to the nearest building surface was $6H$, and the distance from the surface of the last element along the streamwise direction to the outlet was $15H$. The second part of the suggestion concerned the neighbourhood region for the effects of the surroundings on natural ventilation. In general, the neighbourhood region in the normal pattern layout had $9H$ for upstream fetch and $5H$ for the downstream fetch as well as the two lateral fetches. The staggered pattern had $13H$ for upstream fetch and $6H$ for the downstream fetch and the lateral fetches. The computational domain size comprised both regions for natural ventilation study in the urban environment.

5.3 Results and discussion

5.3.1 Flow over the isolated model

Grid sensitivity study

A grid sensitivity study was performed to ensure the grid resolution would not affect the study. It required at least three grid resolutions, and their results were in asymptotic ranges (Franke et al., 2004). The area-weighted average pressure coefficient on the building surfaces was compared amongst the different grid resolutions, as the mean pressure coefficients around the building were commonly used in the study of natural ventilation. The three grid resolutions that were used were systematically refined.

The mean pressure coefficients on the building surfaces are not sensitive to the increase of grid resolution under the current three types of grids. Table 5.2 describes the average pressure coefficient difference on the building surfaces amongst the three types of grids C1, C2, C3. W1 and W2 represent windward and leeward surfaces respectively, W3 and W4 stand for the lateral surfaces and R1 is for the roof. The difference between the coarse grid C1 and medium grid C2 is less than 12%, while the number of grids in C2 is almost three times that of grid C1. The difference between C2 and C3 is less than 8%, but the number of grids in C3 is twice that of grid C2. The large grid resolution changes the pressure coefficient difference slightly. Therefore, the grids can be seen as independent grids. In order to save computational resources, grid C2 was chosen as the sample for the next step of the study.

Table 5.2 Comparison of the average pressure coefficient difference on the model surfaces among the three grid resolutions. W1, W2, W3 and W4 represent the windward, leeward, lateral surfaces respectively; R1 stands for the roof.

Grids	Pressure Coefficient Difference (%)				
	W1	W2	W3	W4	R1
C1 vs. C2	-0.9	11.5	4.2	4.2	3.6
C2 vs. C3	1.4	6.5	6.5	7.3	6.8

The grid sensitivity test shows that the leeward surface is more sensitive to the grid resolution than the other surfaces, whilst the windward wall is the most insensitive to the grid resolution. The reason may be that after separation on the windward surface, the flow is more complicated in the wake region. It implies that grid distribution around the building is dependent upon the type of the surface. The number of grids on the windward surface is usually less than that of other surfaces.

Flow characteristics around the isolated model

The virtual wind tunnel can reveal the flow characteristics of the flow around the isolated model. Figure 5.5 shows the comparison of the mean velocity vectors around the isolated cube by the virtual wind tunnel with the wind tunnel experiment by Murakami and Mochida (1988). Both have similar flow vectors around the model. The characteristics of flows around the bluff body, such as stagnation in the front surface, separation around the sharp edges, reattachment on the roof and recirculation behind the model, are represented by the virtual wind tunnel.

It should be noted that the fine grid near the surface can produce the separation around the model by the standard $k-\epsilon$ turbulence model with the enhanced wall treatment. This result is contrary to the opinion that the standard $k-\epsilon$ turbulence mode cannot simulate the separation (Murakami, 1993). The grid resolution around the building plays a vital role for the prediction of the flow around the building. Consequently, all of the RANS turbulence models with fine grids can be used for the simulation of general flow characteristics around the isolated building. The virtual wind tunnel can qualitatively reveal the flow characteristics around the isolated model, just as the physical wind tunnel does.

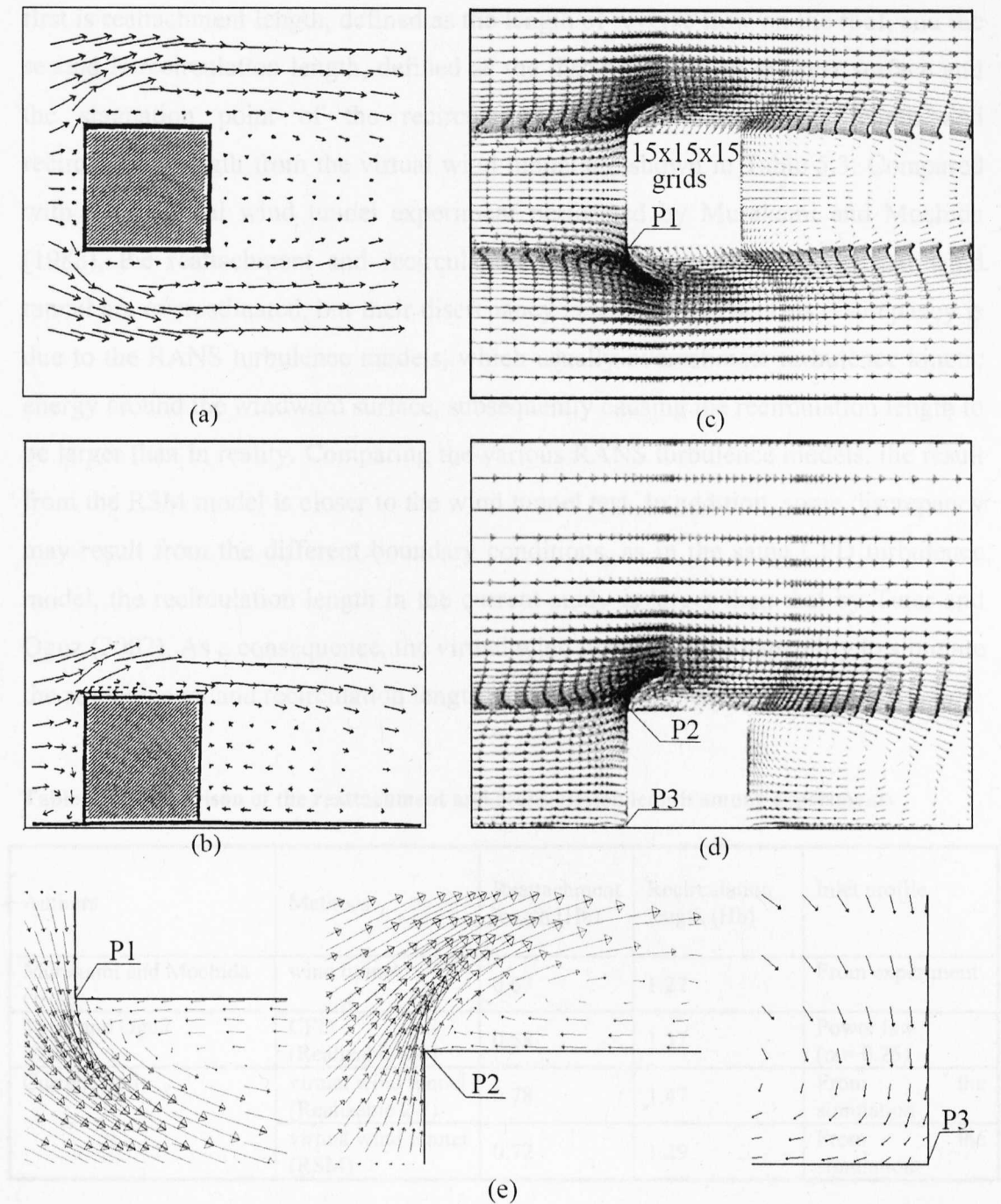


Figure 5.5 Comparisons of the mean velocity vectors at the central plan and section (a), (b): Wind tunnel experiment (Murakami and Mochida, 1988); (c), (d): The virtual wind tunnel; (e): The details of the velocity vectors at P1, P2 and P3.

Besides the qualitative study, validation of the virtual wind tunnel requires a quantitative comparison with the physical wind tunnel experiment. Two parameters of flow pattern were compared between the physical and virtual wind tunnels. The

first is reattachment length, defined as the length of reverse flow on the roof, and the second is recirculation length, defined as the distance between the rear surface and the stagnation point of the recirculation bubble. Reattachment length and recirculation length from the virtual wind tunnel are shown in Table 5.3. Compared with the physical wind tunnel experiment performed by Murakami and Mochida (1988), the reattachment and recirculation lengths achieved by the virtual wind tunnel are overestimated, but their discrepancy is less than 18%. This discrepancy is due to the RANS turbulence models, which usually overestimate turbulence kinetic energy around the windward surface, subsequently causing the recirculation length to be larger than in reality. Comparing the various RANS turbulence models, the result from the RSM model is closer to the wind tunnel test. In addition, some discrepancy may result from the different boundary conditions, as in the same CFD turbulence model, the recirculation length in the current study is larger than that by Tutar and Oguz (2002). As a consequence, the virtual wind tunnel has the capability to simulate the reattachment and recirculation length in the isolated model.

Table 5.3 Comparison of the reattachment and recirculation length among experiments

Authors	Methods	Reattachment length (Hb)	Recirculation length (Hb)	Inlet profile
Murakami and Mochida (1988)	wind tunnel	0.67	1.27	From experiment
Tutar and Oguz (2002)	CFD (Realizable k- ϵ)	0.58	1.37	Power law ($\alpha = 0.25$)
Current study	virtual wind tunnel (Realizable k- ϵ)	0.78	1.47	From the simulation
	virtual wind tunnel (RSM)	0.72	1.29	From the simulation

Comparison of mean pressure coefficients

Since pressure coefficients around buildings are commonly used to estimate wind-induced natural ventilation, they can be taken as the parameters to validate the proposed virtual wind tunnel against the physical wind tunnel. According to the wind tunnel experiments, three series of data, which are the mean pressure coefficients along the central line of the windward, leeward and roof, were used to confirm the

proposed CFD method. The free stream velocity at boundary layer height in the wind tunnel was taken as the reference velocity.

The pressure coefficients on the windward wall can be simulated as well by the virtual urban wind tunnel as the physical wind tunnel experiment. Figure 5.6 describes the pressure coefficients along the central line of the windward wall using the present method and the common method, defined as the method recommended by Richards and Hoxey (1993) against the physical wind tunnel experiment. In general, the CFD data shows agreement with the wind tunnel test. Both of them have a similar tendency, that of a reverse 'S' shape. The largest pressure occurs at about $0.8H_b$ and the lowest data appears at $0.2H_b$. The maximum discrepancy of the pressure coefficient between the virtual and physical wind tunnels is about 15% on the windward surface. The virtual wind tunnel results are generally 10% lower than that of the physical wind tunnel.

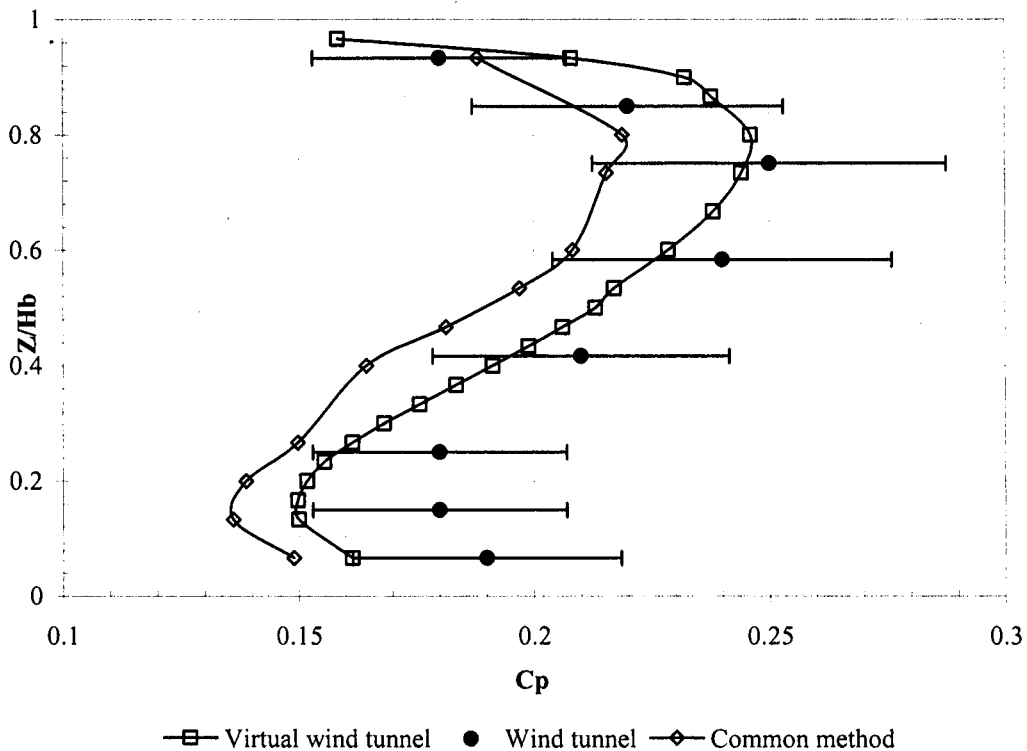


Figure 5.6 Mean pressure coefficients along the vertical central line of the windward wall of the isolated model: The dark dots represent the experiment results with 15% error bars.

However, the larger differences usually occur near the ground and the top edge: a difference of around 15%. It may result in the larger pressure and velocity gradients around the edges, difficult to simulate due to the effect of wiggles around the sharp edges (Murakami, 1998). The complicated turbulence in the near wall region causes the adverse flow. The finer grid near the wall region could improve this result. Another factor is that the inlet of the wind profile in the wind tunnel cannot reach the equilibrium boundary condition due to the limited domain size, which causes its pressure coefficients to be larger than in reality. This implies that the region of $0.1Hb$ around the edges should have the finer grid in order to reduce this discrepancy. The common method has 10% larger discrepancy than the virtual wind tunnel. This further confirms that the virtual wind tunnel is more appropriate for the study of natural ventilation than the common method.

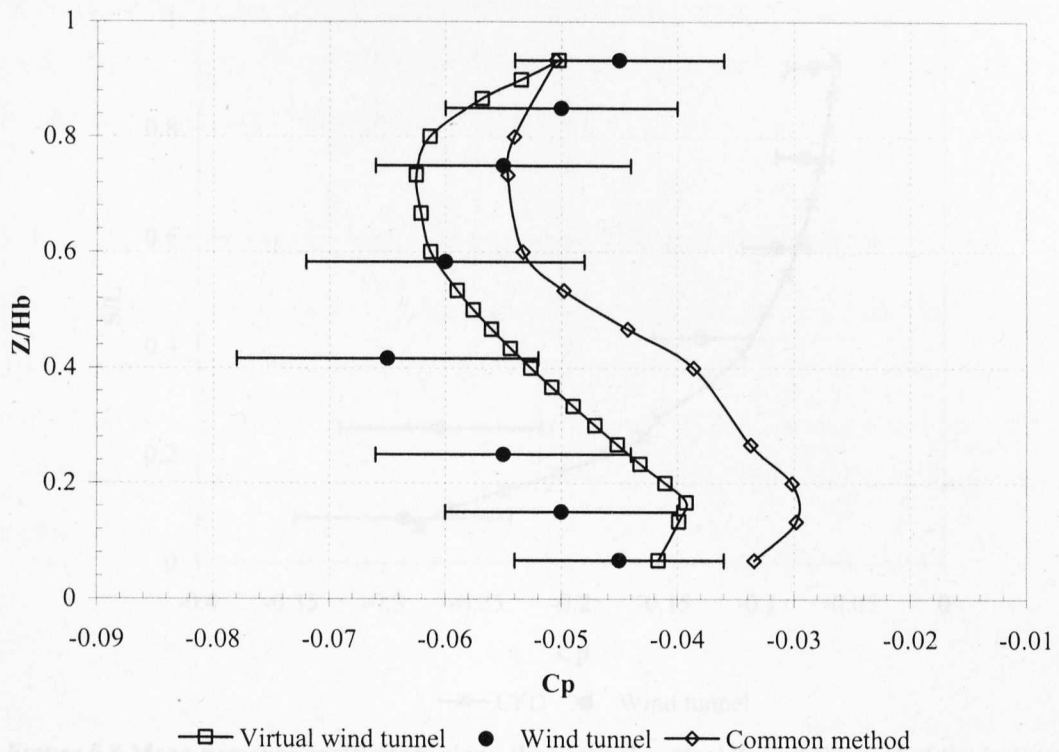


Figure 5.7 Mean pressure coefficients along the vertical central line of the leeward wall of the isolated model: The dark dots represent the experiment results with 20% error bars.

The maximum discrepancy of the pressure coefficients on the leeward wall in the wind tunnel measures about 20% between the virtual wind tunnel and the wind

tunnel. Figure 5.7 shows the pressure coefficient of the central line on the leeward wall generated by the three methods. Compared with the pressure coefficient on the windward wall, the difference between the maximum and minimum data on the leeward wall is insignificant. In general, the present method predicts the tendency of pressure coefficient distribution as well as the wind tunnel. However, there is a discrepancy of 20% between the two methods. The larger discrepancy occurs near the top and bottom edge of the leeward wall. It can be caused because the grid is not fine enough to capture the pressure gradient around the sharp edge. In addition, the wake region is so turbulent that the current steady models have shortcomings when attempting to simulate it. The common method underestimates the suction forces compared with the wind tunnel and the present method, but its tendency is similar to the present method.

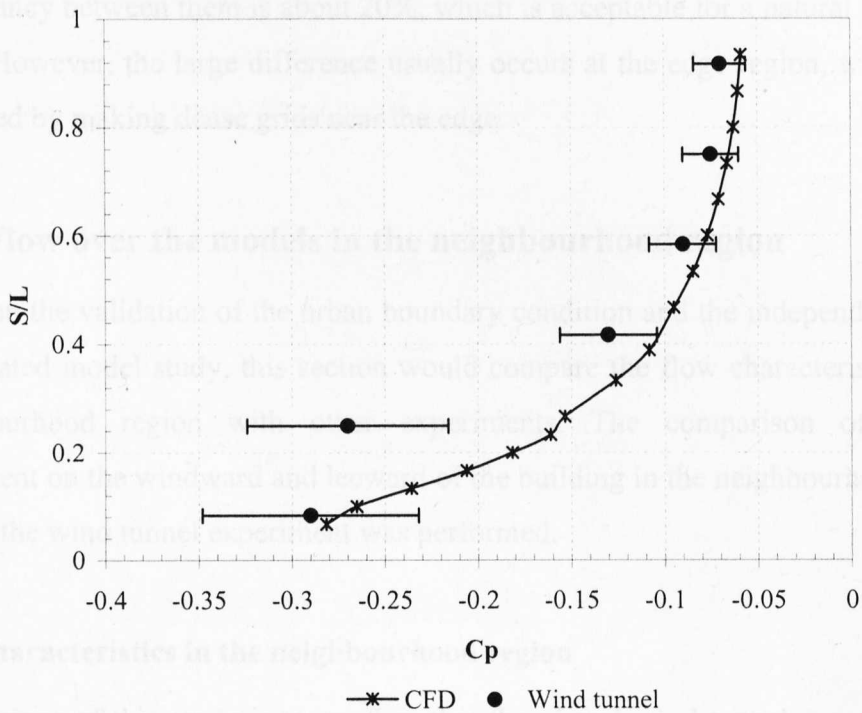


Figure 5.8 Mean pressure coefficients along the vertical central line on the roof of the isolated model: The dark dots represent the experiment results with 20% error bars.

The pressure coefficients on the roof of the isolated model simulated by the virtual wind tunnel have similar results to the wind tunnel, except for the part near the

upstream top edge. The roof is sucked by the flow force (see Figure 5.8). The part of the roof near the front edge undertakes the maximum suction. The results from the virtual wind tunnel show good agreement with the wind tunnel experiment (especially the back of the roof) with an error bar of 20%. However, the front part of the roof cannot be predicted as well. The reasons could be due to the turbulence model and the grid density near the front edges, in which the turbulence kinetic energy increases rapidly, whilst the experiment has constant data (Tamura, et al, 1997), and the reverse flow that occurs after the separation on the top edge requires the fine grid to capture the character of the turbulence.

In summary, the virtual wind tunnel is a more appropriate method to simulate the pressure coefficient around the isolated building than the wind tunnel and the common method. The flow characteristic can be simulated correctly and the discrepancy between them is about 20%, which is acceptable for a natural ventilation study. However, the large difference usually occurs at the edge region, which could be solved by making dense grids near the edge.

5.3.2 Flow over the models in the neighbourhood region

Based on the validation of the urban boundary condition and the independent grid in the isolated model study, this section would compare the flow characteristics in the neighbourhood region with other experiments. The comparison of pressure coefficient on the windward and leeward of the building in the neighbourhood region against the wind tunnel experiment was performed.

Flow characteristics in the neighbourhood region

The purpose of this study is to confirm that the virtual wind tunnel can capture the flow characteristics in the neighbourhood region as in the wind tunnel experiment. Flow in the group of building produces three flow regimes: isolated roughness regime, wake interference regime and skimming regime (Lee et al., 1980, Oke, 1988).

Figure 5.9 shows the flow path line around the building in the normal pattern in the different building densities by the virtual wind tunnel. There are two vortices between the buildings in the 5% building density: one vortex is after the building, the other vortex is in front of the downstream building. It indicates that this flow belongs to the isolated roughness flow regime, which has a fully developed vortex. So the pressure coefficient distribution on the model would be like that on the isolated building. The stagnation point is at about $0.8H$ which has the similar characteristics as the wind tunnel experiment (Hussain and Lee, 1980). In the 10% building density, there is just one vortex between the buildings. The vortex in front of the building is not fully developed due to the interference of the building in the wake. These characteristics insist that this flow belongs to the wake interference flow regime. It can also be seen that the stagnation point on the model in the wake interference flow regime moves upper than that in the isolated roughness flow regime. The flow between the buildings in the 20% building density is much more complicated than others and does not have any distinct vortex. The bulk of the flow does not enter into the canyon, so it belongs to the skimming flow regime.

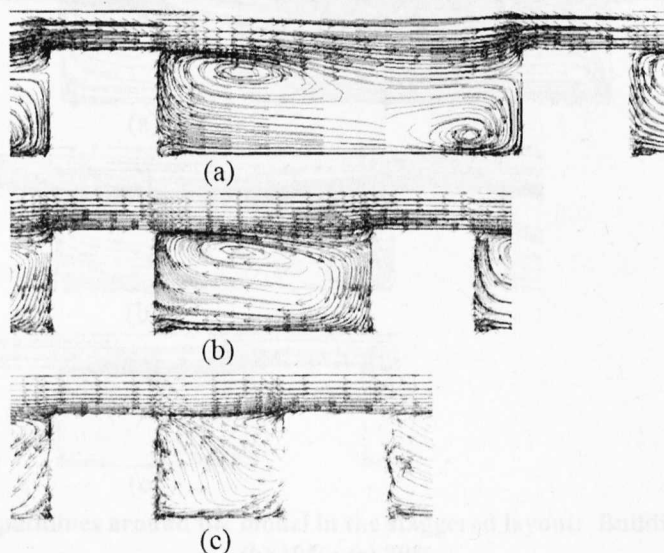


Figure 5.9 Flow pathlines around the model in the normal pattern layout: Building density: (a) 5%, (b) 10%, and (c) 20%.

The flow regimes are divided into three flow regimes according to the ratio of building height to the distance between the two buildings. Compared with the flow regime divided by building density, the current virtual wind tunnel can capture the wind characteristics of the buildings in the normal pattern layout. It would be beneficial to analyse the performance of wind flow in the urban environment.

Figure 5.10 shows the flow pathlines of the three building density in the staggered pattern layout. The flow between the buildings in 5% building density has the characteristics of the isolated roughness flow regime. The stagnation point is around $0.8Hb$. The flow between the buildings in the 10% building density is affected by the downstream building. The vortex in the wake of the building is affected by the secondary flow, while the vortex in front of the building is more distinct than the isolated roughness flow. The bulk of the flow between the buildings passes over the canyon of the buildings in the 20% building density, which belongs to skimming flow regime.

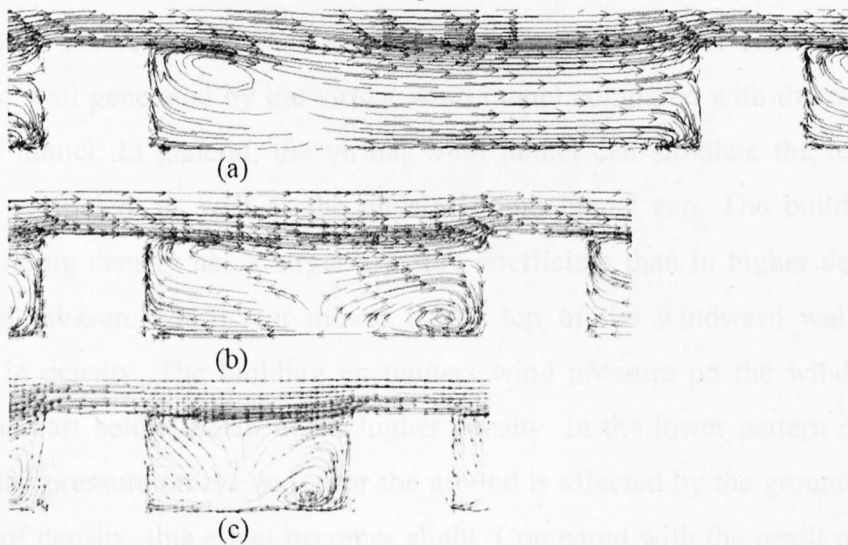


Figure 5.10 Flow pathlines around the model in the staggered layout: Building density: (a) 5%; (b) 10%; (c) 20%.

The flow characteristics between the normal pattern and staggered pattern layouts are similar. This indicates that the ratio of building distance to building height takes

action on the characteristics. However, there are some differences between them. The vortex distribution around the building is different, which could be due to the effect from the lateral building in the staggered pattern. Another difference is that the distance between the buildings along the streamwise direction in the staggered pattern is $\sqrt{2}$ times of that in the normal pattern layout, although their building densities are the same. This implies that the staggered pattern layout can acquire larger wind pressure than the normal pattern at the same building density.

Comparison of mean pressure coefficients in the normal pattern layout

The wind pressure coefficients along the central line of the windward and leeward walls of the building in the normal pattern layout were investigated using the virtual wind tunnel. The results of the three building densities were 5%, 10%, 20% against the wind tunnel experiment. The comparison between them would reveal the capability of the virtual wind tunnel in predicting mean pressure coefficients around the building.

Figure 5.11 shows the pressure coefficients along the vertical central line of the windward wall generated by the virtual wind tunnel compared with the results from the wind tunnel. In general, the virtual wind tunnel can simulate the tendency of pressure coefficient as well as the physical wind tunnel can. The building in the lower building density has a larger pressure coefficient than in higher density. The maximum pressure coefficient moves to the top of the windward wall with the increase in density. The building encounters wind pressure on the windward wall except the part below $0.8H_b$ in the higher density. In the lower pattern of building density, the pressure on the wall near the ground is affected by the ground. With the increase of density, this effect becomes slight. Compared with the result of the wind tunnel test, the virtual wind tunnel usually underestimates the pressure coefficient. The discrepancy between them is around 30%. However, the discrepancy in the higher density tends to be larger, especially near the top edge.

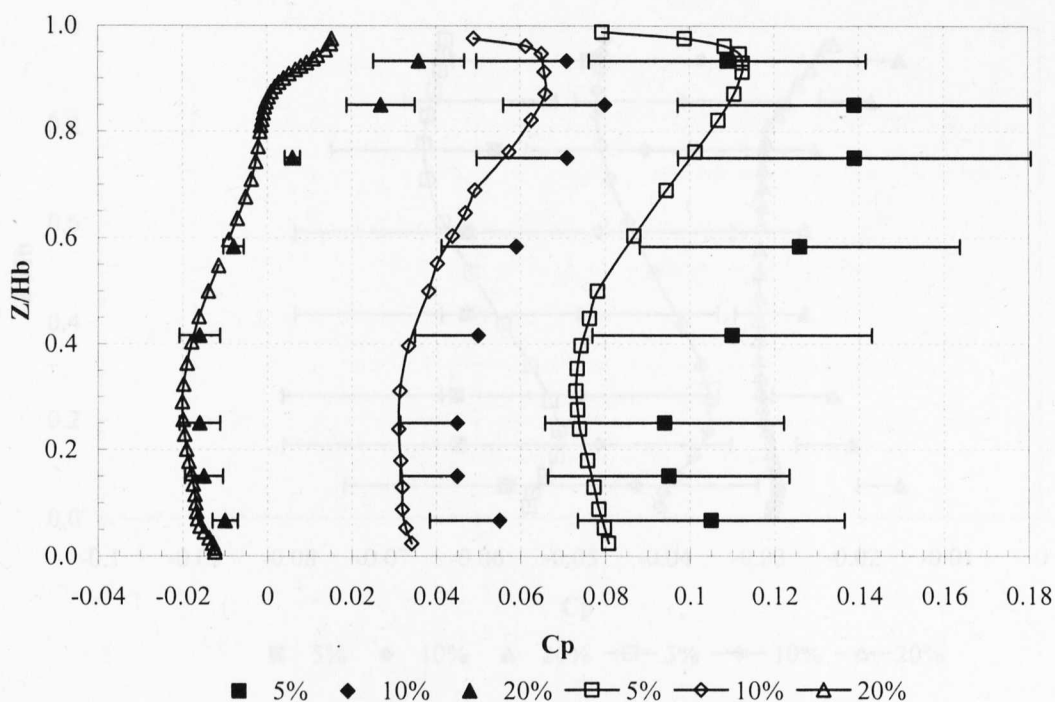


Figure 5.11 Comparison of the mean pressure coefficients along the vertical central line of the windward wall of the model in the normal pattern layout: The dark dots represent the experiment results with 30% error bars.

The leeward wall of the building in the neighbourhood region encounters negative pressure (see Figure 5.12). The pressure coefficients on the leeward wall drop down with the increase in building density, and the difference between the maximum and minimum data tends to be smaller. Compared with the result from the wind tunnel, the predicted pressure coefficient is usually larger than the experiments. The discrepancy between them is around 30%, which is acceptable for the environmental study. The larger difference usually exists near the top and the bottom, because the turbulence near the edge has a larger pressure gradient than at the other positions (Murakami and Mochida, 1988). The solution to this can be to employ more fine grids around the edges. In addition, the significant turbulence around the edges requires the advanced unsteady turbulence model, such as LES, but this would cost more in terms of time and computational resources.

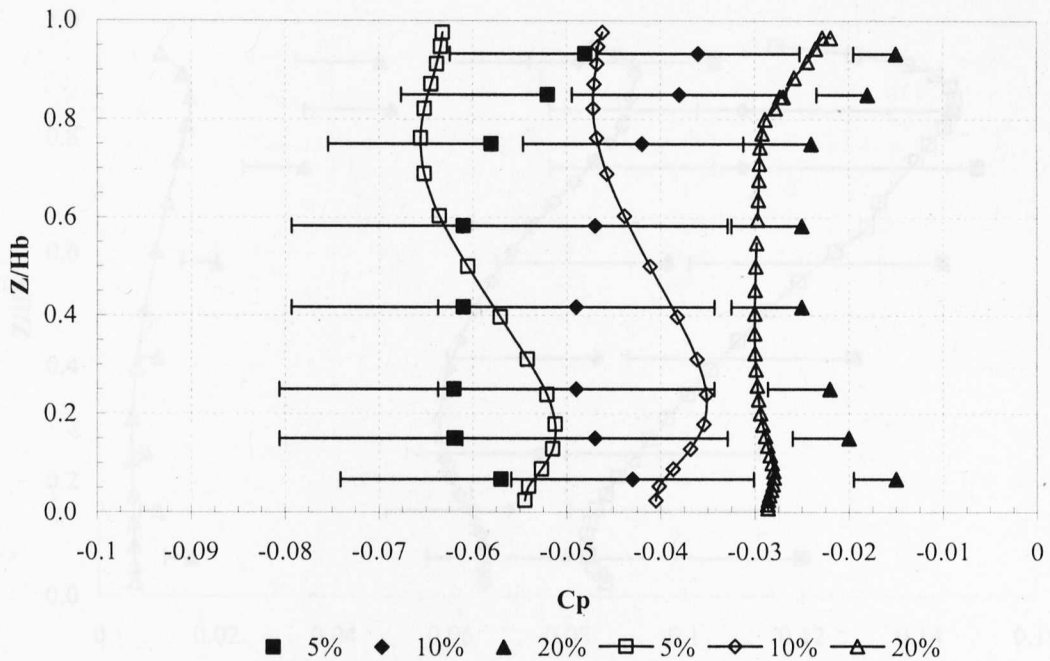


Figure 5.12 Comparison of the mean pressure coefficients along the vertical central line of the leeward wall of the model in the normal pattern layout: The dark dots represent the experiment results with 30% error bars.

Comparison of mean pressure coefficient in the staggered pattern layout

In general, the tendency of the pressure coefficient distribution around the model in the staggered pattern layout can be simulated by the virtual wind tunnel just as well as the physical wind tunnel. Figure 5.13 shows the comparison of pressure coefficients along the vertical central line on the windward wall in the staggered pattern between the virtual wind tunnel and wind tunnel experiments. The data from the virtual wind tunnel are usually lower than those generated by the wind tunnel. The discrepancy is around 30%, which can be tolerated within the environment of this study. The larger difference occurs near the bottom of the model in the isolated roughness flow, and the middle of the model in the wake interference flow. This implies that the pressure coefficients on the windward wall of the building in the higher building density are more difficult to predict, so the grid around this part needs to be refined.

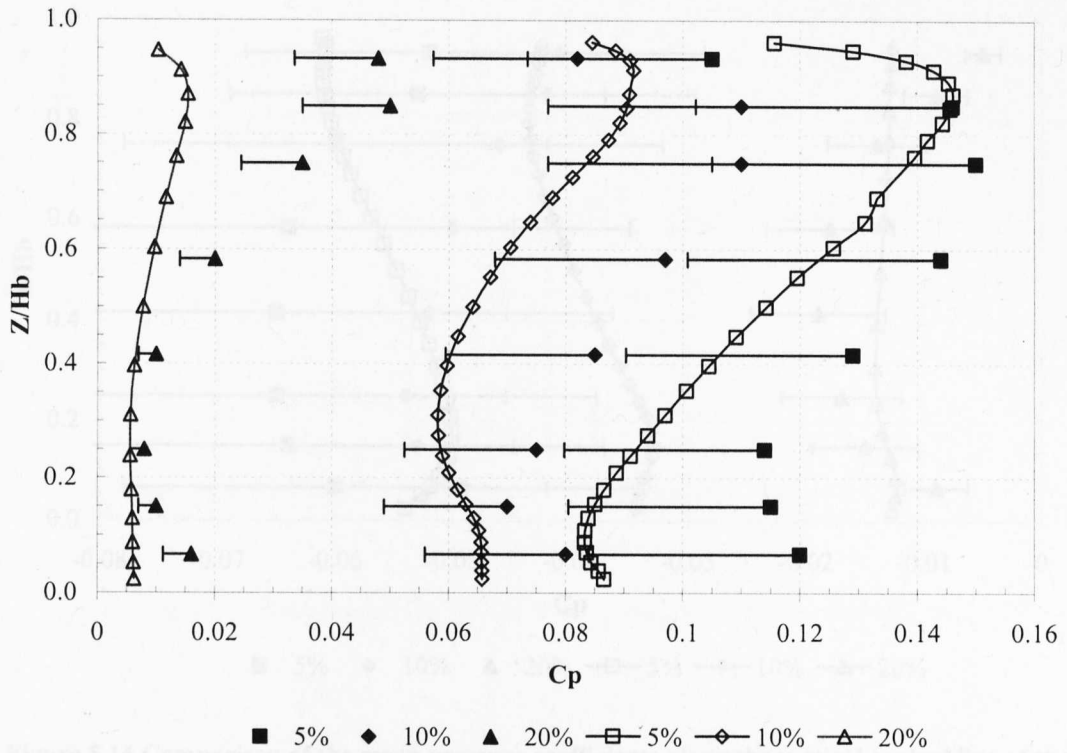


Figure 5.13 Comparison of the mean pressure coefficients along the central line of the windward wall of the model in the staggered pattern layout: The dark dots represent the experiment results with 30% error bars.

The pressure coefficients along the vertical central line of the leeward wall in the staggered pattern layout are shown in Figure 5.14. The tendency of pressure coefficients on the leeward wall is different in the virtual and physical wind tunnels. The worst part is below $0.3H_b$ near the ground, which has a discrepancy larger than 30% between the virtual and physical wind tunnel results. The flow in the wake is hard to predict by the virtual wind tunnel well as the physical wind tunnel, especially near the ground. These phenomena have been mentioned by many researchers (Murakami, 1998, Castro, 2003). A solution to this problem can be to employ the advanced turbulence model, which requires the fine grids and unsteady simulation. However, it needs higher amounts of computational resource and time.

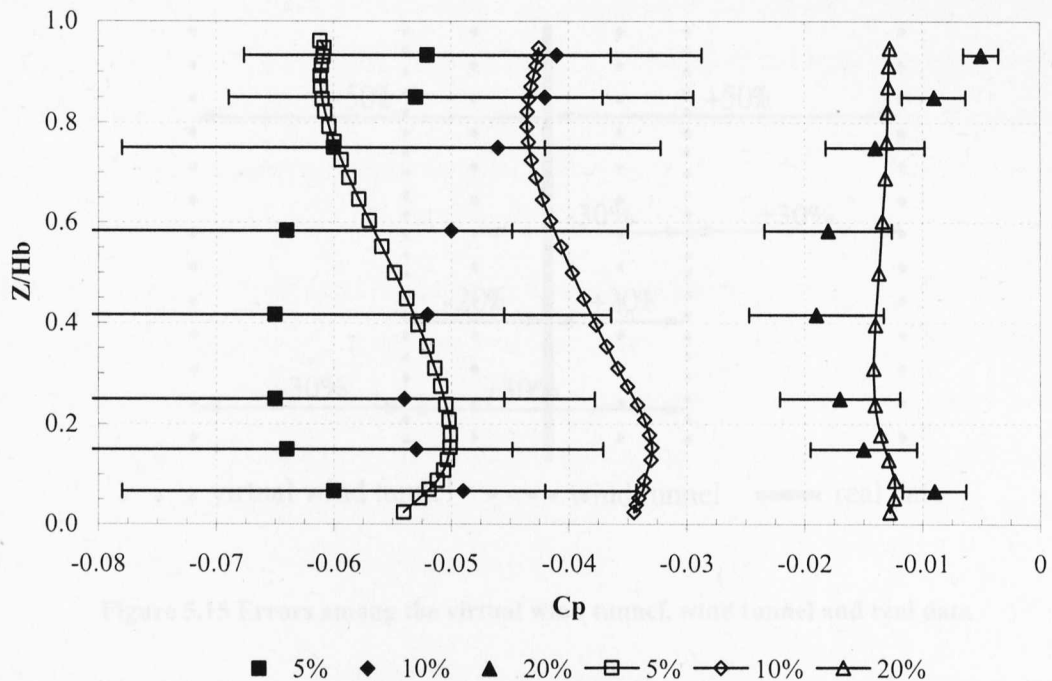


Figure 5.14 Comparison of the mean pressure coefficients along the vertical central line of the leeward wall of the model in the staggered pattern layout: The dark dots represent the experiment results with 30% error bars.

In general, the virtual wind tunnel has the capability to predict pressure coefficients of the model in the neighbourhood region just as the physical wind tunnel experiment does, no matter what the pattern layout is. The current study shows a similar pressure coefficient distribution in the group of models as the wind tunnel test carried out by Cheng et al. (2007). This confirms that the virtual wind tunnel can be used to predict the tendency of the pressure coefficient distribution in the group of buildings. For the pressure coefficient, the discrepancy between the virtual and physical wind tunnel is about 30%. This discrepancy includes the error from numerical errors as well as the wind tunnel experiment. As the wind tunnel pressure measurements have typically about 10% -20% errors (Cook, 1990), the virtual wind tunnel and the real data can be estimated. Provided that the wind tunnel error is 20% and the numerical error of the virtual wind tunnel is 30%, their largest possible discrepancy between the virtual wind tunnel and the real data is 50% (see Figure 5.15). The current discrepancy of 30% is deemed acceptable for studying natural ventilation in the urban environment.

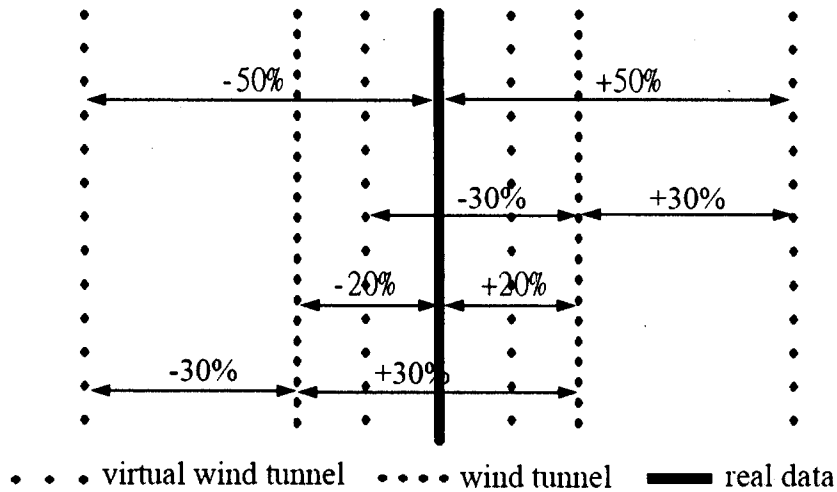


Figure 5.15 Errors among the virtual wind tunnel, wind tunnel and real data

5.4 Summary

The purpose of this chapter is to quantify the performance of the virtual urban boundary layer wind tunnel for studying natural ventilation in the urban environment. The simulation of pressure coefficients around the isolated model and the models in the neighbourhood region were carried out and compared to the physical wind tunnel experiments.

The grid resolution study shows that the independent grid requires 15 grids on the edge of the cube. In order to efficiently utilise computational resources, the grids are denser around the studied building and coarser further from it. The grid size on the ground is the smallest, expanding out away from the ground surface towards the rest of the domain, with an overall expansion factor in all directions.

The boundary condition settings in the virtual wind tunnel are more appropriate for describing the inlet profile than the common method in the urban environment. For the isolated model, the discrepancy of the mean pressure coefficient between the virtual and physical wind tunnels is about 20%, while the discrepancy between the common method and the wind tunnel is greater than 30%. The boundary condition of

the virtual urban boundary wind tunnel is acceptable for natural ventilation study. Care should be taken that the large difference usually occurs near the edge region, which could be solved by the use of denser grids near the edge, and also potentially using the sophisticated, unsteady turbulence model.

The virtual wind tunnel can simulate the flow characteristics around the model in the neighbourhood region and achieve good agreement with the results of the physical wind tunnel experiment. The discrepancy of the mean pressure coefficient of the models in the neighbourhood region generated by the virtual and physical tunnels is around 30%. The larger discrepancy occurs near the top edge and the ground. Higher building density can cause larger discrepancies.

The validations verify that the virtual wind tunnel has the capability to simulate wind flow in the urban environment. The discrepancy of 30% is acceptable for the study of natural ventilation in the urban environment. This method simplified the CFD application, and is effective enough to predict the mean pressure coefficients around buildings in the urban environment.

CHAPTER 6

Planning and the Potential for Natural Ventilation

Planning and sustainability are increasingly affected by policy-makers and planners, since the planning form has significant effects on the sustainability of land use and energy consumption (Hawkes, 1987, Wheeler, 2004). As a sustainable planning strategy, natural ventilation is largely affected by the planning form, because the surrounding buildings play the vital role of wind driven force distributions on the building envelope. Planning decisions on the planning form at the preliminary and conceptual stages have considerable effects on the resulting natural ventilation, but it is impossible to use drawings and data to decide. Therefore, planning guidelines may be used as rules of thumb for policy-makers, developers, planners and architects. In this study, planning was specified as the group of buildings in the neighbourhood region, which was distinguished from large scale urban planning. The purpose of this study is to investigate the effects of planning parameters - including floor area ratio, building density, and building space (gap) - on the potential for natural ventilation. The study also sets out to provide the guidelines to utilise natural ventilation in design at the preliminary and conceptual stages.

This chapter is organised into four main sections: review of the planning and natural ventilation potential and current issues; experiment settings; results; and discussion. The first section contains an overview of previous findings on planning and natural ventilation potential, and a description of current study. The second section describes the experiment settings and methodology. The third section shows the results of the

investigation, and the fourth section discusses the implication of the study, and proposes guidelines for planning.

6.1 Background

6.1.1 Previous findings

Planning parameters can affect the performance of natural ventilation in buildings in the urban environment. Various parameters of the surrounding buildings – including layout, building density and the ratio of building height and spacing - can all weaken wind induced ventilation forces to some extent. Van Moeseke et al. (2005) found that environmental density can change the natural ventilation potential of a building, but this study was limited to describing the planning, which simplified environmental densities into three options: open, suburban and urban area. The study was also affected by Grosso's (1992) parametrical pressure model, which cannot be used in the complex urban environment.

The ratio of building height and space can impact the wind driven forces for natural ventilation. Bauman et al. (1988) investigated the wind pressure distribution on long building rows using a wind tunnel, and concluded that the higher ratio of building height to building space would cause no potential cross ventilation. Tsutsumi et al. (1992) studied wind pressure and building volume ratio in a regularly aligned building cluster by using the wind tunnel test. They concluded that the interval between buildings in the streamwise direction greatly affected the wind pressure coefficient. Chang and Meroney (2003) performed a study on the effect of different distances between surrounding buildings on the surface pressures of a low-rise building. They did this using a wind tunnel and CFD. Their results showed that lower ratios of building height and distance can significantly reduce the pressure coefficient. Syrios and Hunt (2007) examined natural ventilation in the street canyon, and concluded that neglecting to account for surroundings may lead to poor ventilation, as the position of the vent may enhance or dampen natural ventilation.

The above studies confirmed that the planning parameters affected the potential for natural ventilation; however, these researchers each concentrated on the isolated

parameter, and did not answer consider the question in a holistic – or realistic - manner. The practical question is how to integrate these interactive - or contradictive - parameters for measuring natural ventilation potential. For instance, at the planning stage of developing a block in the urban area, developers are concerned with the floor area ratio because the larger floor area ratio can bring the more floor areas with more profits for them, while the planners and architects care about the building density, which is related to the quality of the living environment. Another factor that previous models neglected to consider is the effect of urban neighbourhood buildings on the wind pressures. The urban neighbourhood region for natural ventilation, which has been discussed in Chapter 4, is larger than the range of a street canyon, or two buildings in the urban built-up area. Furthermore, the wind pressure coefficient is a vital parameter when studying natural ventilation, but the limited data from the parametrical method or the previous wind tunnel results cannot meet the necessary requirements when planning in the complex urban environment. In addition, natural ventilation performance should consider buoyancy forces as well as wind induced forces in the urban environment. This is because as the wind force becomes weaker, the buoyancy force becomes the relatively dominant force in the urban environment. Building regulation Part F (2006) is an approved document for ventilation design, but it concentrates on the suggestions of what level of ventilation is sufficient, and does not provide strategies and rules for the designers. All of the limited studies appeal to study planning and natural ventilation potential in order to maximise natural ventilation.

6.1.2 The current study

The effects of planning parameters on wind induced ventilation forces were investigated. These parameters are determined by the procedure of planning, including floor area ratio, building density and space, which are concerned by the policy-makers, developers, planners and architects, mostly at the preliminary or early design stages. Floor area ratio is the first parameter to be carried out under the constant building density, which is taken from the typical urban building density. The suitable floor area ratio would be constant for the next step study on building density. When the appropriate date was found for the floor area ratio and building

density, the space and the gap were carried out to investigate its effect on wind induced ventilation forces.

These investigations of natural ventilation potential were carried out through the cooperation of the virtual wind tunnel and the airflow network model. The virtual wind tunnel makes it possible to study wind pressure distributions around the building in the urban environment. Meanwhile, it has more advantages than the traditional parametrical method and the wind tunnel experiment. The informative data could more accurately study natural ventilation than other method. The airflow network model was used to calculate natural ventilation rates by combining wind induced and buoyancy forces ventilation. As planning does not care about the detail of design, the simple single zone network model AIDA (see Appendix A) is appropriate at this stage to calculate the ventilation rate, which represents the potential of natural ventilation for health, comfort and cooling.

6.2 Experimental settings

6.2.1 Description of model parameters

The model parameters were derived from the ideal planning model in the urban area, as it has been established that the generic method for studying the complicated urban environment is both popular and efficient (Hawkes, 1987, Ratti et al., 2003). The archetype building in this study was set as the regular geometry with a square floor, and the surrounding buildings had the same geometry as the studied model. The planning layouts were set as the normal pattern and staggered pattern, which are typical in the urban area.

The planning model can be represented by one of the repeated units in the whole model. The repeated unit consisted of the following parameters: building height (H_b), building space (S_c) along the wind direction and building gap (G_c) in the spanwise direction (see Figure 6.1). Provided that the model followed the size of one residential floor, the full scale model can be taken as having a side size of 12.6m and the floor height of 2.625m. In the scale model of 1/350, which kept the same scale as the previous urban boundary layer wind tunnel test, the side size (a) was 36mm and

the floor height (H_s) was 7.5mm. The model domain was determined by the building density and building height according to neighbourhood region in Chapter 4.

In addition, the parameters of planning should follow the basic building regulations, such as building density not exceeding 40%, and the interval of buildings should consider the insolation interval and the separation distance. From the parameters of the repeated unit, the planning parameters - such as floor area ratio (ϕ), building density (λ), and the layout - can be calculated.

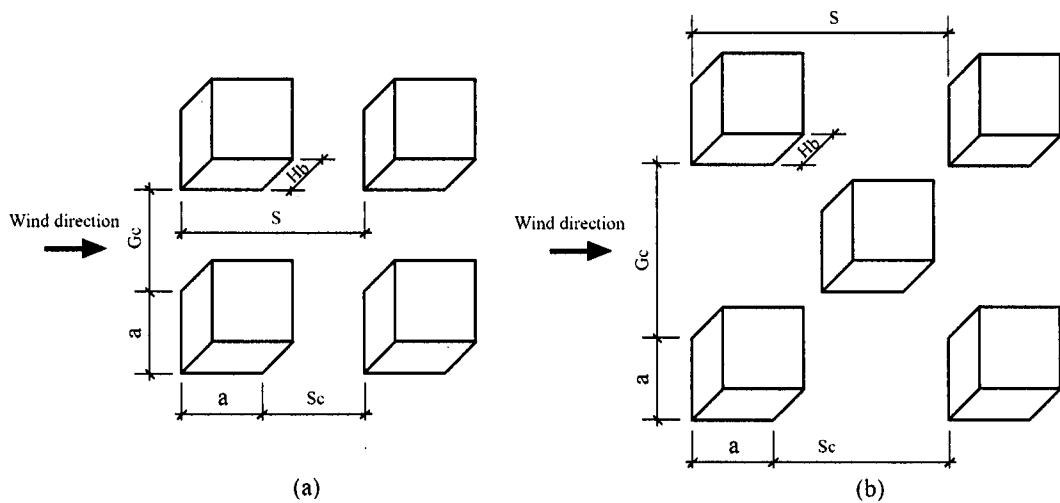


Figure 6.1 Schematics of the repeated unit in planning: (a) Normal pattern; (b) Staggered pattern

The urban environment condition in this study was based on Sheffield, UK. The urban roughness length was set as 1.05m. The prevailing wind direction was perpendicular to the model surface. The wind speed was taken as 9.65ms^{-1} at the gradient height. The outside temperatures were set as 4°C in winter and 20°C in summer. The indoor temperatures were set as 18°C in winter and 27°C in summer, which were dependent upon the adaptive temperature (de Dear and Brager, 2002) for naturally ventilated buildings.

Floor area ratio

The parameters of the model of the floor area ratios are shown in Table 6.1. The building density was taken as a constant 0.2, which belonged to the common building density in the urban residential area. The floor area ratios were set five data

conditions, corresponding with the levels of floors from 3 to 15 (see Equation 6.1), which covered the common building levels in the urban area. As the archetype building plan was a square, the building space (S_c) and gap (G_c) can be calculated by taking the building distance (S) as one unit. In this study, the building side size (a) was set as 36mm under the scale of 1/350, so the building distance was 81mm, and building space was 45mm. the building story height (H_s) was set as 7.5mm. When the planning in the staggered pattern had the same building density and height as the normal pattern, its building space (S_c) was larger than that in the normal pattern.

Table 6.1 Parameters of the models of varying floor area ratios

Building density (λ)	Floor area ratio (ϕ)	Hb (/Hs)	Normal pattern		Staggered pattern	
			S/(a)	Sc=Gc(/a)	S/(a)	Sc=Gc(/a)
0.2	0.6	3	2.236	1.236	3.167	2.167
0.2	1.2	6	2.236	1.236	3.167	2.167
0.2	1.8	9	2.236	1.236	3.167	2.167
0.2	2.4	12	2.236	1.236	3.167	2.167
0.2	3	15	2.236	1.236	3.167	2.167

The domain size consisted of a neighbourhood region and a region for the turbulence to fully develop, in accordance with the recommendation in Chapter 4. The building density was 0.2 in the normal pattern, so its neighbourhood region was $9H_b$ in the upstream fetch, $5H_b$ in the downstream fetch and spanwise fetch. In the staggered pattern, the neighbourhood region was $13H_b$ in the upstream fetch, $6H_b$ in the downstream fetch. The region for the turbulence to fully develop was $6H_b$ in the upstream fetch and $5H_b$ in the downstream and spanwise fetch. The vertical domain size was $6H_b$.

$$\phi = \lambda \cdot H_b / H_s \quad (6.1)$$

Building density

The effects of building densities on the potential for natural ventilation of the area were investigated under the conditions that the floor area ratio was constant, and the building space and gap were equal. After the above section study on the floor area

ratios, the ratio 1.8 was deemed acceptable for the whole building, so this was taken as a constant for the building density study.

Table 6.2 shows the parameters of the models with different building densities in the normal pattern and the staggered pattern. Six types of models on building densities with the same floor area ratio were set in the normal pattern and the staggered pattern layouts.

Table 6.2 Parameters of the models of varying bulding densities

Building density (λ)	Floor area ratio (\emptyset)	Hb (/Hs)	Normal pattern		Staggered pattern	
			S(/a)	Sc =Gc (/a)	S(/a)	Sc =Gc (/a)
0.36	1.8	5	1.667	0.670	2.361	1.361
0.3	1.8	6	1.826	0.826	2.583	1.583
0.225	1.8	8	2.108	1.108	2.972	1.972
0.2	1.8	9	2.236	1.236	3.167	2.167
0.15	1.8	12	2.582	1.582	3.639	2.639
0.12	1.8	15	2.887	1.887	4.083	3.083

Equation 6.2 was used for the normal pattern and Equation 6.3 for the staggered pattern. The surrounding buildings had the same height as the studied building. The domain size of the model referred the building density and building height according to the guidance in Chapter 4.

$$S_c = a \left(\sqrt{\frac{1}{\lambda}} - 1 \right) \tag{6.2}$$

$$S_c = a \left(\sqrt{\frac{2}{\lambda}} - 1 \right) \tag{6.3}$$

Building space and gap

As the above floor area ratio and building density studies assumed that the building space and building gap were equal, this section tried to investigate the effects of building space (S_c) and building gap (G_c) on the potential for natural ventilation.

Table 6.3 shows the parameters of the models with the different building space and gap in the normal pattern and staggered pattern. The building density and floor area ratio were set as constant data. Considering the factors of privacy, fire interval and sunlight interval, the building space was not less than $1H_b$ and the building gap was not less than $0.35 H_b$. The domain size of the model can be derived from the building density and building height in terms of the guidance in Chapter 4.

Table 6.3 Parameters of models of varying building space and gap

Building density (λ)	Floor area ratio (\emptyset)	Hb (/Sc)	Normal pattern		Staggered pattern	
			Sc (/a)	Gc (/a)	Sc/(a)	Gc/(a)
0.2	1.8	0.6	3.125	0.212	3.139	1.425
0.2	1.8	0.75	2.5	0.429	2.500	1.858
0.2	1.8	0.867	/	/	2.161	2.161
0.2	1.8	1	1.875	0.739	1.889	2.478
0.2	1.8	1.5	1.25	1.25	1.25	3.444
0.2	1.8	2	0.938	1.581	/	/

6.2.2 Description of the method to calculate the potential for natural ventilation

The potential for natural ventilation in this study was represented by the comparison between the calculated ventilation rate and the required ventilation rate for health, comfort and cooling. Calculating the ventilation rate was the main approach to evaluating natural ventilation potential in this study. The first step was to calculate the wind pressure coefficients around the model using the validated virtual wind tunnel. The wind pressure coefficient was essential data for the next step, which was calculating the ventilation rate of the model using the airflow network model. This method of combining the wind and thermal buoyancy forces model was an efficient way of estimating the ventilation rate at the planning stage. The following summarised the settings in the models.

The virtual wind tunnel settings

As well as the wind tunnel test, the CFD simulation had also been acknowledged as an alternative method to acquire the pressure coefficients (Suh et al., 1997, van Moeseke et al., 2005). However, this method required the approximate settings prior

to calculation. After the validation of the virtual boundary layer wind tunnel in Chapter 5, this technique was employed to calculate the pressure coefficients around the models. Their results provided more information on wind pressure distributions around the model than the wind tunnel test.

The boundary condition of these models was similar to that in Chapter 5. The inlet boundary was set as the velocity inlet and its profile was taken from the roughness simulation. The computational domain size was dependent upon the building density and building height, which determined the neighbourhood region and the distance between the boundary and the nearest wall, in accordance with the guidance in Chapter 4. The turbulence model employed the SST $k-\omega$ model with y^+ less than 4, which had good performance in the prediction of pressure coefficients on the building surface in the urban environment, as the RSM turbulence model was too sensitive to converge in the complicated model. The second order of upwind scheme was used in this study.

The grid settings followed the rules that the grids around the studied building should be fine enough to capture the important physical phenomena like shear stress and vortices, and the grid stretch ratio should be less than 1.3 (Franke et al., 2004). In this study, each side of the building had 15 grids with fine grids around the side. The resolution of the finest grid along the building height was the same as that of the finest grid of the side, but the amount of the grids along the building height was changeable with the building height. The resolutions of other grids in the domain became coarse with the constant stretch ratio of 1.2 from the studied building. As the model is not complicated, the hexahedra grids were used in these models. In order to reduce the error from the grid resolution, each grid in each case did the grid independent test.

The airflow network model settings

The airflow network model was applied to calculate the natural ventilation rates. Compared with the empirical models, such as British Standard method BS5925 (1991) and ASHRAE (2005) method, the airflow network model was more rigorous, as it considered the condition of complex flow paths. The details of the building at

the planning stage were unknown, so the every floor of the building can be taken as a single zone. The single zone network model may be suitable for the study of ventilation rate of the building at the planning stage, as this model can combine the wind driven force and buoyancy force to calculate ventilation rates. A single zone network method was compiled as a program by Matlab (see Appendix A).

The fundamental elements of the network model were introduced in Chapter 3. The settings of the airflow network model were summarised as follows. The air density (ρ) was set as 1.225kgm^{-3} ; the outside temperature was dependent upon the season and the indoor temperature was dependent upon the adapted temperature. The outside temperatures were 4°C in winter and 18°C in summer, and the inside adaptive temperatures were 20°C in winter and 27°C in summer. The ratio of the maximum opening area of the model to the wall area was set less than $1/10$, so that the pressure distributions were not affected by the size of openings. The flow coefficient was dependent on the size of the openings. The flow exponent was varied by the type of flow - between 0.5 for fully turbulent flow and 1 for completely laminar flow, and its common value was defined as 0.66 (Liddment, 1996).

6.2.3 Cases of the ventilation calculation

In the urban environment, the complex turbulence flow caused by planning parameters generated complicated pressure distribution on the building surfaces. It was difficult to decide the best strategy in different urban environments. Therefore, the effect of the planning parameters on the natural ventilation potential was necessary to this study. The design guidelines would be help designers to correctly choose the appropriate archetypes.

Ventilation calculation in the urban environment included the factors of wind induced force, buoyancy, and the combination of wind and thermal buoyancy forces. Wind induced ventilation can be divided into two categories: single-sided and cross ventilation. On the same floor, the single-sided with single opening ventilation was mainly driven by random turbulent fluctuations, so it was difficult to calculate by the airflow network model. This study did not consider this type of wind induced ventilation. Comparing the single-sided ventilation, the cross ventilation at the same

floor was much more efficient. Consequently, this type of ventilation was commonly used in natural ventilation design. The natural ventilation driven by the combination of wind and thermal buoyancy forces occurred when the openings had a different height. Care should be taken to ensure that the pressure coefficient was independent of the scale of the model, as the stack effect was affected by the scale. Therefore the scale of the model needed to be transferred to the full scale. In addition, a wind direction between 0 and 45 degree incidence in the urban environment may have a small effect on wind induce forces (Sharples and Bensalem, 2001), so the current studies consider only the wind incidence as being 0 degree.

Table 6.4 Cases of the wind induced ventilation at the different levels

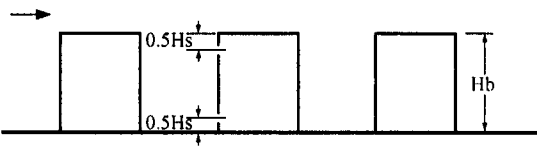
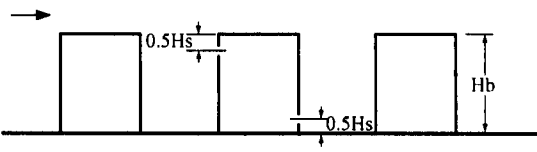
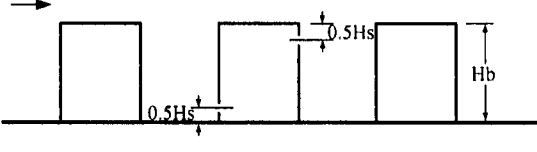
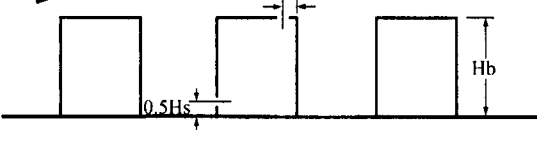
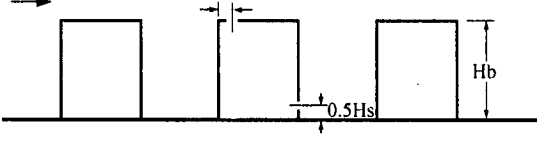
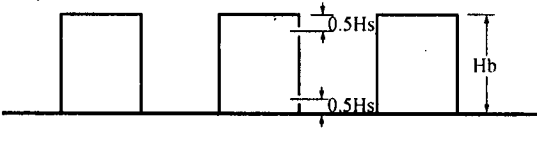
Cases	Schematic	Features
Case1		Pressure coefficient is taken the average-weighted area on the surface.
Case2		The openings are at the top level of the building. The inlet and outlet are located at the vertical level of $0.5H_s$ and at the centre of horizontal level.
Case3		The openings are at the middle level of the building.
Case4		The openings are at the ground level of the building.

Table 6.4 describes the four cases of ventilation on the same floor of the building in the urban environment. Every case had two openings at the centre of the horizontal level. One was located at the windward wall; another was at the leeward wall. The openings were at the same level, so the stack effect of the temperature difference between the inside and outside can be neglected. The two openings had the same area, which can maximise the ventilation rate compared with the different size openings. The ventilation strategy was to ventilate the whole building in order to provide fresh air and dilute and disperse residual water vapour and pollutants. According to building regulations Part F (ODPM, 2006), background ventilation can be acquired by trickle ventilators. The ventilator area was dependent on the dwelling area. For this building, the total floor area of every floor was 158.76m^2 , so the trickle ventilator area was 0.075m^2 in winter time. In summer, the opening area for purge ventilation was taken as $1/20$ of a room's area near the external wall. Here we took the external room area to be $2/3$ of the total area, so the total opening area of two openings was 5.3m^2 .

Besides the above cases of wind induced ventilation on the same floors, the ventilation driven by the combination of wind and buoyancy forces was also common used in the urban environment. This study investigated the models with two openings which had various vertical differences in the urban environment. The standard to evaluate thermal comfort employs the measurement of air change rate per hour (ACH). These models were mainly used to study cooling ventilation strategy for thermal comfort in the summer. The outside temperature in summer was set as 20°C , while the adaptive comfortable temperature indoor was set as 27°C for the natural ventilated building, according to adaptive thermal comfort research (de Dear and Brager, 2002). This figure was larger than the air conditioning comfort upper temperature 25°C . The appropriate opening position on the building surface was one of the efficient natural ventilation design strategies. For example, a top-down ventilation system harnesses wind from the roof to the interior in order to assist stack-driven flow (Gage et al., 2001); Atrium was used to combine wind induced and stack effect ventilation (Holford and Hunt, 2003). All of the strategies involve the airflow path and the opening position. These strategies were mainly used for thermal comfort in summer. According to the opening position, the archetypes of natural

ventilation design strategies can be classified as six cases, illustrated in Table 6.5. Every case had two openings with the same area and total opening area was equal to 1/20 of the floor area, following the building regulation Part F (ODPM, 2006).

Table 6.5 Cases of natural ventilation combined wind and thermal buoyancy forces in the large space

Cases	Schematic	Features
Case5		Both of openings are located at the windward wall and their vertical distances to the top and ground are $0.5H_s$.
Case6		The windward opening is $0.5H_s$ below top edge and leeward opening is $0.5H_s$ above ground. Both are at the centre of horizontal level.
Case7		The windward opening is at $0.2H_b$ and leeward opening is at $0.8H_b$. Both are at the centre of horizontal level.
Case8		The windward opening is $0.5H_s$ above ground and another is at the roof. Both are at the centre of horizontal level.
Case9		One opening is at roof and another is at the leeward. Both are at the centre of horizontal level.
Case10		Both of openings are located at the leeward wall and their vertical distances to top and ground are $0.5H_s$.

6.2.4 Criteria for the natural ventilation potential of the building

The criteria for the natural ventilation potential of the studied building were considered in terms of the building regulation and the relevant research. According to the three main functions of natural ventilation - health, thermal comfort and cooling - Wills et al (1995) reported the generally required ventilation rate for indoor environment in order to avoid or minimise the use of air-conditioning. Building regulation Part F (ODPM, 2006) for ventilation also provided guidance on whole building ventilation rates for dwellings. Compared with Wills et al.'s (1995) report, Part F had a lower requirement of the ventilation rate, but still ensured good indoor air quality. According to the living space of the average house - about 39~44m² per person in the UK (Boardman et al., 2005) - it can be assumed that there are four habitants for every floor (158.76 m² floor area). Table 6.6 summarises the levels of ventilation rates and the opening areas of the building in winter and summer. The criteria of the ventilation rates represented the needs for health in winter, and the purge ventilation rates for the thermal comfort in the shoulder seasons and the cooling ventilation rates for the thermal comfort in summer. The total opening area of the building followed the recommendations of Part F.

Table 6.6 Ventilation criteria for the cases

Ventilation strategies	Total opening area (m ²)	Required ventilation rate
Whole building ventilation	0.075	25ls ⁻¹
Purge ventilation	5.3	4 ACH
Cooling	7.94	25ls ⁻¹ m ²

6.3 Results

6.3.1 Floor area ratio

Pressure coefficient distribution

All of the building surfaces but the windward wall in the case of the floor area ratio 0.6 in the staggered pattern have a negative area-weighted average pressure coefficient in the urban environment with the floor area ratios between 0.6 to 3.0 (see

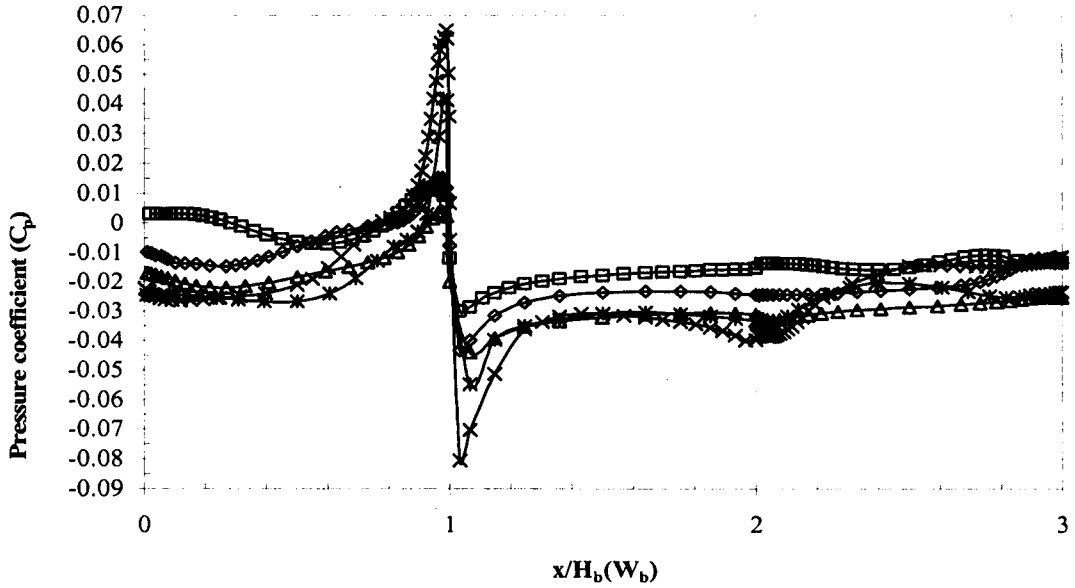
Table 6.7). As the building height is changeable with the floor area ratio, a reference velocity of 9.65ms^{-1} was taken as the undisturbed gradient wind speed at the gradient height. The roof bears the largest suction force amongst all of the surfaces in the same case, and the average pressure coefficient around the building has a random distribution. This phenomenon is because wind flow is disturbed by the surrounding buildings in the urban canopy layer, but around the flat roof the effects of shielding are largely reduced. When comparing the average pressure coefficient difference between the windward and leeward walls in the normal pattern and in the staggered pattern at the same floor area ratio, it was noted that the latter did not always had a larger pressure coefficient difference than the former, though the building space of the latter was larger than the former. That means the comparison of the building space (S_c) among the different layouts cannot be used to decide which layout is better for wind driven ventilation in the planning.

The average data of pressure coefficients on the building surfaces present the general wind pressure distribution around the building, but it is not appropriate in application to the multi-story building. This is because the pressure distribution on the building in the group is irregular, and different opening positions may experience varying pressures. For instance, the windward surface usually measure positive pressures on the upper part and negative pressures on the lower part. The average pressure coefficients cannot express the large difference among the opening positions. This drives a study of the pressure coefficient distributions on the building surfaces.

Table 6.7 Average pressure coefficients on the building surfaces of varying floor area ratios. (the reference velocity is the gradient wind speed 9.65ms^{-1})

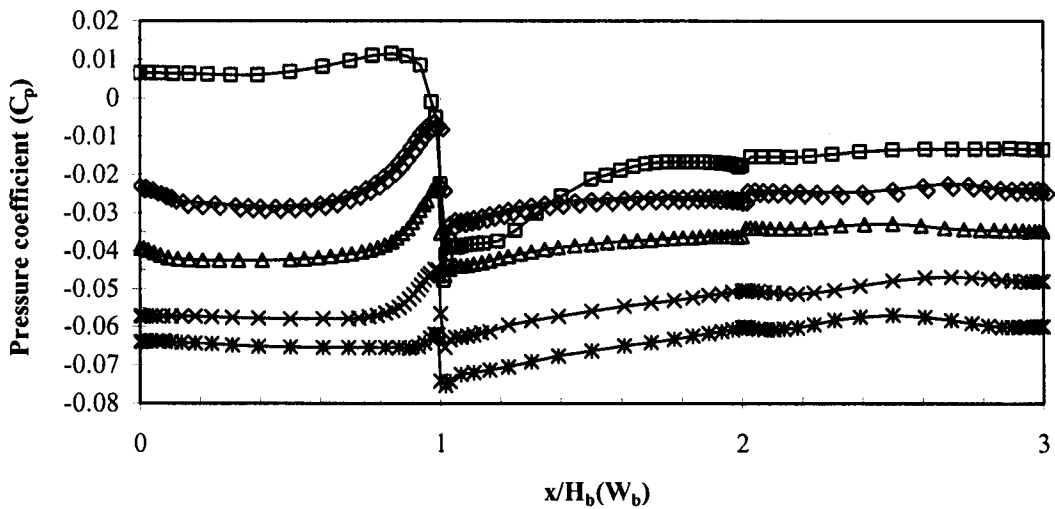
Surface		Floor area ratio				
		0.6	1.2	1.8	2.4	3.0
Normal pattern	Windward wall	-1.1e-03	-5.6e-03	-1.53e-02	-1.18e-02	-1.75e-02
	Leeward wall	-1.47e-02	-2.12e-02	-2.95e-03	-2.51e-02	-2.54e-02
	Lateral wall	-1.90e-02	-2.17e-02	-2.82e-02	-2.63e-02	-2.61e-02
	Roof	-1.97e-02	-2.68e-02	-3.42e-02	-4.07e-02	-3.52e-02
Staggered Pattern	Windward wall	8.38e-03	-2.35e-02	-3.95e-02	-5.64e-02	-6.53e-02
	Leeward wall	-1.54e-02	-2.39e-02	-3.48e-02	-4.94e-02	-5.92e-02
	Lateral wall	-2.16e-02	-2.72e-02	-4.26e-02	-5.95e-02	-6.71e-02
	Roof	-2.50e-02	-2.78e-02	-3.94e-02	-5.64e-02	-6.68e-02

The area-weighted average pressure coefficients along the central lines of the buildings of varying floor area ratios are described in Figure 6.2. On the horizontal axis, 0-1 stands for the central line of the windward wall from the bottom to the top edge; 1-2 represents the central line of the roof from the forward to the backward; 2-3 represents the central line of leeward wall from the top edge to the bottom.



(a) Normal pattern

—□— 0.6 —◇— 1.2 —△— 1.8 —×— 2.4 —*— 3



(b) Staggered pattern

—□— 0.6 —◇— 1.2 —△— 1.8 —×— 2.4 —*— 3

Figure 6.2 Pressure coefficient distributions along the central lines of the models of varying floor area ratios

In general, the pressure coefficients on the surfaces are negative, except the part that is above $0.8H_b$ on the windward wall in the normal pattern and the windward wall of the 0.6 floor area ratio in the staggered pattern. The larger pressure coefficients occur around the top edge of the windward walls, because the wind flow is separated by the top edge. After the flow separation at the top edges, the larger suck forces occur near the windward edge of the roofs. Then the forces on the roofs tend to remain constant until the backward. With the increase of the floor area ratio, the surfaces bear larger suction forces and the pressure difference between the windward wall and leeward walls gradually drop down. This causes the wind driven force for natural cross ventilation is slight on the same floor. From the pressure coefficient distribution, it can be seen that the large potential for natural ventilation could occur when the openings are located on the front of roof and the low part of the leeward wall, because a large difference in the pressure coefficient occurs at these parts. There are some differences between the pressure coefficient distributions of the normal pattern and the staggered pattern. The pressure coefficients of the normal pattern have a larger fluctuation on the windward walls and roofs, while the pressure coefficients of the staggered pattern tend to be uniform.

Natural ventilation rate

As the achieved pressure coefficient only represents the wind driven force and does not express the natural ventilation of the building, it is necessary to consider the natural ventilation rate that is generated by the natural force of combining wind pressure and buoyancy force in the urban environment. According to the three functions of ventilation, whole building ventilation rate (ls^{-1}) for health and air change rate (ACH) for thermal comfort are applied to assess the potential for natural ventilation at the same floor in the cases from Case 1 to Case 4. The ventilation rate unit $\text{ls}^{-1}\text{m}^{-2}$ is used to assess the potential for cooling in the cases from Case 5 to Case 10.

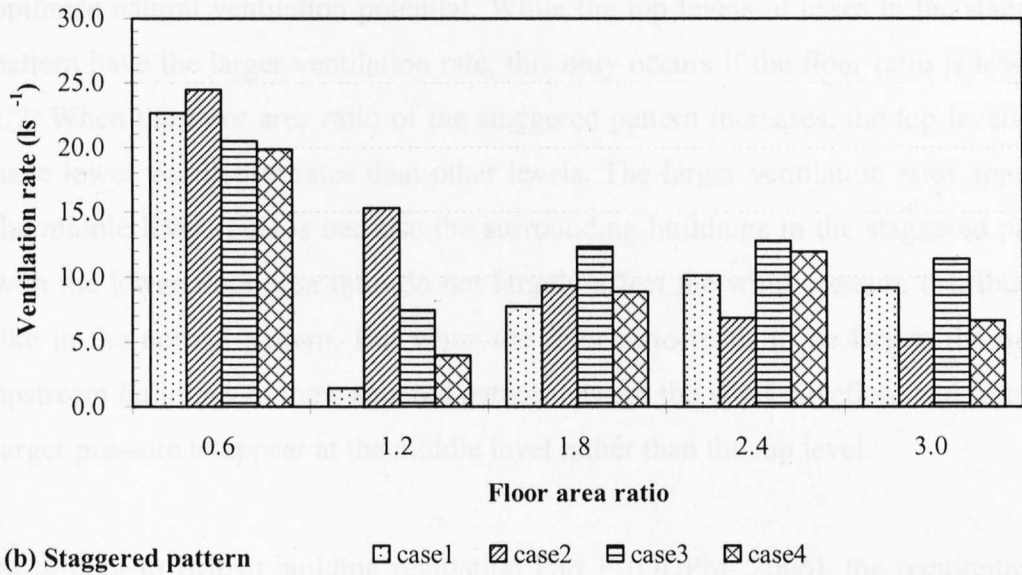
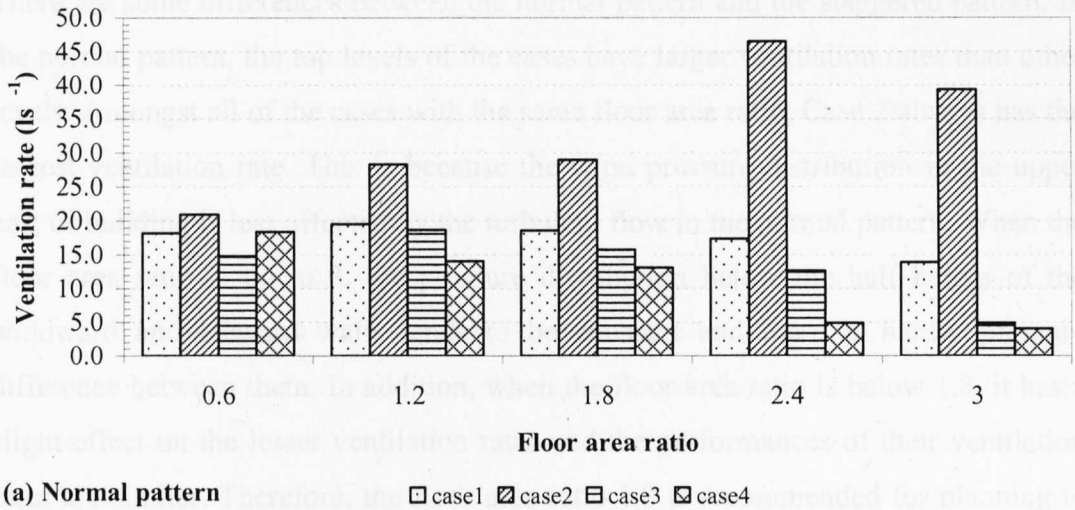


Figure 6.3 Whole building ventilation rates of the buildings of varying floor area ratios

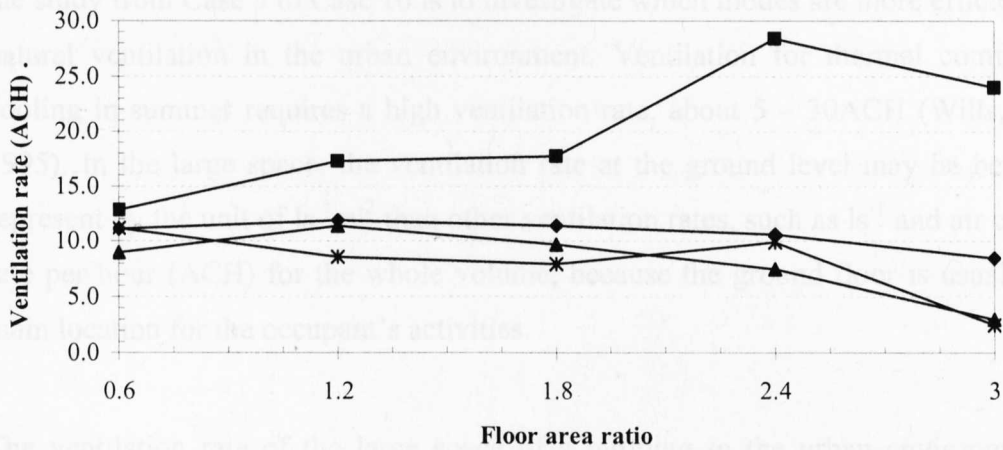
Figure 6.3 shows the effects of floor area ratios on the whole building ventilation rates, for both the normal pattern and the staggered pattern: Case 1 for the average of the building, Case 2 for the top level, Case 3 for the middle level and Case 4 for the ground level. In general, ventilation rates throughout different levels of the whole building are considerably affected by the floor area ratio. The lower floor area ratio has the larger ventilation rates, especially in the staggered pattern. For instance, the lowest floor area ratio 0.6 of the staggered pattern has the largest ventilation rate.

There are some differences between the normal pattern and the staggered pattern. In the normal pattern, the top levels of the cases have larger ventilation rates than other levels. Amongst all of the cases with the same floor area ratio, Case 2 always has the largest ventilation rate. This is because the wind pressure distribution in the upper part of building is less affected by the turbulent flow in the normal pattern. When the floor area ratio is up to 3, the pressure distribution below the half height of the windward and leeward walls tends to be constant and there is hardly pressure difference between them. In addition, when the floor area ratio is below 1.8, it has a slight effect on the lesser ventilation rates and the performances of their ventilation rates are similar. Therefore, the floor area ratio 1.8 is recommended for planning to optimise natural ventilation potential. While the top levels of cases in the staggered pattern have the larger ventilation rate, this only occurs if the floor ratio is less than 1.2. When the floor area ratio of the staggered pattern increases, the top levels may have lower ventilation rates than other levels. The larger ventilation rates appear at the middle level. This is because the surrounding buildings in the staggered pattern with the lower floor area ratio do not largely affect the wind pressure distributions, like in the normal pattern. But when the floor ratio tends to be larger, the nearest upstream buildings in the staggered pattern change the wind direction, and cause the larger pressure to appear at the middle level rather than the top level.

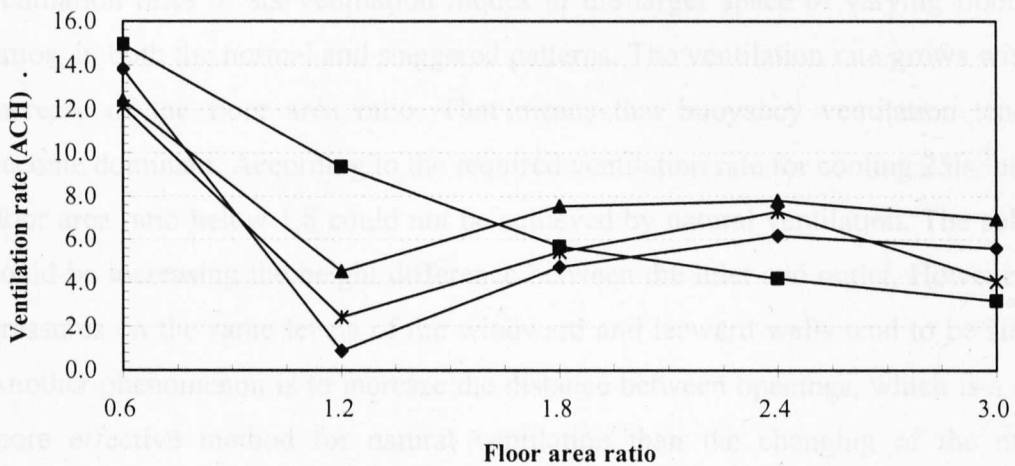
According to British building regulation Part F (ODPM, 2006), the requirement of whole building ventilation rate for the dwelling should be not less than 25ls^{-1} . From the above result, it can be seen that the building in the urban environment cannot achieve the required ventilation rate using the current natural method, except for at its top level. The solution could be the enlarging of the equivalent ventilator area, provided that this does not affect other environmental comforts. If the ventilator area expands to threefold of the current area, the buildings of the floor area ratios below 1.8 can achieve the required ventilation rate by the natural method. Another solution is using mix mode ventilation. The mechanical ventilation can supplement the lower natural ventilation rate.

Purge ventilation rates in the urban environment can be achieved in most cases. Figure 6.4 shows the air change rate in the four cases of the normal pattern and

staggered pattern with the different floor area ratios. The purpose of purge ventilation is for occasionally removing pollution or water vapour of the habitable room. It can also be used for thermal comfort in summertime. In these cases, the opening area follows the suggestion of 1/20 of the near external wall room area. According to building regulation Part F (ODPM, 2006), which requires the minimum purge ventilation rate for the habitable room to be 4ACH, this can be achieved by natural ventilation in these cases. The only exception is the lower levels in floor ratio 3 of the normal pattern, and floor ratio 1.2 of the staggered pattern. In the normal pattern, the top levels of the buildings with 1.2 and 1.8 floor area ratios have about twice the ventilation rates of the ground levels.



(a) Normal pattern



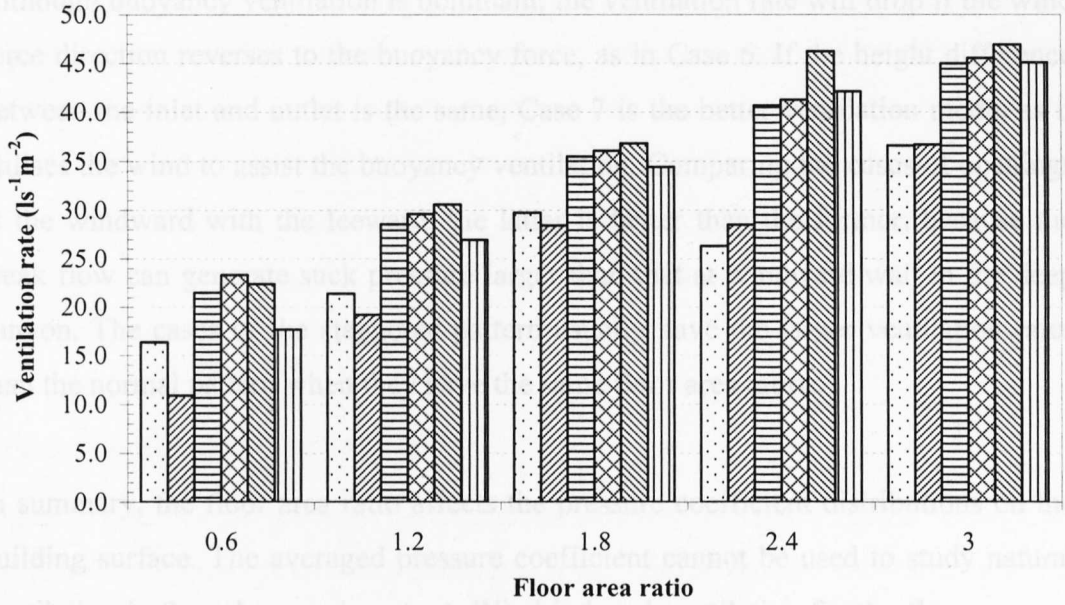
(b) Staggered pattern

Figure 6.4 Purge ventilation rates of the buildings of varying floor area ratios

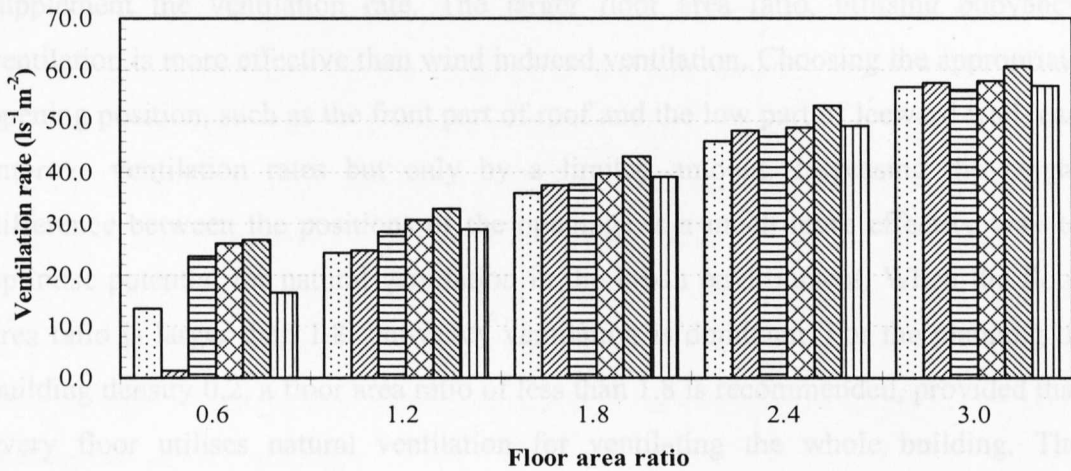
The purge ventilation rates in the staggered pattern are more sensitive to the increase in the floor area ratio, but when the floor area ratio is larger than 1.8, the effects of on ventilation rates are slight. The controllable opening makes purge ventilation intermittent, and the larger ventilation rate could improve thermal comfort in summer, but a too high ventilation rate means higher expenses on opening, so combining the optimum opening area with floor area ratio could bring multiple benefits for the occupants.

Besides the cross ventilation at the same floor, the combination of wind induced and buoyancy ventilation is commonly used for cooling buildings in the urban environment. As the wind can assist or oppose buoyancy ventilation, the purpose of the study from Case 5 to Case 10 is to investigate which modes are more efficient for natural ventilation in the urban environment. Ventilation for thermal comfort or cooling in summer requires a high ventilation rate, about 5 – 30ACH (Wills, et al, 1995). In the large space, the ventilation rate at the ground level may be better to represent by the unit of $\text{ls}^{-1}\text{m}^{-2}$ than other ventilation rates, such as ls^{-1} and air change rate per hour (ACH) for the whole volume, because the ground floor is usually the main location for the occupant's activities.

The ventilation rate of the large space of a building in the urban environment is determined by the height difference between the openings. Figure 6.5 describes the ventilation rates of six ventilation modes in the larger space of varying floor area ratios, in both the normal and staggered patterns. The ventilation rate grows with the increase of the floor area ratio. That means that buoyancy ventilation tends to become dominant. According to the required ventilation rate for cooling $25\text{ls}^{-1}\text{m}^{-2}$, the floor area ratio below 1.8 could not be achieved by natural ventilation. The solution could be increasing the height difference between the inlet and outlet. However, the pressures on the same levels of the windward and leeward walls tend to be similar. Another phenomenon is to increase the distance between openings, which is a much more effective method for natural ventilation than the changing of the natural ventilation modes in the urban environment, especially in the staggered pattern. In the same floor ratio, the difference of ventilation rates of the cases accounts for the small portion of the whole ventilation rate.



(a) Normal pattern □ case5 ▨ case6 ▤ case7 ▩ case8 ▧ case9 ▥ case10



(b) Staggered pattern □ case5 ▨ case6 ▤ case7 ▩ case8 ▧ case9 ▥ case10

Figure 6.5 Cooling ventilation rates of the large space of the buildings of varying floor area ratios

Choosing an appropriate ventilation mode in the urban environment could increase the potential for natural ventilation. For the same floor area ratio, Case 9 usually has the largest ventilation rate among the six cases, while Case 6 has the lowest ventilation rate. The reason is that the positions of openings in Case 9 can form a larger pressure difference, and the wind pressure is coincident with the buoyancy driven flow.

Although buoyancy ventilation is dominant, the ventilation rate will drop if the wind force direction reverses to the buoyancy force, as in Case 6. If the height difference between the inlet and outlet is the same, Case 7 is the better ventilation mode, as it utilises the wind to assist the buoyancy ventilation. Comparing the cases of openings at the windward with the leeward, the latter is better than the former, because the weak flow can generate suck pressure larger than that at windward wall in the deep canyon. The cases of the staggered pattern usually have the larger ventilation rates than the normal pattern when they have the same floor area ratios.

In summary, the floor area ratio affects the pressure coefficient distributions on the building surface. The averaged pressure coefficient cannot be used to study natural ventilation in the urban environment. Wind induced ventilation for the floors cannot meet the requirement of whole building ventilation rates recommended by building regulation. The lower level should consider using mix-mode ventilation in order to supplement the ventilation rate. The larger floor area ratio, utilising buoyancy ventilation is more effective than wind induced ventilation. Choosing the appropriate opening position, such as the front part of roof and the low part of leeward wall, can improve ventilation rates but only by a limited amount. Increasing the height difference between the positions of the openings is a much more effective way to optimise potential for natural ventilation in the urban environment. When the floor area ratio is larger than 1.8, buoyancy ventilation is dominant. For the planning of building density 0.2, a floor area ratio of less than 1.8 is recommended, provided that every floor utilises natural ventilation for ventilating the whole building. The staggered pattern has more advantages for improving ventilation rates than the normal pattern at the lower floor area ratio. However, with the increase of the floor area ratio, the differences of ventilation rates between the staggered pattern and the normal pattern tend to be small, because the buoyancy becomes the dominant ventilation force. With the increase of the floor area ratio, the larger ventilation rate occurs at the top level of the building in the normal pattern, whilst the larger ventilation rate occurs at the middle level of the building in the staggered pattern.

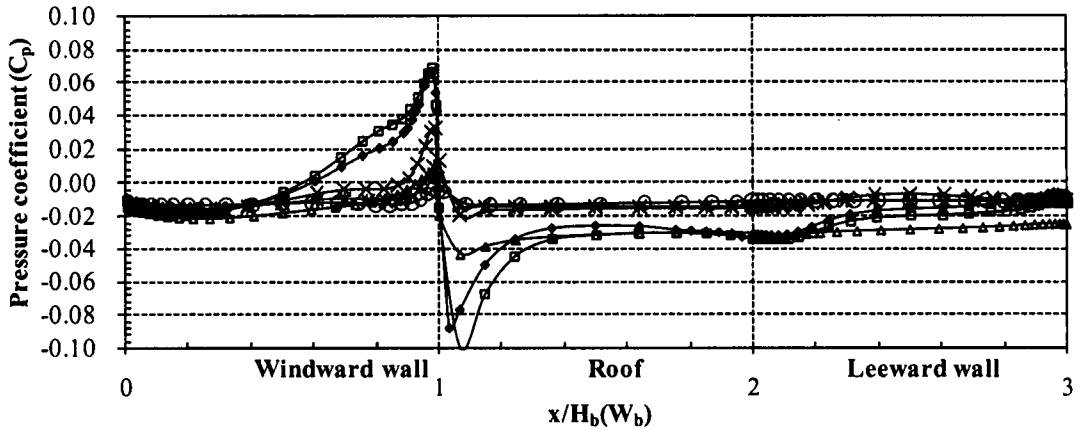
6.3.2 Building density

Building density is another important indicator to consider at the planning stage. Under the constant floor area ratio, changes in building density and average building height can produce various planning forms. The larger building density with the lower building height affects the habitants' life quality. The smaller building density with higher building height could also harm the environment. The purpose of this research is to investigate the effects of varying building densities with the constant floor area ratios on the potential for natural ventilation.

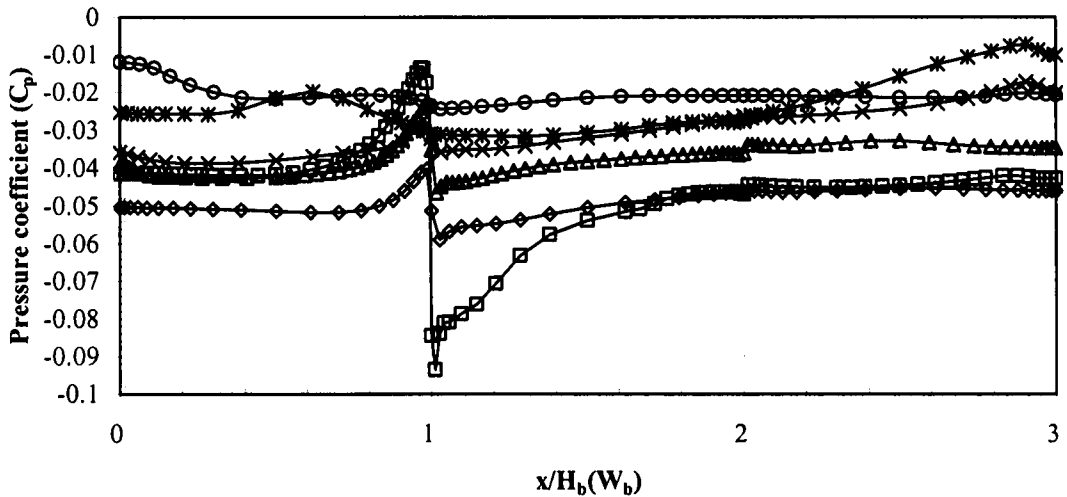
Pressure coefficient distribution

Figure 6.6 shows the pressure coefficient distributions along the central lines of the models in the different building densities. In the normal pattern, the building in the lower building density has larger positive pressure coefficients on the windward wall and larger negative pressure coefficients on the roof and leeward wall than the building in the higher density. This is because the lower building density has a larger space between the buildings for turbulence to develop. In the staggered pattern, all of the pressure coefficients on the surfaces of the buildings are negative. With the increase in building density, the wind pressures around the upwind edge of the roof are weakened. Although the ratio of building height to building space in the staggered pattern is smaller than that in the normal pattern under the condition of the same building density, the building in the staggered pattern does not always acquire larger pressure coefficient difference than that in the normal pattern. Note that the ratio of building height and building distance is not enough to explain the pressure distribution in the planning.

Pressure coefficients on the surfaces of the building in the high density pattern do not have a large difference, except around the upwind edge of the roof. In the high building density, the pressure coefficient difference on the building surface is so slight that it cannot generate enough wind-induced ventilation. It implies that the high-rise low density building would have more natural ventilation potential than the low-rise high density building, provided that their floor area ratios are the same.



(a) Normal pattern —□— 0.12 —◆— 0.15 —▲— 0.2 —×— 0.225 —*— 0.3 —○— 0.36



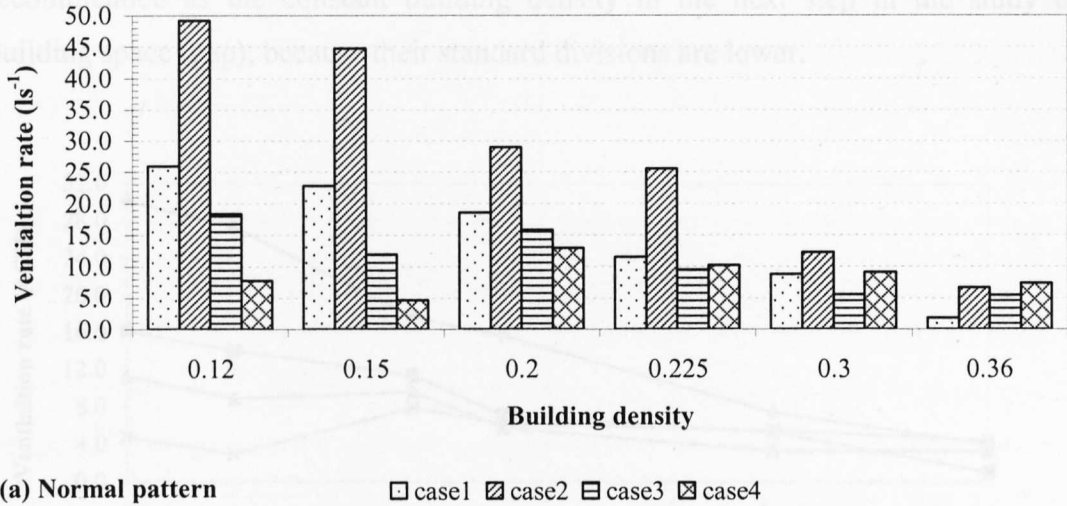
(b) Staggered pattern —□— 0.12 —◆— 0.15 —▲— 0.2 —×— 0.225 —*— 0.3 —○— 0.36

Figure 6.6 Pressure coefficient distributions along the central lines of the models of varying building densities

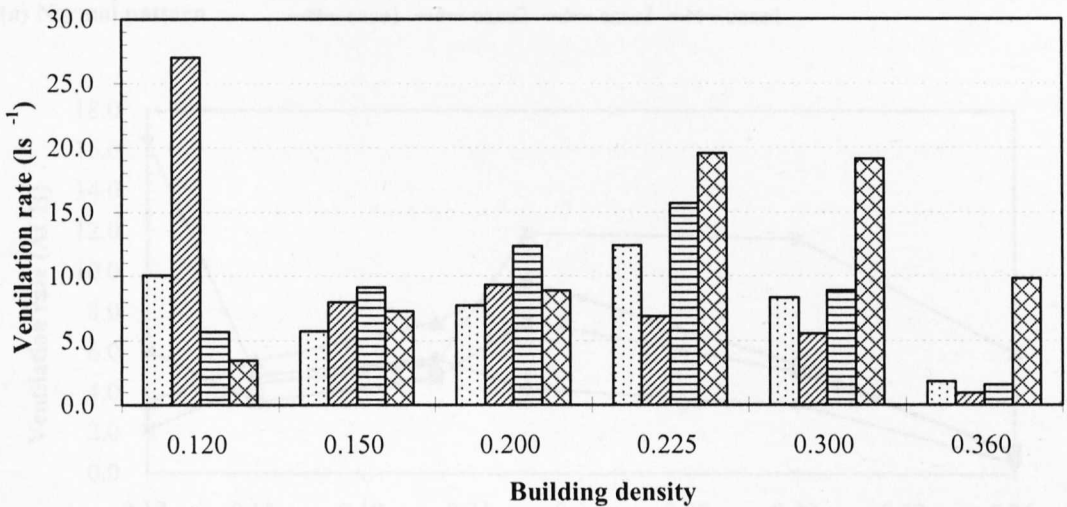
Natural ventilation rate

The building density can affect natural ventilation rates at different levels as well as the floor area ratio. Figure 6.7 shows the whole building ventilation rates of the buildings in varying building densities, keeping the floor area ratio constant at 1.8. In the normal pattern, the ventilation rates of Case 1 and Case 2 drop as the building density increases. Cases 1 and Case 2, which represent the averaged and the top level ventilation rates respectively, imply that the natural ventilation potentials decrease with the increase of the building densities. The ventilation rates of the ground levels in Case 4 have some fluctuation with the change of the building density, the greatest

occurring at building density 0.2. In the staggered pattern, the ventilation rates of Case 4 at the ground level increase as the building density increases. However, the ventilation rates of Case 1 at the top level dramatically drop down,



(a) Normal pattern □ case1 ▨ case2 ▩ case3 ▤ case4

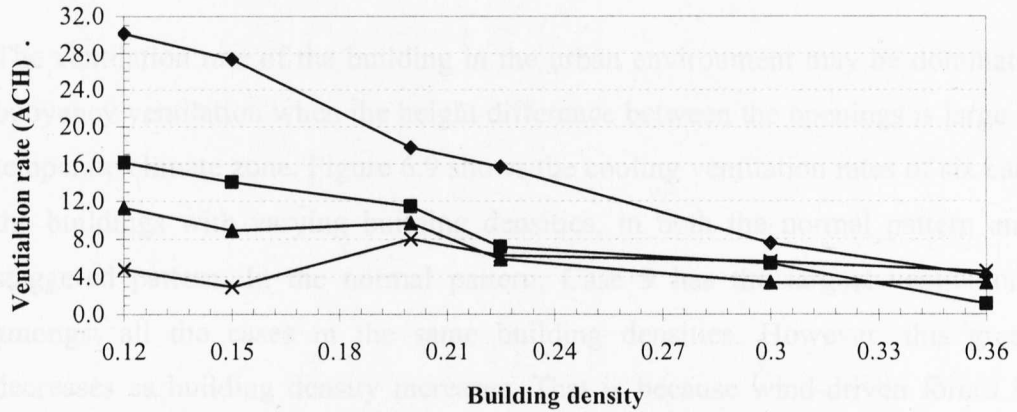


(b) Staggered pattern □ case1 ▨ case2 ▩ case3 ▤ case4

Figure 6.7 Whole building ventilation rates of the buildings of varying building densities

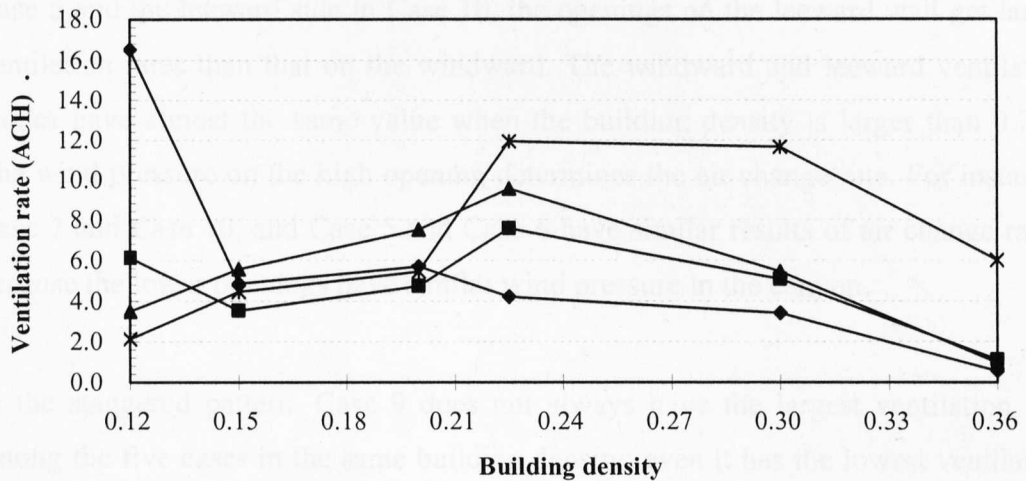
If the required ventilation rate of 25ls^{-1} in dwellings recommended by the building regulation Part F (ODPM, 2006) is taken as the criteria, the current cases, except some top levels, cannot acquire the required ventilation rates for health. Consequently, natural ventilation design in the urban environment should be concerned with opening size and wind pressure distribution on the building.

Regardless, neither the high-rise, lower density building nor the low-rise, high density building can achieve the standard for the whole building, the high density low-rise building performing worse than its counterpart. Among the six building densities in the normal pattern and the staggered pattern, the building density 0.2 is recommended as the constant building density in the next step in the study of building space (gap), because their standard divisions are lower.



(a) Normal pattern

■ case1 ◆ case2 ▲ case3 ✕ case4



(b) Staggered pattern

■ case1 ◆ case2 ▲ case3 ✕ case4

Figure 6.8 Purge ventilation rates of the buildings of varying building densities

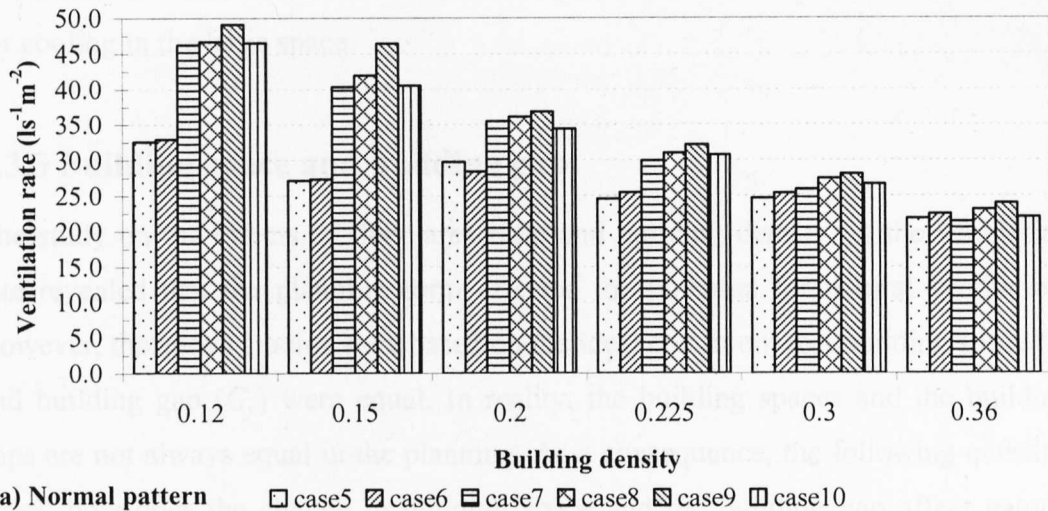
Figure 6.8 shows the purge ventilation rates of the four cases of varying building densities in both the normal pattern and staggered pattern. In the normal pattern, the purge ventilation rates go down with the increase in building density. The top level of Case 2 has the largest ventilation rate in the same building density. The ground

level has the lowest ventilation rate and is not sensitive to building density. In terms of the building regulation requirements on a purge ventilation rate of at least 4ACH, only the cases in the building density 0.12, 0.2 and 0.225 can achieve this requirement. In the staggered pattern, the ventilation rates of the cases keep the relatively stable status between the building density 0.12 and 0.3, except for Case 2 in building density 0.12. When the building density is larger than 0.3, the ventilation rates fall significantly.

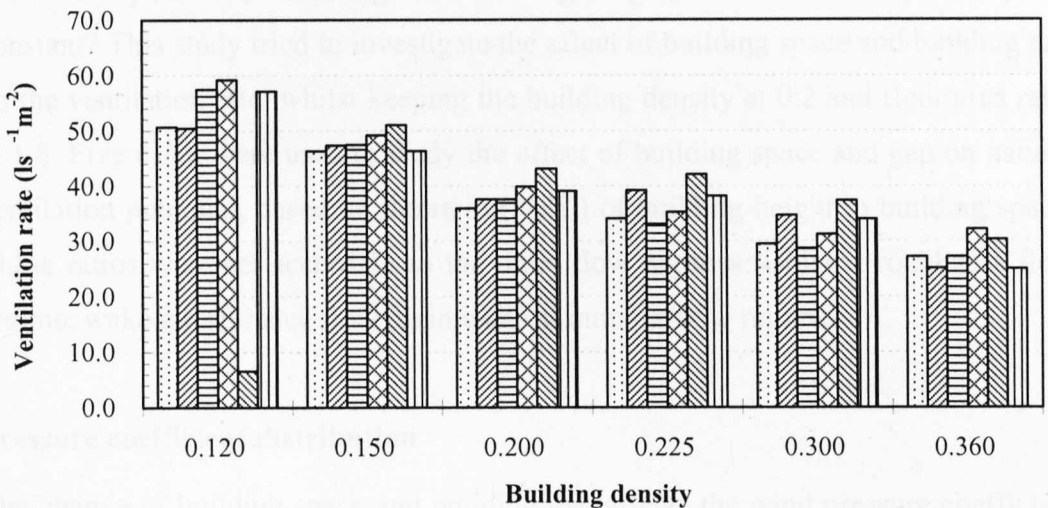
The ventilation rate of the building in the urban environment may be dominated by buoyancy ventilation when the height difference between the openings is large in the temperate climate zone. Figure 6.9 shows the cooling ventilation rates of six cases of the buildings with varying building densities, in both the normal pattern and the staggered pattern. In the normal pattern, Case 9 has the largest ventilation rate amongst all the cases in the same building densities. However, this gradually decreases as building density increases. That is because wind-driven forces in the high building density are weakened and the building height and the height difference between the openings decrease. Comparing the openings on the windward side in Case 5 and the leeward side in Case 10, the openings on the leeward wall get larger ventilation rates than that on the windward. The windward and leeward ventilation modes have almost the same value when the building density is larger than 0.225. The wind pressure on the high opening determines the air change rate. For instance, Case 7 and Case 10, and Case 5 and Case 6 have similar results of air change rates, because the lower openings have similar wind pressure in the canyon.

In the staggered pattern, Case 9 does not always have the largest ventilation rate among the five cases in the same building density; even it has the lowest ventilation rate in the lowest building density. The natural ventilation modes have more effects on ventilation rates in the low building densities than in the higher building densities. The difference between ventilation rates in the cases gradually reduces with the increase of building density. Comparing the ventilation rates of cases in the normal pattern and the staggered pattern, the planning layout at the lower building density affects the ventilation rates, but this is weakened as the building density increases. The reason is that the buoyancy force is the dominant ventilation force in the lower

building density, and there is the lower wind pressure difference in the high building density.



(a) Normal pattern case5 case6 case7 case8 case9 case10



(b) Staggered pattern case5 case6 case7 case8 case9 case10

Figure 6.9 Cooling ventilation rates of the buildings of varying building densities

For a building in a high building density location, the recommended natural ventilation design strategy is using stack effect ventilation. The vents on the roof can be used to increase the difference in height, as well as reducing the effect of building density on the pressure coefficient. For a building in a lower density location, the recommended natural ventilation strategy is using a combination of wind and stack effect ventilation. The recommended mode is like Case 9: the inlet openings are set at the leeward, and the outlet openings are set at the roof near the wind ward wall. As

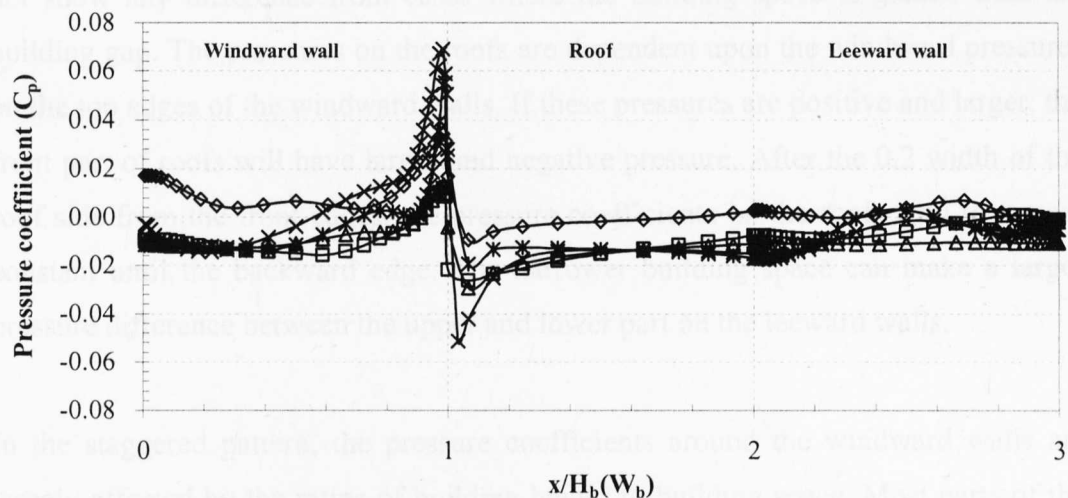
the criteria for cooling is $25\text{ls}^{-1}\text{m}^2$, the maximum building density is 0.3 for the purpose of cooling by natural ventilation in the normal pattern; in the staggered pattern, the building density can be up to 0.36. In a high density location, the layout can affect the ventilation rates of the same level, but little affects the ventilation rate for cooling in the large space.

6.3.3 Building space and building gap

The study on the effects of floor area ratio and building density on the ventilation rate revealed that the planning form affected the potential for natural ventilation. However, the above studies were based on the ideal condition, that building space (S_c) and building gap (G_c) were equal. In reality, the building spaces and the building gaps are not always equal in the planning. As a consequence, the following question arose: how does the change in building space and the building gap affect natural ventilation potential, assuming that building height and the building density are constant? This study tried to investigate the effect of building space and building gap on the ventilation rate, whilst keeping the building density at 0.2 and floor area ratio at 1.8. Five cases were used to study the effect of building space and gap on natural ventilation potential, based on the ratio (H_b/S_c) of building height to building space. These ratios were set according to the three flow regimes: isolated roughness flow regime, wake interference flow regime and skimming flow regime.

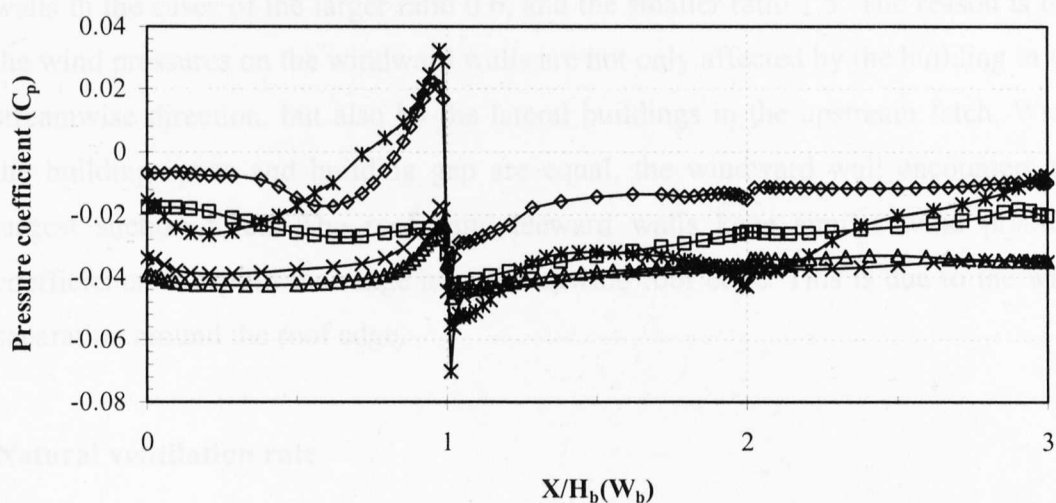
Pressure coefficient distribution

The change of building space and building gap affects the wind pressure coefficient distributions on the building surfaces. Figure 6.10 shows the pressure coefficient distributions along the central lines of the windward walls, roofs and leeward walls of the buildings in the five cases, using different ratios of building height to building space. Buildings in the normal and stagger patterns have similar tendencies when comparing the distribution of wind pressure coefficients. The larger changes usually occur around the top edges of the windward walls, because as the wind flow separates at this edge, there is larger pressure gradient around it.



(a) Normal pattern

—◇— 0.6 —□— 0.75 —△— 1 —×— 1.5 —*— 2



(b) Staggered pattern

—◇— 0.6 —□— 0.75 —△— 0.867 —×— 1 —*— 1.5

Figure 6.10 Pressure coefficient distributions along the central lines of the buildings of varying ratios of building height to building space

In the normal pattern, the pressure coefficients on the windward walls of the case of small ratio (H_b/S_c) can be positive, because the larger building space provides the space for wind flow development, and the reversed wind flow adds the pressure on the windward walls. With the increase of the ratio (H_b/S_c), most parts of the windward wall encounter negative pressure, except the part along the top edge. When the building space is nearly equal to the building gap, the pressure coefficients around the top edge of the windward wall reach the maximum positive pressure. When the building space is less than the building gap, the pressure coefficients do

not show any difference from cases where the building space is greater than the building gap. The pressures on the roofs are dependent upon the windward pressures on the top edges of the windward walls. If these pressures are positive and larger, the front part of roofs will have larger and negative pressure. After the 0.2 width of the roof side from the front edges, the pressure coefficients on the roofs tend to remain constant until the backward edge. The narrower building space can make a larger pressure difference between the upper and lower part on the leeward walls.

In the staggered pattern, the pressure coefficients around the windward walls are largely affected by the ratios of building height to building space. Most parts of the windward walls encounter suction forces, except the upper part of the windward walls in the cases of the larger ratio 0.6, and the smaller ratio 1.5. The reason is that the wind pressures on the windward walls are not only affected by the building in the streamwise direction, but also by the lateral buildings in the upstream fetch. When the building space and building gap are equal, the windward wall encounters the largest suction force. The roofs and leeward walls keep similar wind pressure coefficients, except in the range near the upwind roof edge. This is due to the wind separation around the roof edge.

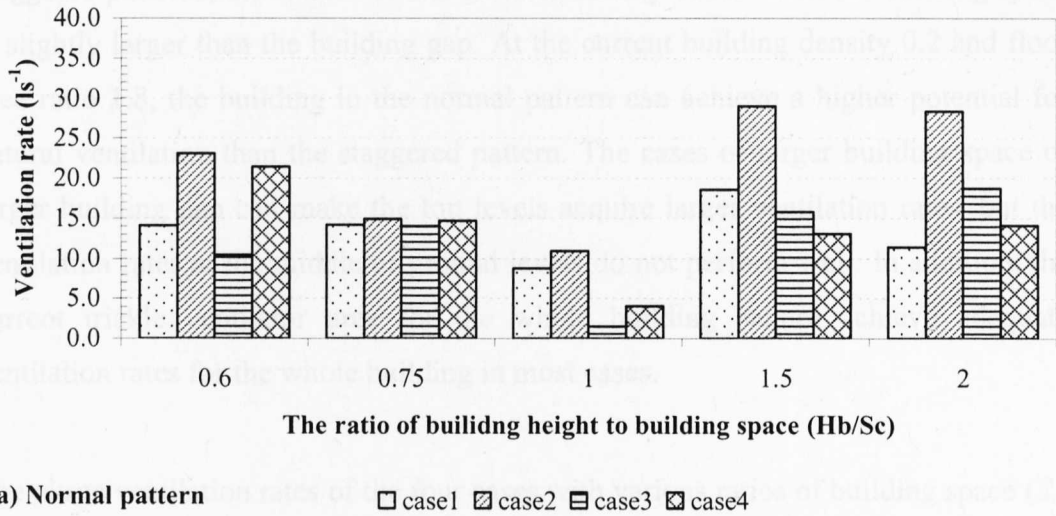
Natural ventilation rate

The change of the building space and the building gap can influence the whole building ventilation rates of the buildings, under the condition that building density and floor area ratio are the same. Figure 6.11 shows the whole building ventilation rate of the four cases, with five different ratios of building height to building space.

In the normal pattern, the ventilation rates reduce with the increase of the ratios (H_s/S_c) until the ratio is equal to 1. When the ratio is 1.5 ($S_c = G_c$), its average ventilation rate is the maximum in the five cases. In the case of 0.6 H_s/S_c , its ground level has a larger ventilation rate than the top level. This is because the flow near the ground level causes larger pressure on the surface, and the minimum pressure exists around $0.5H_b$. The worst case is that the ratio (H_s/S_c) is 1. Its average ventilation rate is less than 10s^{-1} . Apart from the top levels in the cases where the ratios are 1.5 and 2, the whole building ventilation rates are less than the required ventilation rate of

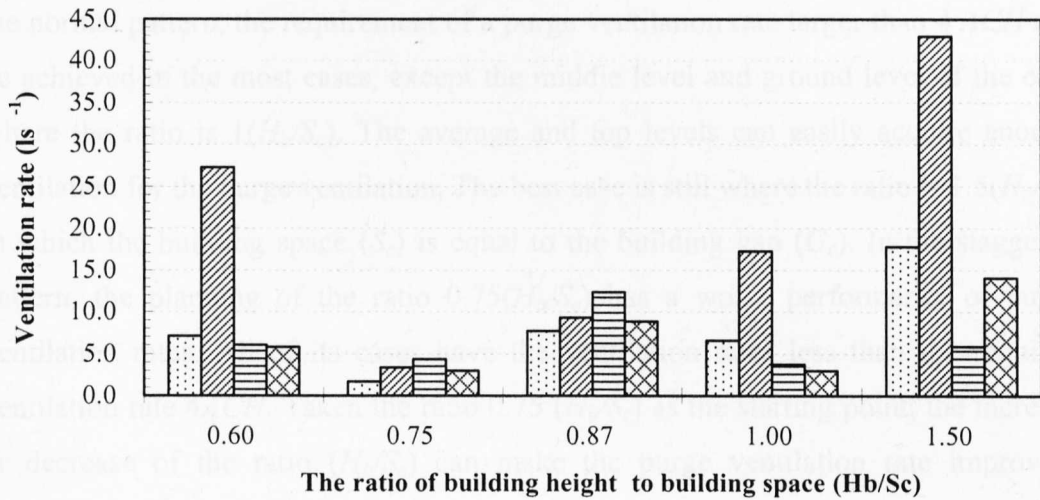
25ls⁻¹. However, when the trickle ventilator area is twice that of the current equivalent area, almost all the levels can achieve the requirement ventilation rate, except in the case where the ratio is equal to 1.

In comparing the whole building ventilation rates of the buildings in the normal and staggered patterns, the lower ventilation rates usually occur when the building space



(a) Normal pattern

□ case1 ▨ case2 ▤ case3 ▩ case4



(b) Staggered pattern

□ case1 ▨ case2 ▤ case3 ▩ case4

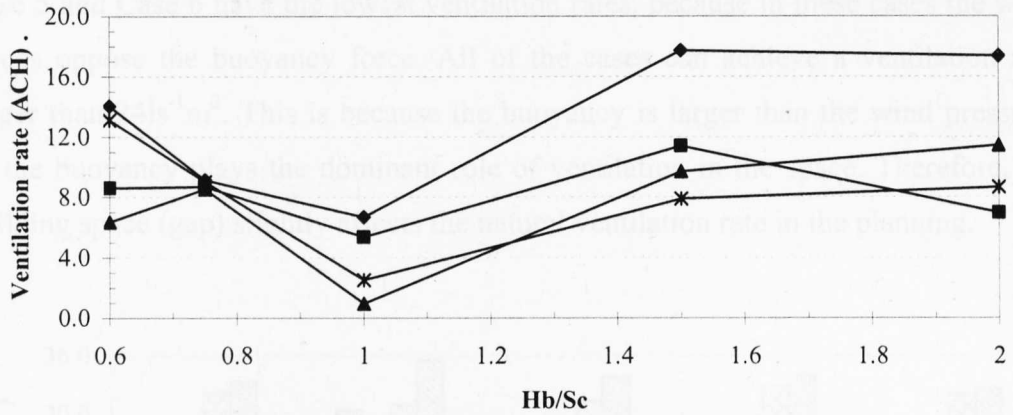
Figure 6.11 Whole building ventilation rates of the buildings of varying of the ratios of building height to building space

In the staggered pattern, the case of the ratio (H_s/S_c) is 1.5 can acquire larger ventilation rates than other cases, especially its top and ground level. When the ratio is 0.87, which means the building space is equal to the building gap, there is not a large difference between the ventilation rates of the three levels and the average one.

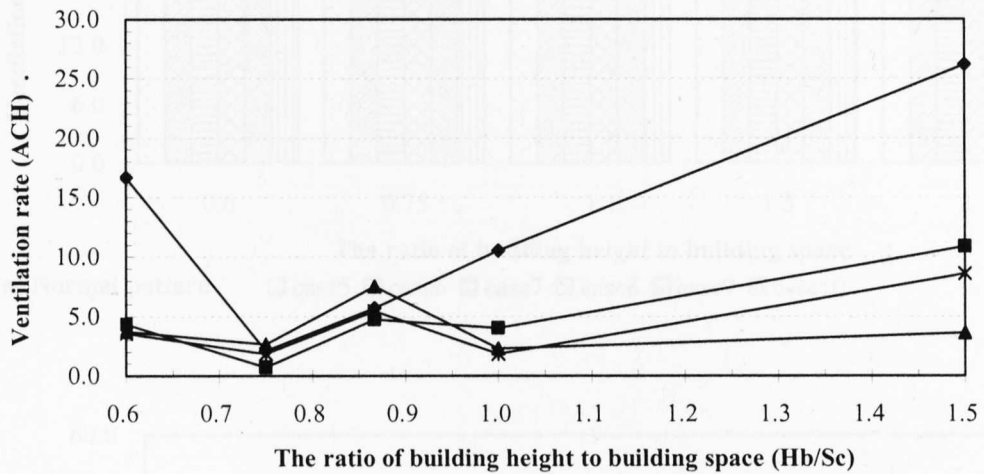
When the ratio is 0.75, the ventilation rates of the building are the lowest among all of the cases.

In comparing the whole building ventilation rates of the buildings in the normal and staggered patterns, the lower ventilation rates usually occur when the building space is slightly larger than the building gap. At the current building density 0.2 and floor area ratio 1.8, the building in the normal pattern can achieve a higher potential for natural ventilation than the staggered pattern. The cases of larger building space or larger building gap can make the top levels acquire larger ventilation rates, but the ventilation rates at the middle or ground levels do not perform well. In addition, the current trickle ventilator area for the whole building cannot achieve adequate ventilation rates for the whole building in most cases.

The purge ventilation rates of the four cases with various ratios of building space (S_c) to building gap (G_c) in the normal and staggered pattern are shown in Figure 6.12. In the normal pattern, the requirement of a purge ventilation rate larger than 4 ACH can be achieved in the most cases, except the middle level and ground level of the case where the ratio is 1 (H_b/S_c). The average and top levels can easily acquire enough ventilation for the purge ventilation. The best case is still where the ratio is 1.5 (H_b/S_c), in which the building space (S_c) is equal to the building gap (G_c). In the staggered pattern, the planning of the ratio 0.75 (H_b/S_c) has a worse performance of purge ventilation rates. All of its cases have the ventilation rates less than the required ventilation rate 4ACH. Taken the ratio 0.75 (H_b/S_c) as the starting point, the increase or decrease of the ratio (H_b/S_c) can make the purge ventilation rate improved, especially the top levels of the buildings. Comparing the normal pattern and the staggered pattern, the former has a relatively stable condition with the increase of the ratio (H_b/S_c). On the contrary, the staggered pattern has the large difference between the top and ground levels in the increase or decrease of the ratio (H_b/S_c). The opening area on the top level can be reduced and the opening area on the ground level can be kept the similar areas.



(a) Normal pattern —■— case1 —◆— case2 —▲— case3 —*— case4



(b) Staggered pattern —■— case1 —◆— case2 —▲— case3 —*— case4

Figure 6.12 Purge ventilation rates of the buildings of varying of ratios of building height to building space

Natural ventilation rates combining wind induced and buoyancy ventilation in the large space are slightly affected by building space and building gap. Figure 6.13 illustrates the cases from Case 5 to Case 10 in various ratios of building space to building gap. This covers cases in the two layout patterns, under the condition of the same floor area ratio and the same building density. In the normal pattern, Case 9 has the largest ventilation rate among the six cases and the second largest is Case 8. The reason is that both of them have larger height differences between the inlet and the outlet. There is a slight difference amongst the cases with the same height between the openings. In the staggered pattern, Case 9 also has the largest ventilation rate.

Case 5 and Case 6 have the lowest ventilation rates, because in these cases the wind forces oppose the buoyancy force. All of the cases can achieve a ventilation rate larger than $24\text{ls}^{-1}\text{m}^2$. This is because the buoyancy is larger than the wind pressure, so the buoyancy plays the dominant role of ventilation in the space. Therefore, the building space (gap) slightly affects the natural ventilation rate in the planning.

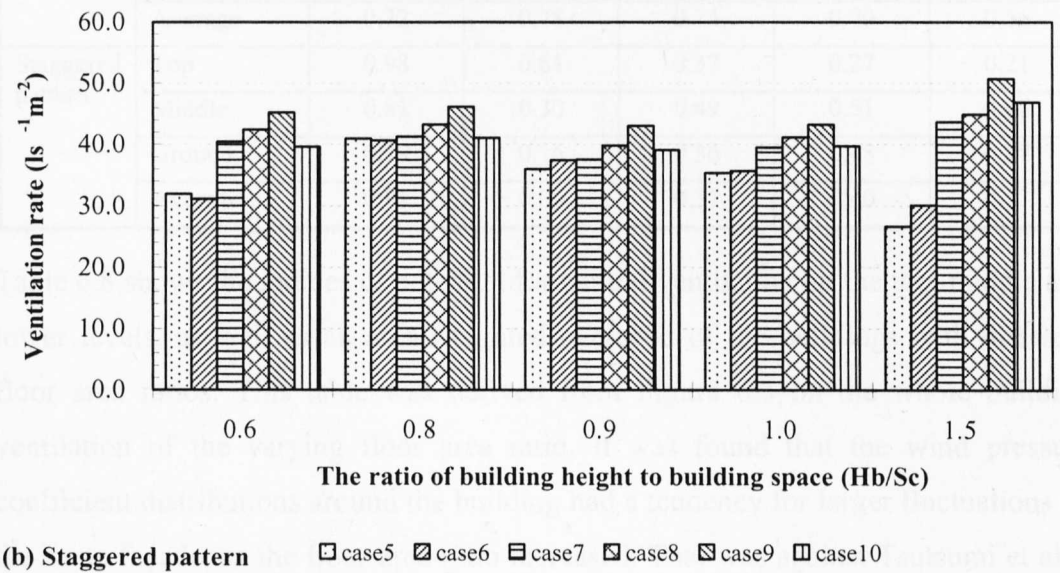
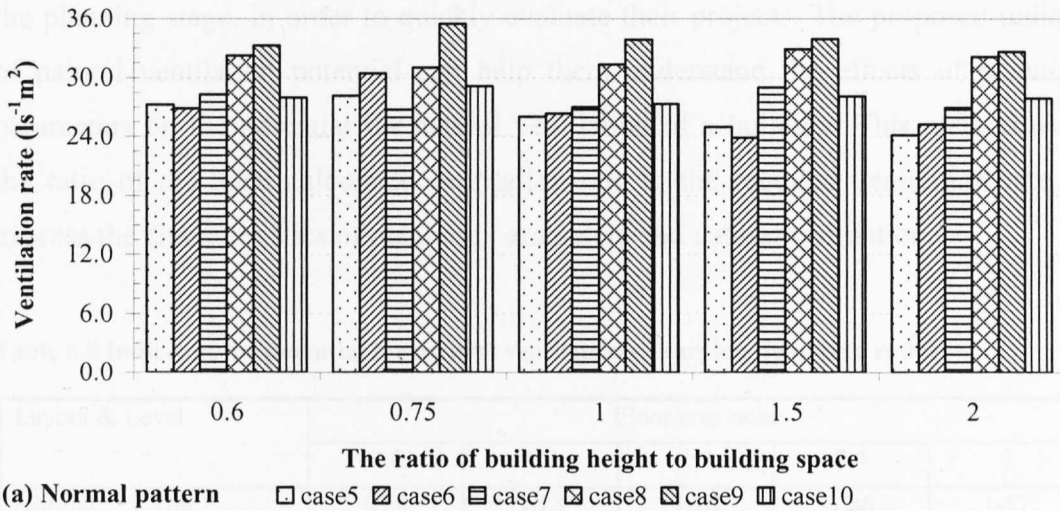


Figure 6.13 Cooling ventilation rates of the buildings of varying of ratios of building height to building space

6.4 Discussion

6.4.1 Planning parameters and natural ventilation potential

From the above results, it can be seen that the planning parameters influenced the buildings access to adequate natural ventilation for a healthy and comfortable indoor environment. So an agreement between the designed ventilation rate and the required ventilation rate is necessary at the planning stage. The planners and architect need to choose the method that can express the natural ventilation potential of the building at the planning stage, in order to quickly evaluate their projects. The proposed indices of natural ventilation potential can help them understand the effects of planning parameters on the potential for natural ventilation of a building. This method used the ratio of the local calculated ventilation rate to the required ventilation rate to express the characteristics of planning parameters and natural ventilation.

Table 6.8 Indices of the potential for natural ventilation of varying floor area ratios

Layout & Level		Floor area ratio				
		0.6	1.2	1.8	2.4	3
Normal Pattern	Top	0.84	1.13	1.16	1.86	1.57
	Middle	0.59	0.75	0.63	0.50	0.19
	Ground	0.73	0.56	0.52	0.20	0.16
	Average	0.72	0.78	0.74	0.70	0.56
Staggered pattern	Top	0.98	0.61	0.37	0.27	0.21
	Middle	0.81	0.30	0.49	0.51	0.46
	Ground	0.79	0.16	0.36	0.48	0.27
	Average	0.91	0.06	0.31	0.40	0.37

Table 6.8 shows the indices of potential for natural ventilation on the top, middle and lower levels, as well as an area-weighted averaged of the buildings with different floor area ratios. This table was derived from Figure 6.3 on the whole building ventilation of the varying floor area ratio. It was found that the wind pressure coefficient distributions around the building had a tendency for larger fluctuations on the same façade, as the floor area ratio increased. That was against Tsutsumi et al.'s (1992) method, which used the average wind pressure coefficient to express natural ventilation potential. This table suggests that the normal pattern can enhance the ventilation rate of the top level but weaken that of the lower level with the increase of building height. It also suggests that the staggered pattern weakens the ventilation rate of all levels.

It is well known that building density has a significant effect on the potential for natural ventilation in the urban environment (Ward, 2003, Germano et al., 2005). However, this cannot answer whether or not the building density is suitable for the building to acquire the required natural ventilation rate. The indices in Table 6.9 show the effects of building density on the potential for natural ventilation. They denote the potential of acquiring natural ventilation in the corresponding level under the prevailing wind environment. The data on the three levels such as the top, middle and ground show there is uneven potential along the vertical of the building in the urban environment. Under the same floor area ratio, the lower density means the building is higher, and vice versa.

Table 6.9 Indices of the potential for natural ventilatino of varying building densities

Layout & Level		Building density					
		0.12	0.15	0.2	0.24	0.3	0.4
Normal pattern	Top	1.97	1.79	1.16	1.02	0.49	0.27
	Middle	0.74	0.48	0.63	0.38	0.22	0.22
	Ground	0.31	0.19	0.52	0.41	0.36	0.29
	Average	1.0	0.9	0.74	0.46	0.35	0.07
Staggered pattern	Top	1.08	0.32	0.37	0.28	0.22	0.04
	Middle	0.23	0.36	0.49	0.63	0.36	0.06
	Ground	0.14	0.29	0.36	0.78	0.76	0.39
	Average	0.40	0.23	0.31	0.50	0.33	0.07

In the normal pattern, compared with the low-rise high density building, the high-rise low density building has a larger natural ventilation potential in the levels above the half of building height, and also has a smaller potential in the levels below the half of the building height. For the multi-storey building, the low-density and high-rise factors may cause the lower part of building to fail to achieve enough natural ventilation. Meanwhile, the higher density, low-rise building may mean the whole building has weak natural ventilation. In the staggered pattern, the high-rise, low density building can acquire relatively similar ventilation rate throughout the building levels; while the low-rise, high density building can mean the lower levels get a larger ventilation rate than the top levels.

When building density and floor area ratio are constant, the building configuration could also have the possibility to affect natural ventilation. Table 6.10 shows the indices of the potential for natural ventilation of buildings with different ratios of building height to building space. In the normal pattern, when the ratio of building height to building space is smaller than 1.5, the worst case occurs at the middle level. This is because the flow near the ground in the isolated or wake interface flow regime has a standing vortex, which imposes more pressure on the lower part of the building. Note that the maximum data of wind pressure distribution may not occur at the top level in these cases. The building can gain the maximum ventilation rate when the building space is equal to the building gap. When the space is equal to the building height, the building has the worst ventilation rate. In the staggered pattern, the larger ventilation rate occurs in the case where building space is less than building gap, and the smaller ventilation rate occurs in the case where building space is larger than building gap. The results are contrary to the conclusion that the larger space along the streamwise direction can gain larger wind pressure difference or natural ventilation from Tsutsumi et al.'s experiments (1992). It implies that the natural ventilation rate of the building in the planning is dependent upon not only the ratio of building height and space, but other planning parameters.

Table 6.10 Indices of the potential for natural ventilation of varying ratios of building height to building space

Layout & Level		The ratio of building height to Space					
		0.6	0.75	0.867	1	1.5	2
Normal pattern	Top	0.92	0.60	/	0.44	1.16	1.14
	Middle	0.42	0.56	/	0.06	0.63	0.75
	Ground	0.86	0.59	/	0.16	0.52	0.56
	Average	0.56	0.57	/	0.35	0.74	0.46
Staggered pattern	Top	1.09	0.14	0.37	0.69	1.72	/
	Middle	0.24	0.17	0.49	0.15	0.24	/
	Ground	0.23	0.12	0.36	0.12	0.56	/
	Average	0.28	0.07	0.31	0.26	0.71	/

6.4.2 Opening area for natural ventilation in the urban environment

The current building regulation Part F for ventilation (ODPM, 2006) guided the opening area of background ventilators for the whole building of dwellings according

to the total floor area and number of bedrooms, and the opening area for the purge ventilation according to the near external wall room floor area. However, the guidance assumed that the ventilation was constant at 1Pa pressure difference. This assumption neglected the effect of terrain on the coefficient, and sheltered location on the pressure. In the planning, the building with various pressures at the different levels on the building surfaces required an appropriate opening area for adequate natural ventilation. The opening area for ventilation should be dependent on its acquired ventilation rate.

As the building air tightness for minimising the uncontrollable infiltration was regulated in building regulation, the purposed ventilation had to consider what was a large enough opening area for health purposes. It is well known that the flow rate through an opening is proportional to the opening area (see Equation 2.4). Assuming that the opening discharge coefficient is constant under the same wind pressure condition, the opening area in the urban environment can be expressed by the above indices of the potentials for natural ventilation, as Equation 6.5:

$$A_u = A_r / \beta \quad (6.5)$$

Where A_u is the opening area in the urban environment; β stands for the indices of the potentials for natural ventilation; A_r means the opening area recommended by the building regulation.

The above indices of the potential for natural ventilation in the planning can be helpful in deciding an opening area for various levels in different situations. The opening area for purge ventilation according to the current building regulation can mostly achieve the required ventilation, so the rules for opening area are not necessary to revise. The suggestion for the dwelling, especially the multi-story building in the urban environment, is to add an extra controllable opening area for the lower levels, which is usually lower than half of the building height. This equivalent opening area can be determined by the difference between the ground level and the required ventilation rate. The inadequate guidance on openings for

natural ventilation design in the current regulations and standards (Karava et al., 2006) can be solved by considering the indices of the potential for natural ventilation.

6.4.3 Natural ventilation modes in the urban environment

Natural ventilation modes for cooling in the large space in the urban environment should consider natural forces combined with wind pressure and stack effect. Wind induced ventilation in the urban environment drops down so largely that it is not enough to acquire an adequate natural ventilation rate. Wind force in the urban canopy layer is disturbed, especially at the lower part of buildings, where wind pressure difference between windward and leeward walls is too slight to generate the enough ventilation for thermal comfort. In the urban environment, buoyancy ventilation plays the main role of natural ventilation with the increase in building height. The wind force can assist or resist the stack effect, which is dependent upon the opening position and airflow path. As a consequence, the incorporation of wind induced ventilation and buoyancy ventilation involving several natural ventilation modes is a good choice in the urban environment.

The position of openings impacts the potential for natural ventilation. For the opening on the roof, the best position is located at the front of 1/10 of roof width, because the separated flow at the front edge of the roof can generate the largest negative pressure in that range. For the openings at the walls, the mode with the inlet at the low part of the windward and outlet at the upper part of the leeward wall is better than the other opening position with the same height difference. For the openings that can only be set at the same side, the openings in the leeward wall have more natural ventilation potential than the openings in the windward wall, because the leeward wall has less interruption by the wind than the windward wall. Sometimes this single side ventilation is more efficient than the cross ventilation.

6.4.4 Guidelines of planning for natural ventilation in the urban environment

The above studies confirmed that the planning parameters affected the potential for natural ventilation in the urban environment. This study considering the combined ventilation by wind and stack effect can compensate for the study by the URBVENT

project (Guiaus and Allard, 2005), which neglected to consider wind induced ventilation in the urban environment. The promoted guidelines for natural ventilation in the urban environment may be useful for planners and architects to optimise the planning at the preliminary and conceptual design stage.

In the temperate climate zone, the ventilation for thermal comfort and cooling can be achieved by natural ventilation. However, the whole building ventilation for health in winter cannot always be achieved by natural ventilation. This can be solved by increasing the opening area. It implies that the current building regulation on the trickle ventilator area cannot guarantee adequate ventilation.

When considering the same building density and building space, the building in the planning with a lower floor area ratio could acquire adequate natural ventilation for health by enlarging threefold the size of the opening area. This suggests that the levels below half of the building height in the building with a larger floor area ratio should adopt the hybrid ventilation mode.

In the case of the same floor area ratio and the same building density, the change of building space and building gap can affect the potential for natural ventilation. When the difference between the building space and building gap is larger, the potential for natural ventilation of the building is more than when the building space is slightly larger than the building gap.

The high-rise low density building can acquire more natural ventilation potential than the low-rise high density building, provided that the floor area ratio is constant. But the high-rise building cannot get adequate natural ventilation on the lower half of the building's height.

With the increase of the floor area ratio, the building in the staggered pattern can generally acquire higher ventilation rates than the normal pattern in most levels, except the top part of the building. In the low building density scenario, the building in the normal pattern can gain larger ventilation rate than that in the staggered pattern.

When utilising the buoyancy ventilation for cooling, the recommended airflow path is the opening positions near the upstream edge of roof and at the low level of leeward wall.

Under the same conditions, the openings on the leeward wall are better than those on the windward wall for natural ventilation in the urban environment. The multi-storey building in the urban environment could utilise the wind induced ventilation for the upper levels, and the lower levels could use buoyancy ventilation.

6.5 Summary

The impacts of three planning parameters - floor area ratio, building density and building space (gap) - on the potential for natural ventilation in the normal pattern and staggered pattern layouts have been investigated. The findings can be concluded as follows.

The wind pressure coefficient distributions on the surfaces of the buildings in both planning layouts have the similar characteristics. They suggest that maximum pressure coefficients exist near the top edges of the windward walls and the minimum pressure coefficients exist near the upwind edges of the roofs. The pressure coefficient differences between windward and leeward walls tend to be smaller and smaller with the increase of the floor area ratio and building density. Building space (gap) can affect the pressure coefficient distributions around the building. The larger or smaller ratio of building height to building space can enhance the pressure coefficient difference between the windward and leeward walls.

The surface average wind pressure coefficient is not appropriate to calculate the whole building natural ventilation rate of the different levels of a building, or a building with many openings in the urban environment. This is because there are considerable differences among the wind pressure coefficient distributions at different positions on the same surface.

In most cases, the building in the planning can acquire adequate ventilation for thermal comfort and cooling in the temperate climate zone. However, the whole building ventilation rates for health in winter are affected by changes in planning. This implies that the current building regulation on the trickle ventilator area cannot guarantee the building adequate ventilation for health.

The current building regulation Part F should consider the cases of building in the urban environment. Its guidance on the opening area for purge ventilation can be achieved, but it should consider enlarging the ventilator area for achieving whole building ventilation rate in the urban environment. An extra and controllable opening for whole building ventilation is suggested for the lower levels in the urban environment.

Wind induced natural ventilation can achieve the required ventilation rate at the upper levels of buildings in the urban environment. The levels are dependent on the planning parameters. However, for the lower levels, the ventilation rate cannot be met by the current regulation.

The building in the staggered pattern can generally achieve larger ventilation rates in most levels than in the normal pattern, except the top part of the building. In the low building density, the building in the normal pattern can gain larger ventilation rate than that in the staggered pattern.

The planning with larger difference between building space and building gap can make the building acquire larger potential for natural ventilation than the case that the building space is similar as the building gap.

The indices of the potential for natural ventilation indicate the possibility of natural ventilation rates at the three levels of the building in the urban environment. They may be useful to estimate the ventilator area and decide the appropriate opening positions and ventilation modes in the urban environment.

It is an effective airflow path for achieving a higher ventilation rate to set the openings on the front of the roof along the wind direction and the lower part of leeward wall. For the single side ventilation, the openings at the leeward walls are better than the windward walls.

The current study on the potential for natural ventilation is solely based on ventilation rates. However, a good ventilation rate cannot ensure that occupants will gain satisfactory ventilation, because it does not represent the overall performance of the ventilation system in the building. The further study would investigate the ventilation effectiveness of the building to ensure the benefits of natural ventilation can be felt by the occupants.

CHAPTER 7

A Case Study to Evaluate the Potential for Natural Ventilation of an Urban Building

In the real urban environment, the uneven terrain and irregular building configurations complicate natural ventilation design. Design for natural ventilation has to consider the effects of the external environment, as well as the internal environment. These complexities make it difficult to design and evaluate the natural ventilation system of an urban building. The evaluation of the building's potential for natural ventilation can help designers to optimise their building schemes and choose sensible design strategies, as well as choosing appropriate building component details. This chapter is designed to demonstrate the application of the methodology to an urban building design, so that it can be used to evaluate the building's potential for natural ventilation, and provide the guidance for the natural ventilation design in the urban environment.

This chapter consists of four sections. Section 7.1 describes the background for predicting the potential for natural ventilation of a building in the urban environment and the framework of methodology. Section 7.2 presents the procedure of modelling the building and calculating its natural ventilation rate in the urban environment. Section 7.3 shows the results of experiments in three cases, including winter, summer and the hottest days under the isolated and urban environment conditions. Section 7.4 discusses the guidance of natural ventilation design in the urban environment and natural ventilation simulation.

7.1 Background

7.1.1 Research context

It is a necessary but challenging task to correctly estimate a building's natural ventilation potential at the design stage. The performance of natural ventilation determines the whole ventilation system, which is related to the indoor air quality and thermal comfort, as well as saving energy. The predication of the natural ventilation potential of the building would help the designers to improve and optimise their design. However, predicting the natural ventilation potential is complicated, because natural ventilation is affected by various factors, such as climate, terrain, surroundings and the building itself.

So far, this study has investigated natural ventilation potential from different angles, including climate region and building region. The method to assess the climate suitability of natural ventilation for cooling was proposed based on offsetting interior heating gain by natural ventilation (Axley and Emmerich, 2002). The method of estimating the potential of the force of the natural ventilation (Luo et al., 2007; Yang et al., 2005) was implemented by evaluating the natural ventilation potential of four cities in different climate zones. A semi-qualitative multi-criteria analysis method (Germano, 2007) was proposed to assess the natural ventilation potential of the region. The above methods may be useful to evaluate the potential of natural ventilation in the region, but they are not appropriate for designers to use in an urban environment in a region that has good conditions for natural ventilation. The designers are concerned with the natural ventilation potential of the building in the micro or neighbourhood scale, rather than the macro scale climate region.

Predicting the natural ventilation potential of the building in the urban environment faces two serious problems. In reality, natural ventilation has to combine wind force and buoyancy force, because when the wind-induced force either assists or opposes the buoyancy force, it can generate complex flow rates (Li and Delsante, 2001). The URBVENT project (Guiaus and Allard, 2005) considered only the buoyancy ventilation, and neglected the wind-induced ventilation in the urban environment, as they assumed that the effect of wind on the ventilation of buildings in the urban

environment was so weak it could be neglected. In reality, the wind force still plays a role in ventilating the upper part of the building in the urban environment. On the other hand, some studies place emphasis on the wind-induced ventilation, but ignore the buoyancy ventilation. Most of these studies were restricted by wind tunnel experiments, which usually cannot deal with the temperature in the scale model. Another problem is the correct estimation of the wind pressure coefficient on the buildings in the urban environment. Wind pressure coefficient generated by the parametrical model or algorithm and the abstract urban model cannot deal with the complicated environment. Van Moeseke et al. (2005) studied wind-induced ventilation in the urban environment and point out that the limitation of the wind pressure coefficient in urban modelling makes the result abstract. The problems drive the search for an appropriate method to predict the natural ventilation potential of a building in the urban environment.

7.1.2 Framework of predicting the potential for natural ventilation

Natural ventilation in the urban environment is a complicated issue, which is affected by many factors. The proposed framework of predicting the potential for natural ventilation in the urban environment is a structure of many factors. It consists of three parts: the first part is calculating the pressure coefficients around the building; the second part is calculating the ventilation rates of the zones in the building; the third part is evaluating the potential for natural ventilation (see Figure 7.1).

The first task can be accomplished using the virtual urban boundary layer wind tunnel. Before using the virtual wind tunnel, it requires inputting the urban morphology data, the wind climate data and the model of the studied building and its urban surrounding buildings. The morphology data can be used to calculate the urban roughness length in the urban area (Counihan, 1969; Gimmond and Oke, 1999; MacDonald et al., 1998). According to the wind data and Equation 7.1, 7.2, the urban friction velocity is calculated. The gradient pressure of the periodic boundary is deduced by Equation 7.3. The building model and domain size can refer to Chapter 4. After the completion of the first task, the pressure coefficients around the building are input to the airflow network model. The ventilation rates of the zones in the building can be calculated, in association with temperatures, humidity, the

occupants' requirements and their schedules. When these ventilation rates are compared with the criteria of the natural ventilation rates for health, thermal comfort and cooling, the potential for natural ventilation of the building in the urban environment will be presented. The methodology shown in the framework can be applied to the design stages to optimise the building form and choose the appropriate natural ventilation strategies at the early design stage in the urban environment. It can also be used to optimising the configuration of building space (zones) and the opening positions of building zones at the design stage.

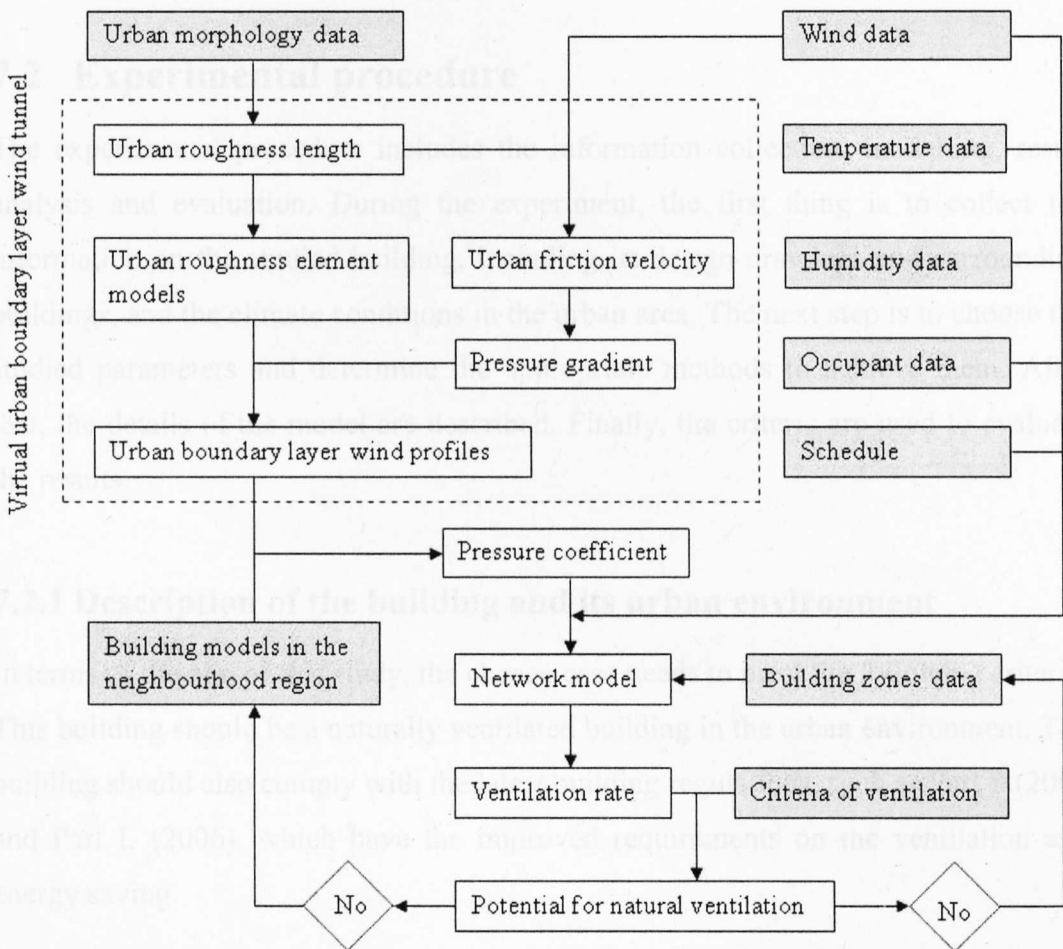


Figure 7.1 Framework of predicting the potential for natural ventilation of buildings in the urban environment: Dark shading indicates the input data.

7.1.3 Aims of this study

This study aims to apply the proposed methodology method to evaluate the potential for natural ventilation of an urban building. One of the objectives is to investigate the effects of the urban surroundings on the wind pressure distribution on the building's

surfaces, and also the characteristics of pressure coefficient distribution in the urban environment. Another objective is to evaluate the potential for natural ventilation of the building in the urban environment. Natural ventilation induced by the combination of wind and buoyancy forces would be investigated in the typical seasons. For natural ventilation design, it is carried out to check whether or not it works well under the common metrological conditions, such as winter, summer and the hottest days; Whether or not the wind and buoyancy ventilation combine well in the urban environment. Based on the current building regulation, the evaluation would provide knowledge to design natural ventilation in the urban environment.

7.2 Experimental procedure

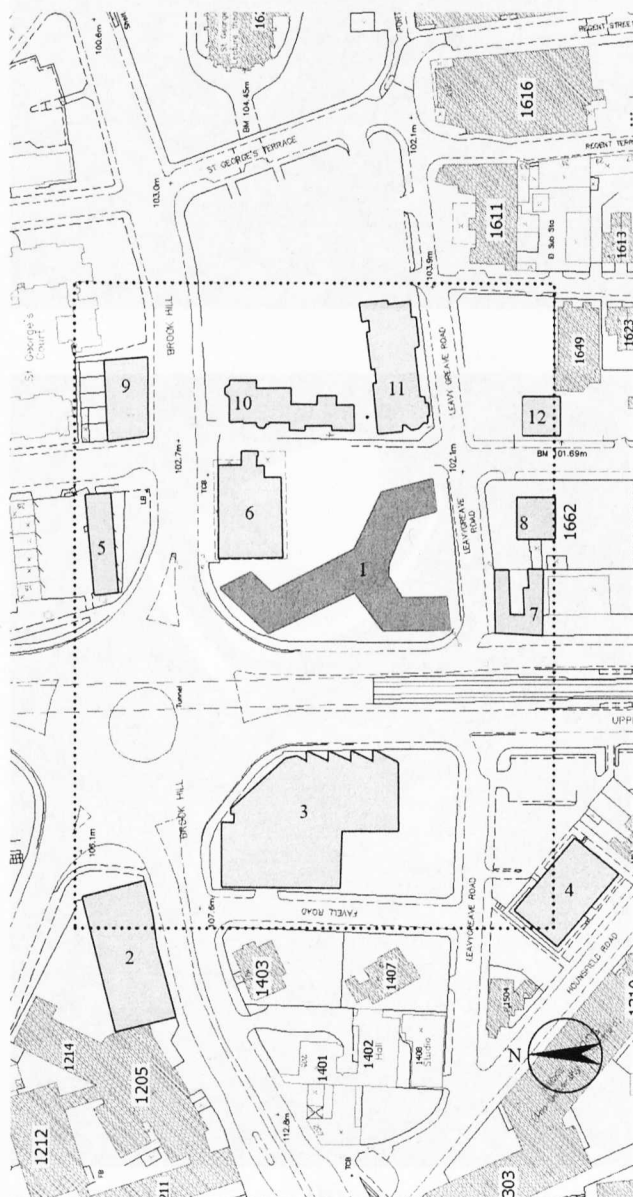
The experimental procedure includes the information collection, modelling, result analysis and evaluation. During the experiment, the first thing is to collect the information on the studied building, including its design drawings and surrounding buildings, and the climate conditions in the urban area. The next step is to choose the studied parameters and determine the appropriate methods to achieve them. After that, the details of the model are described. Finally, the criteria are used to evaluate the results.

7.2.1 Description of the building and its urban environment

In terms of the aim of this study, the chosen case needs to meet the following criteria. This building should be a naturally ventilated building in the urban environment. The building should also comply with the latest building regulations, such as Part F (2006) and Part L (2006), which have the improved requirements on the ventilation and energy saving.

The Jessop West Building was an appropriate case for this study. This teaching and research building of the University of Sheffield, is a naturally ventilated building, designed by Sauerbruch Hutton, RSJM and ARUP, situated in the urban environment and constructed in 2008. This building is surrounded by other buildings (see Figure 7.2,). The building is made up of three wings, like a 'Y' shape, reinforced by variations in height, ranging from six levels to four levels. Its western facade is

opposite the Information Commons, which is higher than the studied building. A main urban road crosses between them, which may cause a noise problem. The Bioincubator building and the Victoria Wing building are at positioned on its eastern side. To the north are the road and residential buildings, and the south faces the lower building. The building density of this area is about 22%. As the region of Sheffield belongs to a temperate climate zone, natural ventilation can be taken as a strategy for achieving sustainable building design.



1. Jessop West Building
2. Richard Roberts Building
3. Information Commons
4. CICS
5. Terraced House
6. Bioincubator Building
7. Henderson's Relish
8. Human Resources Institute
9. Terraced House
10. Victorian Building
11. Jessop Building
12. The Sound House

Figure 7.2 Planning of the Jessop West Building: The domain enclosed by the dot lines stands for the computational domain.



(a)



(b)



(c)

Figure 7.3 Illustrations of the Jessop West Building: (a) view from the outside, (b) atrium in the centre, (c) double façade details.

As an important issue of sustainability, natural ventilation has been emphasized in this building. It has adapted some design strategies to reach this objective (see Figure 7.3, Figure 7.4). The double façade is used in the building surface opposite the road. The configuration of this façade could reduce the noise from the road, whilst keeping natural ventilation working normally. The building layout is a linear shape, consisting of cell offices with a central corridor, and the depth of the wings is less than 15m, which meets the requirements of cross ventilation in the non-domestic building (CIBSE, 2005). Both design strategies consider wind as the main driven force for natural ventilation. In addition, there is an atrium at the building centre, from the ground level to the top level, which can be seen as a shaft.

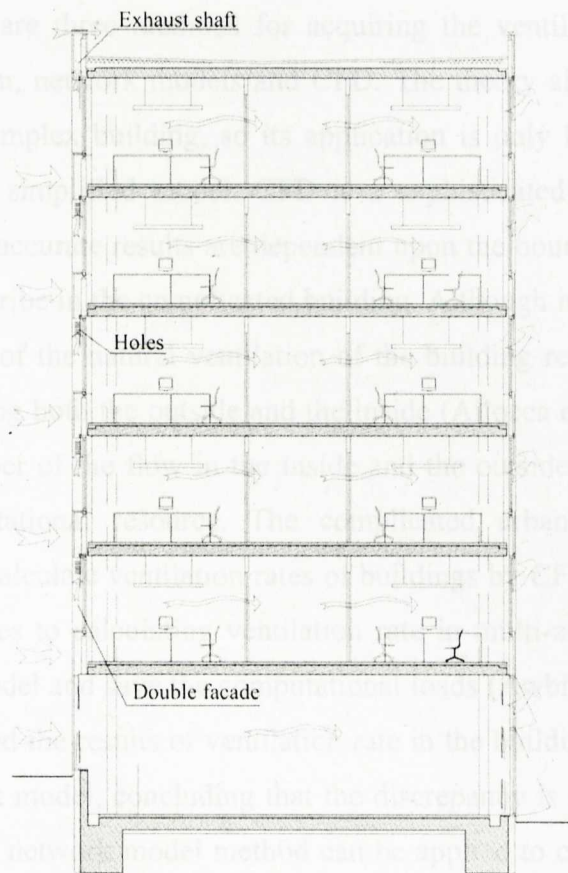


Figure 7.4 Schematic of the building section

7.2.2 Parameters and methods

Ventilation rate

Although there are some standards to evaluate the natural ventilation potential, the ventilation rate is much more appropriate as a parameter to evaluate natural ventilation potential. It can describe the fresh cool air exchange rate between the outside and inside of buildings, so it accurately expresses the ventilation function on health, thermal comfort, and cooling. Meanwhile, many building regulations and societies, including British building regulation Part F (2006), CIBSE (2001) and ASHRAE (2005) regard ventilation rate as the key criteria for the ventilation. As a consequence, ventilation rate can be taken as a standard to evaluate the natural ventilation potential of a building.

It is sensible to calculate the ventilation rate in the complex building by network models. There are three methods for acquiring the ventilation rate, including the theory algorithm, network models and CFD. The theory algorithm is too simple to apply to the complex building, so its application is only limited to the theoretical concept or the simplified model. CFD is a sophisticated method to describe the airflow, but its accurate results are dependent upon the boundary condition, which is difficult to describe in the complicated building. Although it has been confirmed that the calculation of the natural ventilation of the building requires the computational domain including both the outside and the inside (Allocca et al., 2003), the different Reynolds number of the flow in the inside and the outside cause a problem for the limited computational resource. The complicated urban environment makes it impractical to calculate ventilation rates of buildings by CFD. Network models have many advantages to calculating ventilation rate in multi-zone buildings - they can simplify the model and save the computational loads (Awbi, 2003). Asfour and Gadi (2007) compared the results of ventilation rate in the building between CFD and the airflow network model, concluding that the discrepancy is less than 12%. It implies that the airflow network model method can be applied to calculating the ventilation rate.

COMIS (Conjunction of Multi-zone Infiltration Specialist), which is one of the network models for air infiltration calculation, was employed in this study. It had been commonly used in the ventilation design for the multi-zone building (Feustel, 1999). COMIS was carried out to calculate the air flow rate in single side and cross

ventilation, and its results were in good agreement with measured data (Dascalaki et al., 1995). The performance of natural ventilation in a typical residential building by using COMIS was investigated by Bojic and Kostic (2006). They suggest that the multi-zone network method is the best and most feasible way to calculate the ventilation rate of a complicated building. However, the main problem for this method is acquiring pressure coefficients around the building.

Pressure coefficient

Pressure coefficients are essential input data for calculating the airflow rate by the network methods. Their fundamentals are based on the mass and pressure balance between the inside and the outside, while pressure coefficients describe information from the outside. When using COMIS models, the pressure coefficient distributions around the whole building are required, because the isolated horizontal or vertical pressure coefficient can cause the pressures on the network to be incorrect, resulting in errors in the calculation (van Moeseke et al., 2005).

Acquiring pressure coefficients around the building was achieved by using the virtual urban boundary layer wind tunnel, which has been confirmed as a valid method in Chapter 5. Compared with the traditional wind tunnel experiment, this method was more efficient, economic and informative. Its information can meet the requirement of the network model on pressure coefficients. Compared with the parametrical method of estimating pressure coefficients, this method was more accurate, because the studied building was an irregular form with the complicated urban surroundings. The parametrical method does not work at this condition.

Two cases of pressure coefficient were investigated in this study. One was the pressure coefficient of the building in the isolated condition, which was commonly used in the ventilation design. Another was the pressure coefficient of the building in urban surroundings. Comparison of the two cases would supplement the guidelines of pressure coefficient on natural ventilation design in the urban environment. For instance, the CIBSE's guide on depth of building for cross ventilation was for the isolated building (CIBSE, 2005). In fact, the surrounding buildings, especially in the urban environment, will significantly affect the natural ventilation driven forces, and

the wind pressure difference on the building facades. As the wind incidence slightly affects the pressure coefficient of the building in the urban environment (Sharples and Bensalem, 2001), this investigation mainly focuses on the prevailing wind direction in order to simplify the complicated procedure of CFD simulation.

7.2.3 Numerical Model settings

As with the complicated urban environment and limited computational resource, it was unrealistic to model the ventilation of the building in the urban environment by using just one model. The feasible approach was to divide the whole process into two parts. One part was using the models to acquire wind pressure coefficients around the building, and the other part was using the models to calculate the ventilation rate of the building. The first part included the models for the generation of urban wind profiles, and the models for ascertaining wind pressure coefficients around the building under the conditions of being isolated and then with surrounding buildings. CFD models can be applied to accomplish this part. The second part was to model the multi-zones of the building by using the COMIS code, and calculating the ventilation rate of zones under the external various wind pressure coefficients and meteorological conditions.

The urban wind profiles model

Urban wind profiles, including wind velocity and turbulence, were used to describe the inlet boundary condition in the CFD model. They played an essential role in determining the accuracy of the results in the model. However, the commonly used method of the empirical power law or log law has been confirmed as problematic for describing wind profiles in the urban environment (see Chapter 4). Another approach to obtaining the urban wind profile was using the urban boundary layer wind tunnel experiment, but accessing this expensive equipment for many design projects is limited due to the financial and time constraints. It is necessary to turn to other advanced methods to avoid the above problems.

According to the study in Chapter 4, urban wind profiles can be gained from the simulation of the urban roughness model, which is determined by the characters of the urban roughness elements and the friction velocity. When the flow crosses the

long fetch of the urban roughness element, the urban wind profile would be generated. The geometry of the roughness element and the layout of the roughness elements can be used to calculate the urban roughness length Z_0 (Counihan, 1969; MacDonald et al., 1998). The friction velocity can be derived from Equation 7.1:

$$U_* = \frac{U_{ref}}{2.5 \ln((Z_{ref} - d_0) / z_0)} \quad (7.1)$$

Where U_{ref} is the reference velocity at the reference height Z_{ref} , which is about twice of the urban roughness element height; d_0 is the zero displacement height; Z_0 is the roughness length. In the urban environment, it is difficult to get accurate data from Z_0 and d_0 . They can usually be obtained from morphometric and anemometric methods (Gimmond and Oke, 1999). In the design stage, the empirical data (Wieringa, 1993) can be taken as a reference, providing that measurements and morphometric analysis are infeasible. U_{ref} can be gained from the directly measurement or the estimation from the weather station:

$$U_{ref} = U_m \cdot \left(\frac{Z_{ref}}{Z_G} \right) \cdot \left(\frac{Z_m}{H_m} \right)^{\alpha m} \quad (7.2)$$

Where U_m is wind velocity at the measured height H_m at weather station; Z_m and αm are the gradient height and power law exponent at weather station respectively; Z_G and α is the gradient at the building site. The gradient height and power law exponent can refer to BS5925 (1991).

In this study, the urban roughness length in Sheffield was set as 1.05m, which was generated by the geometry of the roughness element, taken as 0.105m (l) x 0.0504m (h) (Lee, 1977). The structure of the urban roughness elements consisted of boxes in the staged pattern layout as the roughness element in the urban boundary layer wind tunnel (see Figure 4.3). The reference velocity was taken as the yearly average wind speed 4ms^{-1} at the reference height, 29m, at Weston park weather station (Pages and Lebens, 1986), which was the nearest station to the site of the building. The friction velocity was 0.5m/s, derived from Equation 7.1.

Using two steps to generate the urban wind profile can reduce the requirement made on computational resources. The first step was to use one of the repeated urban roughness elements to get the wind profile in the urban environment. The periodic boundary condition was employed to get the fully developed wind profile in the urban area. A scaled model of 1/250 was built in CFD, which ensured the Reynolds number did not affect the wind distribution. The domain size of the urban roughness model was $0.63\text{m} (L_x) \times 0.21\text{m} (L_y) \times 0.672\text{m} (L_z)$ and the geometry of the urban roughness element was $105\text{mm} (L) \times 105\text{mm} (W) \times 52.5\text{mm} (H_b)$. The boundary of the urban roughness element was set as the periodical boundary conditions. The pressure gradient was gained from Equation 4.1, as about -0.4594pam^{-1} . The second step was to generate the homogeneous wind profile. The wind profile in the urban roughness element was inhomogeneous in the urban canopy layer, as the wind profile decayed dramatically along the streamwise direction. A homogeneous wind profile is required for the building study, so an extra model was needed to form a homogeneous wind profile. This streamwise dimension of the computational domain was one unit of the urban roughness element, added to $40 H_b$. The section of the domain was the same as the urban roughness model. The inlet boundary condition was taken from the result of the urban roughness model. The outlet boundary condition was set as outflow, and as the flow velocity and pressure at the outlet were unknown, it was extrapolated from the interior. The symmetrical boundary was set for the top boundary. The side boundaries were set as the periodical boundary condition as in the urban roughness model. As the urban roughness element was rectangular, the grid at this part employed structured meshes.

The SIMPLIC scheme was used to couple pressure and velocity. After the convergence of using the first order upwind scheme, the second order upwind scheme was used to improve accuracy. The RSM turbulence model was employed with enhanced wall treatment. The convergence criterion is based on the reduction of all the scaled solution residuals under the threshold of 10^{-5} and the monitor of the area-weighted average pressure coefficient on the building surface being studied.

The isolated model of Jessop West building

The computational domain size of the isolated Jessop West building was determined by the recommended method (Franke et al., 2004). The upstream was $6H_b$, the downstream was $15H_b$, $6H_b$ in the spanwise and the vertical respectively. The inlet boundary was set as the velocity boundary condition, which was from the urban wind profile model. The outlet boundary was set as the outflow boundary condition, in which none of the variables but pressure were affected by the boundary. The side boundary and top boundary were set as symmetry boundary conditions. The wall boundary condition with a roughness height of zero was used by the ground boundary and the building surfaces.

As the geometry of the Jessop West building was irregular, it was time-consuming to use the structured grids in the computational domain, although this kind of mesh has many benefits, such as saving computational memory and enabling faster calculation. The advice from Kim and Boysan (1999) states that the unstructured grid has advantages in terms of flexibility and saving model time, but it increases the calculation time needed. The strategy of this building employed hybrid grids, which contained structured grids around the building and unstructured grids near the building. The near wall region had a high pressure gradient, so the boundary layer was necessary to mesh it. According to the Fluent user guide (2003), the viscous layer needed at least 6~7 layers of grid to catch the viscous flow. Here, 8 grid layers were employed with the enhanced wall treatment y^+ was less than 4. The grid independency was based on the adaptive grid refinement. Three kinds of grids were used to test grid independence by the adaptation function in FLUENT. The unstructured hexahedra grid was employed near the building, and structured grid employed around the building in order to maximise the advantages of unstructured and structured grids (see Figure 7.5).

The turbulence model employed the SST model, which had been proven as more suitable for calculating the wind pressure coefficient on the wall than the other two equation models. The study had used the RSM turbulence model to try to simulate the model, but it was very sensitive in the steady state and could not get convergence. So the SST was the most sensible and feasible among the turbulences in the complex urban build model. The wall treatment for the y^+ was set as being less than 4.

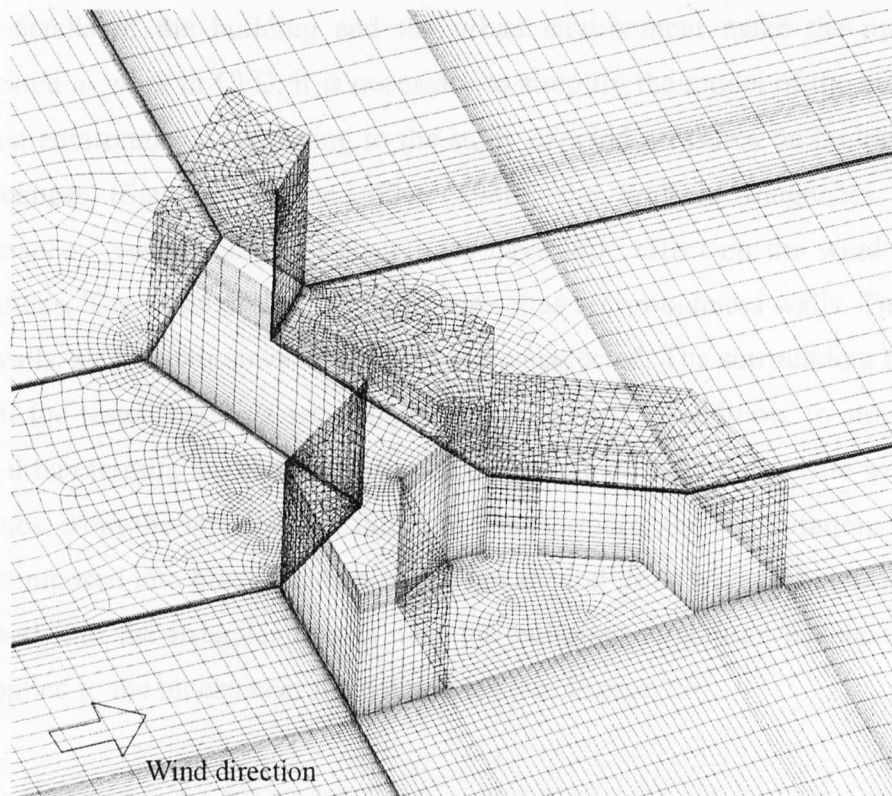


Figure 7.5 Grids around the isolated building

The model of Jessop West building with the urban surrounding buildings

The computational domain size of the Jessop West building with the urban surroundings was determined by the surrounding buildings and the terrain, as well as the building itself. The computational domain size in the urban environment for studying natural ventilation should consider the neighbourhood region, as well as the scope for the wind flow to fully develop. The neighbourhood region was determined by the building density, height, and layout, and the requirement the accuracy was determined by the study carried out in Chapter 4. As the building area density was about 22.5%, which was larger than 20%, the neighbourhood region was taken as $5H_b$ for the upwind stream fetch, and $2H_b$ for the lateral and downstream fetch, taking into consideration the effect of surrounding buildings on urban natural ventilation. The prevailing wind, from west to east, determined the number of building models in the neighbourhood region. The region for full development of the flow followed the recommendation by Franke et al.(2004): $6H_b$ for the upstream, $15H_b$ for the downstream, and $6H_b$ for the spanwise and the vertical.

As the details of the building and the urban environment make the model too complicated to work in CFD, it is necessary to simplify the model of the building in the urban environment. According to the study of wind pressures on buildings with appurtenances (Stathopoulos and Zhu, 1988), the uniform roughness and the appurtenances' width being less than 1.5m have little effect on the wind pressure distributions. The walls of the building were set as non-roughness walls. The details of the walls, such as windows or columns were neglected. The surrounding buildings far from the tested building were simplified as boxes. In addition, to simplify the uneven urban terrain, the characteristics of the terrain of the building site were taken as terraces, from the left down to the right. Furthermore, the computational domain was decomposed into blocks. Unstructured hexahedral grids with 10 boundary layers were used into the irregular blocks near the building; structured hexahedral grids were applied to the blocks near the boundaries (see Figure 7.6).

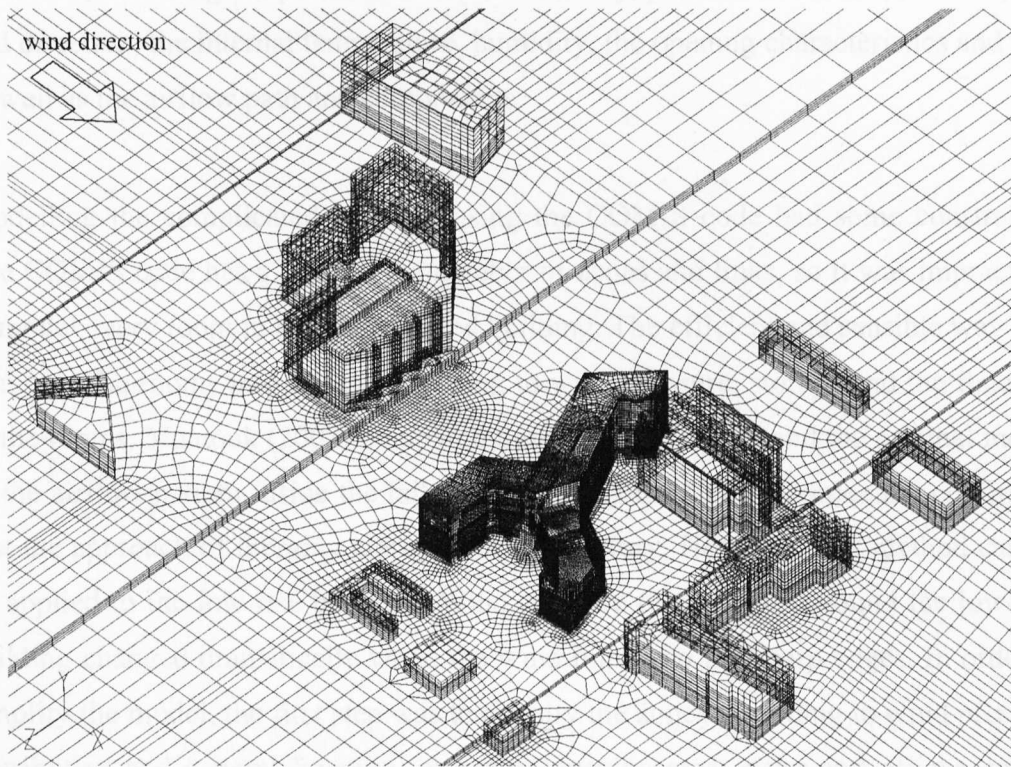


Figure 7.6 Grids around the building with the urban surroundings

The boundary conditions were similar to those of the isolated building. The inlet velocity boundary profile was taken from the urban roughness model. The outlet

boundary was set as the outflow boundary condition, in which none of the variables but pressure were affected by the boundary. The side boundaries and top boundary were set with symmetry boundary conditions. The wall boundary with a roughness height of zero was used for the ground and building surfaces.

COMIS model

The COMIS model, including zones of the building, external nodes and the air flow components, is one of the multi-zone network models used to calculate air change rate, the pattern of air flow between zones, internal pressure, pollutant concentration and so on. This method approximately expresses the true system of ventilation and infiltration air flow. Based on pressure differences resulting from wind, buoyancy, and mechanical ventilation systems, flow equations are solved by an iterative Newton-Ralphson method. This model requires inputting the external climate condition, including temperature, absolute humidity, pressure coefficient, wind speed and direction, the internal temperature, humidity, the opening characteristics and size, as well as the airflow path and components.

Modelling the complicated building using the COMIS code had some constraints. The COMIS code has a limit to the number of zones and links, so it was impractical to model every room in the complicated building. The efficient and sensible way was to merge the rooms into zones, according to wind pressure, storeys and the function of the rooms. Maatouk (2007) compared the simplified model and the original model of the airflow pattern inside the tall building using the COMIS code, and confirmed that the approach of merging storeys was satisfactory. However, this method cannot be applied to the low-rise building. Wind pressure distributions around the low-rise building changed dramatically when the wind impinged the sharp edges. In order to simplify the model, the first step was to classify the zones according to wind pressure distribution and general function, including opening area, stairs and offices, toilets and so on. Figure 7.7 illustrates the zones of every floor plan, and one colour block represents one zone. The second step was to model each wing separately, and connect with the other wings by the zone An-1. The other two wings could be simplified as the single zones, as their connection with the modelled zone was indirect, so they could not affect the tested wing much.

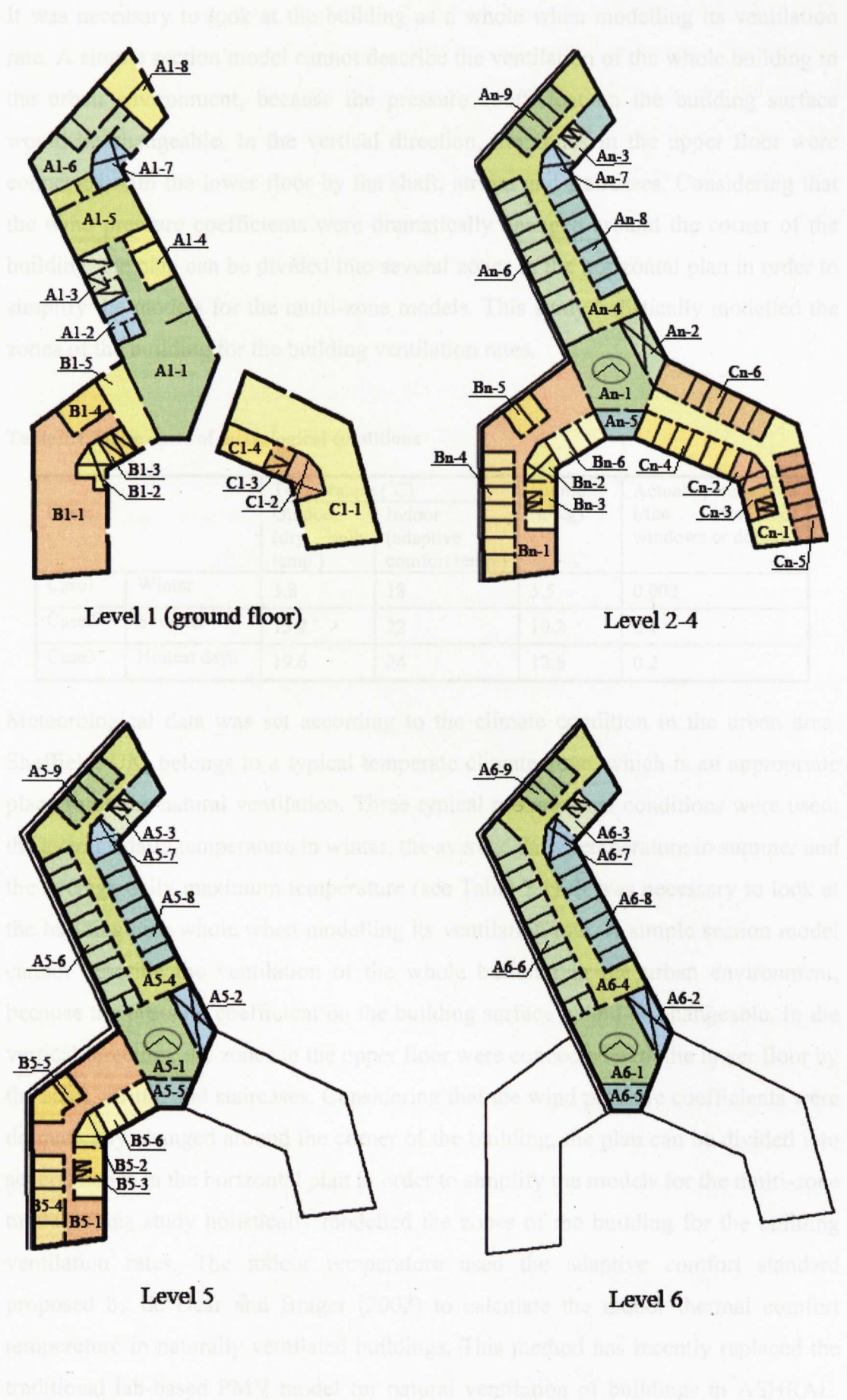


Figure 7.7 Zones of the Jessop West building

It was necessary to look at the building as a whole when modelling its ventilation rate. A simple section model cannot describe the ventilation of the whole building in the urban environment, because the pressure coefficient on the building surface would be changeable. In the vertical direction, the zones in the upper floor were connected with the lower floor by the shaft, atrium and staircases. Considering that the wind pressure coefficients were dramatically changed around the corner of the building, the plan can be divided into several zones in the horizontal plan in order to simplify the models for the multi-zone models. This study holistically modelled the zones of the building for the building ventilation rates.

Table 7.1 Three cases of metrological conditions

Cases		Temperature (°C)		Humidity (g/Kg)	Actual opening area (/the area of windows or doors)
		Outdoor (dry bulb temp.)	Indoor (adaptive comfort temp.)		
Case1	Winter	3.8	18	5.5	0.002
Case2	Summer	15.2	22	10.2	0.1
Case3	Hottest days	19.6	24	12.6	0.2

Meteorological data was set according to the climate condition in the urban area. Sheffield, UK, belongs to a typical temperate climate zone, which is an appropriate place to utilise natural ventilation. Three typical metrological conditions were used: the average daily temperature in winter, the average daily temperature in summer and the average daily maximum temperature (see Table 7.1). It was necessary to look at the building as a whole when modelling its ventilation rate. A simple section model cannot describe the ventilation of the whole building in the urban environment, because the pressure coefficient on the building surface would be changeable. In the vertical direction, the zones in the upper floor were connected with the lower floor by the shaft, atrium and staircases. Considering that the wind pressure coefficients were dramatically changed around the corner of the building, the plan can be divided into several zones in the horizontal plan in order to simplify the models for the multi-zone models. This study holistically modelled the zones of the building for the building ventilation rates. The indoor temperature used the adaptive comfort standard proposed by de Dear and Brager (2002) to calculate the indoor thermal comfort temperature in naturally ventilated buildings. This method has recently replaced the traditional lab-based PMV model for natural ventilation of buildings in ASHRAE.

Humidity was not an issue for this study, so both outdoor and indoor humidity were taken to be the same. Wind speed was taken from the prevailing wind at Weston Park weather station, which is situated within a range of 0.5km from the site of the studied building. It is located in the terrain of the larger town, which is different from the common open area terrain of the weather station, so its reference height was 29m. The yearly average wind speed is 4m/s, exceeding 50% of times (Pages and Lebens, 1986). The prevailing wind direction is from the west to the east. The exponent of power law in COMIS model was set as 0.28.

The opening areas were determined by the requirement of the ventilation rates in the seasons. As the present building emphasized air tightness, the ventilation had to consider the purpose of ventilation through the opening area. The largest opening area was about one fifth of the area of the windows. As the area taken up by windows is approximately 1/4 of the floor area of the office near the external wall, and the opening area is 1/20 of the floor area of the office. In winter, the windows were set as closed, and ventilation was achieved through the trickle ventilator. The trickle ventilator opening area was equal to 1% of the largest opening area of the windows, which followed the building regulation Part F (ODPM, 2006). In summertime, the opening area was set as one half of the largest opening area. In order to keep the ventilation system working efficiently, the area of door openings has to comply with similar rules as the area of the windows. As the external openings of double façades were made of porous steel panel, their opening areas are estimated by the percentage of porous, measured as 70%.

The variables in this study include wind speed, temperature and pressure coefficient value. Wind speeds were set as zero (no wind condition) and 4ms^{-1} (the average wind condition); temperatures were set as the average winter temperature, average summer temperature and the hottest day temperature. Pressure coefficient values were set under two cases: the isolated building, and the building with surrounding buildings.

7.2.4 Criteria of natural ventilation rates for the office building

The criteria of natural ventilation rates are dependent upon the functions of the natural ventilation. For the purpose of health, the ventilation rate affects the indoor

air quality, which is a main concern in winter. According to the perceived air quality and the quantity of air supplied to a space, Ward (2008) classified the ventilation rate for health in three categories (see Table 7.2). The ventilation rates for thermal comfort and cooling can be represented by air change rate (*ACH*). Thermal comfort is dependent on activity and clothing level, as well as air speed, air temperature and humidity. For example, the air speed 0.25ms^{-1} could reduce the temperature 2°C (CIBSE, 2005). As the calculation of indoor air speed distribution requires the CFD model, the air change rate can be used to evaluate the cooling potential of natural ventilation according to Wills et al.'s (1995) statement on the required ventilation rate for the indoor environment. Table 7.2 summarises the ventilation function and the corresponding ventilation rates for the non-domestic building, which can be taken as criteria for evaluating the potential for natural ventilation. The occupancy number of the building can be estimated at 10m^2 per person in the office building, according to the CIBSE standard (CIBSE, 2005).

Table 7.2 Ventilation functions and rates for the non-domestic building (Wills, 1995; Ward 2008)

Requirement		Ventilation rate	Unit	Note
Health	A	>16	l/s per person	<10% dissatisfied
	B	7-16	l/s per person	10-20% dissatisfied
	C	<7	l/s per person	>20% dissatisfied
Comfort		1-5	ACH	
Cooling		5-30	ACH	

7.3 Results

7.3.1 Generation of the homogeneous urban wind profile

The homogeneous urban wind profile in this study was generated by the virtual urban boundary layer wind tunnel, the use of which has been validated in Chapter 5. Figure 7.8 shows the urban wind profiles, including velocity, turbulence kinetic energy, and turbulence dissipation rate at $30H_b$ and $40H_b$ along the streamwise direction from the inlet boundary in the empty domain.

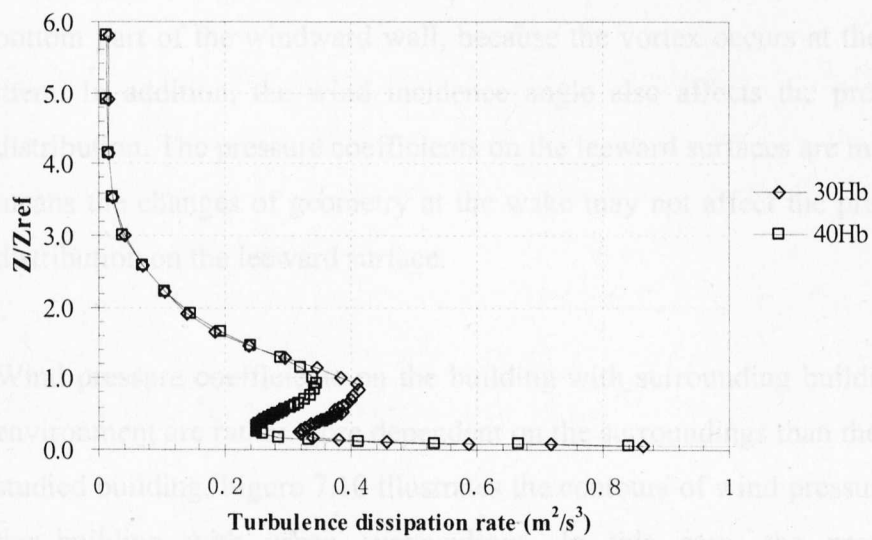
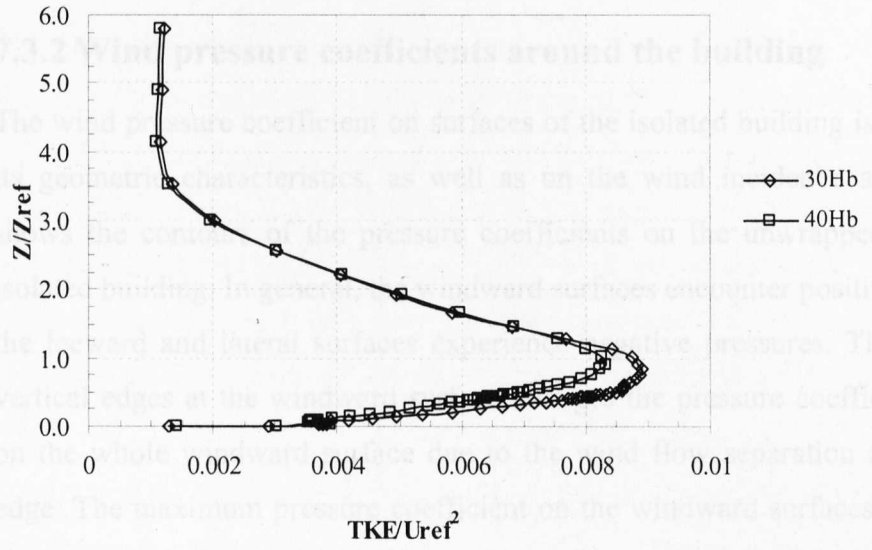
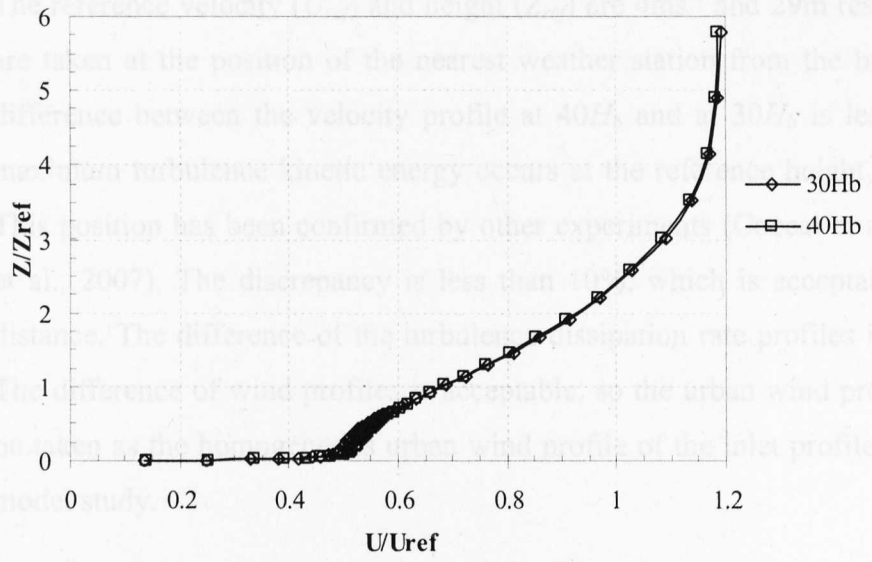


Figure 7.8 Urban wind profiles at the building site (a) mean velocity profile; (b) turbulence kinetic energy profile; (c) turbulence dissipation rate profile

The reference velocity (U_{ref}) and height (Z_{ref}) are 4ms^{-1} and 29m respectively, which are taken at the position of the nearest weather station from the building site. The difference between the velocity profile at $40H_b$ and at $30H_b$ is less than 5%. The maximum turbulence kinetic energy occurs at the reference height, which is $2.3H_b$. This position has been confirmed by other experiments (Coceal et al., 2006; Yoshie et al., 2007). The discrepancy is less than 10%, which is acceptable for the $10H_b$ distance. The difference of the turbulence dissipation rate profiles is less than 15%. The difference of wind profiles is acceptable, so the urban wind profile at $40H_b$ can be taken as the homogeneous urban wind profile of the inlet profile for the building model study.

7.3.2 Wind pressure coefficients around the building

The wind pressure coefficient on surfaces of the isolated building is dependent upon its geometric characteristics, as well as on the wind incidence angle. Figure 7.9 shows the contours of the pressure coefficients on the unwrapped facades of the isolated building. In general, the windward surfaces encounter positive pressures, and the leeward and lateral surfaces experience negative pressures. The first upstream vertical edges at the windward surface changes the pressure coefficient distribution on the whole windward surface due to the wind flow separation around the sharp edge. The maximum pressure coefficient on the windward surfaces occurs near this sharp edge, at about $0.65 H_b$. The ground enhances the pressure distributions on the bottom part of the windward wall, because the vortex occurs at the corner between them. In addition, the wind incidence angle also affects the pressure coefficient distribution. The pressure coefficients on the leeward surfaces are mostly stable. That means the changes of geometry at the wake may not affect the pressure coefficient distribution on the leeward surface.

Wind pressure coefficients on the building with surrounding buildings in the urban environment are rather more dependent on the surroundings than the geometry of the studied building. Figure 7.10 illustrates the contours of wind pressure distribution on the building with urban surroundings. In this case, the pressure coefficient differences between the windward and leeward surfaces are not distinct, and the lower part of the windward surfaces could experience negative pressure as well as

other surfaces could. The maximum pressure coefficient occurs at the right upper corner of the windward surface, because the upstream surrounding building is far away this facade. When the building is sheltered by surrounding buildings, the larger pressure coefficient happens near the top edge of its windward surface. Furthermore, the pressure coefficients on the lower part of building tend to be uniform, as well as on the leeward and lateral surfaces. In addition, the incident angle has little effect on the wind pressure coefficient distribution, which further confirms Sharples and Bensalem's (2001) conclusion that wind incident angles from perpendicular to the building to a 45° incidence angle in the urban environment have a much smaller effect on the wind induced ventilation .

The pressure coefficients on the roof are also affected by the surroundings. Figure 7.11 presents the contours of pressure coefficient distributions on the roofs of the isolated building and the building with surrounding buildings. Their comparison shows that the roof of the building with surrounding buildings encounters smaller negative pressures than the isolated building. However, this reduction is not as large as on the facades, especially the part of the roof near the windward edge, where the pressure coefficients are about half of those of the isolated building.

Comparing the pressure coefficient distribution under both conditions, it can be seen that pressure coefficients are dramatically reduced by the surroundings. The pressure coefficients in the urban environment are generally reduced to 10% of that on the isolated building. The effects of the building's geometry and the position of the first sharp edges are less important in the urban environment than for isolated building. The characteristics of the surroundings play a vital role, and the distance to the upstream buildings and the urban canyon characteristics are important to consider. In addition, the horizontal pressure coefficient distributions are changeable as well as those in the vertical direction, so it is incorrect to describe the pressure coefficient on the urban building by using average data for the ventilation rate calculation.



Figure 7.9 Contours of pressure coefficients on the facades of the isolated building

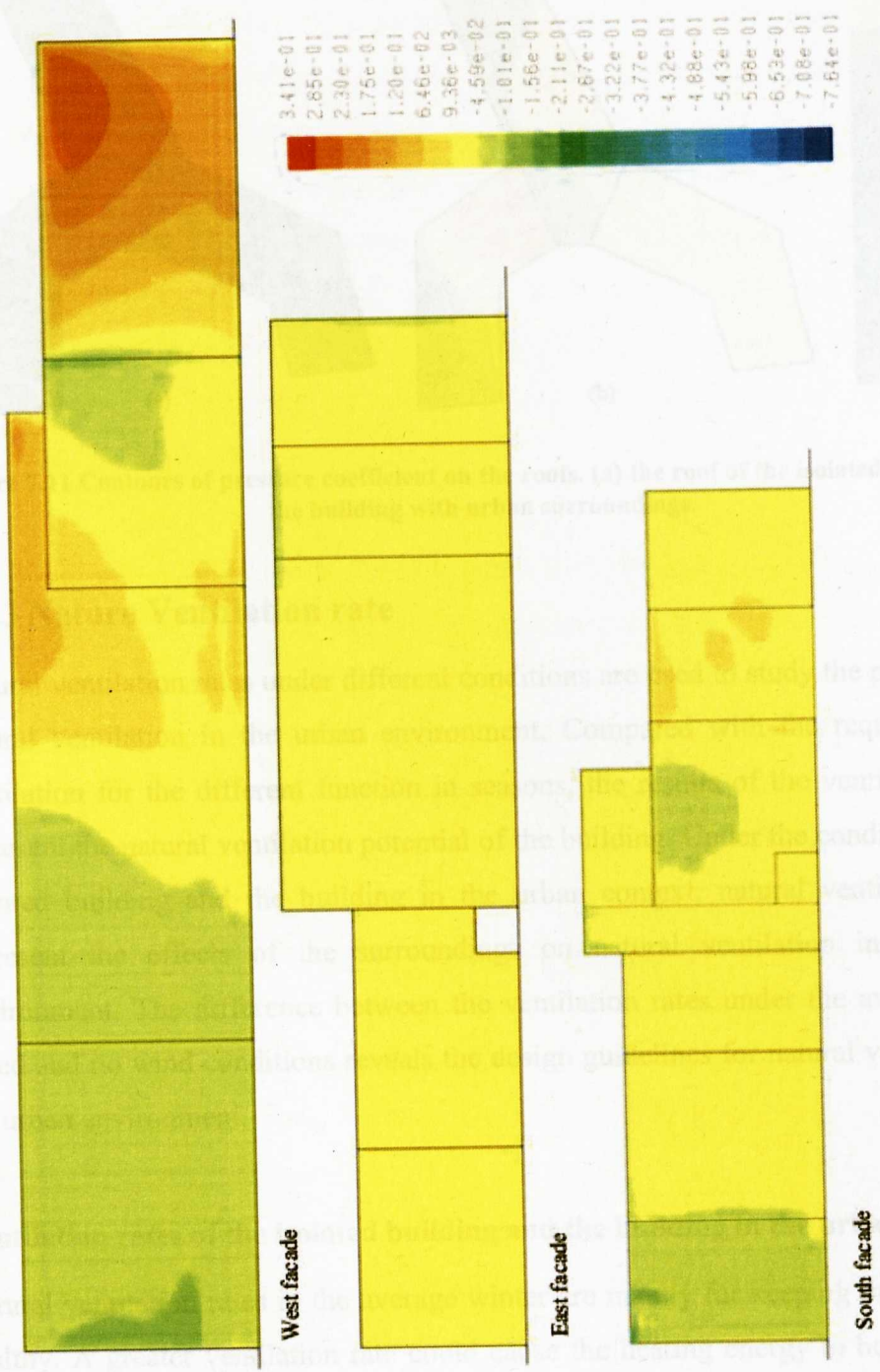


Figure 7.10 Contours of pressure coefficients on the facades of the building with urban surrounding buildings

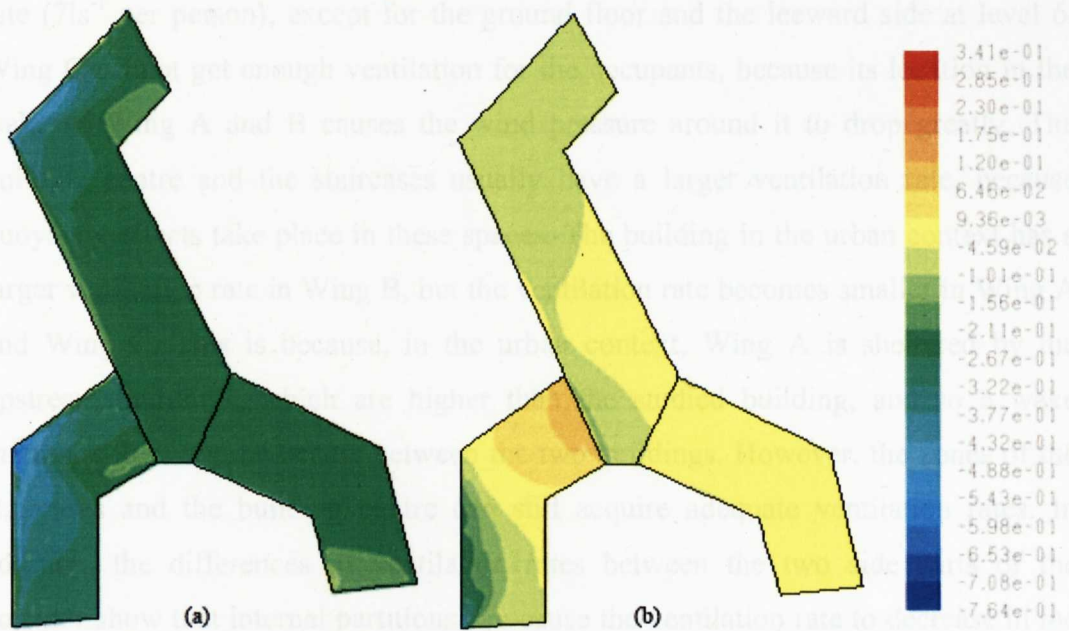


Figure 7.11 Contours of pressure coefficient on the roofs. (a) the roof of the isolated building; (b) the building with urban surroundings.

7.3.3 Nature Ventilation rate

Natural ventilation rates under different conditions are used to study the potential for natural ventilation in the urban environment. Compared with the requirement of ventilation for the different function in seasons, the results of the ventilation rates represent the natural ventilation potential of the building. Under the conditions of the isolated building and the building in the urban context, natural ventilation rates represent the effects of the surroundings on natural ventilation in the urban environment. The difference between the ventilation rates under the average wind speed and no wind conditions reveals the design guidelines for natural ventilation in the urban environment.

Ventilation rates of the isolated building and the building in the urban context

Natural ventilation rates in the average winter are mainly for keeping the air quality healthy. A greater ventilation rate could cause the heating energy to be lost, so the ventilation rate should be kept at the appropriate level. Table 7.3 shows the natural ventilation rate in the zones of the building at 6 levels, under the conditions of being isolated and being in the urban context. Under the isolated condition, Wings A and B can acquire general good ventilation rates, greater than the basic healthy ventilation

rate (7ls^{-1} per person), except for the ground floor and the leeward side at level 6. Wing C cannot get enough ventilation for the occupants, because its location in the wake of Wing A and B causes the wind pressure around it to drop greatly. The building centre and the staircases usually have a larger ventilation rate, because buoyancy effects take place in these spaces. The building in the urban context has a larger ventilation rate in Wing B, but the ventilation rate becomes smaller in Wing A and Wing C. This is because, in the urban context, Wing A is sheltered by the upstream buildings, which are higher than the studied building, and so a wake inference flow regime occurs between the two buildings. However, the zones of the staircases and the building centre can still acquire adequate ventilation rates. In addition, the differences of ventilation rates between the two side parts of the corridor show that internal partitions can cause the ventilation rate to decrease in the zones near the leeward walls.

Comparing the building in the urban context with the isolated building, in general, worse ventilation usually happens at the ground floor and in the wake region, no matter what the conditions. The zones near the windward façades in the urban context have a greater ventilation rate with the increase of the vertical level. The solution for achieving adequate ventilation rates in the urban context is to enlarge the opening area at the lower levels. Another solution is to reduce the wake of the taller, upstream building, or avoid building in its wake, in order to increase the wind pressure on the building's surfaces. This requires that the surroundings should be considered at an early design stage. The poor performance of the less than 15m building plan implies that the general guidelines on the cross ventilation do not suit the building in the urban environment.

Both conditions of the isolated building and the building in the urban context can almost acquire adequate ventilation rates in the average summer. Table 7.4 shows the natural ventilation rate in the zones in the average summer. The isolated building can acquire a ventilation rate that is usually greater than 5 ACH. The building centre and the staircases acquire the largest ventilation rate. However, the worst ventilation rate happens at the north part of Wing A on the ground floor, due to the smaller opening area. In the urban context, the worst ventilation occurs at the ground floor level of

wing B, due to the limited opening area. It is surprising that Wing C can achieve the ventilation rate that it does, although the wind pressure coefficient on its surface is much smaller. The reason could be that the buoyancy force plays the main role of ventilation, rather than the wind force. The comparison of the ventilation rates of the isolated building and the building in the urban context shows that their differences are not distinct in the summer.

Almost all of the zones in both conditions of the isolated and the urban context can acquire a ventilation rate greater than 5ACH for cooling on the hottest days. Table 7.5 shows the natural ventilation rates of zones benched by the four catalogues. In the isolated case, the ground floor of Wing A has the lowest ventilation rate, due to the limited opening area. Above the ground floor, the zones can acquire adequate ventilation rates for cooling. In the urban context, the ground level of Wing C and part of Wings A and B cannot acquire enough natural ventilation for cooling. This is because of the lower wind pressure coefficient and lack of buoyancy effect. On the ground level, almost all of the space can achieve ventilation for cooling. The best zones for this are the building centre and staircases, as a stack effect takes action in these spaces.

Natural ventilation rates of the building under the isolated and in the urban context in the three climatic conditions reveal the design strategies for an adequate ventilation rate. From the results of the ventilation rate in winter, it can be seen that the current opening areas – that followed the building regulation Part F (ODPM, 2006) - are not enough to ensure the ventilation rate for health in winter. In summer and on the hottest days, the ventilation rates could achieve the required ventilation rate for comfort and cooling. Note that the ground floor usually has worse ventilation than other levels. In order to improve the ventilation rate, the solutions in the urban context include enlarging the opening area and reducing internal partitions. Furthermore, the effect of wind on natural ventilation in the lower level of the building in the urban context is limited, so utilising buoyancy ventilation could achieve the ventilation rate for thermal comfort and cooling in the temperate climate region.

Table 7.3 Natural ventilation rates of zones in winter with the different surrounding conditions

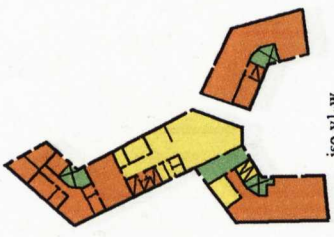
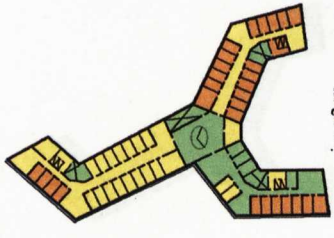
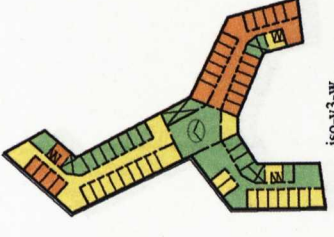
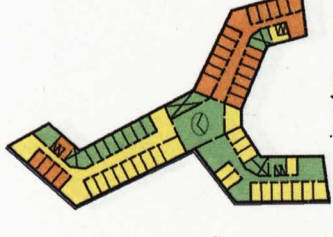
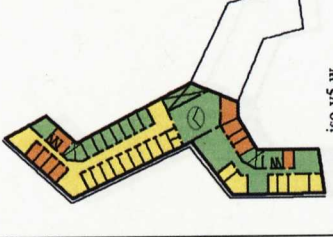
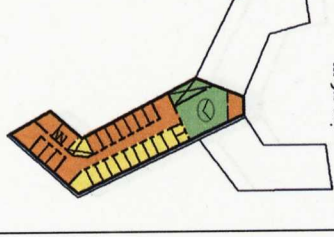
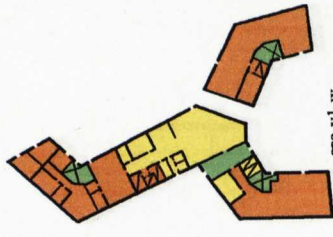
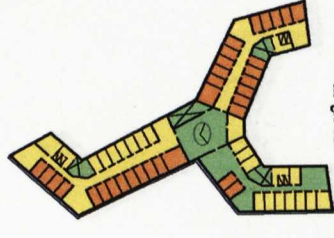
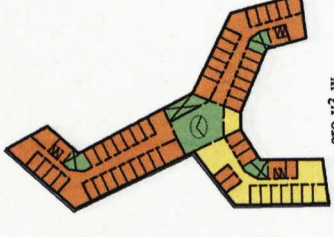
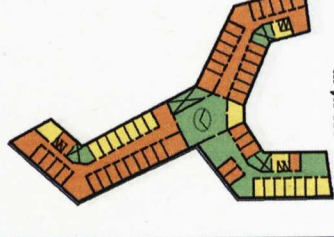
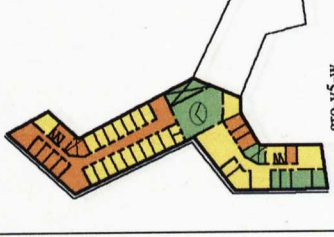
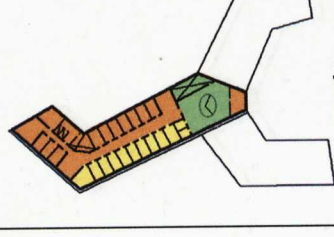

Condition	Level 1	Level 2	Level 3	Level 4	Level 5	Level 6
isolated	 iso-v1-w	 iso-v2-w	 iso-v3-w	 iso-v4-w	 iso-v5-w	 iso-v6-w
Urban context	 gro-v1-w	 gro-v2-w	 gro-v3-w	 gro-v4-w	 gro-v5-w	 gro-v6-w
						

Table 7.4 Natural ventilation rates of the zones in summer with the different surrounding conditions

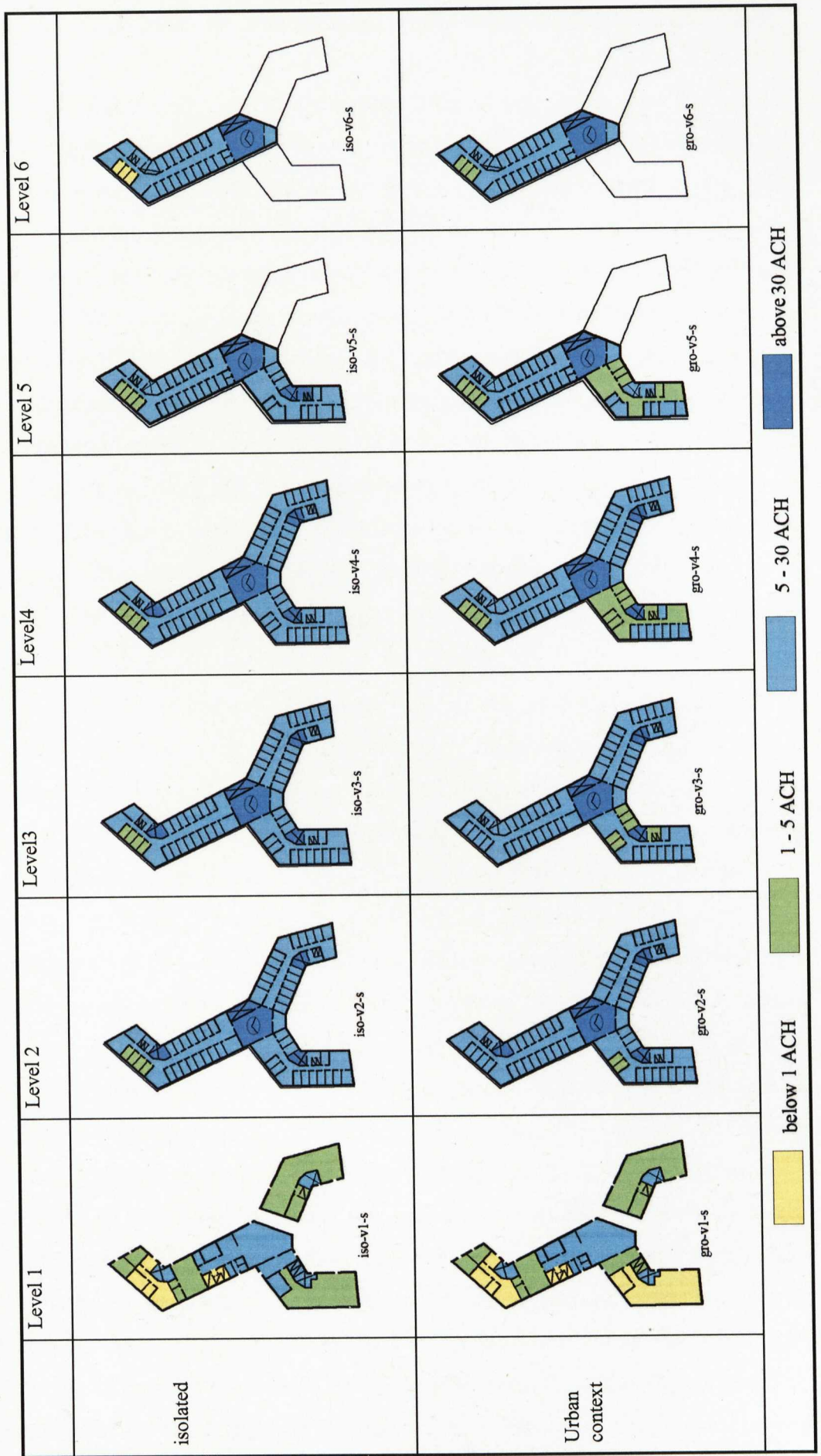


Table 7.5 Natural ventilation rates of the zones on the hottest days with the different surrounding conditions

	Level 1	Level 2	Level 3	Level 4	Level 5	Level 6
isolated	 iso-v1-h	 iso-v2-h	 iso-v3-h	 iso-v4-h	 iso-v5-h	 iso-v6-h
Urban context	 gro-v1-h	 gro-v2-h	 gro-v3-h	 gro-v4-h	 gro-v5-h	 gro-v6-h
	below 1 ACH	1 - 5 ACH	5 - 30 ACH	above 30 ACH		

Ventilation rates under the average wind and no wind conditions in the urban context

Besides the above study, which shows the different ventilation rates between the isolated and the urban context, it is also necessary to understand the individual role of buoyancy and wind pressure in the natural ventilation system in the urban environment. This investigation would reveal how to utilise two types of natural ventilation in the urban environment: wind induced ventilation and buoyancy ventilation. No wind condition means natural ventilation is only generated by the buoyancy force. The difference between the two cases would indicate the role of the wind induced and buoyancy ventilation in the whole natural ventilation system. It can be divided into three cases, explained as follows. When the difference is larger than 50%, this indicates that the wind induced ventilation plays the dominant role; when the difference is less than 50%, it means the buoyancy ventilation is dominant, and if the difference is negative, this implies that the wind flow conflicts the buoyancy flow and reduces the performance of buoyancy ventilation.

Table 7.6 shows the natural ventilation rates of the studied building under the average wind and no wind conditions in winter. In general, buoyancy ventilation plays the main role for ventilating the whole building in winter. Approximate 90% of zones are dominated by buoyancy ventilation, and only 10% of zones are dominated by wind induced ventilation. The zones on the ground level are all dominated by the buoyancy ventilation. However, the wind induced ventilation is dominant in the zones that are closed to the upper windward walls, even when the studied building is sheltered by an upstream building. For the isolated building, the wind induced ventilation is dominant above the second level. This is because wind pressure distributions at the higher levels are usually larger than at the lower levels, and the maximum wind pressures usually exist near the top edge of the building. In addition, about one quarter of the zones have a negative difference value, which means that the wind induced ventilation weakens the buoyancy ventilation. The phenomenon generally occurs in the zones near the leeward wall, because these zones usually have a bit of negative wind pressure. When the wind induced pressures are less than the buoyancy forces, the latter will dominate the flow pour into the interior, and not the flow from the inside to the outside. In conclusion, wind flow may be not important for ventilating the whole building in winter. Usually, buoyancy ventilation can meet

the requirement of natural ventilation rates for health in winter, while care should be taken for the zones in which wind induced ventilation plays the dominant role.

Table 7.7 shows the difference in natural ventilation rates under the average wind and no wind conditions in the urban context in summer. The zones that are dominated by the wind induced ventilation account for 16% of the total zones. These wind dominated zones are located near the windward wall. Compared with winter, this amount increases by 6%, as the temperature difference between inside and outside reduces from 14.2°C to 6.8°C. This indicates that the buoyancy ventilation is still the main natural ventilation mode in summer. Even if there is no wind, the buoyancy ventilation can make most zones reach the standard of thermal comfort, above 1ACH. The worst ventilation rate - less than 1ACH - occurs at 5 zones on level 1, 2 zones on level 4 and 1 zone on level 5, but these only comprise 8% of the total zones. The building can achieve thermal comfort in summer by natural ventilation.

Table 7.8 shows the natural ventilation rates of the building in the urban context under the average wind and no wind conditions on the hottest days. Taking 5ACH as a criterion for cooling, the percentage of that have lower ventilation rates than the criterion is 7% for the average wind conditions and 15% for non wind condition. Most zones are located on level 1. The number of zones that are dominated by wind induced ventilation on the hottest days increase to 25% of the total zones, as the temperature difference between outside and inside reduces to 4.4°C. These zones are mainly located at the upper level of the building and near the windward wall. Even if the building is at no wind condition, there are still 75% of zones that can achieve a ventilation rate that is greater than the criterion. It can be concluded that buoyancy ventilation in the building in the urban context can be taken as the main natural ventilation mode for cooling on the hottest days.

Table 7.6 Natural ventilation rate under the average wind and no wind conditions in the urban context - winter

	Level 1			Level 2			Level 3			Level 4			Level 5			Level 6		
	AW (l/s/p)	NW (l/s/p)	Diff (%)	AW (l/s/p)	NW (l/s/p)	Diff (%)	AW (l/s/p)	NW (l/s/p)	Diff (%)	AW (l/s/p)	NW (l/s/p)	Diff (%)	AW (l/s/p)	NW (l/s/p)	Diff (%)	AW (l/s/p)	NW (l/s/p)	Diff (%)
An-1	14.8	14.2	4.1	50.6	48.1	4.9	70.8	67.0	5.4	88.2	82.9	6.0	99.1	92.0	7.2	379.0	379.0	0.0
An-2	13.6	12.9	5.1	143.0	141.0	1.4	251.0	249.0	0.7	116.0	116.0	0.0	272.0	273.0	-0.4	156.0	156.0	0.0
An-3	0.0	0.0	0.0	8.8	8.9	-0.5	6.2	6.3	-1.8	4.4	4.2	4.6	2.8	3.1	-8.1	2.8	3.1	-9.6
An-4	11.0	10.6	3.6	9.3	6.9	25.4	5.1	8.3	-64.0	6.7	8.3	-25.1	6.3	7.8	-24.4	6.6	3.6	46.1
An-5	1.1	1.0	3.7	14.4	13.8	4.2	11.7	11.0	6.0	9.6	8.8	8.5	7.0	5.8	17.0	3.4	3.6	-6.8
An-6	0.1	0.1	8.2	6.7	5.7	14.7	6.8	4.6	32.1	8.7	1.7	80.7	10.0	2.4	76.3	9.5	9.4	1.0
An-7	26.5	26.6	-0.4	102.0	103.0	-1.0	33.6	35.0	-4.2	7.7	11.6	-50.5	4.1	5.4	-30.2	4.2	5.9	-40.9
An-8	1.2	1.1	1.7	14.0	11.8	15.7	5.1	6.1	-20.2	7.9	10.7	-34.9	7.8	10.8	-38.1	3.9	4.5	-17.1
An-9	n/a	n/a	n/a	4.0	1.7	57.2	4.7	2.9	39.5	2.5	3.9	-55.4	1.8	3.3	-82.4	5.8	2.3	60.2
Bn-1	1.9	1.4	26.3	19.1	15.5	18.8	11.4	9.3	18.7	16.2	15.0	7.4	15.6	15.4	1.3	n/a	n/a	n/a
Bn-2	38.0	37.0	2.6	71.7	70.2	2.1	78.2	76.4	2.3	76.6	76.4	0.3	45.0	44.9	0.2	n/a	n/a	n/a
Bn-3	4.0	3.4	14.6	10.6	11.4	-7.5	5.4	4.7	12.1	11.9	11.4	4.2	15.3	15.2	0.7	n/a	n/a	n/a
Bn-4	3.3	3.0	9.5	11.7	4.8	59.4	13.2	0.3	97.8	13.5	4.0	70.4	17.7	7.9	55.1	n/a	n/a	n/a
Bn-5	16.2	15.5	4.3	4.0	4.9	-22.4	6.3	5.8	8.1	6.9	4.8	31.3	11.4	3.4	69.8	n/a	n/a	n/a
Bn-6	n/a	n/a	n/a	9.2	9.6	-4.0	5.1	5.3	-3.5	4.4	4.2	4.1	4.5	4.7	-3.8	n/a	n/a	n/a
Cn-1	1.5	1.4	5.3	7.1	4.5	36.9	6.8	2.8	58.4	5.7	1.3	77.7	n/a	n/a	n/a	n/a	n/a	n/a
Cn-2	48.4	46.1	4.8	72.9	66.2	9.2	72.9	66.2	9.2	50.7	40.8	19.5	n/a	n/a	n/a	n/a	n/a	n/a
Cn-3	4.1	2.9	28.3	7.4	5.2	29.7	6.1	5.9	2.8	8.3	8.4	-1.3	n/a	n/a	n/a	n/a	n/a	n/a
Cn-4	2.0	1.6	18.0	5.1	3.0	41.8	3.0	2.6	14.7	2.7	2.5	7.8	n/a	n/a	n/a	n/a	n/a	n/a
Cn-5	n/a	n/a	n/a	3.2	3.1	2.8	3.3	3.1	6.1	3.3	3.0	8.9	n/a	n/a	n/a	n/a	n/a	n/a
Cn-6	n/a	n/a	n/a	3.5	3.2	8.7	2.8	2.8	1.4	2.9	2.7	4.9	n/a	n/a	n/a	n/a	n/a	n/a

Note: AW = Average wind condition; NW = No wind condition; Diff = (AW-NW)/AW

Table 7.7 Natural ventilation rates under the average wind and no wind conditions in the urban context - summer

	Level 1			Level 2			Level 3			Level 4			Level 5			Level 6		
	AW (ACH)	NW (ACH)	Diff (%)	AW (ACH)	NW (ACH)	Diff (%)	AW (ACH)	NW (ACH)	Diff (%)	AW (ACH)	NW (ACH)	Diff (%)	AW (ACH)	NW (ACH)	Diff (%)	AW (ACH)	NW (ACH)	Diff (%)
An-1	10.7	9.9	7.6	47.7	43.5	8.8	66.3	60.1	9.4	82.1	73.5	10.5	92.2	81.2	11.9	128.0	99.5	22.3
An-2	9.9	8.9	9.3	122.0	119.0	2.5	148.0	146.2	1.2	167.0	165.9	1.1	135.3	132.5	2.1	132.0	132.0	0.0
An-3	0.0	0.0	0.0	21.8	21.8	0.0	20.2	20.4	-1.0	19.0	18.7	1.6	18.1	18.1	0.0	18.1	18.1	0.0
An-4	7.5	7.0	6.7	8.8	4.9	44.1	7.0	4.6	33.9	7.1	4.2	40.3	7.3	4.7	35.8	6.89	2.37	65.6
An-5	3.6	3.3	7.0	17.0	16.4	3.5	16.3	15.6	4.3	15.1	14.4	4.6	14.1	13.2	6.4	12.9	11.2	13.2
An-6	0.2	0.2	6.7	7.9	3.5	55.4	8.3	3.7	55.2	10.1	0.4	96.32	11.3	2.3	79.9	10.2	1.23	87.9
An-7	7.5	7.6	-0.7	76.0	78.4	-3.2	25.3	28.3	-11.9	11.0	4.4	59.8	8.8	9.3	-6.1	8.9	9.6	-8.4
An-8	1.1	0.7	30.8	21.6	20.7	4.2	19.1	17.2	9.9	17.7	17.8	-0.6	17.5	18.6	-6.3	16.1	16.4	-1.9
An-9	n/a	n/a	n/a	5.6	2.2	60.8	5.7	0.9	83.6	4.5	2.6	42.3	3.4	2.5	27.6	2.4	2.07	13.0
Bn-1	0.3	0.5	-51.8	5.2	6.5	-24.6	18.0	15.2	15.6	3.7	2.2	41.0	3.7	3.5	4.9	n/a	n/a	n/a
Bn-2	12.5	12.2	2.4	33.6	32.8	2.4	36.5	35.1	3.8	35.4	35.1	0.8	20.7	20.6	0.5	n/a	n/a	n/a
Bn-3	1.5	1.5	0.7	6.5	6.5	0.6	3.6	3.3	7.5	5.0	4.7	6.2	6.6	6.5	0.8	n/a	n/a	n/a
Bn-4	0.7	0.7	1.7	6.6	2.5	62.5	6.8	1.2	82.2	6.7	0.8	87.6	8.3	2.7	66.9	n/a	n/a	n/a
Bn-5	4.9	4.6	5.1	4.2	1.7	59.2	4.4	2.8	35.7	4.8	1.7	64.3	7.0	0.1	99.2	n/a	n/a	n/a
Bn-6	n/a	n/a	n/a	5.4	4.8	11.0	3.4	3.0	12.9	1.8	1.7	7.7	1.8	2.0	-7.6	n/a	n/a	n/a
Cn-1	1.1	1.1	4.4	9.4	8.0	15.0	8.6	7.1	17.3	7.2	6.2	13.2	n/a	n/a	n/a	n/a	n/a	n/a
Cn-2	22.5	22.6	-0.4	69.4	68.9	0.7	69.4	68.9	0.7	42.1	43.1	-2.4	n/a	n/a	n/a	n/a	n/a	n/a
Cn-3	4.4	2.3	46.9	17.4	16.0	8.0	17.3	16.8	2.9	18.7	18.0	3.7	n/a	n/a	n/a	n/a	n/a	n/a
Cn-4	2.0	1.2	37.6	16.4	14.5	11.6	14.5	14.0	3.4	14.1	13.9	1.4	n/a	n/a	n/a	n/a	n/a	n/a
Cn-5	n/a	n/a	n/a	19.9	19.9	0.0	20.2	19.9	1.5	20.1	19.8	1.5	n/a	n/a	n/a	n/a	n/a	n/a
Cn-6	n/a	n/a	n/a	15.4	15.1	1.9	14.7	14.7	0.0	14.8	14.6	1.4	n/a	n/a	n/a	n/a	n/a	n/a

Note: AW = Average wind condition; NW = No wind condition; Diff = (AW-NW)/AW

Table 7.8 Natural ventilation rates under the average wind and no wind conditions in the urban context – the hottest days

	Level 1			Level 2			Level 3			Level 4			Level 5			Level 6		
	AW (ACH)	NW (ACH)	Diff (%)	AW (ACH)	NW (ACH)	Diff (%)	AW (ACH)	NW (ACH)	Diff (%)	AW (ACH)	NW (ACH)	Diff (%)	AW (ACH)	NW (ACH)	Diff (%)	AW (ACH)	NW (ACH)	Diff (%)
An-1	19.4	16.9	12.9	80.1	69.0	13.9	108.0	92.1	14.7	133.0	112.0	15.8	151.0	124.0	17.9	198.0	145.0	26.8
An-2	15.9	13.6	14.5	185.0	179.0	3.2	195.0	191.2	1.9	203.0	198.8	1.2	179.0	173.2	3.1	199.0	200.0	-0.5
An-3	0.0	0.0	0.0	32.6	32.7	-0.3	30.2	30.6	-1.3	28.7	27.9	2.8	27.5	27.2	1.1	27.6	27.3	1.1
An-4	11.4	10.2	10.5	14.4	7.3	49.0	12.1	6.2	48.6	13.4	6.1	54.5	14.0	7.0	50.3	11.8	3.8	67.9
An-5	5.7	5.0	11.3	25.4	24.1	5.1	34.7	33.3	4.0	33.5	32.0	4.5	21.8	19.8	9.2	20.2	16.7	17.3
An-6	0.4	0.4	5.6	13.8	4.4	68.5	14.7	4.7	68.3	17.8	2.6	85.2	19.5	4.2	78.5	17.7	2.4	86.7
An-7	11.2	11.3	-0.9	112.0	117.0	-4.5	34.7	42.4	-22.2	20.7	6.7	67.5	14.9	14.4	3.4	14.9	14.5	2.7
An-8	2.1	1.5	29.2	32.8	31.0	5.5	29.4	25.9	11.9	28.3	26.5	6.4	28.2	27.8	1.4	24.8	24.6	0.8
An-9	n/a	n/a	n/a	10.9	3.1	71.7	10.9	1.6	85.8	8.8	4.1	53.4	7.9	4.2	47.3	2.5	4.2	-68.0
Bn-1	6.5	1.7	73.5	16.8	15.7	6.5	13.3	5.6	58.1	17.1	11.4	33.3	15.8	13.9	12.0	n/a	n/a	n/a
Bn-2	38.7	36.0	7.0	107.0	102.0	4.7	122.0	117.0	4.1	116.0	113.0	2.6	68.4	67.3	1.6	n/a	n/a	n/a
Bn-3	14.0	5.7	59.2	22.6	24.3	-7.5	32.0	30.2	5.6	36.8	35.1	4.6	38.9	38.4	1.3	n/a	n/a	n/a
Bn-4	4.6	2.7	41.1	23.1	7.0	69.8	24.1	3.5	85.4	24.1	5.0	79.2	27.3	9.9	63.6	n/a	n/a	n/a
Bn-5	18.3	14.6	20.2	3.0	0.8	74.1	8.4	6.6	21.6	19.2	8.2	57.6	25.5	6.1	75.9	n/a	n/a	n/a
Bn-6	n/a	n/a	n/a	24.9	24.7	0.8	20.1	19.6	2.5	19.6	19.3	1.5	20.3	20.8	-2.5	n/a	n/a	n/a
Cn-1	2.2	2.1	5.5	14.9	11.9	20.1	14.5	10.6	26.9	12.1	9.3	23.2	n/a	n/a	n/a	n/a	n/a	n/a
Cn-2	33.7	33.8	-0.3	104.0	103.0	1.0	104.0	103.0	1.0	62.4	64.7	-3.7	n/a	n/a	n/a	n/a	n/a	n/a
Cn-3	8.7	4.1	52.8	26.7	24.0	10.1	26.2	25.1	4.2	28.4	27.0	4.9	n/a	n/a	n/a	n/a	n/a	n/a
Cn-4	3.9	2.5	36.8	25.8	21.7	15.9	21.9	21.0	4.1	21.1	20.8	1.4	n/a	n/a	n/a	n/a	n/a	n/a
Cn-5	n/a	n/a	n/a	30.1	29.8	1.0	30.5	29.8	2.3	30.4	29.6	2.6	n/a	n/a	n/a	n/a	n/a	n/a
Cn-6	n/a	n/a	n/a	23.1	22.7	1.7	22.1	22.0	0.5	22.2	21.9	1.4	n/a	n/a	n/a	n/a	n/a	n/a

Note: AW = Average wind condition; NW = No wind condition; Diff = (AW-NW)/AW

7.4 Discussion

7.4.1 Characteristics of wind pressure coefficients around the building in the urban environment

Wind pressure coefficients of the building in the urban environment have particular characteristics. They are more affected by the characteristics of surrounding buildings than the geometric characteristic of the building being studied. These characteristics include building density, building height and the ratio of the upstream building height and the distance between them. In the thumb rules, compared with the isolated building, the pressure coefficients on the windward, leeward and lateral and roof of the building in the urban environment are reduced to 10%, 20% and 50% respectively. The maximum positive pressure coefficient usually occurs near the top edge of the windward surface, and the maximum negative pressure coefficient usually occurs around the windward edge of the roof. The pressure coefficients on the lower part of the building surfaces tend to be uniform negative data. The unstable pressure coefficient distribution on the same surface means the average data cannot be used to represent the pressure on the surface. In addition, the effect of the wind incident angle on the pressure coefficient is slight in the urban environment.

These characteristics of pressure coefficients on the building can be explained by the flow features in the urban surroundings. Wind velocity at the upper level of the urban canopy layer decreases, and the difference of the velocity along the vertical height becomes smaller than in the isolated condition. Wind velocity profiles are also affected by the building density, since increasing the building density means the mass conservation constrain area becomes larger, and the difference in velocity along the vertical height tends to be smaller (MacDonald, 2000). The maximum pressure coefficient occurs near the top edge of the windward surface, because the velocity at the upper part is less affected by the surrounding s than at the lower level. This phenomenon has been confirmed by the study on the flow over cube arrays of different packing densities in the wind tunnel (Cheng et al., 2007). Georgakis and Santamouris' (2006) field experiment in the deep canyon claimed that wind speed in the urban street was very weak, but increases considerably at the upper level. This could be because the urban street canyon is a special case, which has a larger length

and ratio of height to width. In this study, the ratio of building height to street width is 0.52 and the length of canyon is 2.2. Therefore, wind pressure coefficients of the building in the urban environment are dependent upon the features of surrounding buildings.

The characteristics of pressure coefficients on the building in the urban environment can help designers to optimise wind induced ventilation design at the early design stage. Using these characteristics, one can choose an appropriate building geometry and layout by analysing the surrounding buildings and the prevailing wind direction. The effect of the surroundings on the roof is less than on the other surfaces, which suggests that the roof can be taken as a key factor for improving the natural ventilation rate. The possible positions of the maximum and minimum data are suggested for setting the openings. When the openings have to be located at a lower potential location, other solutions such as using stack effect and enlarging opening size are recommended. However, wind induced ventilation in the urban environment is reduced largely. The comprehensive natural ventilation design in the urban environment needs to consider buoyancy ventilation as well as wind induced ventilation.

7.4.2 Natural ventilation design strategies in the urban environment

In general, buoyancy ventilation can be taken as the main ventilation strategy in the urban environment in the temperate climate zone, provided that there are possible opening position differences in the building. Wind velocity in the urban canopy layer is significantly reduced, and wind pressure on the building is weak, especially the lower part of building or the building that is sheltered by an upstream building. The temperature difference between the outside and inside has the potential to generate adequate ventilation for health, thermal comfort and cooling. Note that this strategy requires considering the opening positions. Increasing the height difference between the openings can improve the ventilation rate. Using this strategy would bring freedom for the designers to consider the form of building at the low level, as the geometry of building at the low level does not affect its performance. For the buoyancy ventilation strategy, the critical airflow path in the building attaches importance to the building section design.

Since buoyancy ventilation as the only ventilation strategy in the URBVENT project (Guiaus and Allard, 2005) is limited to the special deep urban street canyon, wind induced ventilation can still take action in most urban areas. Wind pressure at the upper part of the building has the potential to acquire adequate ventilation rate for health, thermal comfort and cooling. In addition, the wind force can resist the performance of buoyancy ventilation if the wind flow path opposes the buoyancy flow path. Different opening positions with the same wind flow direction in the urban canyon can cause different ventilation rates (Syrios and Hunt, 2007). Natural ventilation design in the urban environment has to consider wind as the subordinate strategy, so it is better to harness the wind force to assist the buoyancy flow and avoid any potential conflict. The wind induced, top down ventilation strategy proposed by Gage et al (2001) resists buoyancy flow, so it is limited to the low-rise building.

Combining the wind induced ventilation and buoyancy ventilation is necessary for the natural ventilation design in the urban environment. Both natural ventilation strategies have roles to play in the urban environment. However, the current building regulations on ventilation design are limited to applying to the building in the urban environment. CIBSE's (2005) suggestion on narrow building depth for cross ventilation is not suitable for a building in the urban environment. The recommended opening area for the sealed building cannot meet the ventilation requirement, as the natural ventilation potential is changeable. The suggestion is to keep a flexible opening area for the occupants in order to adjust their environment by themselves. The low level of buildings in the urban environment can utilise buoyancy ventilation, and the upper levels of buildings can use wind induced ventilation. The building section design would be important for estimating the possibility of the airflow path at the early design stage.

7.4.3 Simulation to predict the potential for natural ventilation

Coupling the virtual urban boundary layer wind tunnel and multi-zone network model (COMIS) is an efficient method for predicting the natural ventilation potential of the building in the urban environment. This method utilises their individual advantages. COMIS is better for calculating the ventilation rate in the multi-zone

buildings than CFD, as CFD is better for capturing the details of the flow in the single space (Liddment, 1996), while COMIS needs to input the accurate wind pressure coefficients around the building. Van Moeseke et al. (2005) point out that the limited tool for generating pressure coefficients can lead to abstract results. The virtual wind tunnel can comprehensively consider the features of the urban environment, and the effects of surroundings on the building. The wind pressure coefficient that it achieves is acceptable for the study of natural ventilation. This method can be applied to building design for optimisation and evaluation of natural ventilation design in the urban environment.

Using this method is not without its problems. The simulation result usually needs to be validated, by comparison with experiment, but it is difficult to validate the result at the building design stage, because the full scale experiment and wind tunnel experiment is restricted by both finance and time period. The solution is to develop guidelines and a benchmark for natural ventilation study in the urban environment. In addition, the user's experience and knowledge would decide the accuracy of results during the simulation (Cowan et al., 1997). This means the physical conditions in the simulation have to be simplified, which is dependent upon individual experience and knowledge. In this study, the wind flow was set at a steady state and the temperature outside as well as the inside the buildings is isothermal. These conditions are not true in reality. However, we have to emphasise that the value of building simulation is to reveal the tendency of the effect of parameters on the whole system, in order to optimize the building design.

7.5 Summary

This study has applied the propose methodology to evaluating the potential for natural ventilation of a case in the urban environment. It reveals the characteristics of the wind pressure coefficients of the building in the urban surroundings, and summarises the natural ventilation design strategies in the urban environment.

Wind pressure coefficient on the building in the urban environment has certain notable characteristics. Compared with the isolated building, the pressure coefficients of the building in the urban environment are more affected by the characteristics of

surroundings than the geometric characteristic of the building. The ratio of the upstream building height and the distance between them decide the pressure coefficient distribution. The maximum pressure coefficient usually occurs near the top edge of the windward surface. The larger pressure differences between the windward wall and the leeward wall exist at the upper level of building, which may have the potential for natural ventilation. In addition, the wind incident angle has a slight effect on the pressure coefficient in the urban environment.

Natural ventilation design in the urban environment in the temperate climate zone can generally take buoyancy ventilation as the main strategy for ventilation in winter, summer, and even the hottest day. The combination of wind induced ventilation and buoyancy ventilation is essential in natural ventilation design in the urban environment, because wind pressure can both assist and oppose buoyancy force. The ground level and the lower level can mainly use buoyancy ventilation, while the upper levels should consider wind induced ventilation as the dominant ventilation. The stack effect can generate a greater ventilation rate. The narrow building plan from the ventilation point of view does not achieve wind induced ventilation at the lower levels in the urban context, but uses buoyancy ventilation as the main strategy for natural ventilation. The suggestion is to increase the height of the doors. The top to down - wind induced ventilation would oppose any buoyancy ventilation.

Coupling the virtual urban boundary layer wind tunnel and the multizone network method is an efficient approach for predicting the natural ventilation potential of the building. CFD is used to predict the wind pressure coefficients around the building in the urban environment, while the multizone network method is used to predict the ventilation rate of the building in various seasons. Using the current computational resources and limitations of software, it is necessary to simplify the models according to requirements, which includes domain size, the surrounding buildings model, zones and environmental data. The validation of the simulation is still a difficult task with regards to the practical design. However, the knowledge and experience could be helpful to the simulation.

CHAPTER 8

Conclusions

This thesis has developed the methodology for predicting the potential of natural ventilation of buildings in the urban environment, and has also considered the applications of this methodology at the stages of planning and building design. This methodology will be beneficial to policy-makers, planners and building designers for maximising the potential of their projects when designing sustainable buildings. This chapter highlights the main findings and their implications, and also discusses the limitations of this study and recommendations for future study.

8.1 Main conclusions

The presented approach is intended to comprehensively predict the potential for natural ventilation, through considering the effects of the external urban surroundings and thermal buoyancy on natural ventilation at the planning and building design stages. The virtual urban boundary layer wind tunnel is capable of predicting the wind pressure coefficients of buildings for the purpose of building design. This overcomes the inaccuracy of parametrical methods (Grosso, 1992) and the high cost of physical wind tunnels on the prediction of pressure coefficients around the building in the urban environment. The combination of the virtual wind tunnel and airflow network models integrates the effects of wind induced ventilation and buoyancy ventilation, which is more efficient to study in the urban environment than the wind tunnel and direct CFD simulation. The benefits in terms of cost-effectiveness of computational resources, fast running, flexible modelling and accurate results make it possible to use this approach in the planning and building

design stages. The investigation of the effects of planning parameters on the potential for natural ventilation provides some guidance for policy-makers and planners. The evaluation of this potential of an urban building demonstrates the proposed methodology may be popularised in other projects. Some suggestions with regards to building design in the urban environment can help planners and designers to optimise their projects, and fully utilise the potential for natural ventilation when seeking maximum sustainability.

8.1.1 Development of the virtual urban boundary layer wind tunnel

The developed virtual urban boundary layer wind tunnel based on the CFD technique is used for predicting wind pressure coefficients around the building in the urban environment. The step by step simulation of the urban boundary layer wind tunnel is as good as the validated wind tunnel experiment in terms of acquiring a sensible, homogeneous wind profile. The decision to use the neighbourhood region for natural ventilation study provides a feasible approach for determining the computational domain size for the building design practices. The virtual wind tunnel can provide sensible boundary conditions, a turbulence model, and a minimal but effective domain size for studying natural ventilation in the urban environment.

- ◆ The horizontally homogeneous wind profile can be achieved in two steps. The first is to simulate the wind profile in one of the repeated units in the urban roughness element fetch by using the period boundary conditions. This profile is more appropriate in representing urban atmospheric boundary layer than the wind tunnel experiment, because the fully developed profile overcomes the limitation of the urban roughness fetch in the wind tunnel. The second step is to simulate the wind crosses the empty domain. It was found that the horizontally homogeneous profile occurred behind $40H_b$ of the last roughness element. The simulated wind profile, which represents the effects of urban roughness, is more sensible than common methods that usually ignore the wind profile in the urban roughness sublayer. This implies that users can generate the homogeneous urban wind profile using the numerical method, rather than having to complete expensive wind tunnel experiments.

- ◆ The pressure gradient from the global friction velocity (about 2.3 times of the urban roughness element height) is better at generating the wind profile in the urban environment. The surface friction velocity can cause a larger pressure gradient and wind profile, which suggests that the pressure gradient can be estimated from the global friction velocity at the building site. The global friction velocity can be transferred from a meteorological station to the building site, provided that the urban roughness element height is known.

- ◆ The mixed-use turbulence models are efficient for natural ventilation studies in the urban environment. It was found that the RSM turbulence model with enhanced wall treatment can simulate wind profiles more accurately than other RANS models, but it is still difficult to converge when the model is complicated. The SST κ - ω turbulence model is the most accurate in simulating wind pressure on the surface in the RANS models. The sensible decision is to use the RSM turbulence model in the relative simple model to predict the mean wind profile in the urban roughness area. The SST κ - ω turbulence model is the most appropriate model for predicting wind pressure coefficients around an isolated building or a building in the group in the urban environment. The combination of turbulence models can not only reduce the requirement of computational resource, but also achieve a sensible result in a faster time.

- ◆ The computational domain size for natural ventilation study in the urban environment consists of two parts: the region for the turbulence to fully develop, and the neighbourhood region for the effects of surroundings on the wind pressure around the studied building. As the full turbulence development region is known, this study focuses on the neighbourhood region. The neighbourhood region for natural ventilation study is dependent the characteristic of the building height, as well building density, building layout and tolerant error. This study proposed guidelines for computational domain size of natural ventilation in the urban environment (see Table 4.7). It ensures that the simulation results are acceptable without including unnecessary surroundings.

8.1.2 Validations of the virtual urban boundary layer wind tunnel

By comparing the results of wind flow characteristics and the wind pressure coefficient around the buildings from the virtual wind tunnel with the previous wind tunnel experiments, it was found that the virtual wind tunnel can qualitatively study wind flow and the discrepancy with the wind tunnel experiment is acceptable. This means the virtual wind tunnel has the capability of obtaining the mean wind pressure coefficients around the building in the urban environment.

- ◆ For the isolated model, the RANS turbulence model with the enhanced wall treatment can capture the flow characteristics around the building, comparing the reattachment length and recirculation length with those from the wind tunnel experiment. The discrepancy of the mean pressure coefficient around the building surfaces between the virtual wind tunnel and the wind tunnel is about 20%, which is 10% less than between the commonly used methods and the wind tunnel experiments. This implies that the postulated settings of the boundary conditions and turbulence model are better than the other methods.
- ◆ For the models in the neighbourhood region, the virtual wind tunnel can achieve good flow characteristics, but the discrepancy of the mean wind pressure coefficients between the virtual and the real wind tunnels is about 30% in most part of the surfaces. This discrepancy is acceptable in natural ventilation studies.
- ◆ The large discrepancy usually occurs at the parts of near the top edge and the ground. It can be reduced by using a denser grid near the edges. In addition, a more advanced turbulence model could be used as a solution, because the current RANS turbulence models have the drawbacks to simulate the anisotropic flow around the edges.

8.1.3 Planning parameters and the potential for natural ventilation

Planning parameters can affect the wind pressure distribution around a building and their effects can also assist or oppose each other. Investigating the effects of associated parameters can be helpful to design practice. The findings from the study provide guidance for policy-makers and planners to make the best use of natural ventilation in their planning at the early design stage.

- ◆ The wind pressure coefficient distribution on the building surfaces in the building area has its own unique characteristics. Planning parameters like floor area ratio, building density, and building space and gap all affect wind pressure coefficient distribution around the building. The maximum pressure coefficients occur near the top edge of the windward wall, and the minimum pressure coefficient exist near the upwind edge of the roof. The pressure coefficient difference between the windward and leeward walls is determined by the planning parameters. The pressure coefficients at different positions on the same surface are considerably different. The average wind pressure coefficient of the surface cannot represent the wind pressure coefficient distribution on the surface. This suggests that the information of the pressure coefficient on the whole surface is fundamental when calculating the natural ventilation rate of the whole building in the urban environment.

- ◆ The planning layout can affect the potential for natural ventilation. With the increase of floor area ratio, the upper levels of buildings in the normal pattern can acquire larger ventilation rates, whilst the lower parts of the building have the smaller ventilation rates. With the increase of building density, the bottom levels of buildings in the staggered pattern could obtain larger ventilation rates, whilst their upper levels acquire the smaller ventilation rates.

- ◆ In the temperate climate zone, most levels of buildings can acquire the thermal comfort and cooling by natural ventilation. However, the whole building ventilation for health in winter cannot be easily achieved by natural ventilation. Increasing an appropriate opening area of buildings in the urban environment could be a solution.

- ◆ The changes of building density can influence ventilation rates of the different levels with a fixed floor area ratio. High-rise buildings in low building density areas have dramatic fluctuations in the ventilation rate at different levels. The high-rise building in a low building density area has more natural ventilation potential than the low-rise building in a high building density area. This suggests that building planning should balance the building density and building height.

- ◆ Given that the floor area ratio and building density are fixed, changes of building space and gap can also influence the ventilation rate. The larger building space with the smaller gap has a larger ventilation rate at the lowest level, whilst the smaller building space with the larger gap has a larger ventilation rate at the middle level. The best case is that the building space is equal to the building gap, which means a larger ventilation rate at different levels.
- ◆ Planning parameters have effects on the purge ventilation rate, or the ventilation rate for thermal comfort as well as the whole building ventilation rate. However, in most cases, wind induced natural ventilation for purge ventilation or thermal comfort at the same level of the building can be achieved, as the opening area for the purge ventilation rate is larger than the trickle ventilator area.
- ◆ A bigger opening area in the building within the urban environment should be considered to extend the ventilator area for the whole building ventilation. An extra controllable opening for the whole building ventilation is more appropriate for the lower levels in the urban environment. The indices of natural ventilation rate that are affected by planning parameters indicate the potential of natural ventilation in the urban environment (Table 6.9, 6.10, 6.11). They can be useful when estimating the ventilator area and deciding the appropriate ventilation mode in the urban environment. Its application supplements the inadequate guidance of openings area and position in the current building regulations or standard codes, for example Part F(OPDM, 2006).
- ◆ Natural ventilation design strategies for cooling large spaces in the urban environment should consider the combination of wind and buoyancy induced ventilation. Using buoyancy for cooling is more efficient than using wind force in the dense urban environment in the temperate climate zone. The opening position determines the potential for cooling. The best opening positions are the places near the windward edge of roofs and the low level of leeward walls. The worst positions are when the opening is positioned at the upper level of the windward surfaces, and the lower level of leeward surfaces. Providing that the openings have to be at the same surface, the leeward surface is better than the

windward surface. When the building is higher than 6 levels, the ventilation rate for cooling can be achieved.

8.1.4 Prediction of the potential of an urban building

The investigation of the natural ventilation potential of the real building revealed the characteristics of wind pressure coefficient distribution around the building are affected by urban surroundings. The proposed natural ventilation design strategies can guide building design in the urban environment. The method of predicting this potential can be widely applied in practice.

- ◆ The wind pressure coefficients on the building in the urban environment have their own characteristics. The pressure coefficients in the urban environment are more affected by the characteristics of the surroundings than the geometric characteristics of the particular building, compared with the isolated building. This implies that it is not necessary to model all the details of the building. The maximum pressure coefficient usually occurs near the top edge of the windward surface. The larger pressure difference between the windward and leeward walls exists at the upper level of building, which has natural ventilation potential.
- ◆ The impact of the wind incident angle on the pressure coefficient is slight in the urban environment. This suggests that the simulation of the building in the urban environment does not need to analyse many wind incident cases.
- ◆ Natural ventilation design in the temperate climate zone can take buoyancy ventilation as the main source for ventilation in winter and summer, and even on the hottest days. Combining wind induced ventilation and buoyancy ventilation is necessary for the design of natural ventilation in the urban environment. Wind induced ventilation usually changes buoyancy ventilation at the upper level. The ground level and the lower level can mainly utilise buoyancy ventilation, while the upper levels should consider wind induced ventilation as the dominant ventilation. The narrow building plan in terms of ventilation does not achieve wind induced ventilation at the lower levels in the urban context, but it can consider buoyancy ventilation as the main strategy for natural ventilation. The

interior design should consider making the sensible airflow path cross the plan. Cross ventilation is expected, but the ratio of distance between the wall and the surrounding buildings and building height ultimately decides which model is most suitable to choose. The top-to-down ventilation strategies have to consider that the wind induced ventilation resists the buoyancy ventilation.

- ◆ In the urban environment, the lower ventilation rate usually occurs at the ground floor, and the part of the building that is shadowed by the upstream building. One of the solutions for the building to avoid or reduce being sheltered by the upstream building at the early design stage. Another solution is to employ buoyancy ventilation or enlarge the opening area at these places.
- ◆ Coupling the virtual urban boundary layer wind tunnel and the airflow network model is an efficient and feasible method for predicting the potential for natural ventilation of the building in the urban environment. This method holistically considers natural ventilation driven by the combination of wind and thermal buoyancy forces, which is essential in practice. It has the capability of evaluating the effects of a building's surroundings on wind induced ventilation, as well as the effects of buoyancy ventilation in the buildings. Combining the advantages of CFD and airflow network models is more sensible and practical for the building design than other methods, such as empirical calculations and wind tunnel experiments.

8.1.5 Methodology for predicting the potential for natural ventilation

This methodology is an effective approach to predicting the potential for natural ventilation. The virtual urban boundary layer wind tunnel can acquire wind pressure coefficients around the building in the urban environment satisfactorily. The airflow network models can calculate the ventilation rates of zones of buildings quickly. This methodology can holistically predict the potential of natural ventilation of buildings in the urban environment, although natural ventilation in the urban environment is affected by many factors: urban morphology, wind velocity, temperature, building form, building spaces and openings and so on.

The methodology for predicting the potential for natural ventilation can be applied to optimise and evaluate the potential of the planning and building at the design stages. As the building configuration at the planning stage is unknown, the building can be simplified as a single zone or several zones. A simple airflow network model, such as AIDA, can be used to quickly evaluate the potential for natural ventilation of the building during planning. It can help the planners to fast evaluate the potential for natural ventilation of their projects and optimise their planning. At the building design stage, the building configuration is known and the building form is determined. Subsequently, the airflow network model can employ a multizone network model, which can quickly and accurately calculate natural ventilation rates of the zones in the building. This can be used to evaluate the natural ventilation design, and optimise the opening position and size.

8.2 Limitations

The numerical models used in the current study have some differences from the physical wind flow. The current study assumed that the flow was taken as a steady state, and the temperature was set as an isothermal condition. The study did not consider the effect of the urban heat island on the potential for natural ventilation. The turbulence model in this study employed the RANS turbulence models, which have the shortcomings of turbulence fluctuations when simulating the unsteady turbulence flow around a building. In reality, the airflow is unsteady and changeable with space and time. In the airflow network models, the opening discharge rates were assumed to have constant data. In fact, these rates vary with wind incidence angle, opening shape, type and so on.

The current study is limited to validating the results by comparison with the previous wind tunnel experiment and the existing literature. Although the validated wind tunnel experiments can be used to validate the current study, the ideal validation should be made by comparing the results from the simulation and the physical experiment at the same conditions, but this requires extra facilities, more finance and a longer time period. However, the application of the proposed methodology aims to optimise building design, rather than to acquire exact data at the planning and building design stages.

The model in the current study is idealized. The model in the planning was assumed to be a square shape, and the building layout was taken as being normal, in a staggered pattern. This simplified model could possibly cause different results when other shapes are used in planning. The urban surroundings in the urban building study only considered the surrounding buildings and terrain, and neglected the vegetation and fences and so on. The temperate climate zone and the specified weather case were studied.

8.3 Recommendations

Besides the findings described above, some new research areas which need further study have arisen. One is improving the accuracy of the current model; the other is popularizing its application at the planning and building design stages.

- ◆ In the urban environment, natural ventilation could be generated by turbulent fluctuation, which may be a dominant phenomenon in the urban canopy layer. However, it is necessary to employ the advanced turbulence model, which can solve the unsteady anisotropy flow. Further study may investigate the fluctuated ventilation in the urban environment by using the improved numerical model.
- ◆ Natural ventilation in the urban environment is still a complicated issue. In order to improve the reliability of building simulation on natural ventilation in the urban environment, it is necessary to develop guidelines and benchmarks for users. They may be set up by a combination of field tests, wind tunnel experiments and numerical simulations.
- ◆ The current study focuses on the natural ventilation rate, which represents the possibility of air exchange between outside and inside through natural ventilation. However, a higher ventilation rate does not mean that the occupants will acquire more fresh air in the interior, because the position and types of openings, interior partition and so on will affect the efficiency of the ventilation. The possibility for natural ventilation of the building would be eventually determined by the ventilation efficiency. Future study should concentrate on the

possibility for natural ventilation of the building, based on the ventilation efficiency.

- ◆ In addition, a novel code coupling CFD code and airflow multi-zone models for urban natural ventilation study may be worthy of development. The current commercial CFD codes are complicated and expensive systems to use in practice. In reality, urban natural ventilation study employs only a part of the CFD code. The multi-zones model has the potential to predict the whole building, provided that it overcomes its drawbacks such as wind pressure coefficient, and buoyancy stack, which can be complemented by CFD. The new code will consist of different models according to the planning and building design stages, such as the empirical pattern for the preliminary stage, and the turbulence models for the details of building design. The evaluation of the potential for natural ventilation will adapt the dynamic mode. It would be an efficient and flexible method for predicting the potential for the natural ventilation of buildings in the urban environment.

Bibliography

- ALLARD, F. (Ed.). (1998) *Natural ventilation in buildings*. London: James & James.
- ALLOCCA, C., CHENG, Q. and GLICKSMAN, L. R. (2003) Design analysis of single-sided natural ventilation. *Energy and Buildings*, 35 (8), 785-795.
- ANDERSEN, K. T. (2007) Airflow rates by combined natural ventilation with opposing wind--unambiguous solutions for practical use. *Building and Environment*, 42 (2), 534-542.
- ANDERSON, J. D. (2007) *Fundamental of aerodynamics*. Boston: McGRAW-Hill.
- ASFOUR, O. S. and GADI, M. B. (2007) A comparison between CFD and Network models for predicting wind-driven ventilation in buildings. *Building and Environment*, 42 (12), 4079-4085.
- ASHRAE. (2001) *Handbook of fundamental*. Atlanta: American Society of Heating, Refrigeration and Air-conditioning Engineers.
- ASHRAE. (2005) *ASHRE handbook fundamental*. Atlanta: American Society of Heating, Refrigerating and Air-conditioning Engineers.
- AWBI, H. B. (2003) *Ventilation of buildings*. 2nd ed. London: Spon Press.
- AXLEY, J. W. and EMMERICH, S. J. (2002) *A method to assess the suitability of a climate for natural ventilation of commercial buildings*. Paper presented at the Indoor air 2002, 30th June - 5th July, Monterey.
- AYAD, S. S. (1999) Computational study of natural ventilation. *Journal of Wind Engineering and Industrial Aerodynamics*, 82 (1-3), 49-68.
- AYATA, T. and YILDIZ, O. (2006) Investigating the potential use of natural ventilation in new building design in Turkey. *Energy and Buildings*, 38, 959-963.
- BAHADORI, M. N. and HAGHIGHAT, F. (1985) Passive cooling in hot, arid regions in developing countries by employing domed roofs and reducing the temperature of internal surfaces. *Building and Environment*, 20 (2), 103-113.
- BAUMAN, F. S., ERNEST, D. R. and ARENS, E. A. (1988) The effects of surrounding buildings on wind pressure distributions and natural ventilation in long building rows. *ASHRAE Transaction*, 94 (2), 1670-1695.
- BELCHER, S. E., JERRAM, N. and HUNT, J. C. R. (2003) Adjustment of a turbulent boundary layer to a canopy of roughness elements. *Journal of Fluid Mechanics*, 488, 369-398.

- BLOCKEN, B., STATHOPOULOS, T. and CARMELIET, J. (2007) CFD simulation of the atmospheric boundary layer: wall function problems. *Atmospheric Environment*, 41 (2), 238-252.
- BOARDMAN, B., DARBY, S., KILLIP, G. and HINNELLLS, M. (2005) *40% house*. Oxford: University of Oxford.
- BOJIC, M. and KOSTIC, S. (2006) Application of COMIS software for ventilation study in a typical building in Serbia. *Building and Environment*, 41 (1), 12-20.
- BRE. (1994) *BREEZE 6.0 user manual*. Watford: Building Research Establishment.
- BSI (1991) *Code of practice for ventilation - Principles and designing for natural ventilation, 5925*. London: British Standard Institution.
- BSI (1997) *Loading for Buildings-Part 2: Code of Practice for Wind Loads*. London: British Standard Institution.
- BURNETT, J., BOJIC, M. and YIK, F. (2005) Wind-induced pressure at external surfaces of a high-rise residential building in Hong Kong. *Building and Environment*, 40 (6), 765-777.
- CASTRO, I. P. (2003) CFD for external aerodynamics in the built environment. *The QNET-CFD Network Newsletter*, 2 (2), 4-7.
- CASTRO, I. P., CHENG, H. and REYNOLD, R. (2006) Turbulence over urban-type roughness: deductions from wind-tunnel measurements. *Boundary-layer Meteorology*, 118 (1), 109-131.
- CASTRO, I. P. and GRAHAM, J. M. R. (1999) Numerical wind engineering: the way ahead? Paper presented at the Proceedings of the institution of civil engineers, August.
- CERMAK, J. E., POREH, M., PETERKA, J. A. and AYAD, S. S. (1984) Wind tunnel investigations of natural ventilation. *Journal of Transp. Eng. ASCE Trans.*, 110 (1), 67-79.
- CHAKRABARTY, B. K. (2001) Urban Management: Concepts, Principles, Techniques and Education. *Cities*, 18 (5), 331-345.
- CHANG, C.-H. and MERONEY, R. N. (2001) Numerical and physical modeling of bluff body flow and dispersion in urban street canyons. *Journal of Wind Engineering and Industrial Aerodynamics*, 89 (14-15), 1325-1334.
- CHANG, C.-H. and MERONEY, R. N. (2003) The effect of surroundings with different separation distances on surface pressures on low-rise buildings. *Journal of Wind Engineering and Industrial Aerodynamics*, 91 (8), 1039-1050.
- CHEN, Q. (2004) Using computational tools to factor wind into architectural environment design. *Energy and Buildings*, 36 (12), 1197-1209.

- CHENG, H. and CASTRO, I. P. (2002) Near wall flow over urban-like roughness. *Boundary-layer Meteorology*, 104 (2), 229-259.
- CHENG, H., HAYDEN, P., ROBINS, A. G. and CASTRO, I. P. (2007) Flow over cube arrays of different packing densities. *Journal of Wind Engineering and Industrial Aerodynamics*, 95 (8), 715-740.
- CHENG, Y., LIEN, F. S., YEE, E. and SINCLAIR, R. (2003) A comparison of large eddy simulations with a standard k- ϵ Reynolds-Averaged Navier-Stokes model for the prediction of a fully developed turbulent flow over a matrix of cubes. *Journal of Wind Engineering and Industrial Aerodynamics*, 91 (11), 1301-1328.
- CHRISTEN, A., ROTACH, M. W. and PARLOW, E. (2002) *First results from BUBBLE I: Profiles of fluxes in the urban roughness sublayer*. Paper presented at the Proceeding of the 4th symposium on the urban environment, 20-24 May, Norfolk.
- CIBSE. (2003) *CIBSE concise handbook*. London: CIBSE.
- CIBSE. (2005) *Natural ventilation in non-domestic buildings*. London: CIBSE.
- COCEAL, O., THOMAS, T. G., CASTRO, I. P. and BELCHER, S. E. (2006) Mean flow and turbulence statistics over groups of urban-like cubical obstacles. *Boundary-layer Meteorology*, 121 (3), 491-519.
- COOK, N. J. (1978) Wind-tunnel simulation of the adiabatic atmospheric boundary layer by roughness, barrier and mixing-device methods. *Journal of Wind Engineering and Industrial Aerodynamics*, 3 (2-3), 157-176.
- COOK, N. J. (1990) *The designer's guide to wind loading of building structures: Part 2: static structures*. Butterworths: BRE
- COUNIHAN, J. (1969) An improved method of simulating an atmospheric boundary layer in a wind tunnel. *Atmospheric Environment*, 3, 197-214.
- COUNIHAN, J. (1975) Adiabatic atmospheric boundary layers: a review and analysis of data from the period 1880-1972. *Atmospheric Environment*, 9, 871-905.
- COWAN, I. R., CASTRO, I. P. and ROBINS, A. G. (1997) Numerical considerations for simulations of flow and dispersion around buildings. *Journal of Wind Engineering and Industrial Aerodynamics*, 67-68, 535-545.
- DASCALAKI, E., SANTAMOURIS, M., ARGIRIOU, A., HELMIS, C., ASIMAKOPOULOS, D. N., PAPADOPOULOS, K. and SOILEMES, A. (1995) Predicting single sided natural ventilation rates in buildings. *Solar Energy*, 55 (5), 327-341.
- DASCALAKI, E., SANTAMOURIS, M., BRUANT, M., BALARAS, C. A., BOSSAER, A., DUCARME, D. and WOUTERS, P. (1999) Modeling large openings with COMIS. *Energy and Buildings*, 30 (1), 105-115.

- DAVENPORT, A. G. (1961) *The applications of statistical concepts to the wind loading of structures*. Paper presented at the Proceeding of the Institution of Civil Engineers.
- DE DEAR, R. J. and BRAGER, G. S. (2002) Thermal comfort in naturally ventilated buildings: revisions to ASHRAE Standard 55. *Energy and Buildings*, 34 (6), 549-561.
- DUYNKERKE. (1988) Application of the E- ϵ turbulence closure model to the neutral and stable atmospheric boundary layer. *Journal of the Atmospheric Science*, 45 (5), 865-880.
- EMMERICH, S. J., DOLS, W. S. and AXLEY, J. W. (2001) *Natural ventilation review and plan for design and analysis tools*. (NISTIR 6781): National Institute of Standards and Technology.
- ENDO, T., KURABUCHI, T., ISHI, M., KOMAMURA, K., MARUTA, E. and SAWACHI, T. (2006) Study on the numerical predictive accuracy of wind pressure distribution and air flow characteristics. *International Journal of Ventilation*, 4, 269-284.
- ENGINEERING SCIENCES DATA UNIT (1985) *Characteristics of atmospheric turbulence near the ground part II: single point data for strong winds (neutral atmosphere)*, 85020. London: ESDU.
- ERNEST, D. R., BAUMAN, F. S. and ARENS, E. A. (1991) The prediction of indoor air motion for occupant cooling in naturally ventilated buildings. *ASHRAE Transaction*, 97 (1).
- ESDU (1982) *Strong wind in the atmospheric boundary layer*, 82026. London: Engineering Sciences Data Unit.
- ESDU (1985) *Characteristics of atmospheric turbulence near the ground part II: single point data for strong winds (neutral atmosphere)*, 85020. London: Engineering Sciences Data Unit.
- ETHERIDGE, D. and SANDBERG, M. (1996) *Building ventilation: theory and measurement*. New York: John Wiley & Sons.
- EVOLA, G. and POPOV, V. (2006) Computational analysis of wind driven natural ventilation in buildings. *Energy and Buildings*, 38, 491-501.
- FEIGENWINTER, C., VOGT, R. and PARLOW, E. (1999) Vertical structure of selected turbulence characteristics above an urban canopy. *Theory of Applied Climatology*, 62, 51-63.
- FERZIGER, J. H. (1990) Approaches to turbulent flow computation: applications to flow over obstacles. *Journal of Wind Engineering and Industrial Aerodynamics*, 35 (1-3), 1-19.
- FEUSTEL, H. E. (1999) COMIS--an international multizone air-flow and contaminant transport model. *Energy and Buildings*, 30 (1), 3-18.

- FLUENT (2006) *Fluent 6.3 user's guide*. Fluent Inc.
- FRANKE, J., HELLSTEN, A., KRUS, H. W. and SCHATSMANN, M. (2007) *Best practices guidelines for the CFD simulation of flows in the urban environment*. Cost Action 732.
- FRANKE, J., HIRSCH, C., JENSEN, A. G., KRUS, H. W., SCHATSMANN, M., WESTBURY, P. S., MILES, S. D., WISSE, J. A. and WRIGHT, N. G. (2004) Recommendation on the use of CFD in wind engineering. *In: Cost Action C14 Impact of wind and storm on city life built environment*, von Karman Institute, Belgium.
- GAGE, S. A., HUNT, G. R. and LINDEN, P. F. (2001) Top down ventilation and cooling. *Journal of Architecture and Planning Research*, 18 (4), 286-301.
- GAO, X., ASAMI, Y. and KATSUMATA, W. (2006) Evaluating land-use restrictions concerning the floor area ratio of lots. *Environment and Planning C: Government and Policy*, 24, 512-532.
- GEORGAKIS, C. H. and SANTAMOURIS, M. (2006) Experimental investigation of air flow and temperature distribution in deep urban canyon for natural ventilation purpose. *Energy and Buildings*, 38 (4), 367-376.
- GERMANO, M. (2007) Assessing the natural ventilation potential of the Basel region. *Energy and Buildings*, 39 (11), 1159-1166.
- GERMANO, M., GHIAUS, C., ROULET, C. A. and ALLARD, F. (2005) Natural ventilation potential of urban buildings. *International Journal of Ventilation*, 4 (1), 49-56.
- GHIAUS, C. and ALLARD, F. (2006) Potential for free-cooling by ventilation. *Solar Energy*, 80 (4), 420-413.
- GHIAUS, C. and ALLARD, F. (Eds.). (2005) *Natural ventilation in the urban environment: assessment and design*. London: Earthscan.
- GIMMOND, C. and OKE, T. (1999) Aerodynamics properties of urban areas derived from analysis of surface form. *Journal of Applied Meteorology*, 38 (9), 1262-1292.
- GINGER, J. D. and HOLMES, J. D. (2003) Effect of building length on wind loads on low-rise buildings with a steep roof pitch. *Journal of Wind Engineering and Industrial Aerodynamics*, 91 (11), 1377-1400.
- GIVONI, B. (1998) *Climate consideration in building and urban design*. New York: Van Nostrand Reinhold.
- GROSSO, M. (1992) Wind pressure distribution around buildings: a parametrical model. *Energy and Buildings*, 18 (2), 101-131.
- HAGHIGHAT, F. and MEGRI, A. C. (1996) A comprehensive validation of two airflow models - COMIS and CONTAM. *Indoor Air*, 6, 278-288.

- HAMLIN, D. and BRITTON, R. (2005) A numerical study of the flow field and exchange processes within a canopy of urban-type roughness. *Atmospheric Environment*, 39 (18), 3243-3254.
- HARGREAVES, D. M. and WRIGHT, N. G. (2007) On the use of the k- ϵ model in commercial CFD software to model the neutral atmospheric boundary layer. *Journal of Wind Engineering and Industrial Aerodynamics*, 95 (5), 355-369.
- HARRIS (1968) Measurements of wind structure at heights up to 598ft. above ground level. In: *Symposium on Wind Effects on Buildings and Structures*, Loughborough University.
- HAWKES, D. (Ed.). (1987) *Energy and urban built form*. London: Butterworths.
- HE, J. and SONG, C. S. (1999) Evaluation of pedestrian winds in urban area by numerical approach. *Journal of Wind Engineering and Industrial Aerodynamics*, 81 (1-3), 295-309.
- HEE, O. H., KOOP, G. A. and INCULET, D. R. (2007) The UWO contribution to the NIST Aerodynamics database for wind load on low buildings: part3 international pressures. *Journal of Wind Engineering and Industrial Aerodynamics*, 95, 755-779.
- HEISELBERG, P. (2004) Natural ventilation design. *International Journal of Ventilation*, 2, 295-312.
- HOGSTROM, U. (1996) Review of some basic characteristics of the atmospheric surface layer. *Boundary-layer Meteorology*, 78 (3-4), 215-246.
- HOLFORD, J. M. and HUNT, G. R. (2003) Fundamental atrium design for natural ventilation. *Building and Environment*, 2003, 409-426.
- HU, C.-H. and WANG, F. (2005) Using a CFD approach for the study of street-level winds in a built-up area. *Building and Environment*, 40 (5), 617-631.
- HUSSAIN, M. (1978) *A study of the wind forces on low rise buildings arrays and their application to natural ventilation design methods*. Thesis (PhD). the University of Sheffield, Sheffield.
- HUSSAIN, M. and LEE, B. E. (1980) *An investigation of wind forces on three dimensional roughness elements in a simulated atmospheric boundary layer Part I: Flow over isolated roughness elements and the influence of upstream fetch*. (BS 55). Sheffield: University of Sheffield.
- HUSSAIN, M. and LEE, B. E. (1980) A wind tunnel study of the mean pressure forces acting on large group of low-rise building. *Journal of Wind Engineering and Industrial Aerodynamics*, 6, 207-225.
- JAKKOLA, J. J. K. and MIETTINEN, P. (1995) Ventilation rate in offices buildings and sick building syndrome. *Occupational & Environmental Medicine*, 52, 709-714.

- JIANG, Y., ALEXANDER, D., JENKINS, H., ARTHUR, R. and CHEN, Q. (2003) Natural ventilation in buildings: measurement in a wind tunnel and numerical simulation with large-eddy simulation. *Journal of Wind Engineering and Industrial Aerodynamics*, 91 (3), 331-353.
- JIANG, Y. and CHEN, Q. (2001) Study of natural ventilation in buildings by large eddy simulation. *Journal of Wind Engineering and Industrial Aerodynamics*, 89 (13), 1155-1178.
- JIMENEZ, J. (2004) Turbulent flows over rough walls. *Annual Review of Fluid Mechanics*, 36, 173-196.
- KARAVA, P., STATHOPOULOS, T. and ATHIENITIS, A. K. (2006) Impact of internal pressure coefficients on wind-driven ventilation analysis. *International Journal of Ventilation*, 5 (1), 53-66.
- KASTNER-KLEIN, P. and ROTACH, M. W. (2004) Mean flow and turbulence characteristics in an urban roughness sublayer. *Boundary-layer Meteorology*, 111 (1), 55-84.
- KHANDURI, A. C., STATHOPOULOS, T. and BEDARD, C. (1997) Wind-induced interference effects on buildings - a review of the state-of-the art. *Engineering Structures*, 20, 617-630.
- KIEFER, H. and PLATE, E. J. (1998) Modelling of mean and fluctuating wind loads in built-up areas. *Journal of Wind Engineering and Industrial Aerodynamics*, 74-76, 619-629.
- KIM, S.-E. and BOYSAN, F. (1999) Application of CFD to environmental flows. *Journal of Wind Engineering and Industrial Aerodynamics*, 81 (1-3), 145-158.
- KNOLL, B., PRHAFF, J. C. and GRIDS, W. F. (1996) Pressure coefficient simulation program. *Air Infiltration Review*, 17, 1-5.
- LANDSBERG, H. E. (1981) *The urban climate*. London: Academic Press.
- LEE, B. E. (1977) *The simulation of atmospheric boundary layer in the Sheffield university 1.2x1.2m boundary layer wind tunnel* Sheffield: the University of Sheffield.
- LEE, B. E., HUSSAIN, M. and SOLIMAN, B. (1979) *A method for the assessment of the wind induced natural ventilation forces acting on low rise building arrays*. (BS 50). Sheffield: University of Sheffield.
- LEE, B. E., HUSSAIN, M. and SOLIMAN, B. (1980) Prediction natural ventilation forces upon low-rise buildings. *ASHRAE Journal* February, 35-39.
- LETTAU, H. (1969) Note on aerodynamic roughness-parameter estimation on the basis of roughness element description. *Journal of Applied Meteorology*, 8, 828-832.

- LI, L. and MAK, C. M. (2007) The assessment of the performance of a windcatcher system using computational fluid dynamics. *Building and Environment*, 42 (3), 1135-1141.
- LI, X.-X., LIU, C.-H., LEUNG, D. Y. C. and LAM, K. M. (2006) Recent progress in CFD modelling of wind field and pollutant transport in street canyons. *Atmospheric Environment*, 40 (29), 5640-5658.
- LI, Y. and DELSANTE, A. (2001) Natural ventilation induced by combined wind and thermal forces. *Building and Environment*, 36 (1), 59-71.
- LIDDAMENT, M. W. (1996) *A guide to energy efficient ventilation*. Coventry: AIVC.
- LIDDEN, P. F. (1999) The fluid mechanics of natural ventilation. *Annual Review of Fluid Mechanics*, 31, 201-238.
- LIEN, F. S. and YEE, E. (2004) Numerical modelling of the turbulent flow developing within and over a 3-d building array, part i: a high-resolution Reynolds-averaged Navier-stokes approach. *Boundary-layer Meteorology*, 112 (3), 427-466.
- LIN, Z. and DENG, S. (2003) The outdoor air ventilation rate in high-rise residences employing room air conditioners. *Building and Environment*, 38 (12), 1389-1399.
- LUO, Z., ZHAO, J., GAO, J. and HE, L. (2007) Estimating natural-ventilation potential considering both thermal comfort and IAQ issues. *Building and Environment*, 42 (6), 2289-2298.
- MAATOUK, K. (2007) A simplified procedure to investigate airflow patterns inside tall buildings using COMIS. *Architectural Science Review*, 50, 365-369.
- MACDONALD, R. W. (2000) Modelling the mean velocity profile in the urban canopy layer. *Boundary-layer Meteorology*, 97 (1), 25-45.
- MACDONALD, R. W., GRIFFITHS, R. F. and HALL, D. J. (1998) An improved method for the estimation of surface roughness of obstacle arrays. *Atmospheric Environment*, 32 (11), 1857-1864.
- MELARAGNO, M. G. (1982) *Wind in architectural and environmental design*. New York: Van Nostrand Reinhold Co.
- MENTER, F. R. (1994) Two-equation eddy-viscosity turbulence models for engineering applications. *AIAA Journal* 32, 1598-1605.
- MERONEY, R. N., LEITL, B. M., RAFAILIDIS, S. and SCHATZMANN, M. (1999) Wind-tunnel and numerical modeling of flow and dispersion about several building shapes. *Journal of Wind Engineering and Industrial Aerodynamics*, 81 (1-3), 333-345.

- MILES, S. and WESTBURY, P. S. (2003) Practical tools for wind engineering in the built environment. *QNET-CFD Network newsletter*. Available from: [Accessed: 5-10-2007].
- MURAKAMI, S. (1993a) Comparison of various turbulence models applied to a bluff body. *Journal of Wind Engineering and Industrial Aerodynamics*, 46&47, 21-36.
- MURAKAMI, S. (1993b) Discussions of turbulence modelling and their applications: Comparison of various turbulence models applied to a bluff body. *Journal of Wind Engineering and Industrial Aerodynamics*, 46-47, 183-191.
- MURAKAMI, S. (1998) Overview of Turbulence Models Applied in CWE-1997. *Journal of Wind Engineering and Industrial Aerodynamics*, 74-76, 1-24.
- MURAKAMI, S. and MOCHIDA, A. (1988) 3-D numerical simulation of airflow around a cubic model by means of the k- ϵ model. *Journal of Wind Engineering and Industrial Aerodynamics*, 31 (2-3), 283-303.
- NG, E. (2008) An investigation into parameters affecting optimum ventilation design of high density cities. *International Journal of Ventilation*, 6, 349-357.
- NOZAWA, K. and TAMURA, T. (2002) Large eddy simulation of the flow around a low-rise building immersed in a rough-wall turbulent boundary layer. *Journal of Wind Engineering and Industrial Aerodynamics*, 90 (10), 1151-1162.
- ODPM (2006) *Approved document F- means of ventilation*. Office of the Deputy Prime Minister.
- OIKAWA, S. and MENG, Y. (1995) Turbulence characteristics and organized motion in a suburban roughness sublayer. *Boundary-layer Meteorology*, 74, 289-312.
- OKE, T. (1988) Street design and urban canopy layer climate. *Energy and Buildings*, 11, 103-113.
- OLGYAY, V. (1963) *Design with climate: bioclimatic approach to architectural regionalism*. Princeton: Princeton University Press.
- PAGES, J. and LEBENS, R. (1986) *Climate in the United Kingdom*. London: Her Majesty's Stationary Office.
- PITTS, A. C. (2004) *Planning and design strategies for sustainability and profit: pragmatic sustainable design on building and urban scales*. Oxford: Architectural Press.
- PLATE, E. J. (1999) Methods of investigating urban wind fields - physical models. *Atmospheric Environment*, 33 (24-25), 3981-3989.
- RAFAILIDIS, S. (1997) Influence of building areal density and roof shape on the wind characteristics above a town. *Boundary-layer Meteorology*, 85, 255-271.

- RAO, K. S. and NAPPO, C. J. (1998) Turbulence and dispersion in the stable atmospheric boundary layer. *In: Singh, M. P., and Raman, S. eds. Dynamics of the Atmospheric Flows: Atmospheric Transport and Diffusion Processes: Computational Mechanics Publications*, 39-91.
- RATTI, C., RAYDAN, D. and STEEMERS, K. (2003) Building form and environmental performance: archetypes, analysis and an arid climate. *Energy and Buildings*, 35 (1), 49-59.
- REICHRATCH, S. and DAVIES, T. W. (2002) Computational fluid dynamics simulations and validation of the pressure distribution on the roof of a commercial multi-span venlo-type glasshouse. *Journal of Wind Engineering and Industrial Aerodynamics*, 90 (3), 139-149.
- RICHARDS, P. J. and HOXEY, R. P. (1993) Appropriate boundary conditions for computational wind engineering models using the k- ϵ turbulence model. *Journal of Wind Engineering and Industrial Aerodynamics*, 46-47, 145-153.
- RODI, W. (1997) Comparison of LES and RANS calculations of the flow around bluff bodies. *Journal of Wind Engineering and Industrial Aerodynamics*, 69-71, 55-75.
- ROTACH, M. W. (1993) Turbulence close to a rough urban surface, part I: Reynolds stress. *Boundary-layer Meteorology*, 65, 1-28.
- ROTACH, M. W. (1999) On the influence of the urban roughness sublayer on turbulence and dispersion. *Atmospheric Environment*, 33, 4001-4008.
- ROULET, C. A., FURBRINGER, J. M. and CRETTON, P. (1999) The influence of the user on the results of multizone air flow simulations with COMIS. *Energy and Buildings*, 30, 73-86.
- SAGRADO, A. P. G., VAN BEECK, J., RAMBAUD, P. and OLIVARI, D. (2002) Numerical and experimental modelling of pollutant dispersion in a street canyon. *Journal of Wind Engineering and Industrial Aerodynamics*, 2002 (4-5), 321-339.
- SANTIAGO, J. L., MARTILLI, A. and MARTIN, F. (2007) CFD simulation of airflow over a regular array of cubes. Part I: three-dimensional simulation of the flow and validation with wind-tunnel measurements. *Boundary-layer Meteorology*, 122 (3), 609-634.
- SCHMIDT, S. and THIELD, F. (2002) Comparison of numerical methods applied to the flow over wall-mounted cubes. *International Journal of Heat and Fluid Flow*, 23, 330-339.
- SELVAM, R. P. (1997) Computation of pressures on Texas Tech University building using large eddy simulation. *Journal of Wind Engineering and Industrial Aerodynamics*, 67&68, 647-657.

- SHAH, K. B. and FERZIGER, J. H. (1997) A fluid mechanics view of wind engineering: large eddy simulation of flow past a cubic obstacle. *Journal of Wind Engineering and Industrial Aerodynamics*, 67&68, 211-224.
- SHARAG-ELDIN, A. (1998) *Predicting natural ventilation in residential buildings in the context of urban environments*. Thesis (PhD). University of California, Berkeley.
- SHARPLES, S. and BENSALAM, R. (2001) Airflow in courtyard and atrium buildings in the urban environment: a wind tunnel study. *Solar Energy*, 70 (3), 237-244.
- SHIH, T. H., LIOU, W. W., SHABBIR, W., YANG, A. and ZHU, J. (1995) A new k- ϵ eddy- viscosity model for high Reynolds number turbulence flows - model development and validation. *Computer Fluids*, 24, 227-238.
- SIMI, E. and SCANLAN, R. H. (1986) *Wind Effects on Structures: An Introduction to Wind Engineering*. 2 ed.: John Wiley & Sons.
- SIMI, E. and SCANLAN, R. H. (1986) *Wind effects on structures: an Introduction to wind engineering*. 2nd ed. New York: John Wiley & Sons.
- SNYDER, W., H. and CASTRO, I. P. (2002) The Critical Reynolds Number for Rough-wall Boundary Layers. *Journal of Wind Engineering and Industrial Aerodynamics*, 90, 41-54.
- STATHOPOULOS, T. and BASKARAN, B. A. (1996) Computer simulation of wind environmental conditions around buildings. *Engineering Structures*, 18, 876-885.
- STATHOPOULOS, T. and ZHU, X. (1988) Wind pressures on buildings with appurtenances. *Journal of Wind Engineering and Industrial Aerodynamics*, 31, 265-281.
- STERN, F., WILSON, R. V., COLEMAN, H. W. and PATERSON, E. G. (2001) Comprehensive approach to verification and validation of CFD simulations- part 1: methodology and procedures. *Journal of Fluid Engineering*, 123, 793-802.
- STRAW, M. P., BAKER, C. J. and ROBERTSON, A. P. (2000) Experimental measurements and computations of the wind-induced ventilation of a cubic structure. *Journal of Wind Engineering and Industrial Aerodynamics*, 88 (2-3), 213-230.
- SU, B. (2003) Developments in wind tunnel studies for estimating the cross ventilation potential for a low-rise building in a built-up area. *International Journal of Ventilation*, 2 (1), 77-85.
- SU, Y., RIFFAT, S. B., LIN, Y.-L. and KHAN, N. (2008) Experimental and CFD study of ventilation flow rate of a Monodraught(TM) windcatcher. *Energy and Buildings*, 40 (6), 1110-1116.

- SUH, S.-H., ROH, H.-W., KIM, H.-R., LEE, K.-Y. and KIM, K.-S. (1997) Application of computational techniques for studies of wind pressure coefficients around an odd-geometrical building. *Journal of Wind Engineering and Industrial Aerodynamics*, 67-68, 659-670.
- SUMMERS, D. M., HANSON, T. and WILSON, C. B. (1986) Validation of a computer simulation of wind flow over a building model. *Building and Environment*, 21 (2), 97-111.
- SWAMI, M. V. and CHANDRA, S. (1988) Correlations for pressure distribution on buildings and calculation of natural-ventilation airflow. *ASHRAE Transaction*, 94, 243-266.
- SYRIOS, K. and HUNT, G. R. (2007) Urban Canyon Influence on Building Natural Ventilation. *International Journal of Ventilation*, 6 (1), 43-49.
- SYRIOS, K. and HUNT, G. R. (2007) Urban canyon influence on building natural ventilation. *International Journal of Ventilation*, 6, 43-49.
- TSENG, Y. H., MENEVEAU, C. and PARLANGE, M. B. (2006) Modeling flow around bluff bodies and predicting urban dispersion using large eddy simulation. *Environmental Science & Technology*, 40, 2653-2662.
- TSUTSUMI, J., KATAYAMA, T. and NISHIDA, M. (1992) Wind tunnel tests of wind pressure on regularly aligned buildings. *Journal of Wind Engineering and Industrial Aerodynamics*, 43 (1-3), 1799-1810.
- TUTAR, M. and OGUZ, G. (2002) Large eddy simulation of wind flow around parallel buildings with varying configurations. *Fluid Dynamics Research*, 31 (5-6), 289-315.
- UN (2008) *World urbanization prospects: the 2007 revision*. United Nations Publication.
- VAN MOESEKE, G., GRATIA, E., REITER, S. and DE HERDE, A. (2005) Wind pressure distribution influence on natural ventilation for different incidences and environment densities. *Energy and Buildings*, 37 (8), 878-889.
- VERSTEEG, H. K. and MALALASERKRA, W. (2007) *An introduction to computational fluid dynamics: the finite volume method*. 2nd ed. London: Person Education Limited.
- WARD, I. C. (2003) The usefulness of climatic maps of built-up areas in determining drives for the energy and environmental efficiency of building and external areas. *International Journal of Ventilation*, 2, 277-286.
- WARD, I. C. (2008) The potential impact of the new (UK) building regulations on the provision of natural ventilation in dwellings - a case study of low energy social housing *International Journal of Ventilation*, 7, 60-72.
- WARREN, P. (2000) *Multizone Air Flow Modelling (COMIS)*. (IEA ECBCS Annex 23). Coventry: International Energy Agency.

- WHEELER, S. M. (2004) *Planning for sustainability*. London: Routledge.
- WIERINGA, J. (1993) Representative roughness parameters for homogeneous terrain. *Boundary-layer Meteorology*, 63 (4), 323-363.
- WIJK, T. and HANSEN, W. M. (1997) The assessment of wind loads on roof overhang of low-rise buildings. *Journal of Wind Engineering and Industrial Aerodynamics*, 67-68, 687-696.
- WILCOX, D. C. (1998) *Turbulence modelling*. California: DCW Industries.
- WILLS, S., FORDHAM, M. and BORDASS, B. (1995) *Avoiding or minimising the use of air-conditioning- a research report from the EnREI Programme*. (31).
- XIE, Z. and CASTRO, I. P. (2006) LES and RANS for turbulent flow over arrays of wall-mounted obstacles. *Boundary-Layer Meteorology* (76), 291-312.
- YAKHOT, A. and ORSZAG, S. A. (1986) Renormalization group analysis of turbulence: I Basic theory. *Journal of Science Computing*, 1, 1-51.
- YANG, L., ZHANG, G., LI, Y. and CHEN, Y. (2005) Investigating potential of natural driving forces for ventilation in four major cities in China. *Building and Environment*, 40 (6), 738-746.
- YOSHIE, R., MOCHIDA, A., TOMINAGA, Y., KATAOKA, H., HARIMOTO, K., NOZU, T. and SHIRASAWA, T. (2007) Cooperative project for CFD prediction of pedestrian wind environment in the Architectural Institute of Japan. *Journal of Wind Engineering and Industrial Aerodynamics*, 95 (9-11), 1551-1578.
- ZHAI, Z. (2006) Application of computational fluid dynamics in building design: aspects and trends. *Indoor and Built Environment*, 15, 305-313.
- ZHANG, A., GAO, C. and ZHANG, L. (2005) Numerical simulation of the wind field around different building arrangements. *Journal of Wind Engineering and Industrial Aerodynamics*, 93 (12), 891-904.
- ZHAO, Y., YOSHINO, H. and OKUYAMA, H. (1998) Evaluation of the COMIS model by comparing simulation and measurement of airflow and pollutant concentration. *Indoor Air*, 8, 123-130.

Appendix A

Air Infiltration Development Algorithm

```
%*****
%   Air Infiltration Development Algorithm
%*****
%This is the script file of 'aida.m'
d=1.225;                               % Air Density at 15 Deg C
cd=0.61;                               % discharge coefficient
disp('Enter Building Data:');
v=input('Building Volume (m3)=');
disp('Enter Climate Data');
e=input('Ext Temp(Deg C)=');
i=input('Int Temp(Deg C)=');
u=input('Wind Spd(Ref)(m/s)=');
disp('Enter Flow Path Data:');
j=input('Number of Flow Paths=');
h=input('Height(m)=[ ]');
g=input('Opening Area(m2)=[ ]');
n=input('Flow Exp=[ ]');
p=input('Pressure Coef=[ ]');
c=sqrt(2/d)*cd.*g;                     %flow coefficient calculation
w=0.5*d.*p*u*u;                         %wind pressure calculation
s=-3455.*h*(1/(e+273)-1/(i+273));       %stack pressure calculation
t=w+s;                                   %path pressure

%Calculation Infiltration
tt=sum(t);                               %Total pressure
if tt>0
    r=100;                               %Initial positive internal pressure
    y=-1;                                  %Initial flow balance
else
    r=-100;                               %Initial negative internal pressure
    y=1;
end;
x=50;
z=0.0000001;                             %Absolute criteria of convergence
```

```

while abs(y)>z
    r=r+sign(y)*x;
    o=t-r;                                %Pressure difference across flow path
    x=x/2;
    f=sign(o).*c.*abs(o).^n;            %Path flow rate
    y=sum(f);                            %The total mass flow rate
end;
disp('Calculation Results');
disp('Internal pressure (Pa)');
fprintf('%f\n',r);
disp('path flow rate (m3/s)')
q=0;
for m=1:j
    if f(m)>0
        q=q+f(m);                        %Infiltration rate
    end;
    fprintf('path%g %f\n', m, f(m));
end;
disp('Infiltration rate (m3/s),');
fprintf('%f\n',q);
qm=1000*d*q;
disp('Infiltration rate (g/s),');
fprintf('%f\n',qm);
disp('Air Change Rate (ACH),');
ach=q*3600/v;                            %Air change rate per hour
fprintf('%f\n',ach);

```

Appendix B

COMIS Input Data of the Zones of the Jessop West Building

Comis Input File (.CIF) --- Generated by Simulation Studio for COMIS 3.2
 # November 2005

Please send your remarks and questions to software@cstb.fr

=====

&-CIF 1

COMIS Input File

jw-iso-a-w.cif

&-NET-ZONes

Zone	Name	Temp	Ref.	Volume	Humid.	Schedule
ID		Height	[m3]		Name	
		H/D/W				
(-)	[-]	[[temp]]	[m]	[m/m/m]	[[humi]	[-]

<i>a1_2</i>	<i>a1_2</i>	18	0.0	98.41	0
<i>a1_3</i>	<i>a1_3</i>	18	0.0	114.05	0
<i>a1_5</i>	<i>a1_5</i>	18	0.0	359.25	0
<i>a1_1</i>	<i>a1_1</i>	18	0.0	743.21	0
<i>a1_4</i>	<i>a1_4</i>	18	0.0	114.13	0
<i>a1_7</i>	<i>a1_7</i>	18	0.0	93.45	0
<i>ta2_6</i>	<i>ta2_6</i>	18	0	18	0
<i>ta2_9</i>	<i>ta2_9</i>	18	0	6.98	0
<i>a2_6</i>	<i>a2_6</i>	18	0	240.09	0
<i>a2_9</i>	<i>a2_9</i>	18	0	119.46	0
<i>a2_8</i>	<i>a2_8</i>	18	0	227.73	0
<i>a2_3</i>	<i>a2_3</i>	18	0	49.91	0
<i>a2_5</i>	<i>a2_5</i>	18	0	59.27	0
<i>a2_2</i>	<i>a2_2</i>	18	0	81.15	0
<i>ta2_4</i>	<i>ta2_4</i>	18	0	9.55	0
<i>a2_4</i>	<i>a2_4</i>	18	0	517.42	0
<i>a2_7</i>	<i>a2_7</i>	18	0	53.18	0
<i>a2_1</i>	<i>a2_1</i>	18	0	289.51	0

<i>ta3_6</i>	<i>ta3_6</i>	18	0	18	0
<i>ta3_9</i>	<i>ta3_9</i>	18	0	6.98	0
<i>a3_6</i>	<i>a3_6</i>	18	0	240.09	0
<i>a3_9</i>	<i>a3_9</i>	18	0	119.46	0
<i>a3_8</i>	<i>a3_8</i>	18	0	227.73	0
<i>a3_3</i>	<i>a3_3</i>	18	0	49.91	0
<i>a3_5</i>	<i>a3_5</i>	18	0	59.27	0
<i>a3_2</i>	<i>a3_2</i>	18	0	81.15	0
<i>ta3_4</i>	<i>ta3_4</i>	18	0	9.55	0
<i>a3_4</i>	<i>a3_4</i>	18	0	517.42	0
<i>a3_7</i>	<i>a3_7</i>	18	0	53.18	0
<i>a3_1</i>	<i>a3_1</i>	18	0	289.51	0
<i>ta4_6</i>	<i>ta4_6</i>	18	0	18	0
<i>ta4_9</i>	<i>ta4_9</i>	18	0	6.98	0
<i>a4_6</i>	<i>a4_6</i>	18	0	240.09	0
<i>a4_9</i>	<i>a4_9</i>	18	0	119.46	0
<i>a4_8</i>	<i>a4_8</i>	18	0	227.73	0
<i>a4_3</i>	<i>a4_3</i>	18	0	49.91	0
<i>a4_5</i>	<i>a4_5</i>	18	0	59.47	0
<i>a4_2</i>	<i>a4_2</i>	18	0	81.15	0
<i>ta4_4</i>	<i>ta4_4</i>	18	0	9.55	0
<i>a4_4</i>	<i>a4_4</i>	18	0	517.42	0
<i>a4_7</i>	<i>a4_7</i>	18	0	53.18	0
<i>a4_1</i>	<i>a4_1</i>	18	0	289.51	0
<i>ta5_6</i>	<i>ta5_6</i>	18	0	18	0
<i>ta5_9</i>	<i>ta5_9</i>	18	0	6.98	0
<i>a5_6</i>	<i>a5_6</i>	18	0	240.09	0
<i>a5_9</i>	<i>a5_9</i>	18	0	119.46	0
<i>a5_8</i>	<i>a5_8</i>	18	0	227.73	0
<i>a5_3</i>	<i>a5_3</i>	18	0	49.91	0
<i>a5_5</i>	<i>a5_5</i>	18	0	59.27	0
<i>a5_2</i>	<i>a5_2</i>	18	0	81.15	0
<i>ta5_4</i>	<i>ta5_4</i>	18	0	9.55	0
<i>a5_4</i>	<i>a5_4</i>	18	0	517.42	0
<i>a5_7</i>	<i>a5_7</i>	18	0	53.18	0
<i>a5_1</i>	<i>a5_1</i>	18	0	289.51	0
<i>ta6_6</i>	<i>ta6_6</i>	18	0	18	0
<i>ta6_9</i>	<i>ta6_9</i>	18	0	6.98	0
<i>a6_6</i>	<i>a6_6</i>	18	0	279.32	0
<i>a6_9</i>	<i>a6_9</i>	18	0	88.13	0
<i>a6_8</i>	<i>a6_8</i>	18	0	227.73	0
<i>a6_3</i>	<i>a6_3</i>	18	0	49.91	0
<i>a6_5</i>	<i>a6_5</i>	18	0	59.27	0
<i>a6_2</i>	<i>a6_2</i>	18	0	81.15	0
<i>ta6_4</i>	<i>ta6_4</i>	18	0	9.55	0
<i>a6_4</i>	<i>a6_4</i>	18	0	509.52	0
<i>a6_7</i>	<i>a6_7</i>	18	0	53.18	0
<i>a6_1</i>	<i>a6_1</i>	18	0	289.51	0
<i>b1</i>	<i>b1</i>	18	0.0	1045.1	0
<i>b2</i>	<i>b2</i>	18	0	1045.1	0

```

c2    c2    18    0    310.8  0
b3    b3    18    0    1045.1 0
c3    c3    18    0    310.8  0
b4    b4    18    0    1045.1 0
c4    c4    18    0    310.8  0
b5    b5    18    0    1045.1 0
ta6_1 ta6_1  18    0    3.08   0

```

```
&-CIF          2
```

```

|COMIS Input File |
|                  |

```

```

jw-b-iso-w.cif
&-NET-ZONes

```

Zone	Name	Temp	Ref.	Volume	Humid.	Schedule
ID		Height	[m3]		Name	
(-)	[-]	[[temp]]	[m]	[m/m/m]	[[humi]]	[-]

```

b2_4  b2_4  18    0    196.08  0
b2_3  b2_3  18    0    46.88   0
b2_5  b2_5  18    0    37.27   0
b2_6  b2_6  18    0    91.16   0
tb2_1 tb2_1  18    0    9.55    0
tb2_4 tb2_4  18    0    13.22   0
tb2_5 tb2_5  18    0    3.67    0
b2_1  b2_1  18    0    401.53  0
b1_4  b1_4  18    0.0  96.73   0
b1_1  b1_1  18    0.0  649.92  0
b1_3  b1_3  18    0.0  54.04   0
b1_2  b1_2  18    0.0  65.69   0
b2_2  b2_2  18    0    44.98   0
b3_4  b3_4  18    0    196.08  0
b3_3  b3_3  18    0    46.88   0
b3_5  b3_5  18    0    37.27   0
b3_6  b3_6  18    0    91.16   0
tb3_1 tb3_1  18    0    9.55    0
tb3_4 tb3_4  18    0    13.22   0
tb3_5 tb3_5  18    0    3.67    0
b3_1  b3_1  18    0    401.53  0
b3_2  b3_2  18    0    44.98   0
b4_4  b4_4  18    0    196.08  0
b4_3  b4_3  18    0    46.88   0
b4_5  b4_5  18    0    37.27   0
b4_6  b4_6  18    0    91.16   0
tb4_1 tb4_1  18    0    9.55    0
tb4_4 tb4_4  18    0    13.22   0

```


<i>c2_6</i>	<i>c2_6</i>	18	0	210.56 0
<i>c2_2</i>	<i>c2_2</i>	18.0	0	42.84 0
<i>c3_3</i>	<i>c3_3</i>	18	0	60.96 0
<i>c3_4</i>	<i>c3_4</i>	18	0	173.81 0
<i>c3_1</i>	<i>c3_1</i>	18	0	340.61 0
<i>c3_5</i>	<i>c3_5</i>	18	0	122.28 0
<i>c3_6</i>	<i>c3_6</i>	18	0	210.56 0
<i>c3_2</i>	<i>c3_2</i>	18	0	42.84 0
<i>c4_3</i>	<i>c4_3</i>	18	0	60.96 0
<i>c4_4</i>	<i>c4_4</i>	18	0	173.81 0
<i>c4_1</i>	<i>c4_1</i>	18	0	340.61 0
<i>c4_5</i>	<i>c4_5</i>	18	0	122.28 0
<i>c4_6</i>	<i>c4_6</i>	18	0	210.56 0
<i>c4_2</i>	<i>c4_2</i>	18	0	340.61 0
<i>a2_1</i>	<i>a2_1</i>	18	0	420.2 0
<i>a2</i>	<i>a2</i>	18	0	947.58 0
<i>b2</i>	<i>b2</i>	18	0	889.6 0
<i>a1</i>	<i>a1</i>	18	0.0	685.84 0
<i>b1</i>	<i>b1</i>	18.0	0.0	1045.1 0
<i>a3_1</i>	<i>a3_1</i>	18	0	420.2 0
<i>a3</i>	<i>a3</i>	18	0	947.58 0
<i>b3</i>	<i>b3</i>	18	0	889.6 0
<i>a1_1</i>	<i>a1_1</i>	18	0.0	743.21 0
<i>a4_1</i>	<i>a4_1</i>	18	0	420.2 0
<i>a4</i>	<i>a4</i>	18	0	947.58 0
<i>b4</i>	<i>b4</i>	18	0	889.6 0
<i>a5_1</i>	<i>a5_1</i>	18	0	420.2 0
<i>a5</i>	<i>a5</i>	18	0	947.58 0
<i>b5</i>	<i>b5</i>	18	0	889.6 0
<i>a6_1</i>	<i>a6_1</i>	18	0	420.2 0
<i>a6</i>	<i>a6</i>	18	0	947.58 0